Analysis of ATP-Dependent Association of the Smc5/6 Complex with Chromatin

Marc Tarrés Escalona

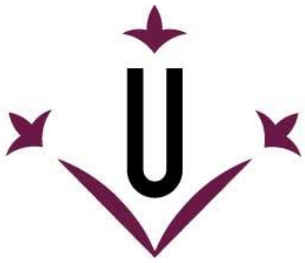

Universitat de Lleida

TESI DOCTORAL

Analysis of ATP-Dependent Association of the Smc5/6 Complex with Chromatin

Marc Tarrés Escalona

Memòria presentada per optar al grau de Doctor per la Universitat de Lleida

Programa de Doctorat en Salut

Director/a

Jordi Torres Rosell

Tutor/a

Jordi Torres Rosell

2022

TABLE OF CONTENTS

TABLE OF CONTENTS

ABSTRACT

The main goal of living organisms is to accurately transmit their genetic information to offspring. At the cellular level, it involves the faithful replication of DNA and the equitable segregation of chromosomes between daughter cells. The family of SMC (Structural Maintenance of Chromosomes) complexes, preserved from prokaryotes to higher eukaryotes, performs essential functions during the processes of DNA replication and segregation, aiding in the organization of chromosomes. In eukaryotes, there are three SMC-type complexes: cohesin, condensin, and the Smc5/6 complex. Its activities as chromosomal organizers require its binding to chromatin in a process dependent on the ATPase activity of the SMC complexes themselves. While this activity is best known for cohesin, condensin, and bacterial SMC complexes, it remains almost unexplored for the Smc5/6 complex.

In this thesis, we have studied how, when and where the Smc5/6 complex is loaded on chromosomes. Our results indicate an increase in the binding of the complex to chromatin as DNA replicates, showing maximum binding shortly before mitosis entry and accumulating due to problems with replication forks. At the molecular level, this association requires the presence of the Nse1/3/4 and Nse5/6 subcomplexes and the binding of ATP to the ATPase of Smc5/6. In contrast, an Smc5 protein unable to hydrolyze ATP is enriched on DNA, indicating that in the absence of ATP hydrolysis, the complex is trapped on DNA during the loading reaction. In addition, we used this observation to determine the loading sites of the complex. By chromatin immunoprecipitation coupled to mass sequencing (ChIP-seq), we observed that the Smc5/6 complex is loaded at the origins of replication and regions of convergent transcription. The Smc5 mutant unable to hydrolyze ATP is a partial dominant negative, reducing viability in cells that have compromised expression of the wild-type allele. In addition, its expression blocks the segregation of ribosomal DNA (rDNA) while its loading onto specific sequences affects the segregation of these regions. These results suggest that Smc5/6 binds to chromatin through an intermediate in the ATP hydrolysis cycle capable of promoting connections between sister chromatids. In addition, DNA binding and rDNA segregation problems are not shared by an equivalent mutation in the Smc6 protein, suggesting that the ATPase head hydrolyzes ATP molecules at different times during chromatin binding.

In conclusion, our results fit with an essential function of the ATPase activity of the Smc5/6 complex, which would be necessary both for the association of the complex with chromatin and for proper disjunction of chromosomal structures, and which would require intermediates of the ATPase cycle of Smc5/6 capable of transiently connecting sister chromatids.

RESUM

Els organismes vius tenen com a principal objectiu la transmissió precisa de la seva informació genètica a la descendència. A nivell cel·lular, implica la replicació fidel de l'ADN i la segregació equitativa dels cromosomes entre les cèl·lules filles. La família de complexos SMC (Structural Maintenance of Chromosomes), conservada des de procariotes a eucariotes superiors, realitza funcions essencials durant els processos de replicació i segregació de l'ADN, ajudant en l'organització dels cromosomes. En eucariotes, hi ha tres complexos de tipus SMC: la cohesina, la condensina i el complex Smc5/6. Les seves activitats com a organitzadors cromosòmics requereixen la seva unió a cromatina en un procés dependent de l'activitat ATPasa dels propis complexos SMC. Mentre que aquesta activitat és més coneguda per a la cohesina, la condensina i els complexos SMC bacterians, segueix quasi sense explorar per al complex Smc5/6.

En aquesta tesi, hem estudiat com, quan i on es carrega el complex Smc5/6 sobre els cromosomes. Els nostres resultats indiquen un increment en la unió del complex a la cromatina a mesura que l'ADN es replica, mostrant un màxim d'unió poc abans de l'entrada en mitosi i acumulant-se per problemes en les forquilles de replicació. A nivell molecular, aquesta unió requereix la presència dels subcomplexes Nse1/3/4 i Nse5/6 i la unió d'ATP a l'ATPasa de Smc5/6. En canvi, una proteïna Smc5 afectada en la hidròlisi d'ATP es troba enriquida en l'ADN indicant que, en absència d'hidròlisi d'ATP, el complex queda atrapat sobre l'ADN durant la reacció de càrrega. A més, hem aprofitat aquesta observació per tal de determinar els punts de càrrega del complex en cromatina. Mitjançant la immunoprecipitació de cromatina acoblada a seqüenciació en massa (ChIP-seq), hem observat que el complex Smc5/6 es carrega habitualment en els orígens de replicació i les regions amb transcripció convergent. El mutant Smc5 afectat en hidròlisi d'ATP és parcialment dominant negatiu, reduint la viabilitat en cèl·lules que tenen compromesa l'expressió de l'al·lel salvatge. A més, la seva expressió bloqueja la separació de l'ADN ribosòmic (ADNr) mentre que la seva càrrega en seqüències específiques afecta la segregació d'aquestes regions. Aquests resultats suggereixen que Smc5/6 s'associa a cromatina a través d'un intermedi en la hidròlisi de l'ATP capaç de promoure connexions entre cromàtides germanes. A més, els fenotips d'unió a l'ADN i problemes en segregació de l'ADNr no són compartits per una mutació equivalent en la proteïna Smc6, suggerint que el cap ATPasa hidrolitza les molècules d'ATP en diferents moments durant la unió de la cromatina.

En conclusió, els nostres resultats encaixen amb una funció essencial de l'activitat ATPasa del complex Smc5/6, que seria necessària tant per a l'associació del complex amb la cromatina com per a la disjunció adequada d'estructures cromosòmiques, i que passaria per intermediaris del cicle ATPasa d'Smc5/6 capaços de connectar les cromàtides germanes de forma transitòria.

RESUMEN

Los organismos vivos tienen como principal objetivo la transmisión precisa de su información genética a la descendencia. A nivel celular, implica la replicación fiel del ADN y la segregación equitativa de los cromosomas entre las células hijas. La familia de complejos SMC (Structural Maintenance of Chromosomes), conservada desde procariotas a eucariotas superiores, realiza funciones esenciales durante los procesos de replicación y segregación del ADN, ayudando en la organización de los cromosomas. En eucariotas, existen tres complejos de tipo SMC: la cohesina, la condensina y el complejo Smc5/6. Sus actividades como organizadores cromosómicos requieren su unión a cromatina en un proceso dependiente de la actividad ATPasa de los propios complejos SMC. Mientras que esta actividad es más conocida para la cohesina, la condensina y los complejos SMC bacterianos, sigue casi sin explorar para el complejo Smc5/6.

En esta tesis, hemos estudiado cómo, cuándo y dónde se carga el complejo Smc5/6 sobre los cromosomas. Nuestros resultados indican un incremento en la unión del complejo a la cromatina a medida que el ADN se replica, mostrando un máximo de unión poco antes de la entrada en mitosis y acumulándose por problemas en las horquillas de replicación. A nivel molecular, esta unión requiere la presencia de los subcomplejos Nse1/3/4 y Nse5/6 y la unión de ATP en la ATPasa de Smc5/6. Por el contrario, una proteína Smc5 afectada en la hidrólisis de ATP se encuentra enriquecida en el ADN indicando que, en ausencia de hidrólisis de ATP, el complejo queda atrapado sobre el ADN durante la reacción de carga. Además, hemos aprovechado esta observación para determinar los puntos de carga del complejo en cromatina. Mediante la inmunoprecipitación de cromatina acoplada a secuenciación en masa (ChIP-seq), hemos observado que el complejo Smc5/6 se carga habitualmente en los orígenes de replicación y las regiones con transcripción convergente. El mutante Smc5 afectado en hidrólisis de ATP es parcialmente dominante negativo, reduciendo la viabilidad en células que tienen comprometida la expresión del alelo salvaje. Además, su expresión bloquea la separación del ADN ribosómico (ADNr) mientras que su carga en secuencias específicas afecta a la segregación de estas regiones. Estos resultados sugieren que Smc5/6 se asocia a cromatina a través de un intermedio en la hidrólisis de ATP capaz de promover conexiones entre cromátidas hermanas. Además, los fenotipos de unión a ADN y problemas en segregación del ADNr no son compartidos por una mutación equivalente en la proteína Smc6, sugiriendo que la cabeza ATPasa hidroliza las moléculas de ATP en momentos distintos durante la unión de la cromatina.

En conclusión, nuestros resultados encajan con una función esencial de la actividad ATPasa del complejo Smc5/6, que sería necesaria tanto para la asociación del complejo con la cromatina como para la adecuada disyunción de estructuras cromosómicas, y que pasaría por intermediarios del ciclo ATPasa de Smc5/6 capaces de conectar las cromátidas hermanas de forma transitoria.

ABBREVIATIONS

ABBREVIATIONS

ACS - ARS Consensus Sequence

AID - Auxin Inducible Degron

AP - Apurinic / Apyrimidinic

APC - Anaphase Promoting Complex

Amp - Ampicillin

ARS - Autonomously Replicating Sequence

ATP - Adenosine Triphosphate

BER - Base Excision Repair

BRCT - BRCA1 Carboxyl Terminal (Domain)

BSA - Bovine Serum Albumin

CDC - Cell Division Cycle

CDK - Cyclin Dependent Kinase

CEN - Centromere

ChIP - Chromatin Immunoprecipitation

clonNAT - Nourseothricin

CMG - Cdc45-MCM-GINS (Complex)

Cq - Quantification Cycle

DDK - Dbf4-Dependent Kinase

dH_2O - Distilled Water

DMSO - Dimethyl Sulfoxide

DNA - Deoxyribonucleic Acid

DRC - DNA Replication Checkpoint

DSB - Double Strand Break

dsDNA - Double Stranded DNA

DTT - Dithiothreitol

EDTA - Ethylenediaminetetraacetic Acid

FACS - Fluorescence-Activated Cell Sorting

FEAR - Cdc14 (Fourteen) Early Anaphase Release

G1 - Gap 1 (Phase of the cell cycle)

G2 - Gap 2 (Phase of the cell cycle)

GAL - Galactose

GALp - Galactose Promoter

GEN - Geneticin Sulfate, G-418 Sulfate

GFP - Green Fluorescent Protein

GGR - Global Genome Repair

GINS - Go, Ichi, Ni and San complex

GLU - Glucose

HA - Hemagglutinin

HAWK - HEAT Proteins Associated with Kleisin

HJ - Holliday Junction

hph - Hygromycin B

HR - Homologous Recombination

HRP - Horseradish Peroxidase

HU - Hydroxyurea

IAA - 3-Indoleacetic Acid

IGS - Intergenic Spacer

IP - Immunoprecipitation

KAN - Kanamycin

KITE - Kleisin Interacting Winged-Helix Tandem Elements

LB - Luria-Bernati

M (Phase) - Mitosis

MCC - Mitotic Checkpoint Complex

MCM - Minichromosome Maintenance (Complex)

MEN - Mitotic Exit Network

MMR - Mismatch Repair

MMS - Methyl Methanesulfonate

MRX - Mre11-Rad50-Xrs2 Complex

NB - Nanobody

NEF - Nucleotide Excision Repair Factor

NER - Nucleotide Excision Repair

NHEJ - Non-Homologous End Joining

NP-40 - Nonidet P40

NSE - Non-SMC Element

Nz - Nocodazole

ORF - Open Reading Frame

PBS - Phosphate Buffered Saline
PCNA - Proliferating Cell Nuclear Antigen
PCR - Polymerase Chain Reaction
PEG - Polyethylene Glycol
Pgp - P-glycoprotein multidrug transporter
PIKK - Phosphoatidylinositol 3-Kinase-Related Kinase
POL - Polymerase
Pre-LC - Pre-Loading Complex
Pre-RC - Pre-Replicative Complex
qPCR - Quantitative Polymerase Chain Reaction
OD - Optical Density
ORC - Origin Recognition Complex
rARS - rDNA Autonomously Replicating Sequence
rDNA - Ribosomal Deoxyribonucleic Acid
RFB - Replication Fork Barrier
RCF - Relative Centrifugal Force
ROS - Reactive Oxygen Species
RPA - Replication Protein A
rpm - Revolutions per Minute
SAC - Spindle Assembly Checkpoint
SBF - Swi4/6 cell cycle box (SCB) Binding Factor
SC - Synthetic Complete
SDM - Site Directed Mutagenesis
SDS - Sodium Dodecyl Sulfate
SDS-PAGE - Sodium Dodecyl Sulfate-Polyacrylamide Gel Electrophoresis
SGD - *Saccharomyces* Genome Database
SMC - Structural Maintenance of Chromosomes
SPB - Spindle Pole Body
S-Phase - Synthesis Phase (in the cell cycle)
SPR18 - SMC partner of Rad18
SSB - Single Strand Break
SSC - Saline-Sodium Citrate Buffer
ssDNA - Single Stranded DNA

STR - Sgs1-Top3-Rmi1 Complex

SUMO - Small Ubiquitin-like Modifier

TAD - Topologically Associated Domain

TAE - Tris-Acetate-EDTA

TBS - Tris Buffered Saline

TCR - Transcription Coupled Repair

TE - Tris-EDTA

TEMED - Tetrametiletilendiamine

TER - Terminator (of Replication)

tetO - Tetracycline Operator

TetR - Tetracycline Repressor

TIC - Total Input Chromatin

TIR1 - Transport Inhibitor Response 1

TLS - Trans-Lesion Synthesis

Top1 - Topoisomerase I

Top2 - Topoisomerase II

tRNA - Transfer Ribonucleic Acid

Ty Element - Yeast Transposable Element

UV - Ultraviolet

WH - Winged-Helix

WT - Wild Type

YFP - Yellow Fluorescent Protein

YP - Yeast Extract Peptone

YPD - Yeast Extract Peptone Dextrose

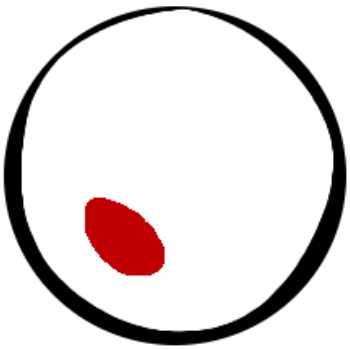

1 INTRODUCTION

1. INTRODUCTION

1.1. The Cell Cycle of Budding Yeast

A common objective of all living beings is the survival of the organism and the perpetuation of the species, which involves the faithful transmission of the genome to the offspring. At the cellular level, this process occurs during the cell cycle, the set of biological processes during which a cell grows and divides. The whole cycle is divided into two differentiated main parts: interphase and mitosis. During interphase, the main events happening to the cell are growth and the replication of the genetic material. Once the genome is duplicated, the cell enters mitosis, the process through which the genetic material is distributed before cell division, giving rise to two daughter cells.

1.1.1. Overview

The eukaryotic cell cycle is characterized by a very long interphase. For instance, mammal cells spend over 90% (Hahn et al., 2009) of the duration of their cell cycle in interphase and budding yeast around 75% (Leitao & Kellogg, 2017). Interphase can be subdivided into three different phases: Gap 1 (G1), Synthesis (S) and Gap 2 (G2). During the gap phases, the cell grows and prepares for either genomic replication or mitosis. In S-Phase, the cell is focused on generating a faithful copy of its chromosomes. Finally, in mitosis, the two genomic copies are segregated equally into two daughter cells and these cells become physically separated through a process named cytokinesis.

As this thesis has used the yeast *Saccharomyces cerevisiae* as a model organism, we will place a special emphasis on the specific organization of the yeast cell cycle. *Saccharomyces cerevisiae* is a unicellular eukaryotic organism belonging to the fungi kingdom. Most fungi perform both sexual and asexual reproduction, for this reason *S. cerevisiae* cells can be either haploid or diploid. Haploid cells are divided into the a and α mating types, which can secrete pheromones to the media named a-factor and α-factor, respectively. When two cells with different mating type find each other, they secrete their pheromones to promote G1 arrest on each other and start the mating process. Finally, these two haploid cells will fuse into a single diploid cell containing two copies for each of its chromosomes (Hartwell et al., 1974). While haploid cells can only divide through mitosis, diploid cells can perform both mitosis and meiosis. Yeast meiosis is also known as sporulation and finishes with the generation of four haploid spores that will eventually enter into a mitotic cell cycle or mate to generate a new diploid cell.

From a morphological point of view, a *S. cerevisiae* cell in G1 is spherical. During G1, the cell grows by increasing its volume without drastic changes in shape. However, when replication of the DNA starts, a bulge named bud appears on the cell wall. This is the reason for calling *S. cerevisiae* the budding yeast. The bud is the structure that eventually will become the daughter cell, so it keeps growing during both S and G2 phases until reaching a size sufficient to become a new cell. During mitosis, there is an

absence of morphological changes until cytokinesis, when the bud separates from the mother cell, giving rise to a newborn daughter cell and ending the cell cycle.

The events that occur during the cell cycle must be consecutive. A tight regulatory layout to ensure a proper advance throughout the cell cycle is conserved in evolution. In budding yeast, a kinase called Cdk1 (cyclin dependent kinase, codified by the *CDC28* gene in budding yeast) regulates the advance along the cell cycle. This protein is activated through binding to a cyclin subunit. During G1, the Cdk1 is inactive due to the absence of cyclins and the presence of Cdk inhibitors. As G1 advances, the Cln3 cyclin promotes the activation of Cdk1. The active kinase then phosphorylates Whi5, an inhibitor of SBF, the transcription factor required for activation of the G1 transcriptional program. Two of the proteins transcribed are the Cln1 and Cln2 cyclins, which generate a positive feedback loop activating Cdk1 even more. At this point, a cyclin dependent kinase inhibitor named Sic1 is tagged for degradation, activating Clb5-Cdk1 and Clb6-Cdk1, the cyclins responsible for the entrance into S-Phase (Zegerman & Diffley, 2007). When Cdk1 is bound to these cyclins, it phosphorylates and inactivates SBF to block the possibility of the cell going backwards through the cell cycle.

1.1.2. The S-Phase: Replication of the DNA

The transference of the genetic material to the offspring is the main objective of any living organism. Generation of a faithful copy of this genetic material is a key step to achieve a positive outcome at the end of the cell cycle. This process starts at replication origins, also known as ARS. Ars1 was the first replication origin discovered in budding yeast. Ars1 sequence was identified as a sequence that, when cloned into an episomal plasmid, conferred to this plasmid the capability to be replicated and inherited by daughter cells (Stinchcomb et al., 1979). These kind of sequences were named autonomously replicating sequence (ARS). Over 350 replication origins have been identified and characterized in *S. cereviasiae* ever since (Cherry et al., 2012; Raghuraman et al., 2001). They all contain a conserved 11 bp ARS consensus sequence (ACS) (DePamphilis, 1993; Newlon & Theis, 1993).

Replication is prepared during G1 with the assembly of the pre-replicative complex (pre-RC). The activity of Cdk1 blocks the formation of the pre-RC, hence the low CDK activity during G1 sets the proper environment for the complex to assemble. The recruitment of the six-subunit origin replication complex (ORC) to ACS is the first step of the pre-RC assembly (Bell & Stillman, 1992). Then, Cdc6 and Cdt1 help recruiting the Mcm2-7 complex to the ORC-bound ACS, becoming a complete pre-RC (Figure 1).

At the end of G1, activation of Clb5/6-Cdk1 promotes the phosphorylation of Sld2 and Sld3 (Zegerman & Diffley, 2007). First, the phosphorylation of Sld3 promotes the recruitment of Cdc45 to the pre-RC (Figure 1). Both Sld3 and Cdc45 are essential for replication origin firing (Zou et al., 1997). Then, phosphorylated Sld2, which carries the

Go, Ichi, Ni and San complex (GINS) and polymerase ε, binds to the C-terminal tandem BRCT domains in Dpb11 forming the pre-loading complex (pre-LC) (Muramatsu et al., 2010). Dpb11 can interact through its N-terminal tandem BRCT domains with phosphorylated Sld3, carrying the whole pre-LC to the pre-RC bound to the replication origin (Figure 1). On the pre-RC complex, the GINS together with Cdc45 and Mcm2-7 form the CMG complex, the DNA helicase that unwinds or rearranges duplex DNA during replication (Moyer et al., 2006). The ARS with all the described proteins bound to its ACS is then ready to be fired. The firing is controlled and activated by Dbf4-Cdc7, the Dbf4-dependent kinase (DDK), which phosphorylates Mcm2-7 (Lei et al., 1997; Sato, 1997). The phosphorylation of this subcomplex, increases its affinity for Cdc45 and GINS, favoring the formation of the active CMG complex, promoting the unwinding of DNA through its helicase activity and initiating DNA replication (Figure 1). The primase activity of polymerase α primes the synthesis and DNA polymerase ε is responsible for the extension of the leading strand. On the lagging strand, polymerase α is recruited to start its replication, generating the Okazaki fragments, which are extended by polymerase δ (Enserink, 2011; Waga & Stillman, 1994).

The replicative process implies the separation of parental DNA strands. Due to the helical structure of the DNA, this separation overwinds DNA ahead of the replication fork, increasing positive supercoiling and generating tension (Champoux, 2001; Peter et al., 1998). Topoisomerase I (Top1) and topoisomerase II (Top2) are the proteins responsible for the alleviation of this tension (Bermejo et al., 2007; R. A. Kim & Wang, 1989). These topoisomerases can transiently break one (Top1) or two (Top2) DNA strands to exchange their position, passing an intact DNA molecule through the break before resealing the broken strands (Champoux, 2001). Topoisomerase function is required not only during DNA replication but also in other processes that alter DNA supercoiling, like transcription of the rDNA (Brill et al., 1987; French et al., 2011), pausing of the replication fork (Fachinetti et al., 2010) and repair of DNA double strand breaks (Mehta & Haber, 2014). In addition, Top2 activity is required to decatenate replicated sister chromatids (Holm et al., 1985).

1.1.3. Mitosis: Chromosome Segregation and Cytokinesis

Mitosis takes places after DNA replication. The genomic material is divided into pieces called chromosomes, formed by two arms joined by a centromere. After DNA replication, chromosomes have two chromatids, also known as sister chromatids, which are identical to each other. During mitosis, microtubules bind to the centromere of each chromatid and pull it apart from its sister in a coordinated manner during anaphase.

1.1.3.1. Chromosome Segregation

The microtubules segregating the chromosomes are coordinated by the spindle pole bodies (SPB). The SPB is the only microtubule organizing element in budding yeast

(Jaspersen & Winey, 2004). It is a trans-nuclear membrane complex, which interacts with both nuclear and cytoplasmic microtubules (Page & Snyder, 1993; Robinow & Marak, 1966). One SPB is inherited from the previous cell division and a second one is assembled during interphase, starting at G1 (Byers & Goetsch, 1975; Jaspersen et al., 2002). During G2, the SPBs separate from each other, moving to opposite poles of the nucleus. Then, the SPBs position rotates 90 º to align with the longer axis in the mother cell and approaches to the neck between the mother cell and the bud, in a process mediated by the cytoplasmic astral microtubules and the actin cytoskeleton (Cottingham & Hoyt, 1997; Palmer et al., 1992). This movement of the SPB to the neck is known as nuclear migration, as it involves the movement of the whole nuclear mass.

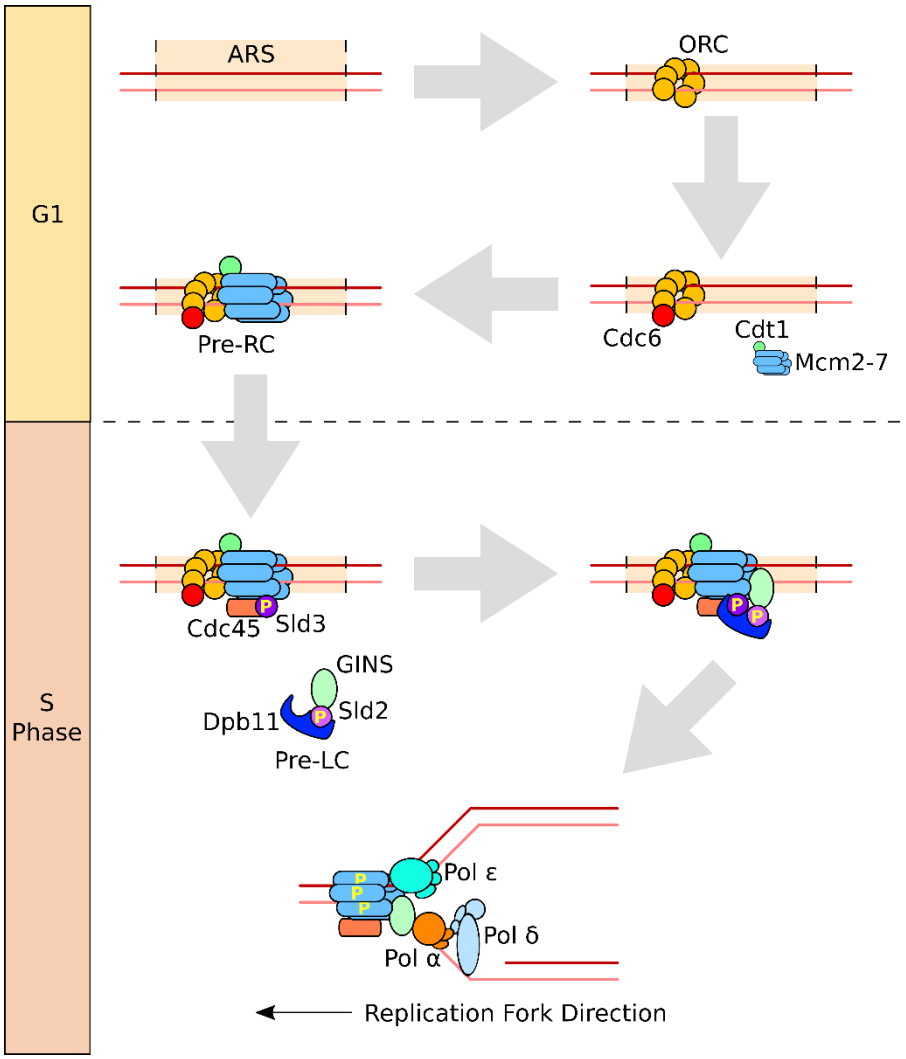

Figure 1. Assembly of the replisome at the replication origin. Scheme showing first the formation of the pre-RC complex during G1 and the posterior recruitment of the pre-LC to fire a replication origin during S phase. Yellow Ps indicate phosphorylated proteins.

Image adapted from L. Wu et al., 2014

In budding yeast, centromeres are already connected to spindle poles through microtubules in S-Phase. This interaction is mediated by the kinetochore, a protein complex that interacts with both centromeres and nuclear microtubules. CBF3A, a protein of the kinetochore, is bound to chromatin already during interphase and to the nuclear microtubules during mitosis (Page & Snyder, 1993). The interaction of the nuclear microtubules to the kinetochore exerts a tension on the centromere. The tension applied by each SPB to the centromere is equilibrated and places the chromosome on the metaphase central plate (Nicklas & Koch, 1969; Palmer et al., 1992). At this point, cohesin (the complex responsible for sister chromatid cohesion) holds sister chromatids together, avoiding their segregation due to the pulling by the spindle (Guacci et al., 1997; Michaelis et al., 1997). Cells in this situation activate Cdc20, a protein that interacts with and activates the anaphase promoting complex (APC) (Prinz et al., 1998). APC^{Cdc20} ubiquitylates Cbl5 and Pds1 (Figure 2), promoting their degradation (Jin et al., 2009; Shirayama et al., 1999). Pds1 (securin) is an inhibitor of Esp1, the separase that cleaves Scc1 (a subunit in cohesin) to release the sister chromatids and permit their segregation, hence anaphase progression (Ciosk et al., 1998; Uhlmann et al., 1999). The absence of Pds1 also promotes the activation of the Cdc14 (Fourteen) Early Anaphase Release (FEAR) pathway, which ends up in a brief release of Cdc14 from the nucleolus, which dephosphorylates Clb5 substrates necessary for anaphase activation (Liang et al., 2013) (Figure 2). Coinciding in time, Clb2 is expressed and interacts with Cdk1 to help in the activation of the FEAR pathway (Figure 2). All these signals together promote the advancement of the cell into anaphase. The nucleolus, containing the rDNA array, displays a delayed segregation (D'Amours et al., 2004; Sullivan et al., 2004; Torres-Rosell et al., 2004). Interestingly, it has been described lately that, in budding yeast, even after chromosome segregation has started, DNA is still replicating sequences close to the telomere (Ivanova et al., 2020).

1.1.3.2. DNA Structure and Condensation

Chromosomes are long threads of DNA which would be difficult to segregate properly in normal conditions. During interphase, DNA is organized into nucleosomes, structures of 147 base pairs wrapped around an octameric subunit complex named histone and separated by linker DNA of 18 base pair average length (Beshnova et al., 2014; Jansen & Verstrepen, 2011). Nucleosomes have a size of 11 nm and fold into a secondary structure of 30 nm, which has been proposed to be either a solenoid or a zigzag structure (B. V. S. Iyer et al., 2011). In budding yeast, the DNA is transiently condensed upon anaphase entrance, although it does not remotely reach the condensation levels of mitotic human chromosomes (Vas et al., 2007). Condensed chromosomes are more compact and shorter due to a high level of chromatin organization, facilitating their segregation. Chromosome condensation in mitosis is mediated by condensin and cohesin complexes, together with topoisomerase II (Lavoie et al., 2002; Strunnikov et al., 1995; Vas et al., 2007).

1.1.3.3. Mitotic Exit and Cytokinesis

Finally, after chromosome segregation, the mitotic exit network (MEN) is activated. The MEN is a pathway that consists of Ras-Like GTPase, Tem1, Mob1 and different kinases, Cdc5, Cdc15 and Dbf2 (D'Amours & Amon, 2004; Frenz et al., 2000; Kitada et al., 1993). The activation of MEN promotes the extrusion of the actomyosin contractile ring, which is followed by the formation of a primary and secondary septum ending cytokinesis (Bhavsar-Jog & Bi, 2017; Tamborrini et al., 2018). MEN activation also promotes a major release of Cdc14 from the nucleolus with different roles (Shou et al., 1999; Visintin et al., 1999). First, the Cdc14 release activates APC together with Cdh1 (APC^{Cdh1}) which ubiquitylates Clb2-Cdk1 for degradation (Schwab et al., 1997). Second, Cdc14 dephosphorylates Clb2-Cdk1 substrates (Jin et al., 2009; Visintin et al., 1998).

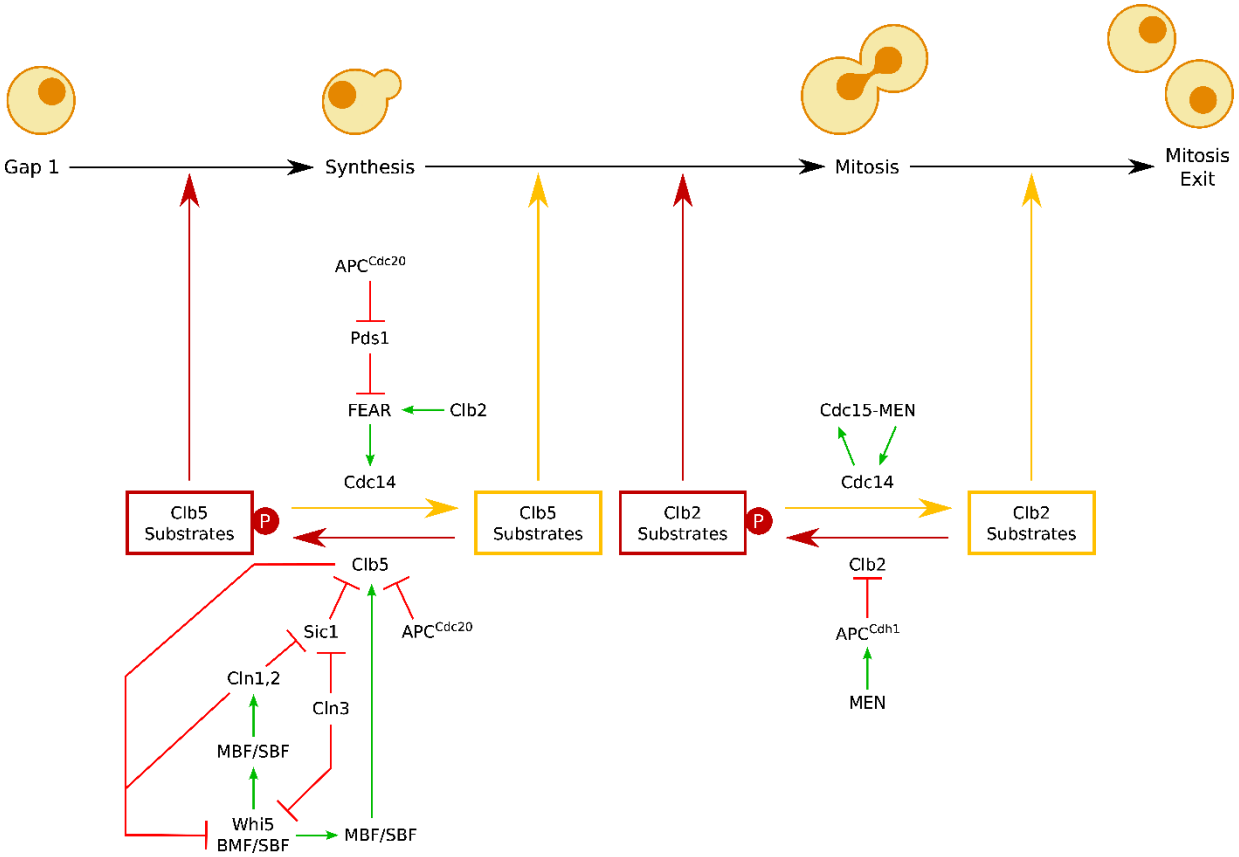

Figure 2. Regulation of the entrance and exit of mitosis. Schematic view of the regulatory pathways controlling the entrance into mitosis, chromosome segregation and the exit through cytokinesis.
Image adapted from Jin et al., 2009; Sherr & Roberts, 2004

1.1.4. Checkpoints in the Cell Cycle

In this text, the cell cycle has been depicted as a continuous stream of ordered events. However, eukaryotic cells have mechanisms to either extend or temporary stop these processes. These mechanisms are used by the cell to ensure a positive outcome

of the cell cycle and are called checkpoints. There are four main checkpoints in the cell cycle: the G1/S checkpoint, the intra-S checkpoint, the DNA damage checkpoint and the spindle assembly checkpoint (SAC). The G1/S checkpoint is activated under adverse environmental conditions such as the lack of nutrients (Coller, 2022; Hartwell et al., 1974; Johnston et al., 1977), osmotic stress (Escoté et al., 2004) or heat stress (Piper, 1993).

1.1.4.1. Intra-S Checkpoint and Checkpoints Dependent on DNA Damage

Two different phosphatidylinositol 3-kinase-related kinases (PIKKs) control the pathways of DNA damage response in *Saccharomyces cerevisiae*: Tel1 and Mec1. Tel1 recruitment requires dsDNA and happens at blunt end double strand breaks (DSB), while Mec1 is recruited to ssDNA, at DSB with ends resected (further info in section 1.2.2.4) (Waterman et al., 2020). These kinases promote a signaling cascade that, through different other kinases and adaptor proteins end up activating Rad53, the effector kinase that promotes a transcriptional response that helps to restrain mitosis, promote other cell cycle arrests or delays, the stabilization of the replication fork and DNA repair (Waterman et al., 2020).

During S-phase, the intra-S checkpoint, also known as DNA replication checkpoint (DRC) is activated (Galanti & Pfander, 2018; D. R. Iyer & Rhind, 2017). The DRC is activated by stalled replication forks, for instance due to a depletion of nucleotides (Alcasabas et al., 2001; Pellicioli et al., 1999). After Mec1 activation, Mrc1 is the main adaptor protein that ends up in the activation of Rad53 (D. Iyer & Rhind, 2017). The DRC is using two different strategies to elongate the S-Phase: (1) inhibition of the DNA primase to delay replication initiation and elongation (Marini et al., 1997) and (2) inhibition of the firing of late replication origins (Donaldson et al., 1998).

The DNA damage checkpoint can be activated during G1, S and G2/M phases. During G1, DSB are repaired mainly using non-homologous end joining (NHEJ. Further information in section 1.2.2.5). The inhibition of resection at DSB sets Tel1 as the sensor kinase that starts the checkpoint activation (Waterman et al., 2020). Through the adaptor kinase Rad9, Rad53 is activated, which promotes the arrest of cells in G1 in the presence of DNA lesions (Siede et al., 1993, 1994; Toh & Lowndes, 2003). Rad53 phosphorylates Swi6 (in the SBF complex) to inhibit Cln1 and Cln2 transcription and arrest the cell in G1 (Sidorova & Breeden, 1997). This G1 extension is used by the cell to repair the DNA damage (Gerald et al., 2002).

Finally, during G2, the adaptor protein Rad9 is essential to achieve cell arrest, hence checkpoint activation (Waterman et al., 2020). Rad9 recruits Rad53 to the damaged locus and promotes its phosphorylation by Mec1, the sensor protein in this case (Emili, 1998; Gilbert et al., 2001).

1.1.4.2. The Spindle Assembly Checkpoint (SAC)

At the end of metaphase, chromosomes are positioned on the metaphase plate due to the equilibrium of forces applied by the spindle apparatus on each side of the

nucleus (Nicklas & Koch, 1969; Palmer et al., 1992). The spindle assembly checkpoint (SAC) tests whether this positioning of the chromosomes in metaphase is achieved by sensing the tension applied on the kinetochores (Li & Nicklas, 1995; Stern & Murray, 2001). A second parameter tested by the cell is the kinetochore occupancy by microtubules, which is a 1:1 proportion in budding yeast (Winey et al., 1995). Different proteins bind to kinetochores that are not attached to any microtubule, forming the mitotic checkpoint complex (MCC) (Funabiki & Wynne, 2013). The MCC interacts with Cdc20, inhibiting the activation of APC and, therefore, the advance into anaphase (Hwang et al., 1998). Binding of a microtubule to the kinetochore promotes the detachment of Mad1 and Mad2, proteins of the MCC (Funabiki & Wynne, 2013). In contrast, Bub1 remains attached to the kinetochore and is the responsible for the recruitment of Sgo1, the protein that plays the role of the tension sensor (Nerusheva et al., 2014). Sgo1 regulates Ipl1 (Aurora B) presence in centromeres, which performs a quality control on the interaction between the kinetochore and the microtubule (Hauf et al., 2003; Nerusheva et al., 2014). The correct microtubule occupancy of the kinetochores and the bioriented tension on the centromeres results in the advance into anaphase and the end of the cell cycle.

1.2. DNA Damage and Repair

DNA can be damaged, inducing the activation of DDC and repair pathways. The different kinds of DNA damage can be classified depending on the agent causing the damage or the method used by the cell to repair it.

1.2.1. Causes of DNA Damage

There are both endogenous and exogenous agents that cause DNA damage. Endogenously, replication itself has an intrinsic error rate as DNA polymerases introduce a base mismatch once every 10^4 to 10^6 nucleotides (Kunkel, 2009; McCulloch & Kunkel, 2008). Other than replication, different compounds produced by the cell may cause DNA damage too. The formation of reactive oxygen species (ROS) affects the DNA structure, modifying nitrogen bases and even generating strand breaks (Cooke et al., 2003; Dizdaroglu, 1992; Melvin et al., 1996) (Figure 3). Alkylating agents can modify the DNA (Holliday & Ho, 1998) leading to undesired modifications on nitrogen bases (de Bont, 2004) (Figure 3). Exogenous physical agents, such as ionizing radiation, can produce ROS, promoting strand breaks and nucleotide modifications (Borrego-Soto et al., 2015; Ray et al., 2012; Santivasi & Xia, 2014) (Figure 3). Exposure to ultraviolet (UV) light is also deleterious as promotes the production of ROS and the formation of intrastrand crosslinks, mostly between pyrimidine nucleotides (Mitchell & Karentz, 1993; Visser et al., 1999) (Figure 3). Finally, different chemical compounds can produce interstrand crosslinks and strand breaks (Deans & West, 2011) (Figure 3).

1.2.2. DNA Damage Repair Pathways

1.2.2.1. Mismatch Repair (MMR)

DNA mismatch repair (MMR) works to solve or avoid three different situations in eukaryotes. It is a pathway coupled to replication as it corrects the nucleotides misplaced by the DNA polymerase (Hombauer et al., 2011; Kolodner & Marsischky, 1999). It also works preventing genome rearrangements by avoiding the recombination between divergent DNA sequences (Datta et al., 1996) and participates in gene conversion, repairing mispaired bases during recombination intermediates formation (Kolodner & Marsischky, 1999) (Figure 3).

The MMR pathway starts with the recognition of a mismatch by one of the two MSH complexes: Msh2-Msh3 or Msh2-Msh6 (Kunkel & Erie, 2005). The first complex detects insertion-deletion loop mismatches of up to 17 nucleotides while the latter detects small insertion-deletion loop and base-base mismatches (Kunkel & Erie, 2005). The sensor MSH complex interacts with Mlh1-Mlh2, a complex with endonuclease activity that nicks the DNA (Kadyrov et al., 2006). At this point, the pathway is divided into three variants, a first one dependent on the exonuclease Exo1, a second one dependent on the nuclease Rad27 and a third variant dependent on nuclease activity of Mlh1-Mlh2 (Calil et al., 2021; P. T. Tran et al., 2001). The Rad27 activity is coupled to polymerase δ activity while in the other two pathways both polymerase δ and ε fill the gap generated by the nuclease in a sequential procedure (Bowen et al., 2013; Calil et al., 2021).

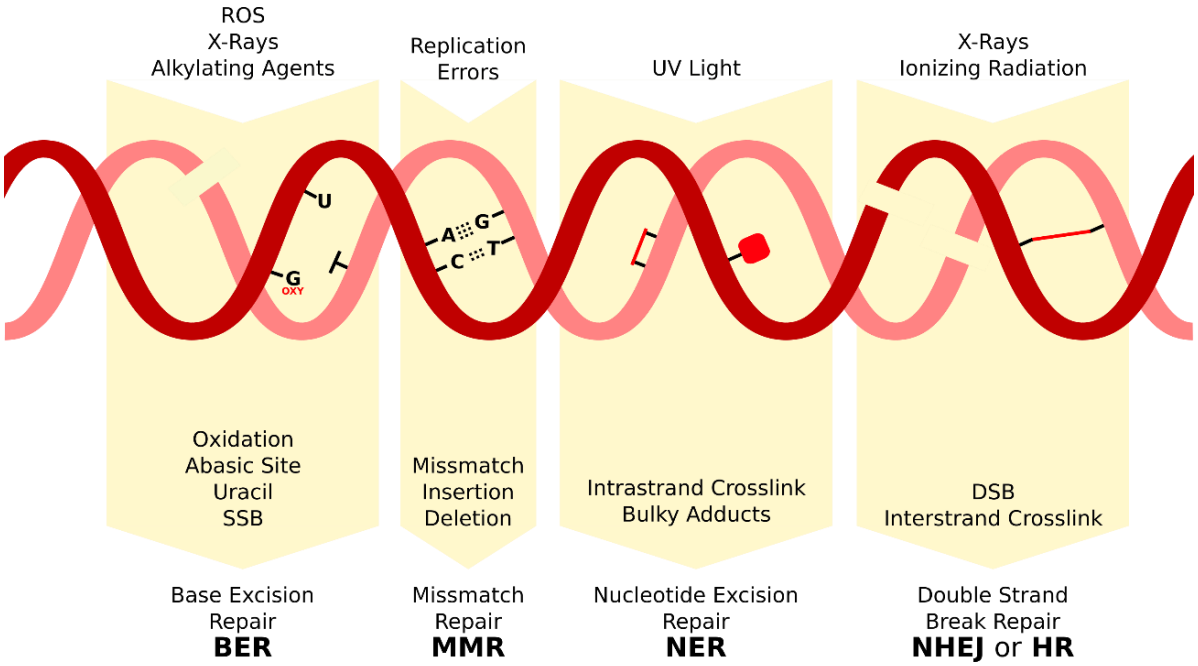

Figure 3. Causes, types and repair pathways of DNA damage. Scheme of the different types of DNA damage that can be found in a cell together with the agents causing it and the pathway that repairs it.
Image adapted from Dexheimer, 2014

1.2.2.2. Base Excision Repair (BER)

Cytosine deamination results in the transformation of the cytosine nitrogen base into an uracil. This transformation, leaves a guanosine-uracil pair in the DNA chain, which is a mismatch but does not distort the double helix structure. It was hypothesized that a nuclease could excise this uracil nucleotide. However, an uracil-DNA glycosylase was discovered to be responsible for the cleavage of the uracil nucleoside from the deoxyribose (Krokan & Bjoras, 2013; Lindahl, 1974). The nucleotide without the excised nitrogen base becomes an apurinic/apyrimidinic (AP) site. It is at this point that a nuclease, an AP-endonuclease, cuts at one site of the AP site. Then, a phosphodiesterase completes removes the remaining of the former nucleotide, a DNA polymerase refills the gap and a DNA ligase seals the repaired DNA strand (Dogliotti et al., 2001; Maclean et al., 2003) (Figure 3).

The BER pathway does not only repair cytosine to uracil transformations, but also repairs other base lesions caused by oxidation, alkylation or deamination (Dogliotti et al., 2001; Maclean et al., 2003; Robertson et al., 2009) (Figure 3). Also, there are two variants of this pathway, the long-patch and the short-patch (Dogliotti et al., 2001; Robertson et al., 2009). The short-patch excises and replaces a single nucleotide and uses DNA polymerase Pol4 and DNA ligase III (Robertson et al., 2009; Sterling & Sweasy, 2006). On the other hand, the long-patch pathway can replace multiple nucleotides and is dependent on the helicase Pol30 (PCNA) and the nuclease Rad27 (Greene et al., 1999; Robertson et al., 2009; van der Kemp et al., 2009), while Pol4 is not essential and uses the DNA ligase I (Dogliotti et al., 2001; Robertson et al., 2009).

1.2.2.3. Nucleotide Excision Repair (NER)

The nucleotide excision repair (NER) pathway is a versatile repair method that recognizes several different types of DNA damage. It solves problems with bulky DNA and helix-distorting lesions that negatively affect both transcription and DNA replication (Tatum & Li, 2011). For instance, UV-induced intrastrand pyrimidine dimers are repaired by NER (Figure 3). This pathway is characterized by the removal of a 25 to 30 nucleotide-long section of the DNA strand, containing the lesion, and the refill of this gap (Prakash & Prakash, 2000).

There are four nucleotide excision repair factors (NEF) involved in NER. The four NEF complexes contain Rad proteins, which are proteins that confer sensitivity to radiation when mutated. The NER pathway can detect DNA damage through two different methods that converge to the same repair system. The global genome repair (GGR) depends on the NEF4 (Rad7-Rad16) detection of the damage in an ATP-dependent manner. NEF4 uses its ATPase to move along the genome until finding the DNA damage, were it stalls and promotes the changes that recruit the other factors needed for NER (Guzder et al., 1998; Tatum & Li, 2011). The transcription coupled repair (TCR) is started upon RNA polymerase II stalling on the DNA and the recognition of the DNA damage by NEF2.

NEF2, formed by Rad4 and Rad23 binds to DNA damage independently of ATP and is also the factor recruited by NEF4, playing a role of tethering of NEF1 and NEF3 in GGR (Prakash & Prakash, 2000). The interaction between NEF2 and NEF4 is due to the interaction between Rad7 and Rad4 (Guzder et al., 1999) while its interaction with NEF1 and NEF3 is mediated by Rad23 and its interaction with Rad14 (in NEF1) and TFIIH (in NEF3). The damaged region of the DNA is excised during its repair in a three-step process. First, NEF3, constituted by a 6-subunit complex named TFIIH and Rad2 (Prakash & Prakash, 2000; Tatum & Li, 2011), is the helicase that unwinds the DNA upon finding of DNA damage (Egly & Coin, 2011). While the DNA strands are separated, the single stranded DNA (ssDNA) is protected by the replication protein A (RPA). Then, Rad2, belonging to NEF3, is the nuclease responsible for cutting the damaged DNA at its 3' end. Finally, NEF1, formed by Rad1-Rad10 and Rad14 (Guzder et al., 2006), cuts the 5' end of the damaged DNA portion thanks to the action of the Rad1-Rad10 endonuclease (Sung et al., 1993; Tomkinson et al., 1994). After the excision of the damaged DNA, polymerases δ or ε refill the created gap and Cdc9 ligates it, sealing the DNA strand (Tatum & Li, 2011; X. Wu et al., 1999).

1.2.2.4. Homologous Recombination (HR)

Homologous Recombination (HR) is a process that repairs double strand breaks (DSB) (Figure 3) and stalled replication forks. To do so, it requires a homologous sequence of the DNA in the genome, which is used as a template for repair. The requirement of the homologous DNA sequences restricts this pathway to S and G2 phases of the cell cycle, when an identical chromosome (the sister chromatid) is available for repair (Takata et al., 1998), although homologous recombination can also occur with non-sister DNAs. When a DSB is detected, the 5' end on each of the sides is resected leaving a 3' overhanging end. Then, the overhanging ends start the invasion of the homologous template strand and new DNA is polymerized from the invading 3' end. Homologous recombination results in formation of DNA recombination intermediates, which physically connect the two recombination products. Finally, different pathways can resolve these intermediates, separating two DNA molecules either with or without crossovers (U. Roy & Greene, 2021; San Filippo et al., 2008).

The first step on the DSB repair is the detection of DNA damage by Rad17 due to the γH2A (Qiu & Huang, 2021). Then, the resection of the 5' ends to expose the 3' end strand. This resection is divided in two steps, a short-range and a long-range resection (U. Roy & Greene, 2021). The responsible for the short-range resection is the Mre11-Rad50-Xrs2 (MRX) complex (Zhu et al., 2008). Afterwards, the helicase Sgs1-Top3-Rmi1 (STR) together with the exonucleases Exo1 or Dna2 resect the DNA at 4.4 Kb/h (Zhu et al., 2008). The whole resection process is coupled to RPA binding to the ssDNA, which is needed to stabilize and protect the ssDNA (U. Roy & Greene, 2021). Then, Rad51 displaces RPA and binds to the ssDNA in a process dependent on Rad55-Rad57, Rad52 and the SHU complex (Gaines et al., 2015; Sung, 1997). The Rad51-bound ssDNA is named presynaptic filament and presents a right-handed helicoidal shape

(Sung & Robberson, 1995). The presynaptic filament invades a double stranded DNA (dsDNA) in a process mediated by Rad54, a protein remodeler that transiently opens the dsDNA (without helicase activity) and changes its topology, facilitating the Rad51-coated ssDNA invasion (Crickard et al., 2020). The invading strand is elongated using the open dsDNA as template and ligated, generating a structure named Holliday junction (HJ) (Hiom, 2001; Holliday, 1964; I. Kobayashi & Ikeda, 1983).

Holliday junctions physically connect recombined sister chromatids, what avoids their segregation (Blanco et al., 2010). These intermediates have to be either dissolved or resolved, to allow separation of the two sister chromatids from one another. Dissolution is the most frequent pathway to separate the sister chromatids linked by HJs. STR plays a role again in HR as it is the complex responsible for HJ dissolution (Bizard & Hickson, 2014; Wyatt & West, 2014). The helicase Sgs1 promotes branch migration, a process through which the two HJs generated during HR are brought close together to an hemicatenate (Bizard & Hickson, 2014; L. Wu & Hickson, 2003). Then, the topoisomerase Top3 releases the hemicatenate, giving as a product the two sister chromatids repaired and without crossover (Bizard & Hickson, 2014; Plank et al., 2006). Rmi1, the third subunit of the STR complex, interacts with both Sgs1 and Top3 and, although it does not have any known catalytic function in HJs dissolution, it greatly stimulates the process (Raynard et al., 2006).

In eukaryotes, there is a canonical and a non-canonical pathway to resolve the HJs. The canonical pathway is mediated by the endonuclease Yen1 (Ip et al., 2008; Wyatt & West, 2014). The nuclease of the non-canonical pathway is Mus81 (Interthal & Heyer, 2000), a structure-specific endonuclease that works in tandem with the noncatalytic subunit Mms4 (Mullen et al., 2001) and forms the SLX-MUS complex with the nucleases Slx1 and Slx4 (Constantinou et al., 2002; West et al., 2015; Wyatt & West, 2014) . Both pathways have been described to produce both crossover and non-crossover products (West et al., 2015). This means that the DNA sequences at each side of the resolution can be both, coming from different original DNA molecules (crossover product) or coming from the same original molecule (non-crossover).

1.2.2.5. Non-Homologous End Joining (NHEJ)

Non-Homologous End Joining (NHEJ) is the method selected to repair DSB in the absence of a homologous sequence (Figure 3). This pathway is used in G1, as there is no sister chromatid for homologous recombination. In NHEJ, the KU heterodimer, formed by Yku70 and Yku80, binds to the dsDNA ends after the DSB (Arosio et al., 2002). This binding, protects the DNA ends from resection, mainly by Mre11, establishing the divergent point between HR and NHEJ repair (Sun et al., 2012). Some studies claim that MRX is also required for NHEJ as it bridges both DNA ends through an ATPase-dependent Rad50 binding (Zhang & Paull, 2005), while others discard any function of MRX on this pathway (Sun et al., 2012). In any case, XRCC4/LigIV complexes (DNA Ligase IV) bind to the KU-protected DNA ends. DNA ligase IV pairs the DNA ends and

ligate them (Reid et al., 2015). This process entails a high risk of loss of information as there are small deletions at the site where the repair takes place (Heidenreich et al., 2003).

1.2.3. Stalling of the Replication Fork and its Bypass

DNA lesions may arrest replication forks, especially if found on the leading strand (Marians, 2018). The presence of DNA damage uncouples the DNA polymerase from the helicase. The stalled replisome at the leading strand does not avoid the unwinding of DNA, what leaves ssDNA ahead of the replisome, while the lagging strand continues to replicate. The single stranded DNA is coated with RPA, which protects it from degradation and is the signal that activates the S-Phase DNA damage checkpoint (Sogo et al., 2002). On the other hand, if the lesion is found on the lagging strand, replication may continue as long as the helicase can unwind the DNA. The priming procedure by polymerase α and the possibility to bind a new polymerase δ on the next Okazaki fragment, avoids the stoppage of replication (Marians, 2018; McInerney & O'Donnell, 2004) (Figure 4). In the case that a replication fork remains stalled for a prolonged period of time and the replisome decouples, it may finally collapse, leading to DNA damage and the formation of DSBs (Cortez, 2015).

The first possible option to overcome the stalling of the replication fork is the activation of trans-lesion synthesis (TLS) (Figure 4). For example, when the replisome stalls due to UV-induced damage or AP sites and the polymerase decouples, polymerase ζ (Rev3-Rev7) can bind to the replisome and place a nucleotide opposite to the lesion (Stone et al., 2011). Due to the low fidelity of DNA polymerase ζ, this may lead to the introduction of mutations. Importantly, this mechanism allow replication to continue, bypassing the lesion, but does not repair the damage on DNA.

Another lesion bypass pathway used to solve the stalling of the replication fork is template switching (Figure 4). The lesion on the leading strand stalls polymerase ε, but permits the unwinding of the DNA (Marians, 2018), which means that replication of the lagging strand continues. A ssDNA gap is generated in the leading strand, due to the lack of advance of the replication (Figure 4). In this situation, the strand with stalled replication invades the newly synthesized lagging strand. This invasion is mediated by Rad5, which unwinds the leading strand with its helicase activity (Shin et al., 2018). This process generates a reversal of the replication fork, permitting the use of the newly synthesized lagging strand as a template for the synthesis of the leading strand by polymerase δ (Marians, 2018) (Figure 4). As a result of template switching, a double Holiday junction is generated and STR is responsible for its resolution (Giannattasio et al., 2014). Interestingly, the dichotomy between TLS and template switching depends on the ubiquitination of the DNA polymerase sliding clamp (known as PCNA or Pol30 in budding yeast). Monoubiquitylation of PCNA by Rad6-Rad18 activates the mutagenic trans-lesion pathway (Chatterjee & Siede, 2013; Stelter & Ulrich, 2003), while

polyubiquitylation of the sliding clamp, mediated by Mms2-Ubc13-Rad5, directs the stalled replication fork towards template switch (Broomfield et al., 1998; Chatterjee & Siede, 2013).

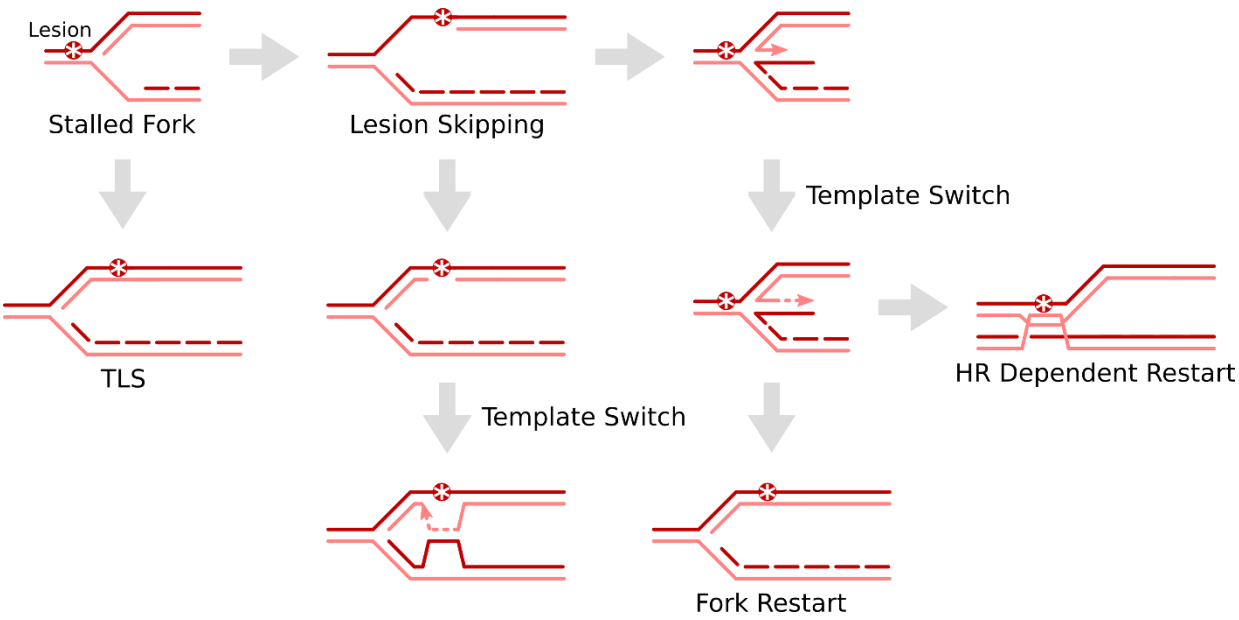

Figure 4. Stalled fork remodeling and repair. Scheme of the pathways through which a stalled replication fork is either bypassed or repaired.

Image adapted from Marians, 2018

1.3. The Structural Maintenance of Chromosomes Complexes

The Structural Maintenance of Chromosomes (SMC) is a family of protein complexes conserved from prokaryotes to eukaryotes. All of them display a similar architecture and participate in sister chromatid segregation by organizing chromosomes.

1.3.1. SMC Proteins and Structure of the SMC Complexes

The structural maintenance of chromosome proteins display a well conserved structure, present both in prokaryotes (Melby et al., 1998) and eukaryotes (Haering et al., 2002). SMCs are long proteins of over 1000 amino acids with 5 differentiated domains: two globular domains (containing Walker A and B motifs) at both ends of the protein, connected by two coiled coils to a central hinge domain (Melby et al., 1998) (Figure 5A). The long coiled-coil domains, at each side of the hinge domain, interact with each other in an antiparallel fashion, leaving the Walker domains in close proximity at one end of a rod-shaped SMC protein, and the hinge domain at the other end (Haering et al., 2002; Soh et al., 2015) (Figure 5B).

The SMC proteins heterodimerize through the hinge domain (Haering et al., 2002; M. Hirano, 2001). These heterodimers are formed by established pairs and bind other subunits to form active SMC complexes. The complex containing the Smc1/3 heterodimer is called cohesin, the one containing Smc2/4 is called condensin and the last SMC complex in yeast has no name other than the Smc5/6 complex (Figure 5C). All SMC complexes have a kleisin subunit that interacts through its N-terminal end with the coiled-coil domain of one of the SMC proteins in the heterodimer and through its C-terminal domain with the globular domain of the other SMC subunit of the heterodimer (Gruber et al., 2003; Hu et al., 2005; Nasmyth & Haering, 2005). Finally, different subunits bind to this structure to form the SMC complexes. These subunits are divided into two groups, the HAWK (HEAT proteins associated with kleisin) and the KITE (kleisin interacting winged-helix tandem elements) proteins (J. J. Palecek & Gruber, 2015; Wells et al., 2017). The kleisin subunit of cohesin is Scc1 and Scc3 is the only other permanent subunit in the complex (Toth et al., 1999). Other proteins can bind cohesin modulating its function and the binding of the complex to chromatin: Wpl1, Scc2-4, Pds5 (Lopez-Serra et al., 2013; Petela et al., 2018; N. Wu & Yu, 2012) (Figure 5C). Brn1 is the kleisin subunit in condensin, which is composed by two other subunits, Ycg1 and Ycs4 (Freeman et al., 2000; Ouspenski et al., 2000) (Figure 5C). The kleisin in the Smc5/6 complex is Nse4, which belongs to a group of 6 subunits in the complex named Non-SMC Elements (Nse1 to 6) (Duan, Yang, et al., 2009; Hu et al., 2005; Zhao & Blobel, 2005) (Figure 5C).

The two SMC proteins in the heterodimer are coupled in an antiparallel manner that generates a complete ABC type ATPase on the combination of both globular domains (Löwe et al., 2001). The ABC ATPases are a family of ATPases with a series of common motifs: Walker A (GXXGXGKS/T), Walker B and signature motif (starting with LSGGQ) (Holland & Blight, 1999). The globular domain on each SMC protein of the heterodimer binds an ATP molecule to the Walker A motif, also called phosphate-binding loop. Then, the signature motif on each protein recognizes the binding of ATP to the Walker domains of its counterpart, what promotes the dimerization of the globular domains. The dimerization of the heads together with the binding of DNA to the hinge, promotes a conformational change on the coiled-coils and the formation of two different compartments into the complex, one between the hinge and the globular domains and the other between the globular domains and the kleisin subunit (Soh et al., 2015; Yatskevich et al., 2019). The dimerization of the globular domains of the SMC subunits also activates a coordinated hydrolysis of ATP at both subunits of the heterodimer (Arumugam et al., 2003; T. Hirano, 2002; Holland & Blight, 1999). The hydrolysis of ATP promotes the globular domains disengagement, switching the conformation of the heterodimer from a ring to an inverted V shape that has a single space from the hinge to the kleisin (Yatskevich et al., 2019). Exists a second type of conformational change of the coiled-coils at the elbow (or joint), a region where their helical structure is broken. Hinges approach to the globular domains by the bending of the elbow (Bürmann et al., 2019).

The SMC complexes can entrap DNA topologically into their lumen. It was proposed that the entry gate of the DNA into the lumen of the complex lumen could be the hinge domain (Gruber et al., 2006). However, other models have been proposed in which the DNA is entrapped due to the opening of the ATPase globular domains (Higashi et al., 2020).

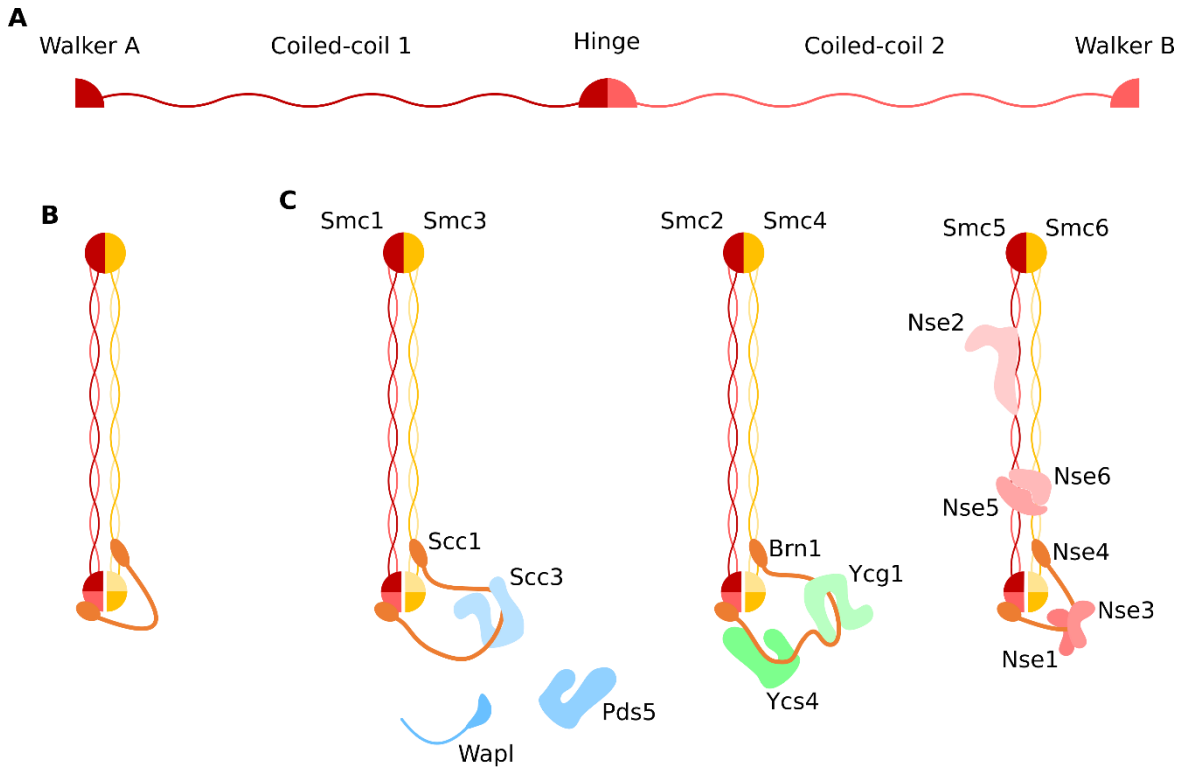

Figure 5. SMC proteins and complexes. Scheme of **(A)** the domains in SMC proteins, **(B)** the trimeric ring formed by the SMC heterodimer and the kleisin subunit, and **(C)** the budding yeast SMC complexes: cohesin, condensin and Smc5/6.

The SMC complexes play different roles on avoiding genomic instability, thus permitting the correct transmission of the genomic information to the offspring. During the cell cycle, the DNA is replicated and segregated. During all this process, DNA can be damaged and the resulting lesions are removed using different repair pathways. The Smc5/6 complex plays a role on the dissolution of intermediate products with sister chromatid linkages (Bermúdez-López et al., 2010; Bermúdez-López & Aragon, 2016). Just before its segregation, the DNA is transiently condensed, an essential role for the correct chromosome segregation that is achieved by condensin (T. Hirano & Mitchison, 1994; Strunnikov et al., 1995; Vas et al., 2007). Afterwards, the condensed chromosomes are positioned on the metaphase central plate by an equilibrated tension applied to the centromere of each sister chromatid. Cohesin is the responsible to avoid the separation of the sister chromatids at this point (Guacci et al., 1997; Michaelis et al., 1997). Other than the classical functions of the SMC complexes, novel properties have

been described afterwards, for instance cohesin works on DNA damage repair (Litwin et al., 2018) and participates on the regulation of transcription (Dorsett & Merkenschlager, 2013).

1.3.2. Roles of the SMC Complexes and Loop Extrusion

Loop extrusion consists on the binding of an SMC complex to a small loop and the active enlargement of the loop until reaching a position that blocks the advancement of the complex (Hassler et al., 2018). *In vitro*, this process is mediated by ATP hydrolysis in cohesin and condensin (Davidson et al., 2019; Ganji et al., 2018). *In vivo*, the loop extrusion mediated by cohesin permits the organization of the genome into topologically associated domains (TADs) (de Wit et al., 2015; Fudenberg et al., 2016; Wutz et al., 2017). This organization permits a better interaction between sequences that belong to the same TAD. In the case of the bacterial SMC, a model proposes that loop extrusion could explain the role of the complex at the origin of replication separating the two arms of the replication fork just after their replication (Davidson & Peters, 2021; Karaboja et al., 2021).

Different models could explain the loop extrusion mechanistic, however there are two main models, the one-sided, related to condensin, and the two-sided, related to condensin (Banigan et al., 2020; Higashi & Uhlmann, 2022; E. Kim et al., 2020). On the two-sided model, the DNA is topologically entrapped into the SMC complex and DNA at both sides, upstream and downstream of the entrapment site, is pumped through the complex (Banigan et al., 2020; Hassler et al., 2018). In contrast, the one-sided model requires at least one anchor point of the complex onto the DNA and the ATPase activity as a motor that pumps the DNA at the other side, entrapping DNA from only one of the sides into the loop (Banigan et al., 2020; Hassler et al., 2018).

Recent studies on loop extrusion performed on cohesin of both budding yeast and mammals, have revealed a mechanism dependent on the bending of the elbows at the coiled-coils in an ATP-independent manner (Bauer et al., 2021; Higashi et al., 2021). This bending of the coiled-coils of Smc1/3 permits the transfer of the DNA between the hinge and the ATPase heads. Although the mechanisms differ on their details, the general idea of a spontaneous swinging of the hinge mediating the loop extrusion in cohesin is shared.

Condensin loop size is connected to that of other loops on the same DNA substrate. When a new loop is created, it can shrink a previously formed loop, indicating that DNA can move backwards during extrusion (E. Kim et al., 2020). Moreover, condensin loops can traverse each other. These observations are important since they could explain the condensation levels of chromosomes during mitosis. A simple loop extrusion model would generate a structure less compacted.

The Smc5/6 complex can compact DNA *in vitro*, shortening its length (Gutierrez-Escribano et al., 2020; Serrano et al., 2020). However, remains unknown whether this complex can perform loop extrusion or achieves DNA compaction through other similar mechanisms.

1.3.3. The Smc5/6 Complex

The Smc5/6 complex was first described in 2000 in the fission yeast *Schizosaccharomyces pombe* (Fousteri & Lehmann, 2000). Rad18 (homologous to Smc6 in budding yeast) was purified as part of a six-subunit complex, being one of the two proteins in the heterodimeric core together with Spr18 (SMC partner of Rad18). In *Saccharomyces cerevisiae* it is described as an 8-subunit complex with different functions, mostly related to recombinational DNA repair and chromosome disjunction. Interestingly, the components of this complex are essential in yeast (Aragón, 2018). Similar functions have been reported to be responsibility of Smc5/6 in mammalians, including repair, chromosome replication, recombination and chromosome segregation (Gómez et al., 2013; N. Wu & Yu, 2012). Moreover, it has also been related to cellular immunity, preventing the replication of Hepatitis B virus DNA (Livingston et al., 2017).

1.3.3.1. Structure of the Smc5/6 Complex

The Smc5/6 complex is composed of 8 subunits, the two SMC proteins and 6 non-SMC elements, Nse1 to 6. The SMC proteins in the complex, Smc5 and Smc6, form a heterodimer, interacting through their hinge domains, as described for other SMC complexes. However, this hinge domain has two differential characteristics: a latch-like domain on Smc5 that interacts with Smc6 and stabilizes the dimerization of the two subunits and the capability to interact with ssDNA (Alt et al., 2017). The coiled-coil domains of Smc5 and Smc6 are also more divergent from those in the other SMC proteins. These domains in the Smc5/6 complex present a thicker region in the middle, containing the elbow that is still unclear whether it can bend like other SMC complexes (Gutierrez-Escribano et al., 2020) or it presents a stiffer configuration (Hallett et al., 2021).

The possible stiffness of the coiled-coil domains of Smc5 and Smc6 might be due to the high occupancy of non-SMC proteins in comparison to the free coiled-coil domains in cohesin and condensin (Yu et al., 2021). The first of the non-SMC proteins interacting with the coiled-coil region of Smc5/6 is Nse2, also known as Mms21, which interacts with the coiled-coil of Smc5 through its N-terminal domain (Duan, Sarangi, et al., 2009; Sergeant et al., 2005). Also, Nse5 and Nse6 form a subcomplex that interacts with lower regions of the coiled-coils, close to the globular heads (J. Palecek et al., 2006). Altogether, Nse2 and Nse5/6 cover a large fraction of the coiled-coil length and leave free the region next to the hinge domain of Smc5/6.

The kleisin subunit of the Smc5/6 complex is Nse4, also known as Qri2, which bridges the globular head domains of Smc5 and Smc6 (J. Palecek et al., 2006). This kleisin subunit forms a subcomplex with two other proteins: Nse1 and Nse3 (Sergeant et al., 2005), two KITE subunits structurally related to the non-SMC components of the prokaryotic condensing complex (J. J. Palecek & Gruber, 2015). This feature makes the Smc5/6 complex different to the other two SMC complexes in *Saccharomyces cerevisiae*, both cohesin and condensin non-SMC subunits belong to the HAWK group (Wells et al., 2017).

Finally, the ATPase heads of Smc5 and Smc6 are similar to those in the other SMC complexes. The ATPase activity of the two SMC subunits is essential for the interaction of the complex with DNA (Kanno et al., 2015; Taschner et al., 2021). The binding of ATP to Smc6 is required for the interactions of the complex with DNA *in vivo* (Kanno et al., 2015) while dimerization of the head domains of the SMC heterodimer is required for those interactions *in vitro* (Taschner et al., 2021).

1.3.3.2. Functions of the non-SMC Subunits in Smc5/6

The functionality of the non-SMC subunits in Smc5/6 is also differential in comparison to cohesin and condensin. Smc5/6 is the only SMC complex in budding yeast that has 2 subunits with enzymatic capability other than the ATPase of the SMC subunits. Nse1 contains a RING domain that permits an E3 ubiquitin ligase activity, stimulated by Nse3 (Doyle et al., 2010; Kolesar et al., 2022). Nse2, the subunit bound to the coiled-coil of Smc5 coiled-coil, is a SUMO-ligase activated by the interaction between the coiled-coil of Smc5 and ssDNA (Andrews et al., 2005; Varejão et al., 2018).

The Nse5/6 subcomplex has an inhibitory effect on the ATPase of the Smc5/6 heterodimer *in vitro* (Hallett et al., 2021; Taschner et al., 2021). This inhibition is due to the obstruction of the SMC globular domains dimerization upon ATP binding due to the location of the Nse5/6 subcomplex in between of the SMC ATPase heads (Taschner et al., 2021). The inhibitory effect of the Nse5/6 complex on the ATPase is lost in the presence of DNA, which is an enhancer of the ATPase activity of the Smc5/6 complex (Hallett et al., 2021; Taschner et al., 2021). These non-SMC subunits do not have the ability to interact with DNA (Hallett et al., 2021). However, they can work as a bridge for the recruitment of Smc5/6 to chromatin mediated by Rtt107, a protein recruited to γH2A, an indicator of the presence of DSB on DNA. Nse6 can interact with Rtt107 through its N-terminal end and promote the recruitment of Smc5/6 to the damaged location (Li et al., 2012; Wan et al., 2019; Williams et al., 2010). On the other hand, Nse5, which binds to Smc5 in a position proximal to Nse2, is an enhancer of the Nse2-mediated sumoylation of Smc5 and Smc6 (Bermúdez-López et al., 2015; Bustard et al., 2012). Additionally, Nse5 is essential for the integrity of the Smc5/6 complex *in vivo*, which is needed for the recruitment and repair of stalled replication forks (Bustard et al., 2012).

The Nse1/3/4 subcomplex is most probably required for the interaction of the Smc5/6 complex with chromatin (Moradi-Fard et al., 2016, 2021; Zabrady et al., 2016).

Nse3 contains a winged-helix (WH) domain that interacts with DNA (Zabrady et al., 2016), which explains the role of the Nse1/3/4 subcomplex. More specifically, Nse3 has been described to be important for the recruitment of the Smc5/6 complex to telomeres (Moradi-Fard et al., 2016) and the IGS regions in the rDNA (Moradi-Fard et al., 2021). The KITE subunits Nse1 and Nse3 are also responsible for a change on the kleisin subunit stiffness and conformation in the presence or absence of ATP bound to the SMC subunits of the complex (Vondrova et al., 2020). This role of the KITE subunits is key on permitting the interaction between Nse4 and the coiled-coil of Smc6. Upon binding of ATP to the SMC head domains, Nse4 detaches from the coiled-coil of Smc6 and permits the dimerization of the ATPase heads. (Vondrova et al., 2020).

1.3.3.3. The Smc5/6 Complex on Replication and Fork Remodeling

During DNA replication, the encounter of DNA damage with the replisome causes fork stalling, which mostly happens at the leading strand. If stalling is prolonged in time, the fork collapses and has to be remodeled to restart replication. It has been described in multiple occasions that Smc5/6 dysfunction promotes the accumulation of sister chromatid junctions coming from collapsed replication forks remodeling, also named X-shaped molecules (Bermúdez-López et al., 2010; Choi et al., 2010; Torres-Rosell, Machín, et al., 2005). The mutation of the helicase activity of Mph1, the helicase involved in remodeling of the collapsed fork (Scheller et al., 2000; Schurer, 2004), alleviates the phenotype of Smc5/6 complex mutant strains, as it inhibits the formation of sister chromatid junctions by Mph1 (Chen et al., 2009). The inhibition of the formation of X-shaped structures is due to direct binding of Smc5 to Mph1 (Xue et al., 2014).

During DNA replication, topological stress accumulates on DNA and has to be removed by topoisomerases. The Smc5/6 complex can interact with Top2. This interaction and the ATPase activity of Smc5 is required by Top2 to catenate DNA (Kanno et al., 2015). In the absence of an active Top2, Smc5/6 is accumulated on chromatin, indicating the formation of sister chromatid junctions after generation of topological stress (Jeppsson et al., 2014).

1.3.3.4. Roles of Smc5/6 on Ribosomal DNA

The replication of the ribosomal DNA (rDNA) encoding region has special characteristics. This region is constituted by approximately 150 tandem repeats of the *RDN1* locus of 9,1 Kb each (T. Kobayashi et al., 1998). This locus is well-characterized and contains two intergenic regions, IGS1 and IGS2, and two coding regions, one encoding for the ribosomal 35S RNA and the other for the ribosomal 5S RNA (Egidi et al., 2020). Two different structures are present in the IGSs of the rDNA, an ARS (rARS) is located in IGS2 (Skryabin et al., 1984) and a barrier for replication named replication fork block (RFB) is present in the 5' end of IGS1 (Brewer & Fangman, 1988; T. Kobayashi et al., 1992). Three different RNA polymerases transcribe this region, RNA polymerase I transcribes the 35S RNA while RNA polymerase III transcribes the 5S RNA in the opposite direction (Klemenz & Geiduschek, 1980); RNA polymerase II has a low

transcriptional activity on the intergenic regions (Mayan & Aragón, 2010). Replication in the rDNA starts at the rARS, in one every three copies of the locus (Egidi et al., 2020), in a bidirectional manner. When the replication fork reaches the RFB, upstream of its position, it stops to avoid collisions with the transcribing RNA Pol I (Brewer & Fangman, 1988). The replication fork advancing downstream, co-directionally with RNA Pol I arrives to the stalled fork of the next rDNA unit and can fuse with it, terminating the replication of one rDNA repeat (Egidi et al., 2020). An important protein binding to the RFB is Fob1, which is involved not only in replication fork arrest, but also in regulation of recombination events occurring at the rDNA and modulation of gene expression (Buck et al., 2016; Johzuka & Horiuchi, 2002; T. Kobayashi et al., 1998; T. Kobayashi & Horiuchi, 1996; Stegmeier et al., 2004).

The ribosomal DNA is an especially vulnerable region in the genome. Thus, one of the first roles found for the Smc5/6 complex was on maintaining the stability of the rDNA. Smc5/6 complex mutants display a phenotype in which nucleolar integrity is compromised without activation of any DNA damage dependent checkpoint (Torres-Rosell, Machin, et al., 2005). In fact, the Smc5/6 complex is required for disjunction of the rDNA locus and its telomeric side (Torres-Rosell, Machín, et al., 2005). rDNA missegregation in Smc5/6 mutants is due to the accumulation of recombination and replication intermediates (Torres-Rosell, de Piccoli, et al., 2007; Torres-Rosell, Machín, et al., 2005). Smc5/6 mutants suffer from excessive recombination (Torres-Rosell, de Piccoli, et al., 2007; Torres-Rosell, Machín, et al., 2005). In addition, Smc5/6 participates in rDNA stability by preventing homologous recombination in the nucleolus (Torres-Rosell, Sunjevaric, et al., 2007). The Smc5/6 complex promotes the translocation of the heterochromatic DSBs for proper repair. At the same time, the complex maintains the stalled replication fork in a recombination-competent conformation (Irmisch et al., 2009). This translocation is dependent on the SUMO-ligase activity of the complex (Whalen et al., 2020).

1.3.3.5. Roles of the Smc5/6 on Homologous Recombination Intermediates Removal

Homologous recombination is the method selected by the cell to repair DSB after replication, when homologous DNA molecules are present. The accumulation of structures derived from homologous recombination in cells without a functional Smc5/6 results in a loss of cell viability (Torres-Rosell, Machín, et al., 2005). The relation between Smc5/6 and homologous recombination becomes patent upon deletion of proteins related to this pathway, which reverts the phenotype of the Smc5/6 mutants (Aragón, 2018). Moreover, the complex binds to DNA around DSB in a process mediated by Mre11, a subunit of the MRX complex (de Piccoli et al., 2006; Lindroos et al., 2006). This interaction of Smc5/6 with DNA enhances its sumo-ligase activity and Smc5 is sumoylated (Varejão et al., 2018). STR, the complex responsible for the long-term resection in HR, is able to specifically recognize and bind to sumoylated Smc5/6 (Bermúdez-López & Aragon, 2016).

1.3.3.6. Localization of the Smc5/6 Complex on DNA Along the Cell Cycle

There are several studies that have performed chromatin immunoprecipitation of the Smc5/6 complex under different circumstances. These publications indicate that the complex has a low interaction with chromatin during G1 (Kanno et al., 2015; Lindroos et al., 2006). In fact, telomeres are the only constitutive binding region for Smc5 along the whole cell cycle (Lindroos et al., 2006). During S-Phase, in the presence of replicative stress, binding is observed around early firing origins, indicating the loading of the complex to a region just after its replication (Lindroos et al., 2006). Finally, binding of the complex to centromeres and the telomeric side of the rDNA can be observed during G2/M (Lindroos et al., 2006; Torres-Rosell, Machín, et al., 2005). The binding profile of Smc6 in these studies is largely coincident with that of the kleisin subunit of cohesin, Scc1.

1.3.3.7. Functions of the Smc5/6 Complex on Telomeres

The telomeres, located at the end of chromosomes are clustered in 6 to 8 loci next to the nuclear envelope in a region with exclusion of HR in a Sir4 dependent manner (Simon et al., 2016). This clustering displays problems in strains bearing mutant alleles of Nse2 and Nse3 (Moradi-Fard et al., 2016). These problems are related to the relation between Sir4 and the two NSE proteins. In the presence of both mutants, Sir4 displays a disperse localization, which in case of the Nse2 mutant is accompanied by lower sumoylation levels (Moradi-Fard et al., 2016). The other way around, Smc5/6 localization on telomeres is dependent on the presence of Sir4 (Moradi-Fard et al., 2021). Regarding telomere integrity, the Smc5/6 complex plays a role on maintaining a stable telomere length (Moradi-Fard et al., 2021)

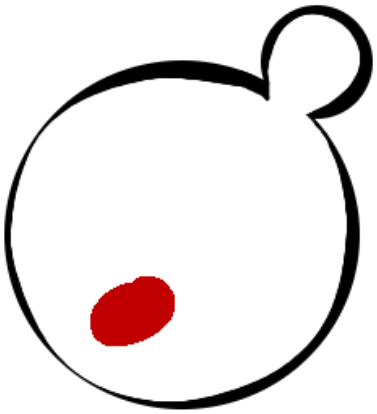

2 OBJECTIVES

2. OBJECTIVES

The Smc5/6 complex is essential to prevent the accumulation of sister chromatid junctions at the rDNA, thus ensuring chromosome segregation (Aragón, 2018). One of the many mechanisms underlying this function is the ability of the complex to interact with and organize chromatin fibers. In all SMC complexes studied so far, the latter depends on the ATPase activity of their head domains. ATP binding and hydrolysis induces sequential conformational changes in SMC complexes, allowing them to dynamically associate with chromatin, in a series of unknown molecular events that promote loop extrusion and ultimately alter the topological organization of chromosomes.

In this work, we aimed to get a better understanding of the chromatin association of the Smc5/6 complex and the roles of its ATPase head domains in sister chromatid disjunction and cell survival. For these reasons, we set the following objectives:

First. To analyze the molecular requirements for the association of the Smc5/6 complex with chromatin.

Second. To determine the loading sites of the Smc5/6 complex on the yeast genome.

Third. To study the role of the Smc5/6 ATPase cycle and the symmetry in each SMC head domain on chromatin association, cell growth, and chromosome segregation.

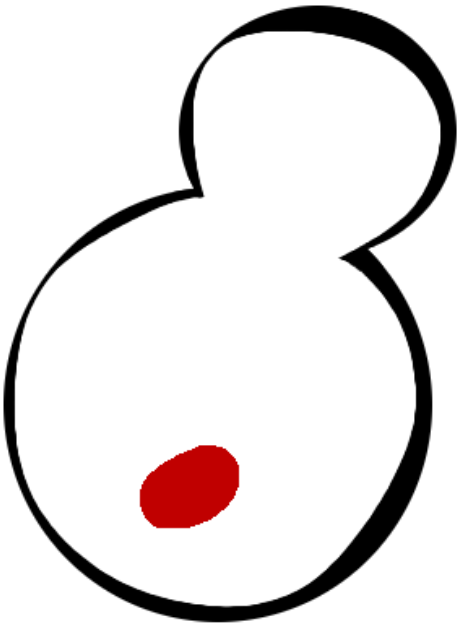

3 MATERIALS AND METHODS

3. MATERIALS AND METHODS

3.1. Yeast Methods

3.1.1. Strains

Table containing the strains used for the completion of this work together with their genotypes.

Strain	Background	Genotype	Source
	AS499	*MATa bar1Δ leu2-3,112 ura3-52 his3Δ200 trp1Δ63 ade2-1 lys2-801 pep4*	A.Strunnikov
	BY4733	*MATa his3Δ1 leu2Δ0 met15Δ0 ura3Δ0*	
	BY5563	*MATalpha can1Δ::MFA1pr-HIS3 lyp1Δ ura3Δ0 leu2Δ0 his3Δ1 met15Δ0*	
	SY2080	*HKY579-10A MATa bar1Δ leu2-3,112 trp1-1 can1-100 ura3-1 ade2-1 his3-11,15 RAD5+*	E.Nadal
	W303	*MATa leu2-3,112 trp1-1 can1-100 ura3-1 ade2-1 his3-11,15*	J.A.Tercero
YTR172	AS499	*TetR-YFP:ADE2 TetO(5.6Kb):487Kb:ChrXII:HIS3 smc6-9:NAT*	Lab Collection
YTR969	AS499	*TetR-YFP:ADE2 TetO(5.6Kb):487Kb:ChrXII:HIS3 smc5-6:NAT*	Lab Collection
YTR1100	AS499	*nse5-1-9MYC:TRP SMC5-6HA:HIS3*	Lab Collection
YMB1345	AS499	*nse3-ts2-9MYC:TRP1 6HF-SMT3:KanMX SMC5-6HA:hph*	Lab Collection
YTR1372	W303	*ura3-1::ADH1-OsTIR1-9Myc:URA3 smc5-AID:KanMX*	Lab Collection
YTR1428	AS499	*SMC5-6HA:HIS3 6HF-SMT3:hph*	Lab Collection
YTR1437	AS499	*TetR-YFP:ADE2 TetO(5.6Kb):487Kb:ChrXII:HIS3 ura3-1::ADH1-OsTIR1-9Myc:URA3 smc5-AID:KanMX*	Lab Collection
YMB1452	AS499	*ura3-1::ADH1-OsTIR1-9Myc:URA3 nse4-AID:KanMX 6HF-SMT3:hph SMC5-6HA:HIS3*	Lab Collection
YMB1905	BY4733	*bar1::URA3 GALp-3HA-SMC5:KanMX 6HF-SMT3:hph NSE4-6HA:NAT*	Lab Collection
YMB1937	BY4733	*bar1::URA3 GALp-3HA-SMC5:KanMX 6HF-SMT3:hph NSE4-6HA:NAT pADH1p-SMC5:9Myc:TRP1*	Lab Collection
YMB1938	BY4733	*bar1::URA3 GALp-3HA-SMC5:KanMX 6HF-SMT3:hph NSE4-6HA:NAT pADH1p-smc5(K75I):9Myc:TRP1*	Lab Collection
YSI3497	BY5563	*SMC5-6HA:NAT 6HF-SMT3:hph*	Lab Collection

Strain	Background	Genotype	Source
YSI3501	BY5563	*SMC5-6HA:NAT 6HF-SMT3:hph mms2::KanMX*	Lab Collection
YSI3528	BY5563	*SMC5-6HA:NAT 6HF-SMT3:hph sgs1::KanMX4*	Lab Collection
YSI3531	BY5563	*SMC5-6HA:NAT 6HF-SMT3:hph rad5::KanMX4*	Lab Collection
YSI3582	BY5563	*SMC5-6HA:NAT 6HF-SMT3:hph rad52::KanMX4*	Lab Collection
YSI3588	BY5563	*SMC5-6HA:NAT 6HF-SMT3:hph mms4::KanMX4*	Lab Collection
YTR3690	BY4733	*bar1::URA3 GALp-3HA-SMC5:KanMX 6HF-SMT3:hph NSE4-6HA:NAT pADH1p-smc5(E1015Q):9myc:TRP1*	Lab Collection
YTR3691	BY4733	*bar1::URA3 GALp-3HA-SMC5:KanMX 6HF-SMT3:hph NSE4-6HA:NAT pADH1p-smc5(S987R):9myc:TRP1*	Lab Collection
YTR3713	BY4733	*GALp-3HA-SMC6:HIS3*	This Study
YTR3714	BY4733	*GALp-3HA-SMC6:HIS pSMC6:URA3*	This Study
YTR3715	BY4733	*GALp-3HA-SMC6:HIS psmc6(D1047A):URA3*	This Study
YTR3716	BY4733	*GALp-3HA-SMC6:HIS psmc6(S1020R):URA3*	This Study
YTR3717	BY4733	*GALp-3HA-SMC6:HIS psmc6(E1048Q):URA3*	This Study
YMT3971	W303	*ura3-1::ADH1-OsTIR1-9Myc:URA3 SMC5-6HA:TRP1:smc5-AID:KanMX*	This Study
YMT4013	W303	*ura3-1::ADH1-OsTIR1-9Myc:URA3 smc5(E1015Q)-6HA:TRP1:smc5-AID:KanMX*	This Study
YMT4046	W303	*ura3-1::ADH1-OsTIR1-9Myc:URA3 smc5(D1014A)-6HA:TRP1:smc5-AID:KanMX*	This Study
YMT4106	W303	*ADH1-OsTIR1-9Myc:URA3 SMC5-6HA:TRP1:smc5-AID:KanMX HTB2-mCherry:hph*	This Study
YMT4270	AS499	*TetR-YFP:ADE2 TetO(5.6Kb):487Kb:ChrXII:HIS3 ADH1-OsTIR1-9Myc:URA3 SMC5-6HA:TRP1:smc5-AID:KanMX*	This Study
YMT4272	AS499	*TetR-YFP:ADE2 TetO(5.6Kb):487Kb:ChrXII:HIS3 ADH1-OsTIR1-9Myc:URA3 smc5(D1014A)-6HA:TRP1:smc5-AID:KanMX*	This Study
YMT4656	AS499	*TetR-YFP:ADE2 TetO(5.6Kb):487Kb:ChrXII:HIS3 ADH1-OsTIR1-9Myc:URA3 smc5(E1015Q)-6HA:TRP:smc5-AID:kanMX*	This Study
YMT4799	AS499	*TetR-YFP:ADE2 TetO(5.6Kb):487Kb:ChrXII:HIS3 smc6-9:NAT pSMC6:URA3*	This Study
YMT4800	AS499	*TetR-YFP:ADE2 TetO(5.6Kb):487Kb:ChrXII:HIS3 smc6-9:NAT psmc6(E1048Q):URA3*	This Study
YMT4890	AS499	*TetR-YFP:ADE2 TetO(5.6Kb):487Kb:ChrXII:HIS3 SMC5-6HA:TRP1:smc5-6:NAT*	This Study

Strain	Background	Genotype	Source
YMT4892	AS499	*TetR-YFP:ADE2 TetO(5.6Kb):487Kb:ChrXII:HIS3 smc5(E1015Q)-6HA:TRP1:smc5-6:NAT*	This Study
YMT4896	AS499	*TetR-YFP:ADE2 TetO(5.6Kb):487Kb:ChrXII:HIS3 ADH1-OsTIR1-9Myc:URA3 smc5-AID:KanMX fob1::hph*	This Study
YMT4898	AS499	*TetR-YFP:ADE2 TetO(5.6Kb):487Kb:ChrXII:HIS3 ADH1-OsTIR1-9Myc:URA3 SMC5-6HA:TRP1:smc5-AID:KanMX fob1::hph*	This Study
YMT4900	AS499	*TetR-YFP:ADE2 TetO(5.6Kb):487Kb:ChrXII:HIS3 ADH1-OsTIR1-9Myc:URA3 smc5(E1015Q)-6HA:TRP1:smc5-AID:kanMX fob1::hph*	This Study
YMS5026	AS499	*TetR-YFP:ADE2 TetO(5.6Kb):487Kb:ChrXII:HIS3 ADH1-OsTIR1-9Myc:URA3 smc5-AID:KanMX rad51::hph*	This Study
YMS5029	AS499	*TetR-YFP:ADE2 TetO(5.6Kb):487Kb:ChrXII:HIS3 ADH1-OsTIR1-9Myc:URA3 SMC5-6HA:TRP1:smc5-AID:KanMX rad51::hph*	This Study
YMS5030	AS499	*TetR-YFP:ADE2 TetO(5.6Kb):487Kb:ChrXII:HIS3 ADH1-OsTIR1-9Myc:URA3 smc5(E1015Q)-6HA:TRP1:smc5-AID:KanMX rad51::hph*	This Study
YMT5153	W303	*ura3-1::ADH1-OsTIR1-9Myc:URA3 smc6-AID*-9myc:hph*	This Study
YMT5157	W303	*ura3-1::ADH1-OsTIR1-9Myc:URA3 smc6-AID*-9myc:hph pSMC6-6HA:KanMX*	This Study
YMT5160	W303	*ura3-1::ADH1-OsTIR1-9Myc:URA3 smc6-AID*-9myc:hph psmc6(EQ)-6HA:KanMX*	This Study
YMT5375	AS499	*TetR-YFP:ADE2 TetO(5.6Kb):487Kb:ChrXII:HIS3 ADH1-OsTIR1-9Myc:URA3 smc5-AID:kanMX*	This Study
YMT5550	SY2080	*bar1Δ TIR1-9myc:LEU2 smc5-AID*-9myc:KanMX*	This Study
YMT5551	SY2080	*bar1Δ TIR1-9myc:LEU SMC5-6Flag:smc5-AID*-9myc:KanMX*	This Study
YMT5553	SY2080	*bar1Δ TIR1-9myc:LEU2 smc5(D1014A)-6Flag:smc5-AID*-9myc:KanMX*	This Study
YMT5554	SY2080	*bar1Δ TIR1-9myc:LEU2 smc5(E1015)-6Flag:smc5-AID*-9myc:KanMX*	This Study
YMT5784	AS499	*TetR-YFP:ADE2 TetO(5.6Kb):450Kb:ChrXII:URA3 Tir1-9myc:LEU::AmpR SMC6-3myc-NB(GFP):hph smc5-AID:KanMX*	This Study
YMT5797	AS499	*TetR-YFP:ADE2 TetO(5.6Kb):450Kb:ChrXII:URA3 Tir1-9myc:LEU::AmpR SMC6-3myc-NB(GFP):hph smc5-AID:KanMX pRS314-SMC5-6HA:TRP*	This Study
YMT5799	AS499	*TetR-YFP:ADE2 TetO(5.6Kb):450Kb:ChrXII:URA3 Tir1-9myc:LEU::AmpR SMC6-3myc-NB(GFP):hph smc5-AID:KanMX pRS314-smc5(E1015Q)-6HA:TRP*	This Study
YMT5817	AS499	*TetR-YFP:ADE2 TetO(5.6Kb):487Kb:ChrXII:HIS3 ADH1-OsTIR1-9Myc:URA3 smc5-AID:kanMX cdc15-9myc-AID:NAT pRS314-SMC5-6HA:TRP*	This Study
YMT5819	AS499	*TetR-YFP:ADE2 TetO(5.6Kb):487Kb:ChrXII:HIS3 ADH1-OsTIR1-9Myc:URA3 smc5-AID:kanMX cdc15-9myc-AID:NAT pRS314-smc5(E1015Q)-6HA:TRP*	This Study

Table 1. List of strains used in this thesis.

3.1.2. Media

We grew yeast in specific media depending on its requirements, always supplemented with a carbon source, either glucose (GLU) or galactose (GAL) at 2%. We used YP media when the cultured yeast strain had no specific requirements, prepared with 1% yeast extract (Quimega, 1702) and 2% peptone. This media could be supplemented with different antibiotics: clonNAT (100 µg/mL, Sigma Aldrich, 74667), hph (300 µg/mL, Invivogen, ant-hg-5) or GEN (200 µg/mL, Duchefa-Biochemie, G0175) to select cells containing the NAT, hph or KAN cassettes respectively.

We also used SC media prepared with 0.67% yeast nitrogen base (BD Difco, BD 291940) and 0.2% drop-out (Formedium, DCS1389). This media was complemented with amino acids when necessary: histidine (0.02 mg/mL), leucine (0.06 mg/mL), tryptophan (0.04 mg/mL) and uracil (0.02 mg/mL). We used a drop-out without adenine when either the yeast strain or the procedure required it (Formedium, DCS1229).

In both cases, we prepared solid media adding 2% bacteriological agar powder to the mentioned recipes. In different experiments, we supplemented YP media with 0.01 to 0.1% MMS (Sigma Aldrich, 129925) to test DNA damage tolerance and 1 mM IAA (Sigma Aldrich, I5148) to promote the degradation of selected proteins.

Media was sterilized at 121 ºC for 15 minutes in the autoclave.

3.1.3. Competent Cells Preparation

To prepare a batch of competent cells, we collected 50 mL of an exponential growing culture (OD_{620}≈0.6-1) by centrifugation (4000 rpm for 2 minutes, Eppendorf Centrifuge 5810 R). Then, we discarded the supernatant and transferred the pelleted cells to a 1 mL tube with distilled water. We spun the cells at 14000 rpm in a tabletop centrifuge and washed them with SORB Buffer (100 mM LiOAc, 1 mM EDTA, 10 mM Tris-HCl pH 8 and 1 M sorbitol), centrifuging at low speed. Finally, we resuspended the cells again in 360 µL of SORB buffer and added 40 µL of denatured salmon sperm DNA (Roche, 11467140001) to act as carrier, as explained by Knop et al., 1999. We aliquoted the competent cells in 50 µL in 1 mL tubes and immediately stored at -80 ºC.

3.1.4. Transformation

The transformation method described below is based on the protocol described by Knop et al., 1999.

We started the transformation procedure thawing a 50 µL aliquot of competent cells on ice for 5 minutes. Then, we added 1 µg of linear DNA (coming from a PCR) or 0.2 µg of plasmidic circular DNA to the competent cells, we never added DNA over a 10% of the total volume of competent cells. Next, we added 6 volumes of PEG buffer (100 mM

LiOAc, 1mM EDTA pH 8 and 50% PEG 3350 -Sigma Aldrich, 1546547-) and the mix was incubated at room temperature for 30 minutes. At the end of the incubation, we added 10% dimethyl sulfoxide (Fisher Bioreagents, BP231) and performed a heat shock at 42 ºC for 15 minutes.

We pelleted the cells at low speed and either resuspended in distilled water and plated them (when the selection marker was an auxotrophy) or resuspended in YPD and left at room temperature for at least 3 hours before plating them (when the selection marker required gene expression, for example in antibiotic resistance).

3.1.5. Genomic DNA Extraction

3.1.5.1. Promega Kit

To obtain the genomic DNA of yeast cells, we resuspended a small quantity of cells in 292.5 µL of 50 mM EDTA and added lyticase (40 U/mL, Sigma Aldrich, L2524). After 1 hour at 37 ºC, we centrifuged the sample at 14000 rpm for 2 minutes in a tabletop centrifuge. Then, we resuspended the pelleted cells in 300 µL of Nuclei Lysis Solution (Promega, A7941) and once resuspended, 100 µL of Protein Precipitation Solution (Promega, A7951) were added before vortexing the sample for 20 seconds. We left the mix on ice for 5 minutes and centrifuged it at 14000 rpm for 2 minutes. Next, we transferred the supernatant to a new tube containing 300 µL of isopropanol and mixed by inversion before centrifuging again at 14000 rpm for 2 minutes. The pellet was resuspended in 300 µL of ethanol, centrifuged once again with the same settings and left drying with the top of the tube open. Finally, we resuspended the DNA in 50 µL of dH_2O.

3.1.5.2. Extraction with Lithium Acetate

We used a second method to extract the genomic DNA of yeast cells. First of all, we resuspended a small quantity of cells 100 µL of 200 mM LiOAc and 1% SDS. This mix was incubated at 70 ºC for 5 minutes. Afterwards, we added 300 µL of ethanol and centrifuged the tube at 14000 rpm for 3 minutes in a tabletop centrifuge. We resuspended the obtained pellet in 300 µL of 70% ethanol and centrifuged once again. After letting it dry, we used 100 µL of buffer TE (10 mM Tris-HCl pH 8 and 1 mM EDTA) to resuspend the DNA and spun the at 14000 rpm to precipitate any remaining debris. The supernatant was used as a DNA extract.

3.1.6. Plasmid Extraction

To obtain a centromeric plasmid from a yeast strain, we incubated cultures overnight at 30 ºC. Once exponentially growing (OD_{620}≈1), we collected 10 mL by centrifugation at 14000 rpm. The cell pellet was resuspended in 250 µL of Resuspension

Buffer from the GeneJET Plasmid Miniprep Kit (Thermo Scientific, K0503). Then, we added 1 volume of glass beads (Sigma Aldrich, G8772) to the resuspended cells and broke them using a Mini-Beadbeater-24 (BioSpec, 112011) at maximum power for 45 seconds. Once the cells were broken, we pierced the top and the bottom of the tube and placed it on top of a new Eppendorf tube. The two tubes were placed into a tabletop centrifuge and spun at 500rpm for 1 minute in order to transfer the liquid to the clean tube at the bottom. After obtaining this cell extract, we followed the instructions provided by the manufacturer for the GeneJET Plasmid Miniprep Kit (Thermo Scientific, K0503). We eluted the plasmid in 20 µL of Elution Buffer and transformed 5 µL of this elution into DH5α competent cells.

3.1.7. Protein Extraction

3.1.7.1. Post Alkaline Extraction

This is a method for a rapid protein extraction with the aim of checking the presence or absence of a tagged protein expression. The protocol is based on that described by Kushnirov, 2000.

After overnight incubation into 1 mL of liquid media, we centrifuged cells at 14000 rpm to get a pellet and discard the supernatant. Then, we resuspended the pelleted cells in 90 µL of dH_2O and added 90 µL of 0.3 M NaOH. This mix was incubated at room temperature for 5 minutes and centrifuged at 14000 rpm for 1 minute. Next, we eliminated the supernatant and resuspended the pellet in 50 µL of 1xSSR (2% SDS, 125 mM Tris-HCl pH 6.8, 4% β-mercaptoethanol, 5% sucrose and 0.01% bromophenol blue). The mix was heat at 95 ºC for 3 minutes. Finally, we spun the samples at 14000 rpm and loaded 8 µL of the supernatant into a gel for SDS-PAGE (Section 3.3.5).

3.1.7.2. Urea Extraction

This protocol was selected when protein levels between different samples had to be compared. It permits quantification of total protein in the sample before loading into the SDS-PAGE gel.

We started this protocol collecting a 10 mL sample of an exponentially growing culture (OD_{620}≈1) by centrifugation (4000 rpm for 2 minutes, Eppendorf Centrifuge 5810 R). We transferred the pellet into a new Eppendorf tube by diluting it in cold dH_2O and spun it at 14000 rpm to eliminated the supernatant. Then, we resuspended the cell pellet in 30 µL of 5 M urea and added two micro-spoons of glass beads (Sigma Aldrich, G8772). Cells were broken in a Mini-Beadbeater-24 (BioSpec, 112011) at maximum power for 30 seconds. At this point, we added 150 µL of 1xSR (2% SDS and 125 mM Tris-HCl pH 6.8) to the mix and vortexed it for 5 seconds. After a 2-minute incubation at 95ºC, we pierced the tube both on its top and its bottom and placed it on top of a new Eppendorf tube. The liquid was transferred to the bottom tube by centrifugation at 500 rpm for 30 seconds,

leaving the glass beads in the tube on top. Next, we cleared the extract by centrifuging it at 14000 rpm for 5 minutes in a tabletop centrifuge. The supernatant was recovered and transferred to a new Eppendorf tube.

Once we had obtained the extract, the total protein in it was quantified by following the instructions provided by the manufacturer for the DC Protein Assay (BioRad, 5000112). We obtained the reads for the colorimetric assay using a VERSAmax Microplate Reader (Molecular Devices LLC). Finally, we took a volume equivalent to 30 µg of protein and mixed it with 4xSS (20% sucrose and 0.04% bromophenol blue, left at 1x) and β-mercaptoethanol (left at 4%). We loaded the whole volume of the mix into a gel for SDS-PAGE (Section 3.3.5).

3.1.8. Mating, Sporulation and Tetrad Dissection

In some cases, we mated two haploid yeast strains of different mating type to combine alleles from different genes into a diploid strain. Afterwards, we sporulated the obtained diploid cells and selected the desired spores to generate new haploid strains containing a desired combination of alleles.

First, we mixed the desired MATa and MATα strains into a small patch on an YPD plate. This plate was incubated at 25 ºC for 5 hours before checking under the microscope the presence of zygotes. Then, we spread a sample of the patch on an YPD plate and grew it at 30 ºC. Once colonies appeared, those that were bigger where transferred onto a plate with selective pressure to obtain only diploid cells.

After the obtention of the diploid cells, we grew them for a couple of days on YPD. We transferred the grown diploid cells to plates with Sporulation Media (1% KOAc, 0.1% yeast extract, 0.05% glucose) making a small patch, trying to extend the cells as less as possible. After a one-week incubation at 25 ºC, we checked the presence of spores under the microscope. Then, we resuspended the spores in water and incubated them for 15 minutes at 30 ºC in the presence of β-glucuronidase (Sigma Aldrich, G8420). To stop the digestion of the asci, we carefully added 1 mL of dH_2O, avoiding the disruption of the tetrads. The spores where then placed on ice and centrifuged for 1 minute at 800 rpm.

Finally, we placed 15 µL of the sample containing the tetrads on one side of an YPD plate and tilted it to distribute the spores along a straight line. We placed this plate onto the micromanipulator (Singer MSM 400) and tetrads were dissected to get isolated ascospores. After the dissection, the plate was placed at 25 ºC until haploid colonies started to grow from each ascospore. We tested the haploid colonies with selective media in order to pick the desired ones.

3.1.9. Cell Cycle Synchronization

We arrested Cells in G1 phase by adding the yeast pheromone alpha factor to the media. In wild type cells for the gene BAR1, we used 10^{-6} M of alpha factor (Genscript, RP01002), while in *bar1Δ* cells, we diluted the pheromone to 10^{-8} M. We maintained this treatment until at least 95% of the cells showed schmoo shape under the microscope. In BAR1 cells, in case that the arrest exceeded the two hours, we added 5 x 10^{-7} M of alpha factor to the media in order to avoid the entrance of some cells into S-Phase. When the protocol required a release from G1, we washed cells twice with culture media and added pronase (protease from *Steptoccocus griseus*, Roche, 10165921001) at a concentration of 0.1 µg/mL.

To arrest cells in S-Phase, we added hydroxyurea (Sigma Aldrich, H8627) to the media at 0.2 M. The hydroxyurea powder was weighted in a clean, sterile tube and the culture was added on top. Then, we incubated the culture at the desired temperature for 2 hours. If the culture to stop came from a G1 arrest, we added the hydroxyurea 30 minutes after the release from G1 to permit the entrance of the arrested cells into S-phase.

To synchronize cells in metaphase, we used two different methods. For the first method, we added 1% DMSO to the media 30 minutes before adding nocodazole (Sigma Aldrich, M1404) at 15 µg/mL. Cells were observed under the microscope until 95% of them had a bud with a size similar to that of the mother cell. If the arrest had to be extended over 2 hours, we added an extra 7.5 µg/mL of nocodazole. For the second method, we constructed yeast strains to have the endogenous CDC20 tagged with an auxin inducible degron. In this case, addition of 1 mM IAA to the media activated the spindle checkpoint, promoting the G2/M arrest. We generated a strain with the AID tag on CDC15 to stop the cell cycle after chromosome segregation, inhibiting the activation of cytokinesis. In this case, proper cell cycle arrest required 6 mM IAA to be added to the media.

3.1.10. Phenotype Analysis on Plate

We diluted exponentially growing cells to OD_{600}≈0.3. Then, we placed 200 µL of the cells into a 96-well plate (Falcon, 353072) and generated sequential dilutions (usually 1/10 dilutions). A 48-pin metallic tool was used to plate the cells on 100 mm plates containing the chosen solid media.

3.1.11. Fluorescent-Activated Cell Sorting (FACS)

We fixed growing cells by adding pure ethanol to the media (to a final concentration of 70%) for 1 hour at room temperature or overnight at 4 ºC. After the fixation step, we pelleted the cells by centrifugation (4000 rpm for 2 minutes, Eppendorf Centrifuge 5810

R) and removed the supernatant to add 500 µL of Saline-Sodium Citrate buffer (SSC; 150 mM NaCl and 150 mM Sodium Citrate) containing 100 µg of RNAse A (Qiagen, 19101). After an incubation of at least 1 hour at 50 ºC, we added 100µL of 1xSSC containing 60 µg of Proteinase K (Qiagen, 19131) and incubated the mix at 50 ºC for 1 hour. Finally, we stained the DNA by adding 1 mL of 1xSSC containing either 3 µg/µL of propidium iodide or 0.3% of SYTOX green (Invitrogen, S7020) and incubating for at least 1 hour at room temperature.

Before analyzing the samples at the FACSCanto II cytometer (BD Biosciences), we sonified them for a few seconds at power 8 with a Soniprep 150 (MSE). The data obtained at the cytometer was analyzed using WinMDI 2.9 software (RRID: SCR_013745).

3.2. Bacterial Methods

3.2.1. Plasmids

Table containing the plasmids used for this work.

Name	Alias	Description	Source
pTR1071		*pRS416-[CEN, URA3, AMP]-SMC6*	Lab Collection
pTR1094		*YCplac22-[CEN, TRP1, AMP]-(SphI,KpnI)-ADH1p-SMC5:9Myc*	Lab Colleciton
p1359	BYP6740	*plinker-IAA17:KanMX*	Yeast Genetic Resource Center
p1361	BYP6744	*ADH11p-OsTIR1-9Myc:URA3*	Yeast Genetic Resource Center
pTR1621		*YCplac22-[CEN, TRP1, AMP]-(SphI,KpnI)-ADH1p-SMC5(K75I):9Myc*	Lab Colleciton
pTR2500		*YCplac22-[CEN, TRP1, AMP]-(SphI,KpnI)-ADH1p-SMC5(E1015Q):9Myc*	Lab Colleciton
pIR2621		*YCplac22-[CEN, TRP1, AMP]-(SphI,KpnI)-ADH1p-SMC5(S987R):9Myc*	Lab Colleciton
p2680	p2151	*AID*-9myc:hph H.Ulrich*	H.Ulrich
p2684	p2188	*AID*-9myc:KanMX H.Ulrich*	H.Ulrich
p2685	p2189	*AID*-9myc:nat H.Ulrich*	H.Ulrich
p3267	pCJ097	*pRS402-[ADE2, AMP]-tetR-YFP*	Lab Colleciton

Name	Alias	Description	Source
pTR3696		*pRS416-[CEN, URA3, AMP]-SMC6(E1048Q)*	Lab Colleciton
pTR3699		*pRS416-[CEN, URA3, AMP]-SMC6(S1020R)*	Lab Colleciton
pTR3702		*pRS416-[CEN, URA3, AMP]-SMC6(D1047A)*	Lab Colleciton
pMT3952		*pRS304-[TRP1, AMP]-(SacI-SpeI)-SMC5p-SMC5-6HA*	This Study
pMT3955		*pRS304-[TRP1, AMP]-(SacI-SpeI)-SMC5p-SMC5-6Flag*	This Study
pMT4005		*pRS304-[TRP1, AMP]-(SacI-SpeI)-SMC5p-SMC5(E1015Q)-6HA*	This Study
pMT4040		*pRS304-[TRP1, AMP]-(SacI-SpeI)-SMC5p-SMC5(D1014A)-6HA*	This Study
p4096	pBS35	*mCherry:hph*	Addgene
pMT4097		*pRS304-[TRP1, AMP]-(SacI-SpeI)-SMC5p-SMC5(D1014A)-6Flag*	This Study
pMT4098		*pRS304-[TRP1, AMP]-(SacI-SpeI)-SMC5p-SMC5(E1015Q)-6Flag*	This Study
p4449	pYM15	*6HA:HIS3MX6*	Lab Colleciton
p4450	pYM16	*6HA:hphNT1*	Lab Colleciton
p4451	pYM17	*6HA:natNT2*	Lab Colleciton
pMT5191		*pRS314-[CEN, TRP1, AMP]-(SacI-SpeI)-SMC5p-SMC5-6HA*	This Study
pMT5193		*pRS314-[CEN, TRP1, AMP]-(SacI-SpeI)-SMC5p-SMC5(E1015Q)-6HA*	This Study
pMT5258		*pRS305-[LEU2, AMP]-Tir1-9myc*	This Study
pMT5279		*TetO(5.6Kb):450Kb ChrXII URA3 (pRS406 - EcoRI-XbaI-BamHI-XmaI)*	Lab Collection

Table 2. List of plasmids used in this thesis.

3.2.2. Media

We grew *Escherichia coli* in Luria-Bernati (LB) broth: 1% peptone, 0.5% yeast extract and 1% NaCl. Solid media was obtained by addition of 2% agar. Both in liquid and solid conditions, we grew bacteria 37 ºC. These media could be supplemented with

either ampicillin (50 µg/mL, Sigma Aldrich, A9518) or kanamycin (50 µg/mL, Sigma Aldrich, 60615).

Media was sterilized at 121 ºC for 15 minutes in the autoclave.

3.2.3. Competent Cells Preparation

To prepare a batch of competent cells, we collected an exponential growing culture (OD_{620}≈0.4) by centrifugation (4000 rpm for 5 minutes, Eppendorf Centrifuge 5810 R). We washed the cells with 1/50th of the original culture volume of ice cold 50 mM $CaCl_2$. Then, we resuspended the cells in the same volume of 50 mM $CaCl_2$ and left them on ice for 2 hours. Finally, we centrifuged the cells again at 4000 rpm for 5 minutes and resuspended them in 4 mL for every 100 mL of the original culture of ice cold 50 mM $CaCl_2$ containing 15% glycerol and stored them in aliquots at -80 ºC.

3.2.4. Miniprep Plasmid Extraction

We used the GeneJET Plasmid Miniprep Kit (Thermo Scientific, K0503) to obtain plasmids stored in bacterial strains. We cultured bacteria overnight at 37 ºC on LB plates containing antibiotic to maintain selective pressure and assure a good plasmid extraction yield. We performed the extraction following the instructions provided by the manufacturer. Finally, we eluted the plasmid in either 50 or 30 µL of Elution Buffer included in the kit, depending on the desired concentration.

3.2.5. Transformation

3.2.5.1. DH5α Transformation

We used the commercial bacterial strain Subcloning Efficiency DH5α Competent Cells (Invitrogen, 18265-017) for plasmid and ligation transformations. The competent cells were stored at -80 ºC in 50 µL aliquots. We thawed an aliquot on ice for 5 minutes and added 0.2 µg of circular DNA or 5 µL of a ligation reaction (explained in section 3.3.4), never exceeding the 5 µL, which represents a 10% of the total aliquot volume. Then, we left this mix on ice for 30 minutes before performing a 20 second heat shock at 42 ºC and return to ice for 2 minutes. Finally, we pelleted the cells at low speed and resuspended them in LB. After an incubation of at least 1 hour at 37 ºC, we plated the transformed cells on selective LB plates containing antibiotics.

3.2.5.2. Homemade Competent Cells Transformation

For transformations with special needs, we used two different bacterial strains: MC1061, a $RecA^+$ strain; and STBL3, a strain without recombinative activity. In this case, we followed the protocol used for DH5α transformation with two changes: (1) we used

100 µL aliquots of the competent cells and (2) the heat shock was extended to 2 minutes at 42 ºC and another 2 minutes on ice.

We used MC1061 competent cells to recombine two independent PCRs. These two PCRs had been performed with complementary primer oligonucleotides that generate 40 nucleotide-long homology regions to allow homologous recombination in bacteria (Figure 6). We co-transformed these PCRs into bacteria, maintaining the maximal proportion of DNA at 10% of the competent cell volume.

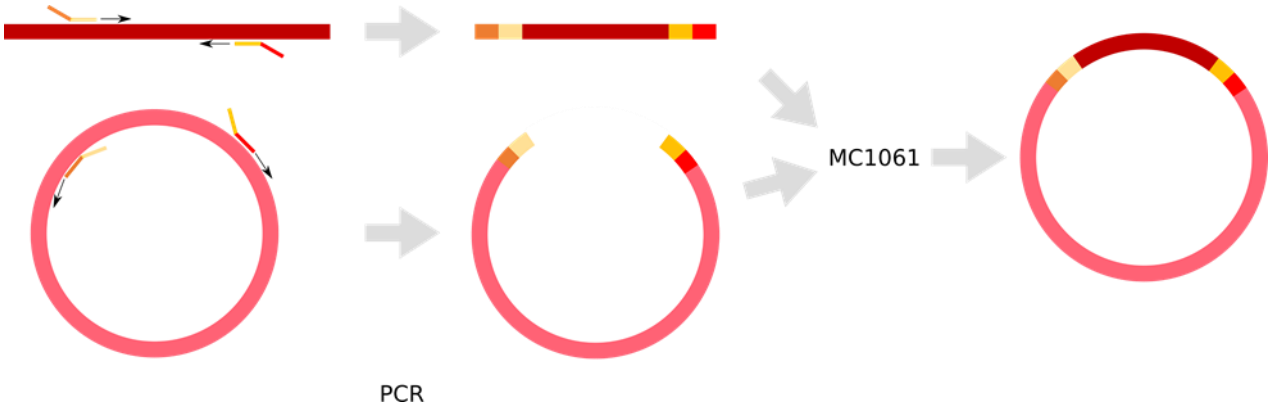

Figure 6. PCR and homologous recombination performed in MC1061 cells. Schematic view of the PCR and recombination used to construct plasmids in MC1061. The sections represented with the same color in primer oligonucleotides have complementary sequences.

3.3. Molecular Biology Methods

3.3.1. Polymerase Chain Reaction (PCR)

3.3.1.1. Amplification PCR

To amplify DNA fragments, we used different polymerases depending on the final objective of the reaction. When the main objective was processivity, we chose Expand High Fidelity PCR System (Roche, 11732650001). In contrast, when we needed to get a good fidelity on the DNA product, we chose between iProof High-Fidelity DNA Polymerase (BioRad, 1725331) and Phusion High-Fidelity DNA Polymerase (Thermo Scientific, F530S). For reactions in which the product would have no further use, such as testing colonies coming from a cloning protocol, we used SupraTherm Taq DNA Polymerase (Genecraft, GC-022).

We used each kit following the instructions provided by the manufacturer regarding to DNA amount, buffer concentration and polymerase units to use in each reaction. We also adjusted PCR programs to each kit. The PCR program consisted basically in a first denaturation step followed by a set of cycles with a brief denaturation, a brief annealing

and the required time of polymerization (1 minute per kilobase to amplify); after these cycles, a final polymerization step and storage at 4 ºC. In the case of the Expand PCR kit, cycles were divided in two parts, 10 normal cycles first and then 30 more cycles in which polymerization is extended 5 seconds per cycle. These reactions were performed in a Gene Amp PCR System 2700 (Applied BioSystems).

Depending on the next steps to perform on the DNA product, we added a purification step with the QIAquick PCR Purification Kit (Qiagen, 28104), following the instructions provided by the manufacturer. Finally, we eluted the DNA with either 30 or 50 µL of Elution Buffer provided in the kit.

3.3.1.2. Quantitative PCR (qPCR)

In this study, we used the qPCR method to quantify different loci in samples obtained after a chromatin immunoprecipitation (ChIP, section 3.3.6). At the end of ChIP, we purified the co-immunoprecipitated DNA with the QIAquick PCR Purification Kit (Qiagen, 28104) and eluted the sample in 50 µL of Elution Buffer provided in the kit. We assume that after the whole protocol, an equivalent quantity of DNA is obtained from each sample and, therefore, the same volume is added to each qPCR reaction.

We used the PowerUp SYBR Green Master Mix (Applied Biosystems, A25779) to prepare the reactions. We first diluted the Master Mix in water and separated it into different aliquots. Then, we added the oligonucleotide pairs to these diluted Master Mix aliquots at 0.2µM. Finally, we added 17 µL of the different primer-containing mixes into each well of a qPCR strip (Real-Time PCR Tube Strips and Masterclear Cap Strips, Eppendorf, 951022109). Finally, we added 3 µL of DNA to each well.

The qPCR reaction was carried out in a CFX96 Touch Real-Time PCR Detection System (BioRad) and the results analyzed with Bio-Rad CFX Manager software and Microsoft Excel 2013. We used the Cq determined by the software to make the calculations (detailed in the ChIP section of this Materials and Methods, section 3.3.6).

3.3.1.3. Oligonucleotides

Table containing the oligonucleotides used for this work.

Name	Description	Sequence	Usage
CYO901	MMS2 (-263)	GTCCACTCAATGCACTGAAGAA	Deletion
CYO902	MMS2 (+269)	GCAACAGTCTTTCTGTCGTCTGTTT	Deletion
CYO903	MMS2 (-417)	TGTAACGCCTGAATCTGACGATTAC	Test

Name	Description	Sequence	Usage
CYO1791	Fw SMC6 (797)	AGTGCTATTCACGATAGTGC	Sequencing
CYO1792	Fw SMC6 (1504)	ATTGCAGAATATTGCTAAGG	Sequencing
CYO1795	S2-SMC5	CATCTATATGTGTATAATTAATTATGCAATA GTGAAAGAATCGATGAATTCGAGCTCG	Tagging
CYO1804	Fw SMC5 D1014A	GAAATCAATCAAGGTATGGACTCTAG	SDM
CYO1805	Rv SMC5 D1014A	AGCAACCACTCTAAATGGTGCAGAG	SDM
CYO1807	Rv SMC6 (833)	TTCAAATTCTCCAGGTGCAGAG	Sequencing
CYO1836	S3-SMC5	AAGATGATACATTTCGGTGAAACTTCTAACTA CTCATTCGATCGTACGCTGCAGGTCGAC	Tagging
CYO1849	Fw SMC6 D1047A	AGCCGAATTCGACGTTTTCATGG	SDM
CYO1850	Rv SMC6 D1047A	AGCGCAATAATCCTTGACCGC	SDM
CYO1968	Fw SMC5 E1015Q + SalI	GACCAAATCAATCAAGGTATGGACTCTAG	SDM
CYO1969	Rv SMC5 E1015Q + SalI	GACCACTCTAAATGGTGCAGAGG	SDM
CYO2002	S3-SMC6	ATGAGAGACCCTGAGAGACAGAATAATTCC AATTTTTATAATCGTACGCTGCAGGTCGAC	Tagging
CYO2003	S2-SMC6	AGACGATTACACAATATTTTGAATAATTACAT GAAGAAACAATCGATGAATTCGAGCTCG	Tagging
CYO2015	Fw SMC5 S987R	AGGTGGTGAAAGAGCTGTTTC	SDM
CYO2016	Rv SMC5 S987R	CTTTGCGTGTGGGAATCTAAC	SDM
CYO2137	Fw SMC6 E1048Q + XbaI	GACCAATTCGACGTTTTCATGGAC	SDM
CYO2138	Rv SMC6 E1048Q + XbaI	TAGAGCAATAATCCTTGACCGCATC	SDM
CYO2139	Fw SMC6 S1020R	GAGGTGGTGAAAAATCGTTTTCCC	SDM
CYO2140	Rv SMC6 S1020R	TCAAGGTGTCAACGTTTCTTGCC	SDM
CYO2166	Rv SMC6 (+75)	TTTCAAATATGCTGCCGTGAAAACG	Sequencing
CYO2174	Fw ChrIII 61 KB	TCACAAGCACTCTTCCGACACACT	qPCR

Name	Description	Sequence	Usage
CYO2175	Rv ChrIII 61 KB	AGGGAGACTGGTGAATTGGAGGAA	qPCR
CYO2189	Fw Smv5 (-220) + SacI	GCGCGCGAGCTCTTTGTCTGACAACACACTTGTTGCC	Cloning
CYO2233	Fw Smc5 (-882) + SacI	AGGAATGAGCTCTCTTGGCTATATATAACGGCAGAC	Cloning
CYO2239	Fw CEN4	GACTAAGTCCATATCGACTTTGTAAAAGTTCAC	qPCR
CYO2240	Rv CEN4	GCAAGCAATTAAATTTTGCAATTTGTGATTTAGG	qPCR
CYO2252	Fw pRS MCS	CCAGGGTTTTCCCAGTCACGACG	Sequencing
CYO2253	Rv pRS MCS	CAATTTCACACAGGAAACAGCTATGACC	Sequencing
CYO2395	Fw Tags in pYM	CATCAGAGCAGATTGTACTGAGAGTGC	Tagging
CYO2607	Rv pYM + NB 1	CAACTTTTGTTCACCACTAGCAGCAGAACCGG	SDM
CYO2608	Fw pYM + NB 1	GTTACTGTTTCTTCTTAAAAAGTGGAACGATCATTCA	SDM
CYO2609	Rv pYM + NB 2	TCGTTCCACTTTTTAAGAAGAAACAGTAACTTGAGTACC	Sequencing
CYO2610	Fw pYM + NB 2	GGTTCTGCTGCTAGTGGTGAACAAAAGTTGATTTCTG	Tagging
CYO2655	Fw pRS + Tir1-9myc (p1361) 1	GAGGTCGACGGTATCGATAAC GGTATCGATAAGCTTGATATCG	SDM
CYO2656	Rv pRS + Tir1-9myc (p1361) 1	CTGCAGGAATTCGATATCAAGC ATCTCTTGAATGATCGTTCCAC	SDM
CYO2657	Fw pRS + Tir1-9myc (p1361) 2	GTGGAACGATCATTCAAGAGAT GCTTGATATCGAATTCCTGCAG	SDM
CYO2658	Rv pRS + Tir1-9myc (p1361) 2	CGATATCAAGCTTATCGATACC GTTATCGATACCGTCGACCTC	SDM
CYO2694	Fw Bar1 (-313)	AGATGCGTTGTCCCTGTTTTTC	Tagging
CYO2695	Rv Bar1 (+207)	CAGATCGGGGTTCAATTCCC	Tagging
CYO2707	S3-CDC15	GATAAAAGTGACGGCTTTTCCGTCCCCATTAC AACATTTCAAACACGTACGCTGCAGGTCGAC	SDM
CYO2708	S2-CDC15	GTATTATTTCTCTATATATGTATGTATGCACAT GCAATTCCTACAATCGATGAATTCGAGCTCG	SDM
CYO2709	S3-CDC20	ATTCATACAAGGAGGCCCTCTAGTACCAGCCA ATATTTGATCAGGCGTACGCTGCAGGTCGAC	SDM

Name	Description	Sequence	Usage
CYO2710	S2-CDC20	ATTTCATTATATGCCTTGACATGAACTTTTAT TTTTTTTATTTTAATCGATGAATTCGAGCTCG	SDM
CYO2763	Fw TER1004	CCATCTTGTTGTCCATGTCC	qPCR
CYO2764	Rv TER1004	CGCATGGGATTTTGCTATC	qPCR
CYO2810	Fw ARS1617	CGCAAATACACCAACTTATGACGATAGTG	qPCR
CYO2811	Rv ARS1617	CGTCACTTCTTTAGTGGGTTCAAGAC	qPCR
CYO2812	Fw ARS418	ACATCTTCTCAACGCGAAAATGACG	qPCR
CYO2813	Rv ARS418	ACTTTGTCTCTAAATCCTTGTAAAATGTGTACG	qPCR
CYO2814	Fw ChrIII 382 Kb	TTCTACTACTGTTTAGTTTCTACGGCCTG	qPCR
CYO2815	Rv ChrIII 382 Kb	AAACCATCAAAGTTCTTGGAACTAGCC	qPCR
CYO2816	Fw rDNA - 35S	GCACTTTACAAAGAACCGCACTCC	qPCR
CYO2817	Rv rDNA - 35S	CGAGTTGTAATTTGGAGAGGGCAAC	qPCR
CYO2818	Fw rDNA - ARS1200-1	CCCACCACACTCCTACCAATAACG	qPCR
CYO2819	Rv rDNA - ARS1200-1	GAGGAAAAGGTGCGGAAATGGC	qPCR
CYO2820	Fw rDNA - RFB	CTCCATTTCCCTCTCTTCTACGG	qPCR
CYO2821	Rv rDNA - RFB	GTAATGCGGCAAAATGTTAGTGCAG	qPCR

Table 3. List of Oligonucleotides used in this thesis.

3.3.2. DNA Electrophoresis

We used electrophoresis in an agarose gel to determine the length of nucleic acid fragments. We prepared the gel by dissolving agarose D1 low EEO (Condalab, 8010) in 1x TAE Buffer (40 mM Tris-HCl, 20 mM acetic acid and 1 mM EDTA pH 8) at a concentration between 0.8 and 2%. We heated the mix using a microwave and avoiding any boiling that would produce an increase of the agarose concentration in the gel. Then, we poured liquid agarose into an appropriate mold and left cooling down until it was fully polymerized.

We prepared the DNA sample to load into the gel with FLB (3% Ficoll-400, 20 mM EDTA pH 8, 0.02% SDS and, optionally, 0.01% bromophenol blue) and loaded it into the gel. Next to the samples, we added a DNA ladder: GeneRuler 1 Kb DNA Ladder (Thermo Scientific, SM0311) or 100 bp DNA Ladder (Genecraft, GC-015-004). Next, we placed the gel into a buffer tank containing 1x TAE buffer and run the electrophoresis at constant voltage between 90 and 100 V. Finally, after the electrophoretic run was completed, the gel was submerged into ethidium bromide (0.5 mL/L in dH_2O) for 15 to 30 minutes, longer times if necessary. We obtained images of the gel by placing it over a UV transilluminator.

3.3.3. DNA Purification from Agarose Gel

To purify a DNA fragment among a mix of different fragments, we used an agarose electrophoresis followed by the recovery of the needed DNA. In this case, we pre-stained the sample using SYBR-Gold before loading it into the agarose gel. We ran the electrophoresis at 90 V since higher voltages promote poor resolution of the bands in the gel. Once the electrophoresis was finished, we transferred the gel to a piece of aluminum foil paper to protect DNA from UV-induced damage and brought it to a transilluminator. With the help of a scalpel, we cut the band from the gel, avoiding excessive UV exposure as it could generate thymine dimers and, therefore, mutagenize de DNA. The agarose piece was cut as small as it was possible.

Once we had obtained the agarose band containing the DNA, we extracted the nucleic acid following the manufacturer instructions of the QIAquick Gel Extraction Kit (Qiagen, 28704).

3.3.4. Site Directed Mutagenesis (SDM)

We used this technique to introduce a desired mutation into a gene, in our case for this thesis the ATPase point mutations in *SMC5* and *SMC6*. We started the SDM process amplifying by PCR a plasmid containing a cloned wild type gene to mutagenize using the Expand High Fidelity PCR System (Roche, 11732650001). The forward primer oligonucleotide contained a modified sequence with the desired mutation to be generated into the gene.

The Expand PCR system does not leave blunt ends on the PCR product; hence we incubated the obtained product with Platinum *Pfx* DNA Polymerase (Invitrogen, 11708013), which has proofreading exonuclease activity 3’ to 5’. Then, we circularized the plasmid using the Rapid DNA Ligation Kit (Roche, 11635379001) as indicated by the manufacturer. Finally, we transformed the ligation product into DH5α competent cells (section 3.2.5.1).

When possible, we designed the oligonucleotides to generate a restriction site at the ligation point. The addition of the transcription site was introduced without disturbing

the protein sequence after transcription and translation. We used the restriction site to check the result of the SDM. However, when the sequence did not permit the addition of a restriction site without disturbing the protein sequence, we sequenced the plasmid using the You Tube It method (Sanger sequencing by Stab Vida).

3.3.5. SDS-PAGE and Western Blot Analysis

To analyze proteins in denaturing conditions, we performed SDS-PAGE (Sodium Dodecyl Sulfate-Polyacrylamide Gel Electrophoresis) followed by immunoblotting (Western Blot).

We casted a polyacrylamide gel into 1mm Mini-PROTEAN Glass Plates (BioRad), with two separated parts: the stacking gel on top and the resolving gel at the bottom. First, we prepared the resolving gel, containing 375 mM Tris-HCl pH 8.8 (1.5 M stock from BioRad, 1610798), 0.1% SDS and 7.5 to 10% Achrylamide/Bis Solution (30% stock from BioRad, 1610158) in water. We activated the polymerization reaction adding 0.08% ammonium persulfate and 5 µL of TEMED. Then, we poured the mix into the casting glass plates with 1 mL of isopropanol on top to avoid the inhibition of polymerization by the oxygen present in the air. Next, we prepared the mix for the stacking gel, containing 125 mM Tris-HCl pH 6.8 (0.5 M stock from BioRad, 1610799), 0.01% SDS and 5% Achrylamide/Bis Solution (30% stock from BioRad, 1610158) in water. When the resolving gel was fully polymerized, we removed the isopropanol on top by decantation and rinsed the top of the resolving gel with water. Finally, we activated the polymerization of the stacking gel adding ammonium persulfate and TEMED to the mix. We poured it on top of the polymerized resolving gel and placed a 10 or 15-well comb on top to create the wells to load the samples afterwards.

After casting the gel, we placed it into a running cell and filled both the running module and the running cell with Running Buffer (25 mM Trizma base, 192 mM Glycine and 0.1% SDS adjusted to pH 8.3). Then, we incubated the samples at 95 ºC for 3 minutes and spun them at 14000 rpm before loading them into the corresponding wells. The electrophoresis was run at 20 mA per gel in the running cell. We used the advance of the PageRuler Prestained Protein Ladder (10 to 180 KDa, Thermo Scientific, 26617) loaded next to the samples to determine the running time of the gel.

When the running finished, the proteins in the gel had to be transferred to a PVDF Amersham Hybond membrane (Cytiva, 10600021). First, we activated the membrane in methanol for a few seconds, rehydrated it by rinsing with water and incubated it in Transfer Buffer (39 mM glycine, 48 mM Trizma base, 0.0375% SDS and either 10 or 20% ethanol). Then, we prepared a sandwich stacking a Whatman filter paper, the membrane, the gel and a second Whatman filter paper. The transfer was carried out at 60 mA per gel for 1 hour and 15 minutes.

Once the proteins were on the membrane, the remaining area had to be blocked to avoid unspecific binding of the antibody to the membrane, since the antibody is also a protein and would have affinity to bind the membrane. We blocked the membrane for 45 minutes in a 50 mL tube containing 10 mL of freshly prepared 5% non-fat milk dissolved into PBST (1% PBS and 0.2% Tween-20) rolling at room temperature. Then, we removed the milk and added 5 mL of the primary antibody in 0.25% non-fat milk dissolved into PBST (concentrations and antibodies in Table 4). After an overnight incubation rolling at 4ºC or a 2-hour incubation at room temperature, we washed the membrane three times shacking for ten minutes in a box with PBST to remove the exceeding primary antibody. Then, we transferred the membrane again into a 50 mL tube and added 5 mL of the secondary antibody if necessary. Finally, we washed the membrane three more times in PBST, shacking for ten minutes to remove the secondary antibody unspecifically bound to the membrane.

The secondary antibodies used for this study were bound to horseradish peroxidase (HRP). We used Immobilon Western Chemiluminescent HRP Substrate (Merck MIllipore, WBKLS0500) to generate the chemiluminescent signal on the membrane and detected with a ChemiDoc XRS+ (BioRad).

Antigen	Clone	Type	Species	Dilution	Reference
FLAG	M2	Primary	Mouse	1:5000	Sigma Aldrich, F3165
HA	3F10	Primary	Rat	1:5000	Sigma Aldrich, 11867423001
MYC	9E10	Primary	Mouse	1:1000	Enzo Life Sciences, ENZ-ABS462-0200
Hexokynase		Primary	Rabbit	1:5000	USBiological, H2035-02
Mouse IgG		Secondary	Sheep	1:10000	GE Healthcare, NXA931
Rat IgG		Secondary	Goat	1:10000	GE Healthcare, NA935

Table 4. List of antibodies used for Western Blot for this thesis.

3.3.6. Chromatin Immunoprecipitation (ChIP)

3.3.6.1. Chromatin Immunoprecipitation Coupled to qPCR (ChIP-qPCR)

The ChIP method was used to obtain information about the binding of a protein to DNA, the regions and quantity. The main idea of the technique is to perform an immunoprecipitation on the protein of interest after a crosslinking step. Then, digestion

of the proteins present in the sample will leave only the DNA which will be identified and quantified by either qPCR or sequencing.

To start the protocol, we crosslinked a 100 mL culture at OD_{620}≈1 adding 1% formaldehyde. After 30 minutes shaking at room temperature, we transferred the culture containing formaldehyde to 4 ºC overnight (also shacking). After crosslinking, all steps were performed on ice and with cold buffers. We collected the crosslinked cells by centrifugation at 4000 rpm for 2 minutes (Eppendorf Centrifuge 5810 R) to obtain a pellet that we washed 3 times with cold 1x TBS (20 mM Tris-HCl pH 7.6 and 150 mM NaCl) and transferred to a clean DNA LoBind tube (Eppendorf, 0030108051). We spun the sample at 13000 rpm at 4 ºC and removed the supernatant.

Then, we resuspended the cell pellet in 100 µL of Buffer I (50 mM HEPES pH 7.4, 140 mM NaCl, 1 mM EDTA, 1% Triton-X100, 0.5% Nonidet P40, 1 mM PMSF and 1x Protease Inhibitor -Roche, 11873580001-) and added 1 volume of glass beads (Sigma Aldrich, G8772). We used a FastPrep-24 (MP Biomedicas, 116004500) at 4 ºC to homogenize the samples for 80 seconds at 6.5 N/m^2. Next, we pierced the tube containing the lysate on the top and the bottom to transfer its content to a new DNA LoBind tube by centrifugation at 800 rpm for 30 seconds at 4 ºC. Then, we added 350 µL of Buffer I on top of the glass beads and spun again to transferred it to the tube containing the lysate to obtain a total volume of 450 µL.

We sonicated the cell lysate at 20% amplitude for a total time of 2 minutes and 30 seconds with cycles of 15 seconds ON and 30 seconds OFF in a 450 Digital Sonifier (Branson). After sonication, we centrifuged the samples at 13000 rpm for 20 minutes at 4 ºC. We recovered the supernatant into a new DNA LoBind tube and repeated the cleaning step to obtain a clear lysate. We took note of the total volume obtained after this step and named it as V_{TOTAL} for calculations at the end of the protocol. We also transferred 5 µL (V_{TIC}) of this lysate to a new DNA LoBind tube with 95 µL of Elution Buffer (50 mM Tris-HCl pH 8, 10 mM EDTA and 1% SDS) and stored this sample at -20 ºC, named as TIC. Finally, we started the immunoprecipitation on the remaining lysate adding 4 µg of anti-FLAG M2 antibody (Sigma Aldrich, F3165) and incubated it overnight, rotating at 4 ºC.

To continue with the immunoprecipitation, we took 40 µL per sample of ProteinG-coupled DynaBeads (Invitrogen, 10003D) and washed them twice with Buffer I. After the washes, we resuspended the beads in their original volume with Buffer I and added 40 µL of the clean beads to each sample. The samples were incubated with the beads for 2 hours, rotating at 4 ºC. We recovered the supernatant after the incubation and transferred in into a new DNA LoBind tube. We brought the supernatant to a total volume of 500 µL adjusting the conditions to 1% SDS and 10 mM EDTA, we labeled this sample as DNA_{QC} (Quality Control). Then, we washed the beads 4 times with 900 µL of Buffer I, twice with Buffer II (50 mM HEPES PH7.4, 500 mM NaCl, 1 mM EDTA, 1% Triton-X100, 0.5% NP-40, 1 mM PMSF and 1x Protease Inhibitor), twice with Buffer III (10 mM Tris-

HCl pH 8, 250 mM LiCl, 1 mM EDTA, 0.5% sodium deoxycholate, 0.5% NP-40, 1 mM PMSF and 1x Protease Inhibitor) and once in 1x TE (10 mM Tris-HCl pH 8 and 1 mM EDTA). Finally, we resuspended the beads in 100 µL of Elution Buffer and incubated them at 65 ºC for 10 minutes, mixing well every 2 minutes. We recovered the supernatant of the elution and performed a secondary elution using 50 µL of Elution Buffer.

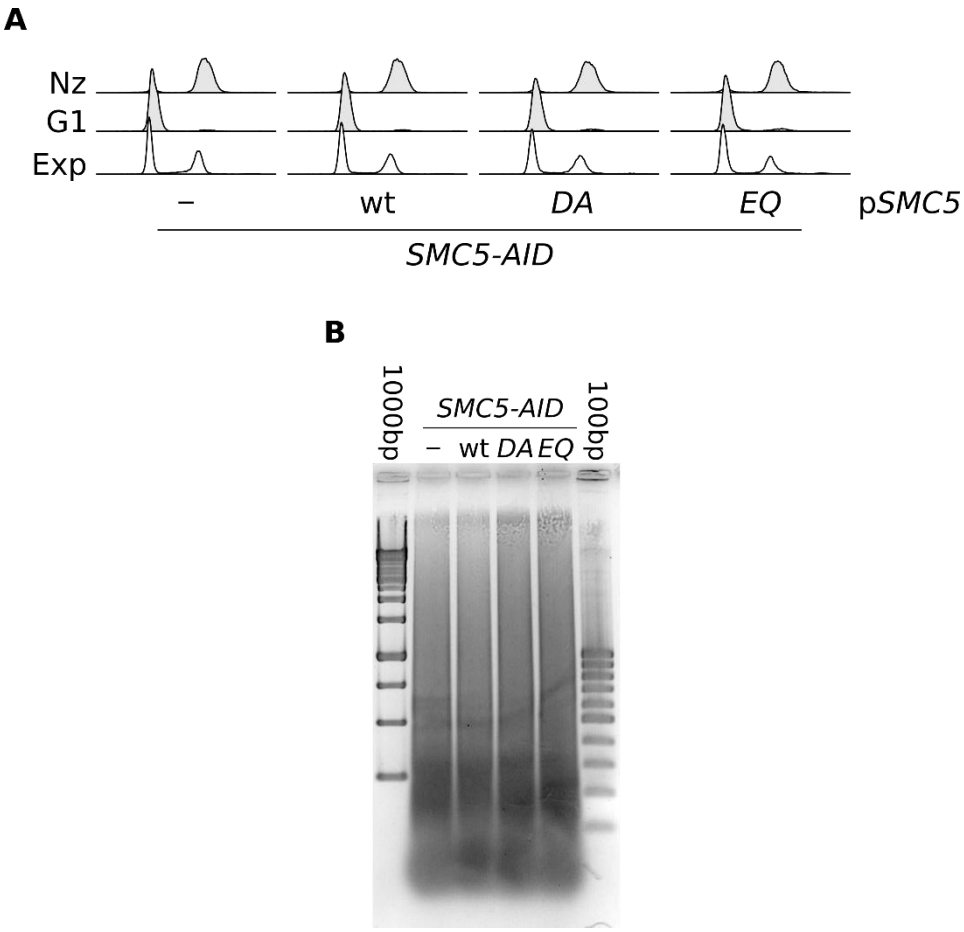

Figure 7. Parameter test for ChIP-qPCR. (A) FACS analysis of the cell arrests performed to collect the samples for ChIP-qPCR experiments displaying a good arrest in G2/M (Nz). **(B)** 2% agarose gel electrophoresis of DNA precipitated from the supernatant after the IP process.

After the immunoprecipitation, we processed the samples labeled as TIC, DNA_{QC} and IP. First, we incubated them overnight at 65 ºC in a water bath, to de-crosslink its content. After the decrosslinking step, we used the QiAquick PCR Purification Kit (Qiagen, 28104) as indicated by the manufacturer and eluted in 50 µL of the Elution Buffer included in the kit. The DNA obtained was used to perform a qPCR (section 3.3.1.2). We used the Cq determined by the Bio-Rad CFX Manager software to calculate the enrichment of a DNA sequence as follows:

$$\%\mathrm{IP} = (\mathrm{Cq_{TIC}} - \log_2 \frac{\mathrm{V_{TOTAL}}}{\mathrm{V_{TIC}}} - \mathrm{Cq_{IP}})^2 \cdot 100$$

To test the quality of the DNA obtained (regarding its quantity and sonication homogeneity), we added 125 µg of Proteinase K to the DNA_{QC} samples and incubated it at 37 ºC for 2 hours. Then, we added 1 volume of Phenol-Chloroform solution (Sigma Aldrich, P2069) to each sample and left it rotating for 5 minutes at room temperature into the fume hood before centrifuging it at 14000 rpm for 10 minutes. We recovered the upper layer in the tube and added NaOAc to a concentration of 0.3 M. We precipitated the DNA adding 1 mL of ethanol to the sample and incubating at -20 ºC for 30 minutes. Next, we centrifuged the sample at 13000 rpm for 20 minutes at 4 ºC and discarded the supernatant. Next, we washed the pellet in 70% ethanol and left it drying at room temperature. Finally, we resuspended the dry pellet with 39.2 µL of 1x TE containing 1.25 µg of RNAse A. After a 2-hour incubation at 37 ºC, we added 8.5 µL of Loading Buffer (3% Ficoll-400, 20 mM EDTA pH 8 and 0.02% SDS). We loaded an 8 µL aliquot into a 2% agarose gel (prepared with TAE buffer) to check its quality (Figure 7).

As it will be shown in the Results section of this document (section 4.1.1), Smc5 is bound to DNA in a higher quantity towards the end of S-Phase and mitosis. We decided to arrest cells in G2/M using nocodazole to perform the ChIP method. We checked this cell cycle arrest by FACS (Figure 7).

3.3.6.2. Chromatin Immunoprecipitation Coupled to Mass Sequencing (ChIP-seq)

The chromatin immunoprecipitation method described below is based on the protocol described by Bermejo et al., 2009.

To start the protocol, a 100 mL culture at OD_{620}≈1 was crosslinked by addition of 1% formaldehyde. After 30 minutes shaking at room temperature, the culture containing formaldehyde was transferred to 4 ºC overnight (also shacking). All steps after crosslinking were performed on ice and with cold buffers. The crosslinked cells were collected by centrifugation at 4000 rpm for 2 minutes (Eppendorf Centrifuge 5810 R) to obtain a pellet that was washed 3 times with cold 1x TBS and transferred to a clean DNA LoBind tube (Eppendorf, 0030108051). The sample was spun at 13000 rpm at 4 ºC and removed the supernatant.

The pellet was resuspended in 0.8 mL of Buffer I (50 mM HEPES PH 7.4, 500 mM NaCl, 1 mM EDTA, 1% Triton-X100, 0.1% sodium deoxycholate, 1 mM PMSF and 1x Protease Inhibitor) and separated into two 0.4 mL aliquots in screw-cap tubes. Then, glass beads were added up to the meniscus and the cells were broken in a multibead shaker (Bertin Instruments Precellys 24), five times at 5000 rpm and keeping the cells on ice for 5 minutes between cycles. Next, the bottom of the tube was punctured and the cap unscrewed to transfer the cell extract to a 15 mL tube by centrifugation at 2850 RCF for 1 minute at 4 ºC, twice. After each centrifugation, the flowthrough extract was resuspended and transferred to a 1.5 mL tube. The resulting extract was centrifuged at 13400 RCF for 1 minute at 4 ºC and a 5 µL sample of the SN was taken (for future western blot) before discarding it. Then, 450 µL of Buffer I were added and the DNA was sheared in a Sonifier 2508 (Branson) for 5 cycles of 15 seconds at tune 1.5, centrifuging

the samples at 2300 RCF for 1 minute at 4 ºC between sonication cycles. Finally, the extract was cleared by centrifugation at 16000 RCF for 5 minutes at 4ºC. The resulting supernatant was transferred to a pre-lubricated 1.7 mL tube and 5 µL were taken for western blot analysis.

The day before the experiment, protein G-coupled magnetic beads were prepared, taking 60 µL of beads per sample and placing them into a 1.7 mL pre-lubricated tube. The supernatant was removed and the beads were washed twice in 500 µL of PBS/BSA (1x Phosphate Buffered Saline containing 5 mg/ml Bovine Serum Albumin) before resuspension in 60 µL of PBS/BSA containing 20 µg of anti-FLAG M2 antibody (Sigma Aldrich, F3165). The beads with the antibody were incubated rotating overnight at 4 ºC. Immediately before use, the beads were washed twice with ice-cold PBS/BSA and resuspended in their original volume before adding 15 µL to each tube of cleared, sheared extract. The extract with the magnetic beads was incubated rotating at 4 ºC for 5 hours.

After the binding of the sample to the antibody in the beads, 5 µL of the supernatant were transferred to a new 1.5 µL tube to use it as the hybridization control and 5 µL more were taken for western blot analysis. Then, the beads were washed twice with 1 mL of Buffer I without protease inhibitors, twice in 1 mL of Buffer II (Buffer I without protease inhibitors and supplemented with 360 mM of NaCl), twice in Buffer III (10 mM Tris-HCl pH 8, 250 mM LiCl, 1 mM EDTA, 0.5% sodium deoxycholate, 0.5% NP-40) and once in ice cold 1x TE. After removing the TE, the beads were centrifuged at 800 RCF for 3 minutes at 4 ºC and the remaining supernatant was eliminated. Finally, the beads were resuspended in 40 µL of Elution Buffer (idem to section 3.3.6.1) and incubated at 65 ºC for 10 minutes before centrifugation at 16000 RCF for 1 minute at room temperature. 5 µL were taken for western blot analysis and the remaining supernatant was transferred to a new tube containing 4 volumes of 1x TE with 1% SDS (IP from now on). At this point, 95 µL of 1x TE with 1 % SDS were added to the sample that had been taken earlier for hybridization control (SUP from now on). Both SUP and IP were incubated overnight at 65 ºC to reverse the crosslinking.

Once the crosslink was reversed, the IP sample was brought to 200 µL with clean 1x TE. Then, 0.5 volumes of TE containing 60 µg of glycogen and 350 µg of Proteinase K were added to both SUP and IP and the samples were incubated at 37 ºC for 2 hours. After that, 12 µL of 5 M NaCl were added to the IP and 6 µL to the SUP. The DNA in the samples was separated from the protein twice with 1 volume of phenol-chloroform-isoamyl alcohol pH 8 at room temperature, with a centrifugation at 13400 RCF for 5 minutes after each extraction. Next, the DNA was precipitated with 2 volumes of ethanol at -20 ºC for 1 hour and centrifuged at 13400 RCF for 10 minutes at 4 ºC before washing the pellet with 1 mL of 80 % ethanol and let the pellet dry. Finally, the pellet was resuspended in 30 µL of TE containing 10 µg of RNAse A and incubated at 37 ºC for 1 hour before rejoining the two IP aliquots from each sample. A PCR Purification Kit was

used as indicated by the manufacturer, eluting the IP in 50 µL of the Elution Buffer in the kit and the SUP in 25 µL of the same buffer.

The ACCEL-NGS 1S Plus DNA Library Kit (Swift Biosciences, 10024) was used to create the libraries for the samples. The main protocol designed by the manufacturer was followed. However, only 7.5 µL of the sample (without adding TE) were used and the volumes of each reagent in the kit were also adapted to a half. During the indexing, the oligonucleotides used were the U001-U096 (Swift Biosciences, 19096 and 190384) in PCRs of 13 cycles for the IP samples and 11 cycles for the SUP. AMPure XP beads (Beckman Coulter, A63880) were used for the purification steps in the protocol.

The libraries obtained were analyzed using a BioAnalyzer (Agilent, G2939BA) to check the size and quality of the fragments in each library. The expected size of the fragments in the libraries for this experiment is 500bp. Afterwards, the DNA in the libraries was quantified by qPCR (section 3.3.1.2) using two dilutions for each library. The libraries and the quantification were able to be sequenced only if the difference in the quantification between both dilutions was under 10%. Finally, aliquots from each library were mixed in order to start the sequencing process using Illumina NextSeq 2000.

The bulk sequencing data was analyzed aligning it to the S288C reference genome using Bowtie 2, Samtools and Bedtools libraries. Further analyses were performed using R and Microsoft Excel with lists of features obtained from OriDB (for ARS, Siow et al., 2012), Fachinetti et al., 2010 (for terminators of replication) and SGD (Cherry et al., 2012). For the overlapping analysis, an overlapping feature was described as any feature that had coincided in at least 1 nucleotide with a peak detected in the samples. The sequencing data was also normalized in order to make it comparable between samples. For each kind of feature, the loci present in the list for that feature were placed randomly into the genome and the number of reads on those new locations was quantified. This process was repeated 10 times and the mean was subtracted from the original data, equaling the background for each of the samples.

3.3.7. Chromosome Spreads

This technique consists on the lysis of cells on a glass slide. During the lysis, only chromatin and the proteins bound to it remain attached to the glass slide. Then, an immunofluorescence permits the observation and quantification of the chromatin association of a protein.

We collected 5 mL of an exponentially growing culture (OD_{620}≈1) by centrifugation at 4000 rpm for 2 minutes. We suspended the cell pellet in 1 mL of dH_2O and transferred it to a new tube. Then, we washed the pellet with 900 µL of ice-cold Solution 1 (80 mM K_2HPO_4, 20 mM KH_2PO_4, 0.5 mM $MgCl_2$, 1.2 M sorbitol and 0.1% sodium azide, adjusted to pH 7.4 using KOH 3 M and filtered), centrifuging at 6000 rpm for 1 minute. Next, we resuspended the pellet in Spheroplasting Buffer (20 mM DTT, 0.2 mg/mL zymolyase

Z100T in Solution 1) and incubated it at 37 ºC until spheroplasts could be observed under the microscope (usually it took around 30 minutes). Once spheroplasts had been obtained, we stopped the cell wall digestion adding 500 µL of ice-cold Solution 2 (100 mM MES, 1 mM EDTA, 0.5 mM $MgCl_2$ and 1 M Sorbitol, adjusted to pH 6.4 using KOH 3 M and filtered). Since spheroplasts are fragile, we centrifuged them at 800 rpm for 8 minutes at 4ºC and eliminated the supernatant. We resuspended the pellet in 60 µL of Solution 2.

Once spheroplasts were ready, we placed a 10 µL droplet on a glass slide (at the center of its bottom quarter) into the fume hood on a flat surface. Then, we added a sequence of substances to the droplet stirring with the tip until seeing a homogenous mix at each step- First, we added 20 µL of Fixative Solution (4% paraformaldehyde, 3.4% sucrose), then, 40 µL of Lipsol 2% and finally, 40 µL of Fixative Solution. Then, we used the tip horizontally to spread the liquid over the bottom quarter of the slide, avoiding to touch the glass with it. All these steps have to be performed swiftly, having 3 pipettes ready, one for each volume used. We left the spreads drying overnight at room temperature inside the fume hood with the ventilation turned on.

The next day, when the liquid on the slides had dried, we placed them into a Coplin jar containing 1x PBS (0.58 M Na2HPO4, 0.17 M NaH2PO4 and 0.68M NaCl) for 10 minutes. Then, we dried their back on a clean paper tissue and placed them on a flat surface before adding 100 µL of freshly prepared Blocking Buffer (0.1 g milk powder, 0.25 g BSA -PAN Biotech, P06-139350- in 5 mL 1x PBS) all over the spread surface. After 10 minutes, we removed the Blocking Buffer and added 20 µL of freshly prepared primary antibody (1:500 in Blocking Buffer, precleared by spinning at 14000 rpm for 2 minutes) at the starting point of the last quarter of the slide. We used a coverslip to homogeneously extend the antibody all over the spread surface and left the slides incubating at room temperature for 1 hour into a humidity chamber. To remove the coverslip, we sunk the slides in 1x PBS, letting the coverslip slide slowly away from the glass slide. Next, we washed the slides three times in a Coplin jar containing 1x PBS for 10 minutes each wash. We prepared the secondary antibody at 1:1000 and used it on the slides in the same way as we had done for the primary antibody, with the three 1x PBS washes included, the only difference was that this time the incubation and washes were held in darkness.

After the immunofluorescence, we left the slides drying on a flat surface in darkness. Then, we added 5 µL of SlowFade (Life Technologies, S36936) containing Hoechst (1 µg/mL, Thermo Scientific, 62249) to each slide. A coverslip was used to spread the liquid and protect the chromosome spreads until we observed them under the microscope (Olympus BX51). We analyzed the pictures using ImageJ (Schneider et al., 2012) or AutoCD-fm (not published yet), a specific software developed for this study.

Alternatively, we used 2.5 mL of the initial culture instead of using 5 mL as described. We did so to mix these 2.5 mL with 2.5 mL of an internal standard. This

internal standard consists of a strain identical to the wild type condition used in the experiment and expressing a tagged version of histones, *HTB2-mCherry*. The red fluorescent tag permits identifying the internal standard cells and quantifying them to standardize any technical difference generated between slides.

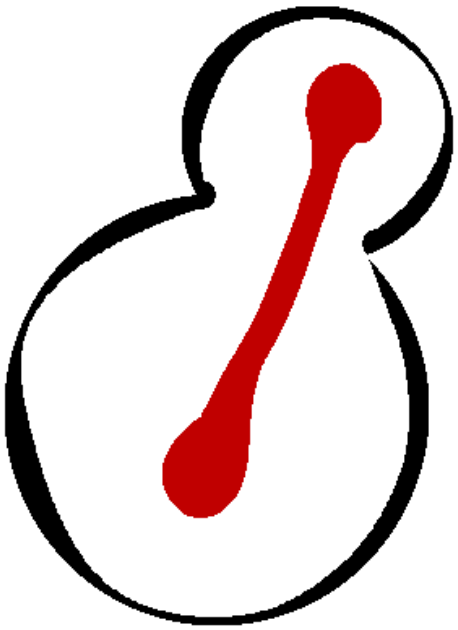

4 RESULTS

4. RESULTS

4.1. Analysis of Smc5/6 binding to Chromatin

SMC complexes are chromosome organizers that dynamically associate with DNA. Their essential functions are directly related to their ability to interact with chromatin and organize it into superstructures such as chromatin loops or sister chromatid pairs. While we start to understand how cohesin and condensin interact with DNA to arrange chromosomes, very little is known about how, when and where Smc5/6 associates with DNA. To fill this gap, we decided to analyze the binding of Smc5/6 to chromatin using immunofluorescence on chromosome spreads. In this part of the thesis, we aim to understand different aspects of the binding of Smc5 to chromatin such as its dependence on the cell cycle progression, DNA damage, accumulation of replication/recombination intermediates or the role of different Smc5/6 subcomplexes.

4.1.1. Smc5 Binding to Chromatin Increases During DNA Replication and Mitosis

First, we addressed whether the cell cycle has any effect on the association of Smc5/6 with chromatin. Other groups have previously performed ChIP experiments of the Smc5/6 complex at different stages of the cell cycle (Lindroos et al., 2006) showing that the association of Smc5/6 subunits with chromatin increases as the cell cycle advances, reaching a peak during G2/M, after nocodazole treatment. To validate this observation, we took an exponentially growing *Saccharomyces cerevisiae* culture, expressing a 6xHA-tagged version of Smc5, and arrested the cells in G1 with alpha factor. Next, we released them from the G1 block in the presence of different drugs to arrest cells at later phases in the cell cycle. Hydroxyurea, which reduces nucleotide availability, stalling replication forks. MMS, an alkylating agent which induces lesions on DNA, blocks replication forks and activates the DNA damage checkpoint in S-Phase. And nocodazole, which inhibits microtubules polymerization and activates the spindle assembly checkpoint during mitosis.

Cell cycle arrests were confirmed by FACS (Figure 8C). Next, we performed chromosome spreads and checked that the signal was specific, using a control sample from cells expressing no HA (Figure 8A, B). We quantified the signal in the different samples and observed that Smc5 binding to chromatin increased as cells were arrested at more advanced points in the cell cycle. Nocodazole-treated cells displayed the highest Smc5-6xHA signal on chromatin, followed by those cultures arrested in MMS or HU and with G1 arrested cells showing the lowest signal (Figure 8A, B).

To avoid artifacts due to replicative (HU), DNA damage (MMS) or spindle (Nz) checkpoint activation, we repeated the experiment without further arrest after the release from G1. Instead, we collected samples from the synchronous culture every 15 minutes. FACS analysis showed that cells entered into S-Phase 30 minutes after G1 release, with genome replication being completed at 75 minutes after release (Figure 9C). Chromosome spreads showed that chromatin-bound Smc5 increased as cells exited

from the G1 arrest, reaching a peak 60 minutes after release, towards the end of the S-Phase (Figure 9A, B). From then onwards, the binding of Smc5 to chromatin decreased. At later time points, when the culture loss synchronicity, the signal from chromosome spreads started to look more similar to an exponentially growing culture

Overall, we conclude that the binding of Smc5 to chromatin increases during DNA replication. This binding becomes maximal at the end of DNA replication, shortly before chromosome segregation. After mitosis, binding of Smc5 to chromatin gradually reduces until the cell enters the next cell cycle.

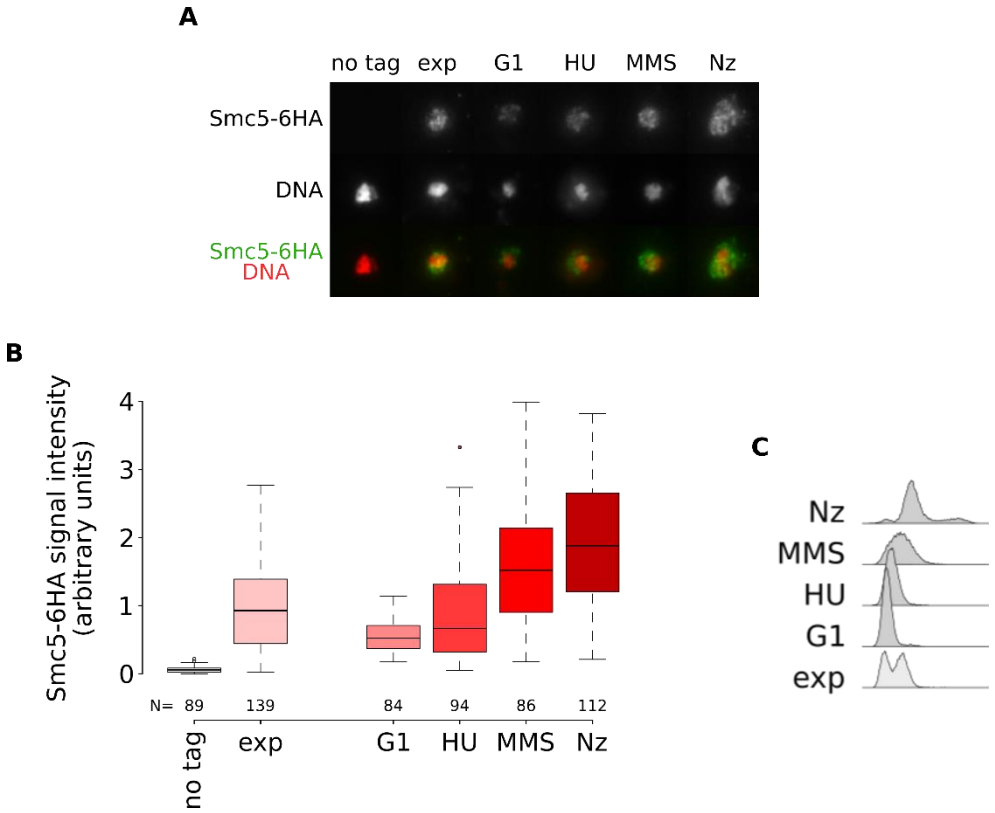

Figure 8. Smc5 binding to chromatin is increased towards the end of cell cycle. (A) Collage of images taken from the different samples after performing chromosome spreads. Cultures treated with hydroxyurea, MMS or nocodazole had been previously arrested in G1 with alpha factor. For each sample, it is shown a representative nucleus of the whole population. The images have been processed to add colors, HA has been colored with green and DNA with red. Rat monoclonal antibody was used to perform the immunofluorescence against HA (clone 3F10). DNA was stained with Hoechst **(B)** Quantification of the signal obtained in the chromosome spreads images. The N represents the number of nuclei quantified for each sample. All images were taken with the same settings in the microscope and, afterwards, the quantifications have been normalized with the mean of the values in the exponential sample. The highest quantification belongs to samples treated with nocodazole. **(C)** FACS profiles for the samples to which chromosome spreads have been performed. 20000 cells were analyzed for each sample.

Strain in this figure: AS499

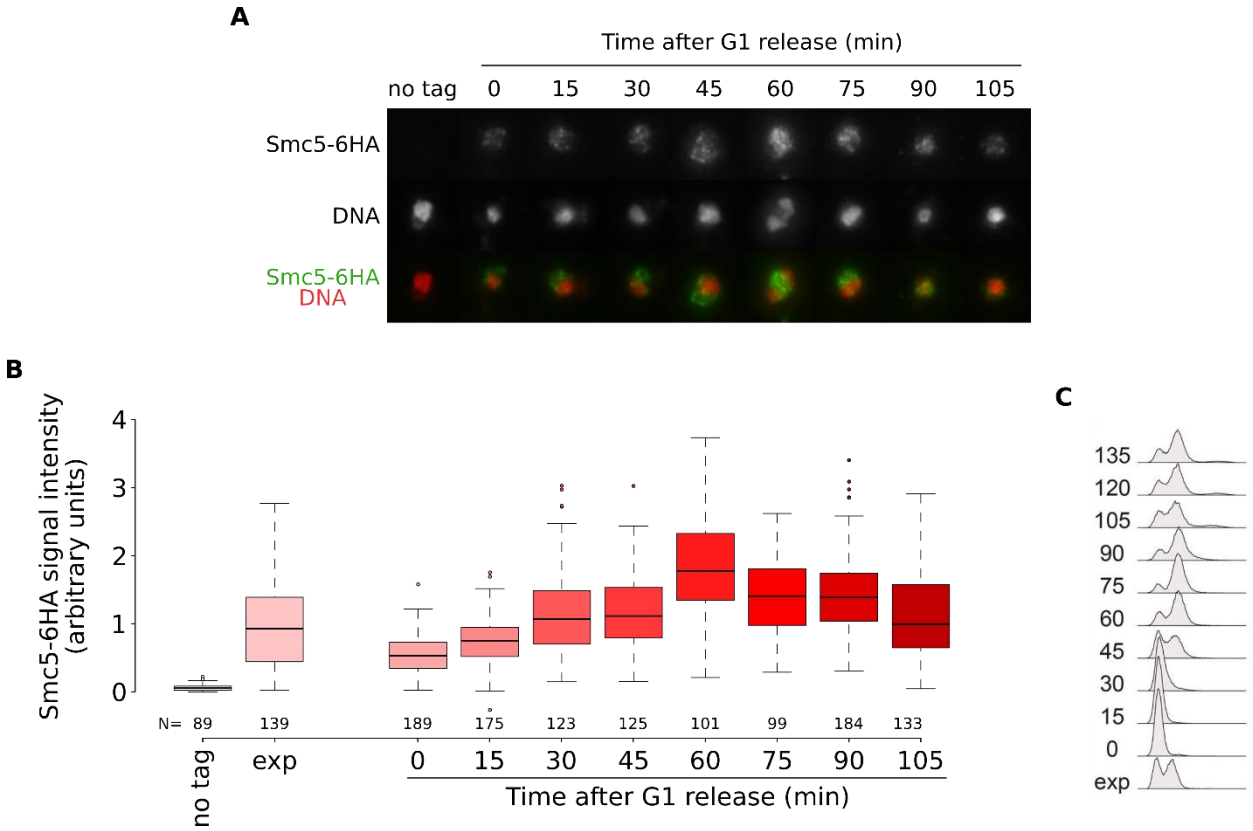

Figure 9. Smc5 binding to chromatin is increased towards the end of DNA replication. (A) Collage of images taken from the different samples after performing chromosome spreads. For each sample, it is shown a representative nucleus of the whole population. The images have been processed to add colors, HA has been colored with green and DNA with red. Rat monoclonal antibody was used to perform the immunofluorescence against HA (clone 3F10). DNA was stained with Hoechst **(B)** Quantification of the signal obtained in the chromosome spreads images. The N represents the number of nuclei quantified for each sample. All images were taken with the same settings in the microscope and, afterwards, have been normalized with the mean of the values in the exponential sample. The highest quantification belongs to samples taken at 60 minutes after G1 release. **(C)** FACS profiles for the samples to which chromosome spreads have been performed. 20000 cells were analyzed for each sample. Replication of DNA starts 30 minutes after G1 release and reaches an end after 60 minutes total time, which correspond to the highest quantification in panel (B).

Strain in this figure: AS499

4.1.2. Smc5 Binding to Replication and/or Recombination Intermediates

The Smc5/6 complex plays a key role in chromosome disjunction. This is more evident in the rDNA array. However, chromosome segregation defects can also be observed at other genomic locations after replication fork damage, even when induced by very low doses of alkylation damage (Bermúdez-López et al., 2010). Disjunction defects seem to stem from the presence of replication and/or recombination intermediates that are not properly resolved before anaphase onset. Thus, we hypothesized that Smc5 could be binding to specific structures to promote their removal.

When a replication fork encounters a lesion in the template strand, it stalls. Different proteins are recruited to damaged forks to tolerate lesions through bypass of the lesion (Figure 10). There are two main DNA damage tolerance pathways in yeast: One of them involves the activation of translesion synthesis polymerases, but plays a minor role in DNA damage tolerance. The other one promotes a switch in the template used by DNA polymerases and depends on PCNA poly-ubiquitination and recombination to swap the damaged template for the undamaged strand on the newly replicated sister chromatid, thus generating recombination intermediates. These intermediates are finally resolved by the STR (Sgs1-Top3-Rmi) dissolvase complex, the Mus81-Mms4 structure selective endonuclease or the Yen1 resolvase. STR is the major activity involved in elimination of recombination intermediates in S-Phase, while Mus81-Mms4 and Yen1 become active at the G2/M transition and late mitosis, respectively (Pfander & Matos, 2017). Importantly, inactivation of dissolvases/resolvases leads to the accumulation of recombination intermediates upon DNA damage.

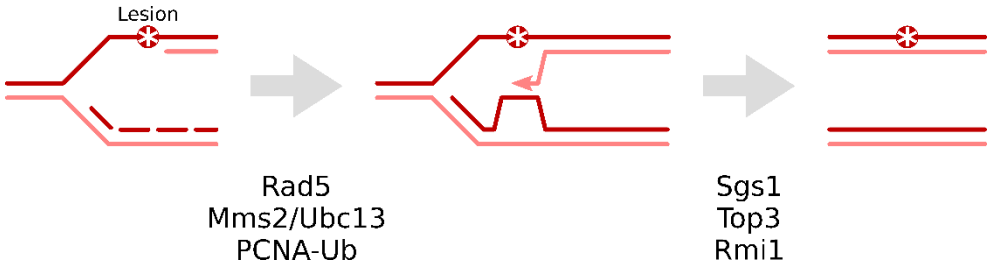

Figure 10. Template switch during DNA replication in the presence of a lesion. Schematic explanation of template switch. Rad5 and Mms2 play a role in strand invasion and, afterwards, Sgs1 is involved in the resolution of recombination intermediates.

To test the effect of accumulating recombination intermediates on Smc5/6 association with chromatin, we deleted *SGS1* or *MMS4* in a strain expressing Smc5-6xHA. We treated exponentially growing cultures of these strains with 0.02% MMS for 30 minutes and performed chromosome spreads. As expected, MMS treatment of wild type cells increased the levels of Smc5 chromatin binding (Figure 11). Deletion of *SGS1* did not significantly affect the binding of Smc5 to DNA upon MMS treatment, relative to wild type cells (Figure 11). MMS treatment on the *mms4* mutant strain, slightly increased the quantity of Smc5 bound to chromatin (Figure 11).

Next, we analyzed the effects of *mms2Δ* and *rad5Δ* on Smc5/6 association with chromatin. Mms2 is the E2 and Rad5 the E3 for PCNA polyubiquitination, and their inactivation preclude template switch (Branzei et al., 2004). We performed chromosome spreads on these strains treated or not with 0.02% MMS. Again, we could observe an increase in the chromatin-associated Smc5 in wild type cells upon DNA damage (Figure 12). However, chromatin binding was significantly higher in *mms2Δ* or *rad5Δ* cells (Figure 12).

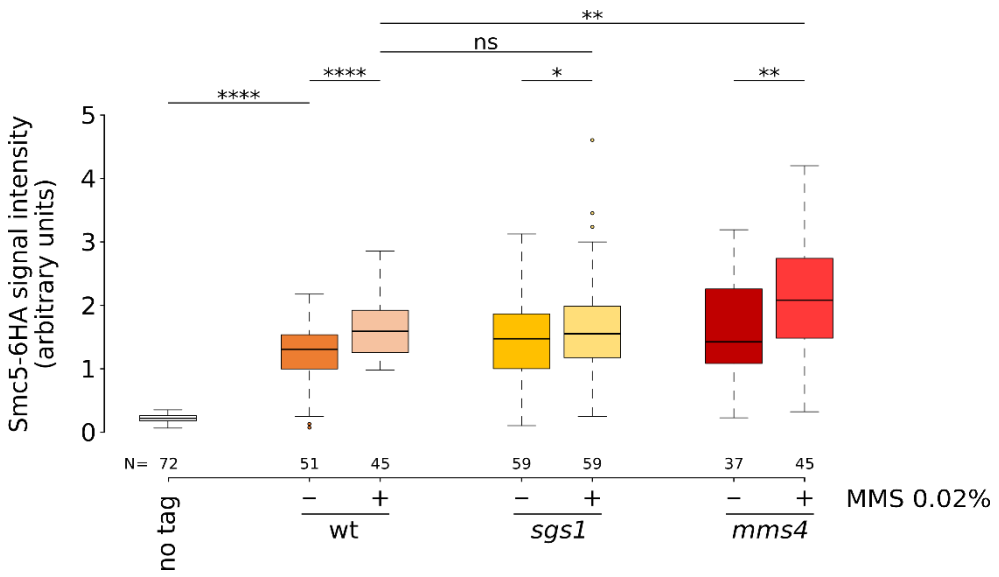

Figure 11. Accumulation of recombination intermediates recruits a slightly higher quantity of Smc5 to chromatin compared to a normal situation. (A) Quantification of the signal obtained in the chromosome spreads images. The N represents the number of nuclei quantified for each sample. All images were taken with the same settings in the microscope. All samples contained an internal standard to normalize all the quantifications. Accumulation of recombination intermediates (X shaped structures) is induced with MMS in sgs1 and mms4 mutant strains. Student's test has been performed for each pair of samples. This is the result of one technical and biological repetition out of three repetitive results.

Significance levels are indicated with the following key: p>0,05 (ns), p≤0,05 (*), p≤0,01 (**), p≤0,001 (***), p≤0,0001 (****).

Strains in this figure: BY5563, YSI3497, YSI3528 & YSI3588

Finally, we also tested a *rad52Δ* mutant strain. This strain is not able to perform strand invasion after the replication fork stalls. Interestingly, compared to a wild type strain, these cells had a higher quantity of Smc5 bound to chromatin in the absence of DNA damage (Figure 13). Upon treatment with MMS, *rad52Δ* cells substantially increased Smc5 binding to DNA (Figure 13).

Overall, our results indicate that mutations in template switch lesion bypass significantly increase the binding of Smc5 to chromatin in response to DNA damage, while inactivation of recombination intermediate resolution does not seem to have an effect. These results suggest that Smc5/6 preferentially binds to damaged replication forks, rather than to the recombination intermediates generated after bypass of DNA lesions.

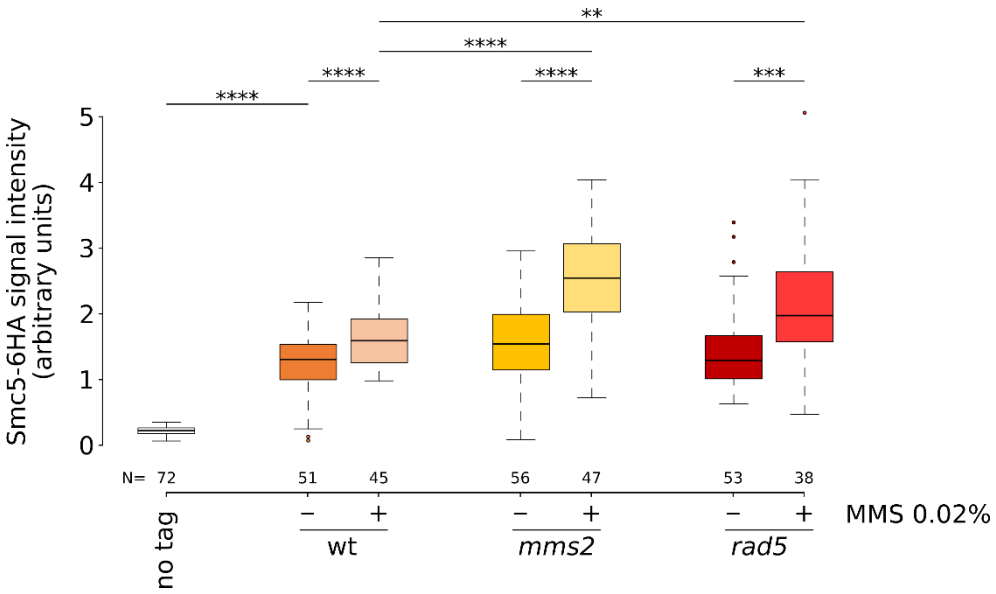

Figure 12. Accumulation of stalled replication forks promotes the recruitment of Smc5 to chromatin. **(A)** Quantification of the signal obtained in the chromosome spreads images. The N represents the number of nuclei quantified for each sample. Each of the dots shows the quantification for a single nucleus and the black bar is the median of all the nuclei in the sample. All images were taken with the same settings in the microscope. All samples contained an internal standard to normalize all the quantifications. Mutant strains for mms2 or rad5 were used to accumulate stalled replication forks. Both mutant strains promote the binding of Smc5 on chromatin. Student's test has been performed for each pair of samples. This is the result of one technical and biological repetition out of three repetitive results.

Significance levels are indicated with the following key: p>0,05 (ns), p≤0,05 (*), p≤0,01 (**), p≤0,001 (***), p≤0,0001 (****).

Strains in this figure: BY5563, YSI3497, YSI3501 & YSI3531

4.1.3. An Integer Smc5/6 Complex is Required for Binding to Chromatin

Besides the core Smc5 and Smc6 proteins, other subunits of the complex were proposed to have DNA binding domains and may modulate association of the complex with DNA. For example, the Nse1/3/4 subcomplex has been shown to associate with DNA in vitro, using a positively charged patch on Nse1/Nse3 as a docking site (Zabrady et al., 2016). In addition, the Nse5/Nse6 subcomplex has been proposed to regulate the association of Smc5/6 with DNA (Bustard et al., 2012). Therefore, we tested the effect of downregulating different subunits in the complex: Nse3, Nse4 and Nse5. To do so, we used either an auxin inducible degron, which promotes the degradation of the protein upon auxin treatment, or thermosensitive alleles.

We fused an auxin inducible degron (AID) tag to Nse4, the kleisin subunit of Smc5/6, in a strain expressing Smc5-6xHA from its endogenous location. We took

samples of exponentially growing cultures treated or not with 1 mM auxin. It is worth noting that the cells containing the AID tagged Nse4 displayed lower levels of Smc5 than the wild type strain (Figure 14D). This observation was independent of the presence of auxin in the media.

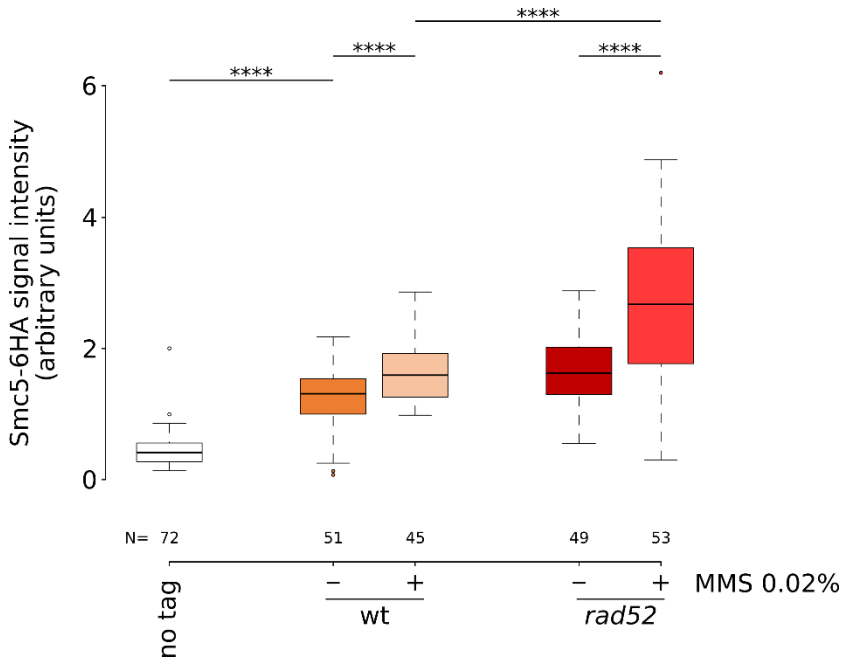

Figure 13. Blocking strand invasion after a double strand break promotes Smc5 recruiting to chromatin. (A) Quantification of the signal obtained in the chromosome spreads images. The N represents the number of nuclei quantified for each sample. Each of the dots shows the quantification for a single nucleus and the black bar is the median of all the nuclei in the sample. All images were taken with the same settings in the microscope. All samples contained an internal standard to normalize all the quantifications. A mutant strain for rad52 was used to block strand invasion. It displays a variable behavior even in the absence of induced DNA damage. Levels of Smc5 bound to chromatin in the presence of double strand breaks is increased in comparison to a non-treated sample. Student's test has been performed for each pair of samples. This is the result of one technical and biological repetition out of three repetitive results.

Significance levels are indicated with the following key: p>0,05 (ns), p≤0,05 (*), p≤0,01 (**), p≤0,001 (***), p≤0,0001 (****).

Strains in this figure: BY5563, YSI3497 & YSI3582

In agreement with the western blot, a lower quantity of Smc5 was bound to chromatin in *nse4-AID* cells (Figure 14A, B). Treatment of the wild type strain with auxin did not affect the binding of Smc5 to chromatin (Figure 14A, B). In contrast, Smc5 bound to chromatin was significantly decreased when Nse4-AID was degraded (Figure 13A, B), indicating that the kleisin subunit in the Smc5/6 complex is required for its association with chromatin.

Next, we tested the binding of Smc5 to chromatin in strains containing thermosensitive alleles *nse3*-2 or *nse5-2*. Cultures were grown overnight at 25 ºC and shifted to 35 ºC for 1 hour before preparation of chromosome spreads. At the permissive

temperature, there was no difference in Smc5-6xHA binding to chromatin between wild type and mutant cells (Figure 15). However, while wild type cells maintained Smc5 on chromosomes after shift to the restrictive temperature, thermosensitive alleles significantly reduced Smc5 binding to chromatin. We conclude that both the Nse1/Nse3/Nse4 and Nse5/Nse6 subcomplexes are required for efficient association of Smc5/6 with chromatin.

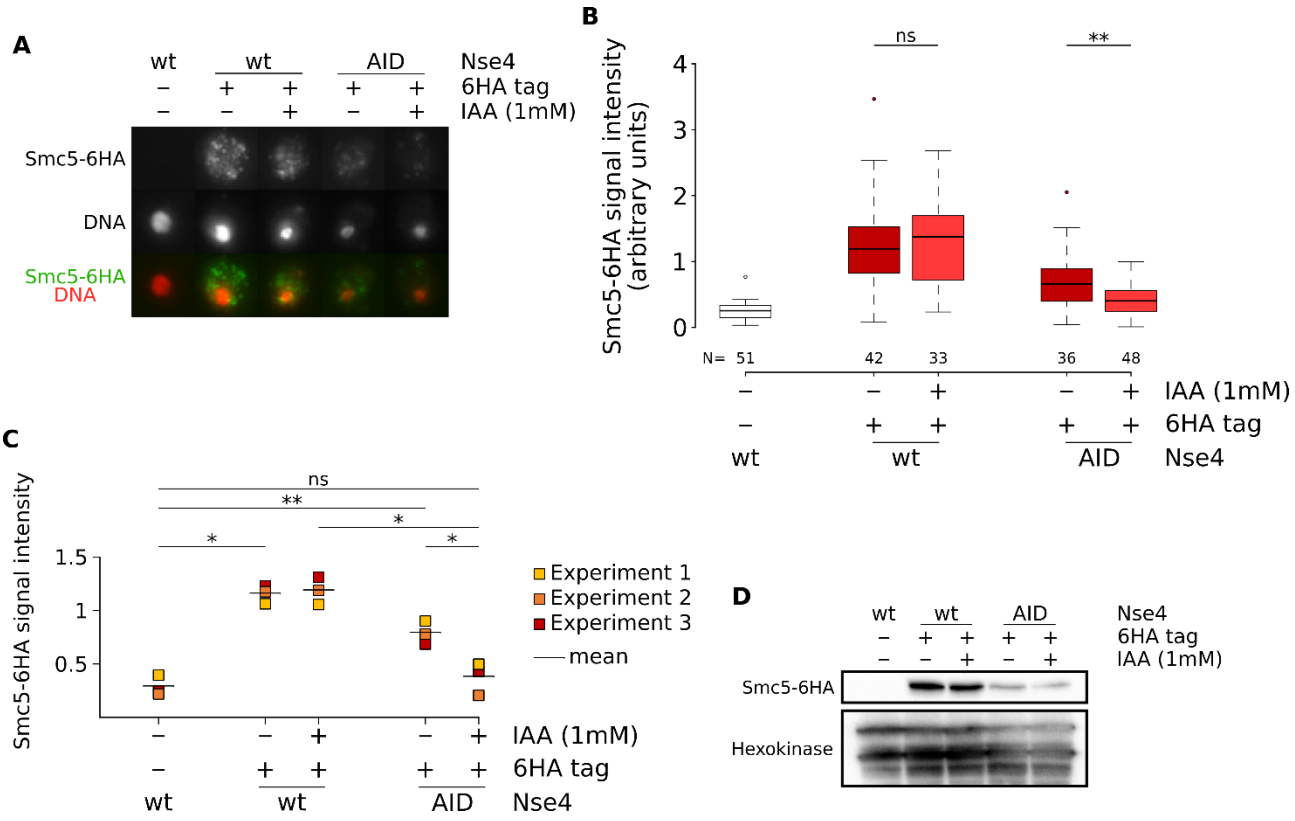

Figure 14. Smc5 binding to chromatin is dependent on its kleisin subunit, Nse4. (A) Collage of images taken from the different samples after performing chromosome spreads. For each sample, it is shown a representative nucleus of the whole population. The images have been processed to add colors, HA has been colored with green and DNA with red. Rat monoclonal antibody was used to perform the immunofluorescence against HA (clone 3F10). DNA was stained with Hoechst **(B)** Quantification of the signal obtained in the chromosome spreads images. The N represents the number of nuclei quantified for each sample. All images were taken with the same settings in the microscope. All samples contained an internal standard to normalize all the quantifications. Depletion of Nse4 by addition of auxin (IAA) decreases the amount of Smc5 bound to chromatin. Student's test has been performed for each pair of samples. **(C)** Summary of the quantifications for three independent repetitions of the chromosome spreads. Each point shows the mean obtained for each sample and the black bar is the mean value of the three experiments. Paired Student's test has been performed for each pair of samples. **(D)** Western Blot showing the total quantity of Smc5 in the samples taken to perform the chromosome spreads represented in panel (B). Detection of Hexokinase was used as a loading control. Rat monoclonal antibody against HA (clone 3F10) and rabbit polyclonal antibody against Hexokinase were used. Tagging Nse4 with an auxin inducible degron decreases the total amount of Smc5 in the cell extract.

Significance levels are indicated with the following key: p>0,05 (ns), p≤0,05 (*), p≤0,01 (**), p≤0,001 (***), p≤0,0001 (****).

Strains in this figure: AS499, YTR1428 & YMB1452

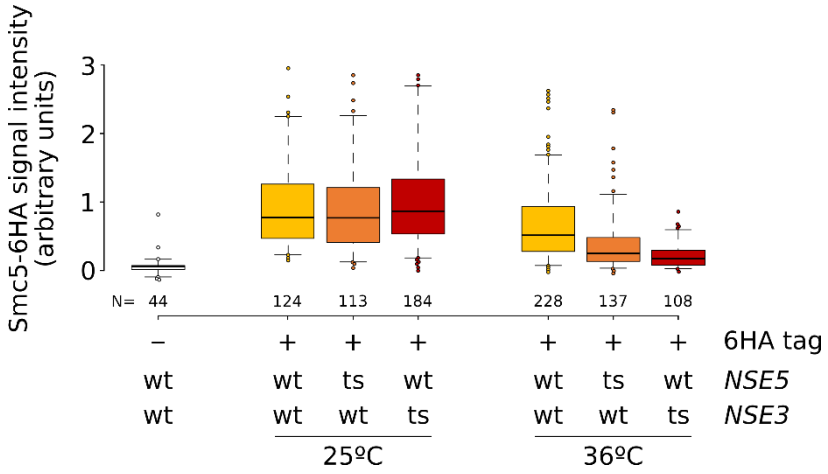

Figure 15. Smc5 binding to chromatin is dependent on Nse3 and Nse5. Quantification of the signal obtained in the chromosome spreads images of *nse3-2* and *nse5-2*cells. The N represents the number of nuclei quantified for each sample. All images were taken with the same settings in the microscope.

Strains in this figure: AS499, YTR1100 & YMB1345

4.2. Analysis of ATPase Function in Smc5

The ATPase at the globular domains of the SMC subunits in cohesin and condensin controls the dynamic interaction and loading of the complex onto DNA (Arumugam et al., 2006; Thadani et al., 2018). This mechanism has also been demonstrated in the bacterial SMC complex (M. Hirano, 2001). We hypothesized that the ATPases of Smc5 and Smc6 could be playing a similar role in the interaction of the complex with chromatin. In the following section, we analyze the role of the ATPase of Smc5 in binding to chromatin.

4.2.1. Generation of Smc5 ATPase Mutants and Phenotypical Study

To study the ATPase of Smc5, we designed similar mutations as those used to study the ATPase of cohesin (Arumugam et al., 2003). Different mutant alleles of the gene can block the ATPase cycle at different steps (Figure 16B, C). A lysine to isoleucine point mutation in the Walker A domain and an aspartic acid to alanine mutation in the Walker B domain can block the binding of ATP to the ATPase head. A serine to arginine mutation in the signature motif of the ATPase prevents the dimerization of the ATPase heads of both SMC subunits. Finally, a glutamic acid to glutamine mutation, located in the catalytic domain in Walker B, blocks ATP hydrolysis.

The equivalent residues and mutations in the yeast Smc5 proteins are: K75I (KI), D1014A (DA), S987R (SR) and E1015Q (EQ) (Figure 16A).

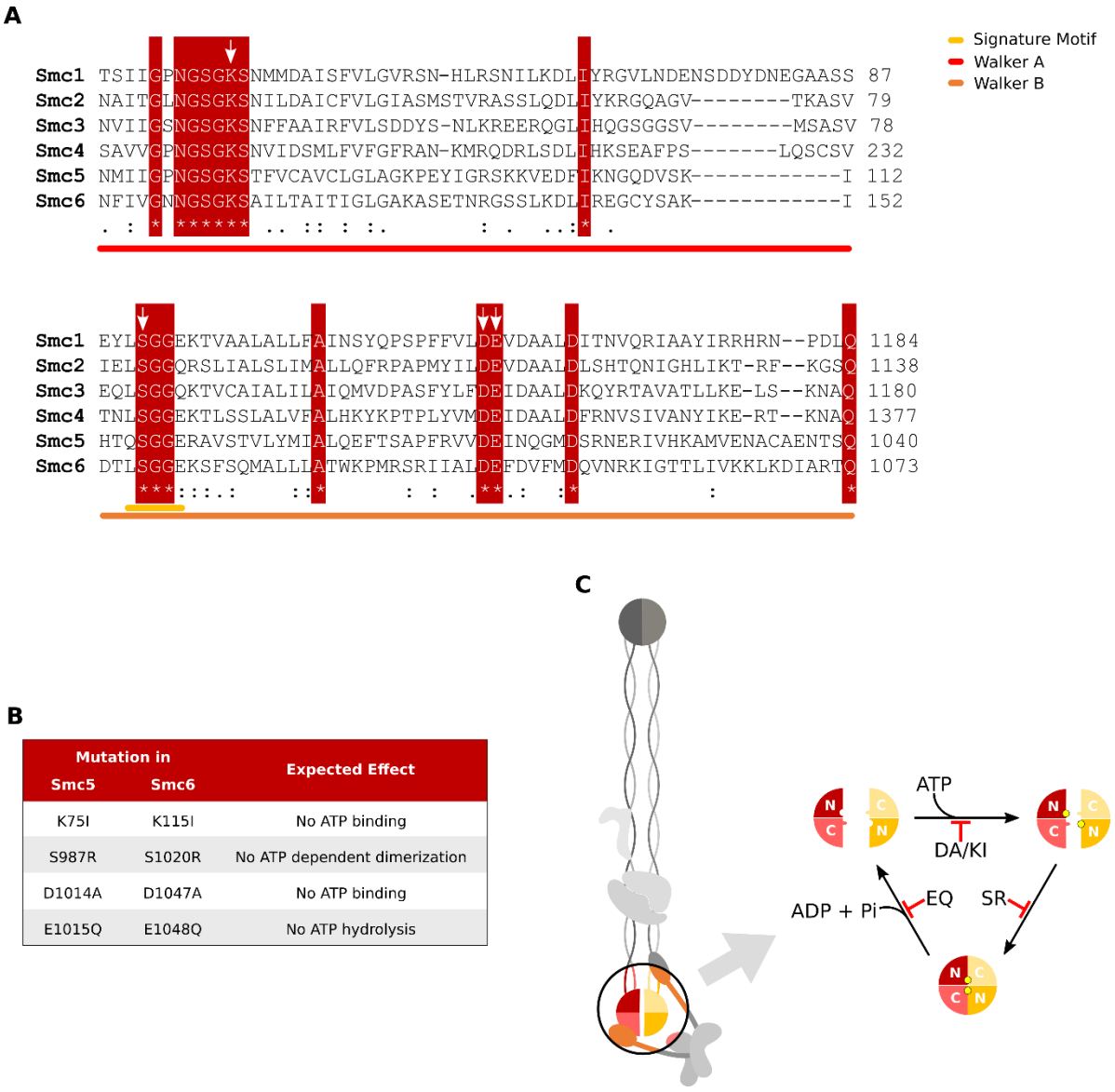

Mutation in Smc5	Mutation in Smc6	Expected Effect
K75I	K115I	No ATP binding
S987R	S1020R	No ATP dependent dimerization
D1014A	D1047A	No ATP binding
E1015Q	E1048Q	No ATP hydrolysis

Figure 16. Diferent mutant alleles can be generated to block the ATPase cycle of Smc5 and Smc6. **(A)** Allignment of the different SMC proteins of Saccharomyces cerevisiae. Red highlight indicates conserved residues in all the proteins. Coloured lines below the alignment indicate the domain to which the aligned region belongs. White arrows point the residues that were mutated in order to block the different steps of the ATPase cycle. **(B)** Table indicating the different mutations performed on the Smc5 and Smc6 ATPases and the expected effect for each of these mutations. **(C)** Schematic representation of the ATPase cycle of the Smc5/6 complex. First, they bind ATP, then by interaction with the signature motive, the heads of both subunits interact and dimerize. Finally, the heads dimerization activates de catalytic activity of both subunits and they hydrolyze ATP, losing interaction and restarting the cycle. Each of these steps can be blocked with a mutant allele: ATP binding with the KI or DA alleles, heads dimerization with the SR allele and hydrolysis with the EQ allele.

4.2.1.1. The ATPase Function in Smc5 is Essential for Cell Growth

Smc5/6 subunits are essential in yeast, and mutations in the ATPase cycle are expected to be lethal (Bustard et al., 2016; Hu et al., 2005; Moradi-Fard et al., 2016;

Torres-Rosell, Machin, et al., 2005). To analyze the role of ATPase mutants, we first introduced the mutations in centromeric or integrative Smc5-expressing plasmids. The mutant alleles displayed a recessive effect when co-expressed with the endogenous *SMC5*. Hence, we decided to use strains in which we could conditionally control the expression or degradation of the Smc5 protein expressed from the endogenous location.

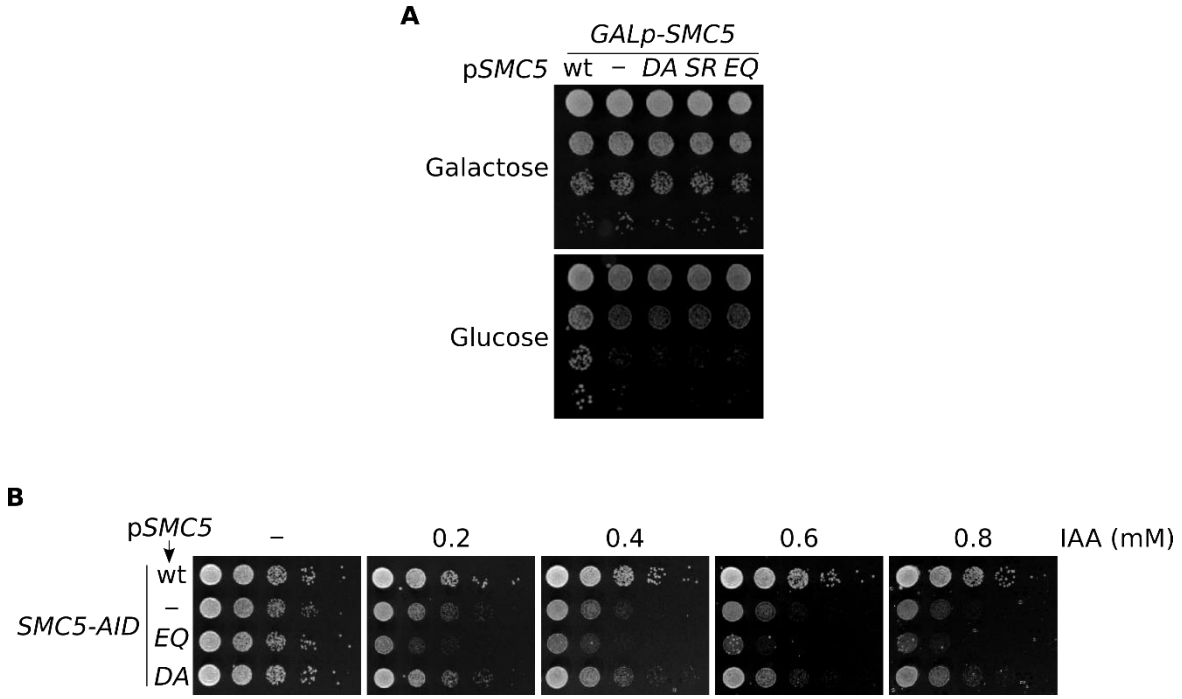

Figure 17. Smc5 ATPase mutations result in loss of viability. (A) Plates displaying serial dilutions of a strain dependent on the different ATPase mutant alleles. The endogenous SMC5 was under control of a galactose promoter to control its expression depending on the carbon source. None of the ATPase mutant alleles can sustain cell viability, while a wild type copy of Smc5 recovers normal growth. **(B)** Plates displaying serial dilutions of a strain dependent on the different ATPase mutant alleles. The endogenous SMC5 is tagged with an auxin inducible degron (AID) to deplete it with the addition of auxin (IAA). None of the ATPase mutants can sustain cell viability, while a wild type copy of Smc5 recovers normal growth. At lower concentrations of IAA can be observed a dominant negative effect of the EQ allele (ATP hydrolysis blockage).

Strains in this figure: YTR1437, YMB1905, YMB1937, YMB1938, YTR3690, YTR3691, YMT4270, YMT4272 & YMT4656

First, we transformed centromeric plasmids containing each of the ATPase mutant *smc5* alleles into a *GALp-SMC5* strain, which expresses the wild type *SMC5* gene from the *GAL* promoter. We cultured cells in galactose, co-expressing the endogenous Smc5 with the different ATPase mutant versions of the protein. The growth of all these strains was equal to that of the wild type strain. In contrast, when glucose was added to the media, none of the ATPase mutants could sustain cell viability either on plate (Figure 17A) or in liquid media.

Next, we used a yeast strain with the endogenous *SMC5* gene fused to an auxin inducible degron, which sensitizes cells to the presence of auxin (Indole-3-acetic acid, IAA). We introduced the mutant *smc5* alleles by integration of a plasmid into the endogenous *SMC5* locus. This integration generates two tandem copies of *SMC5*, first the ATPase mutant allele followed by the *smc5-AID* allele. We plated serial dilutions of cultures from these strains on plates with increasing auxin concentration, from 0 to 0.8 mM IAA. We observed that the strain containing only the AID tag on Smc5, grew worse at higher IAA concentrations (Figure 17B). The addition of a wild type copy of Smc5 rescued growth independently of the auxin concentration. Blocking ATP binding to Smc5 with the DA mutant allele resulted in a growth similar to the strain with no Smc5 expression. Interestingly, the cells bearing an EQ version of Smc5 displayed a poorer growth than the cells not expressing Smc5, in the presence of even low auxin concentrations. Thus, the *smc5-EQ* mutant is a partially dominant negative allele, whose penetrance becomes more evident as its intracellular concentration increases relative to a functional protein (in this experiment, the Smc5-AID protein). In contrast, KI, DA or SR alleles are recessive. We conclude that the *smc5-EQ* mutant has a gain of function that might be toxic to the cell in the absence of the wild type *SMC5* allele.

4.2.2. The ATPase Activity in Smc5 Controls Chromatin Association of the Smc5/6 Complex

To test if the ATPase activity of Smc5/6 controls its binding to chromatin, we transformed the 6HA-tagged *smc5* ATPase mutant alleles into an *smc5-AID* strain. Then, we treated exponentially growing cultures with 1 mM IAA at 25ºC for 30 minutes. Subsequently, we collected samples for chromosome spread analysis, a technique that allows cell-to-cell quantification of the chromatin-bound fraction of a DNA-binding protein.

Cells that did not express Smc5 displayed no signal in the immunofluorescence, (Figure 18A, B). Expression of the DA mutant allele, which blocks the binding of ATP to the protein, reduced the signal on chromosome spreads, relative to the wild type Smc5, suggesting that ATP binding mutants do not efficiently associate with DNA. Surprisingly, the Smc5-EQ protein displayed an increase in binding to chromatin, compared to the wild type protein, accompanied by an increase of the sumoylated fraction of the protein detected by Western Blot (Figure 18D) (Bermúdez-López et al., 2015). These results indicate that binding of ATP to the Smc5 head domain, but not its hydrolysis, is required for chromatin association of the Smc5/6 complex. In addition, they suggest that ATP hydrolysis might be required to remove the Smc5/6 complex from chromatin. This hypothesis could be compatible with a model in which a complete ATPase cycle is required for the dynamic engagement and release of the Smc5/6 complex with chromatin. Thus, defects in ATP hydrolysis might leave Smc5/6 complexes trapped on DNA during the loading reaction.

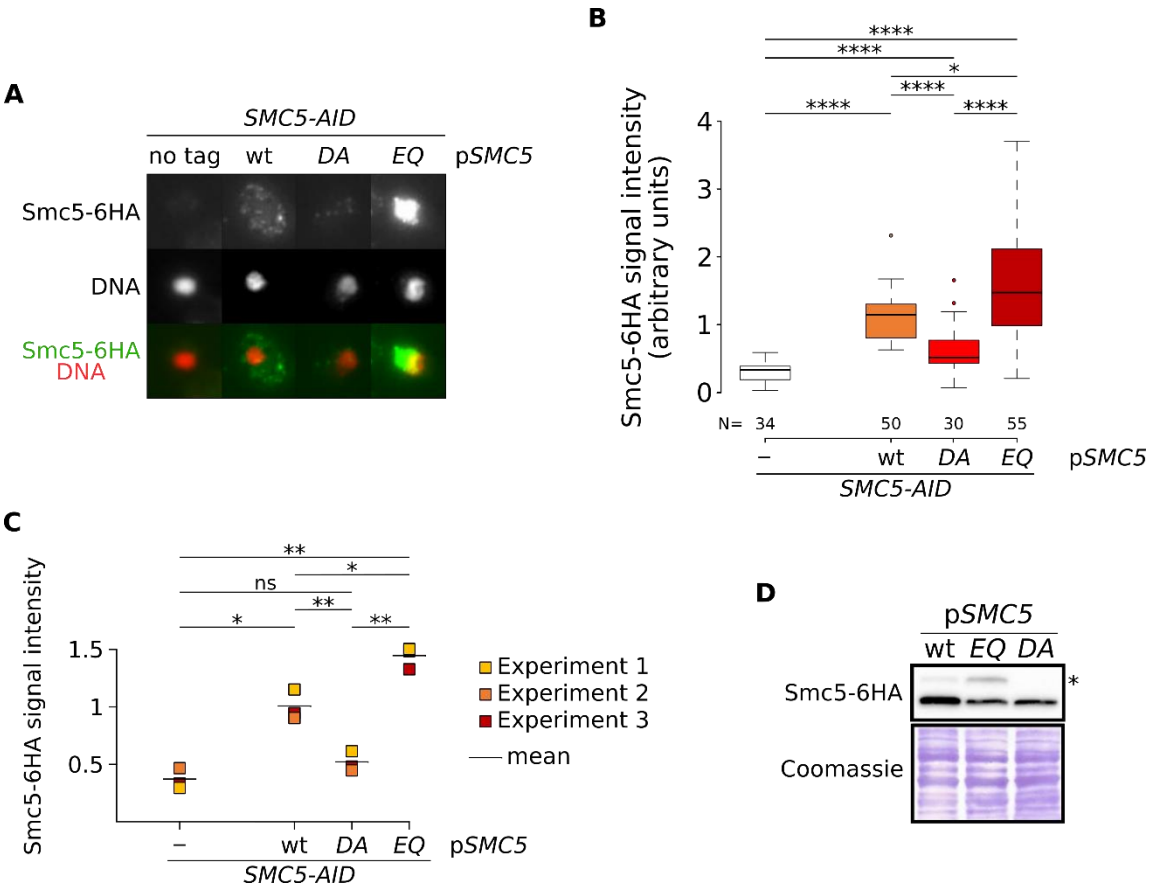

Figure 18. Binding of Smc5 to chromatin is dependent on its ATPase activity. (A) Collage of images taken from the different samples after performing chromosome spreads. For each sample, it is shown a representative nucleus of the whole population. The images have been processed to add colors, HA has been colored with green and DNA with red. Rat monoclonal antibody was used to perform the immunofluorescence against HA (clone 3F10). DNA was stained with Hoechst **(B)** Quantification of the signal obtained in the chromosome spreads images. The N represents the number of nuclei quantified for each sample. All images were taken with the same settings in the microscope. All samples contained an internal standard to normalize all the quantifications. ATP binding is required for Smc5 binding to chromatin. In contrast, binding of ATP but blockage of hydrolysis ends up in a higher binding of Smc5 to chromatin. Student's test has been performed for each pair of samples. **(C)** Summary of three independent repetitions of the chromosome spreads. Each point shows the mean obtained for each sample and the black bar is the mean value of the three experiments. Paired Student's test has been performed for each pair of samples. **(D)** Anti-HA Western Blot. The asterisk indicates the position of sumoylated Smc5, which was detected in a higher proportion in the EQ sample. Coomassie staining was used to test the loading of the samples into the gel.

Significance levels are indicated with the following key: p>0,05 (ns), p≤0,05 (*), p≤0,01 (**), p≤0,001 (***), p≤0,0001 (****).

Strains in this figure: YTR1372, YMT3971, YMT4013 & YMT4046

The observation that the Smc5-EQ protein binds to DNA in a higher proportion than wild type Smc5 can be explained by (at least) two different mechanisms. First, the Smc5-

EQ mutant protein could bind with higher affinity, relative to the wild type protein, to the same chromosomal locations. For example, more complexes are loaded at the same site or more cells display binding at that particular locus. Alternatively, the mutant Smc5-EQ protein could bind to new sites, not occupied by the wild type Smc5 protein. To distinguish between the two hypotheses, we expressed wild type or ATPase mutant Smc5 tagged with the 6xFlag epitope and we performed chromatin immunoprecipitation mass sequencing (ChIP-seq). This experiment was performed in collaboration with the group led by Dr Bermejo in the Center for Biological Research (CIB) of the Spanish National Research Council (CSIC). As Smc5/6 binding to chromatin is maximal in G2/M (Figure 8), exponentially growing cells were arrested in G1 with alpha factor and released into a metaphase block with nocodazole. Samples were collected for ChIP and FACS analysis to monitor cell cycle arrest (Figure 7).

The sequencing results were analyzed by peak calling and differences were readily detected between wild type and ATPase mutant Smc5 (Figure 19A). First, when there was no Smc5-6xFlag to immunoprecipitate (UnTag), the number of peaks detected was very low (229). In comparison, the ChIP performed on the wild type Smc5-6xFlag presented 885 peaks, from which 187 coincided with the UnTag sample (Figure 19B). When the *smc5-DA* allele was expressed, the total amount of peaks compared to the wild type was lower (631) and 76% of those peaks coincided with binding sites for wild type Smc5 (Figure 19C). Blockage of ATP hydrolysis in the *smc5-EQ* mutant resulted in 1451 peaks, 840 of which were different from those found in the wild type Smc5 ChIP (Figure 19D). This result suggested that Smc5-EQ was interacting with new sites instead of just binding in higher amounts to the same places as Smc5.

Since ChIP-seq analysis is not quantitative, we analyzed Smc5 binding to specific sites by chromatin immunoprecipitation followed by qPCR (ChIP-qPCR). All primer pairs used for this study have a melting temperature of 60 ºC and amplify regions of 100 to 150 nucleotides.

Smc5 is known to bind centromeres, so we used primers to test the immunoprecipitation of the centromere in chromosome four (CEN IV). The results of the qPCR were processed to calculate the DNA immunoprecipitated as a percentage of the total DNA in the whole cell extract (input). A comparison between the strain with no Smc5 expression and the wild type Smc5 proved that there is significant enrichment of Smc5 at CEN IV (0.002% vs 0.321% enrichment; Figure 20). As expected from the chromosome spread results, when the ChIP-qPCR is performed on a strain expressing the ATP binding mutant Smc5-DA, binding to CEN IV is 10 times lower than the one observed for the wild type Smc5. When ATP hydrolysis is blocked, Smc5 can still bind to CEN IV, although the enrichment is lower relative to wild type Smc5. As a control for background signal in the ChIP, we analyzed a region where Smc5 does not bind, 62 Kb into chromosome III (Jeppsson et al., 2014). In agreement with published data, Smc5 coimmunoprecipitated very low amounts of DNA for this locus (0.011%), similar to ATP

binding Smc5 mutant. However, we could observe a slight increase in the immunoprecipitated DNA when we quantified the Smc5-EQ sample (0.028%).

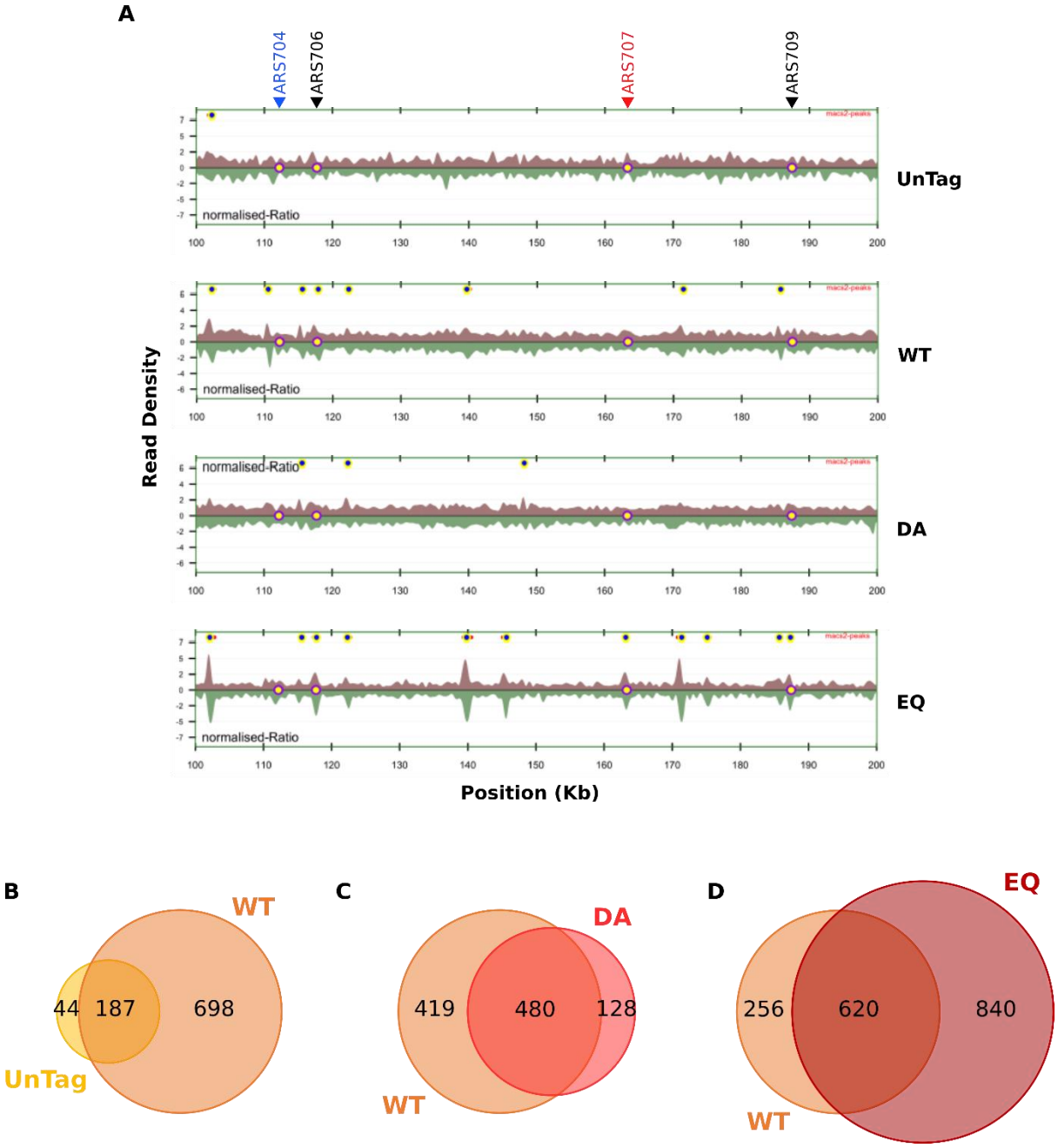

Figure 19. Smc5-EQ binds to more sites in the genome than WT Smc5. (A) Graphical representation of the number of reads over each nucleotide on the genome after performing ChIP-seq. Each lane represents a strain expressing either no Smc5 (UnTag), a wild type copy of the gene or one of its ATPase mutant alleles. Blue dots with yellow rim and red bars extending next to them identify the peaks detected for each sample. **(B, C, D)** The total number of peaks for each sample was quantified and represented in Venn diagrams to identify overlapping peaks between samples. Diagrams proted compare **(B)** UnTag with WT and WT with either **(C)** DA or **(D)** EQ.

Strains in this figure: YMT5550, YMT5551, YMT5553 & YMT5554

Overall, we conclude that ATP binding to Smc5 is required for Smc5/6 association with specific chromosomal sites. In contrast, blocking ATP hydrolysis exposes new binding sites for Smc5/6, leading to higher amounts of chromatin associated Smc5/6 complexes, while slightly reducing its association with usual binding sites, such as centromere IV.

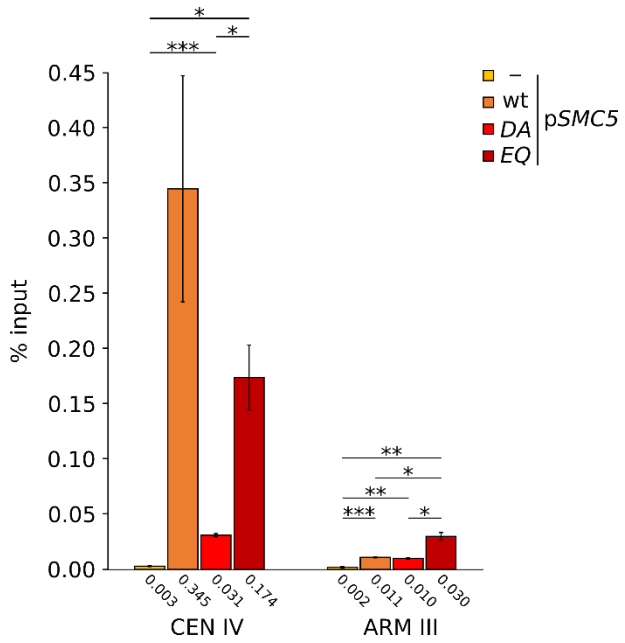

Figure 20. Binding of the EQ ATPase mutant allele of Smc5 to chromatin is lower in usual Smc5 binding sites but increased in other loci. Barplot showing the results for a quantitative PCR (qPCR) analysis of a chromatin immunoprecipitation (ChIP) of cells arrested in G2/M with nocodazole (Nz). Endogenous Smc5 was tagged with an auxin inducible degron (AID) to deplete it with the addition of auxin (IAA). These cells did also have a plasmid integrated into the TRP1 locus to express either a wild type or an ATPase mutant copy of Smc5 tagged with 6 copies of the FLAG epitope. Cultures were arrested in G1, then auxin was added and they were released into a synchronous S phase in the presence of auxin before being arrested again with Nz. Immunoprecipitation was performed using a mouse monoclonal antibody against FLAG epitope (clone M2). Different loci were selected to perform a qPCR and see the quantity of DNA that had been co-immunoprecipitated with the Smc5-6Flag.

Significance levels are indicated with the following key: p>0,05 (ns), p≤0,05 (*), p≤0,01 (**), p≤0,001 (***), p≤0,0001 (****).

Strains in this figure: YMT5550, YMT5551, YMT5553 & YMT5554

4.2.3. *smc5-E1015Q* Binds Preferably to Replication Origins and Convergent Replication Sites

The Smc5-EQ mutant protein seems to interact more with DNA than the wild type protein. In addition, this increase is related to the presence of new binding loci, instead of increased binding of the Smc5-EQ protein to the usual Smc5 binding sites. Next, we

used the information from ChIP-seq data to analyze if blocking ATP hydrolysis in Smc5 results in higher binding of Smc5 to specific chromosomal regions.

The amount of chromatin-associated Smc5 increases as cells progress in S-Phase (Figure 9). In agreement with this observation, previous reports indicate that both Smc6 and Nse1 bind around early firing ARS after HU treatment (Lindroos et al., 2006). Thus, we first analyzed if wild type and/or ATP hydrolysis mutants bind to regions with specific functions in DNA replication: origins of replication (ARS) and terminators of replication (TER).

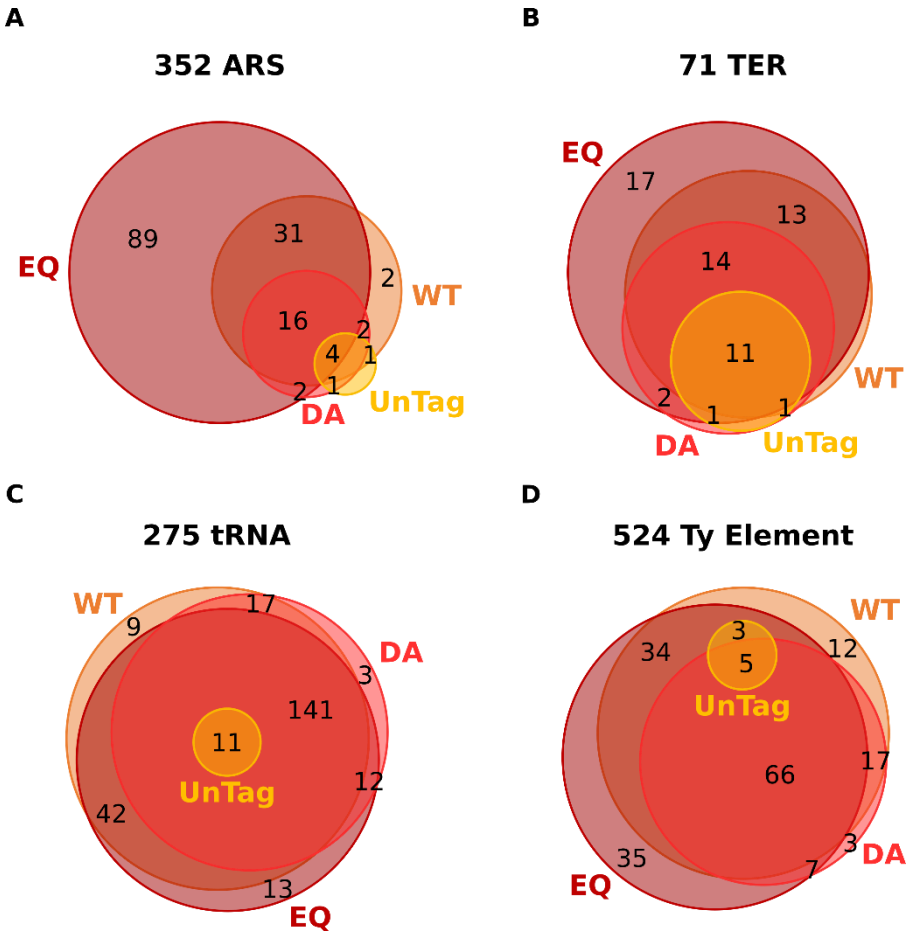

Figure 21. Replication origins are loci where the Smc5/6 complex loads onto chromatin. Venn diagrams obtained from the sequencing results of a chromatin immunoprecipitation (ChIP) of cells arrested in G2/M with nocodazole (Nz). Endogenous Smc5 was tagged with an auxin inducible degron (AID) to deplete it with the addition of auxin (IAA). These cells did also have a plasmid integreated into the TRP1 locus to express either a wild type or an ATPase mutant copy of Smc5 tagged with 6 copies of the FLAG epitope. Cultures were arrested in G1, then auxin was added and they were released into a synchronous S phase in the presence of auxin before being arrested again with Nz. Immunoprecipitation was performed using a mouse monoclonal antibody against FLAG epitope (clone M2). Each Venn diagram shows the number of peaks of each sample overlapping a feature on the DNA: **(A)** origin of replication, **(B)** replication terminator, **(C)** transcription RNA or **(D)** Ty Elements.

Strains in this figure: YMT5550, YMT5551, YMT5553 & YMT5554

A list of the identified replication origins in budding yeast was obtained from OriDB (Siow et al., 2012). There is a total of 352 ARS in the yeast genome and we could detect 56 peaks of wild type Smc5 overlapping with these regions (Figure 21A). Interestingly, Smc5-EQ peaks overlapped with 142 ARS, 89 of which were exclusive for this mutant variant of the protein. Then, we analyzed the overlapping with a list of TERs, which includes 71 sites in *Saccharomyces cerevisiae* (Fachinetti et al., 2010). Wild type Smc5 was present in 55% of them, while the ATP hydrolysis mutant was found associated with 82% of TERs, with 17 TER-binding sites unique to the Smc5-EQ protein (Figure 21B).

Next, we tested two other chromosomal features present in the yeast genome that are natural pausing sites for the replication fork, tRNAs and Ty elements, and are also highly enriched in Smc5/6 (Menolfi et al., 2015; Pebernard et al., 2008). There are 275 tDNA elements (encoding for tRNAs) in budding yeast. We observed that wild type Smc5 binds to 220 of these regions while the *EQ* mutant allele binds to 219 tDNA (Figure 21C). Thus, it seems that the EQ allele has no specific preference for binding to tRNA genes. Next, we checked the binding of Smc5 to Ty elements. These elements have been related to chromosomal rearrangement events (Mieczkowski et al., 2006). Smc5 bound to 137 out of 524 Ty elements in the yeast genome. Blocking ATP hydrolysis, did not significantly increase the association of Smc5 with Ty elements (Figure 21D). In the four types of loci studied, the number of elements to which Smc5/6 binds is lower when the protein cannot bind ATP (Figure 21).

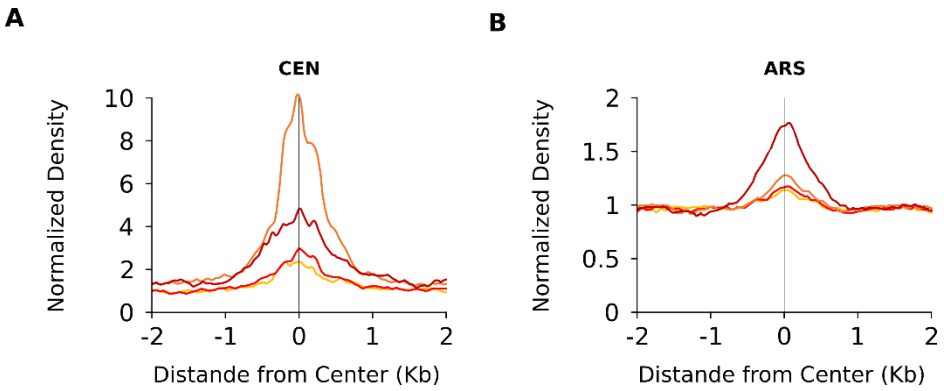

Figure 22. Replication origins are loci where the Smc5/6 complex loads onto chromatin, number of reads. Histogram plotted from the sequencing results of a chromatin immunoprecipitation (ChIP) of cells arrested in G2/M with nocodazole (Nz). Endogenous Smc5 was tagged with an auxin inducible degron (AID) to deplete it with the addition of auxin (IAA). These cells did also have a plasmid integrated into the TRP1 locus to express either a wild type or an ATPase mutant copy of Smc5 tagged with 6 copies of the FLAG epitope. Cultures were arrested in G1, then auxin was added and they were released into a synchronous S phase in the presence of auxin before being arrested again with Nz. Immunoprecipitation was performed using a mouse monoclonal antibody against FLAG epitope (clone M2). Each histogram shows the number of reads of each sample overlapping each position of a specific type of feature: **(A)** centromeres and **(B)** origin of replication.

Strains in this figure: YMT5550, YMT5551, YMT5553 & YMT5554

Sequencing data was also analyzed taking the number of reads as a starting point. This data is not quantitative when comparing between different samples. However, it has a quantitative value when comparing different loci from the same sample. Data was normalized in order to make it comparable between samples (see M&M for further details). This method was validated by analyzing the cumulative binding of Smc5 to centromeres (Figure 22A). In accordance with qPCR data (Figure 20), we observed higher binding of wild type Smc5, relative to ATP hydrolysis mutant, to centromeres. In addition, the Smc5 ATP-binding mutant showed very poor binding to centromeres, to a level similar to the UnTag (Figure 22A). Aggregates for Smc5 binding to origins of replication confirmed the higher binding of Smc5-EQ relative to wild type Smc5 (Figure 22B).

Cohesin can translocate from loading sites to loci of convergent transcription (Lengronne et al., 2004). In contrast, bacterial SMC interaction with chromatin is diminished on those sites with convergent transcription, due to conflicts between the complex and RNA polymerases (N. T. Tran et al., 2017). For the Smc5/6 complex, results from ChIP-seq performed in G2/M demonstrate that the complex accumulates at convergent transcription sites around the centromeres (Jeppsson et al., 2014). Hence, we studied the association of Smc5 with the different classes of intergenic regions (Figure 23).

Smc5 was able to coimmunoprecipitate DNA fragments overlapping with 27% of convergent transcription sites. In contrast, the Smc5-EQ protein was detected in 68% of the convergent transcription sites, with 484 sites (out of 1226) unique to Smc5-EQ (Figure 23A).

There are 1328 divergent transcription sites in *Saccharomyces cerevisiae* genome, which are reduced to 1320 when the peaks detected in the UnTag sample are subtracted. Wild type Smc5 was found associated to 8% of these sites, while Smc5-EQ was found in 7% of them (Figure 23B). Thus, wild type Smc5 seems to bind more proficiently to convergent than divergent transcription sites. In addition, blocking ATP hydrolysis drastically increase Smc5/6 binding to convergent transcription sites, with no effect on binding to divergent transcription sites.

Finally, we analyzed Smc5/6 binding to codirectionally transcribed intergenic regions. Wild type Smc5 coimmunoprecipitated with 10% of the codirectional transcribing intergenic regions, while the EQ mutant allele covered 16% of these loci (Figure 23C). Separating the list of codirectional transcription regions into the ones on Watson strand and on Crick strand did not make much difference on the results (Figure 23D, E).

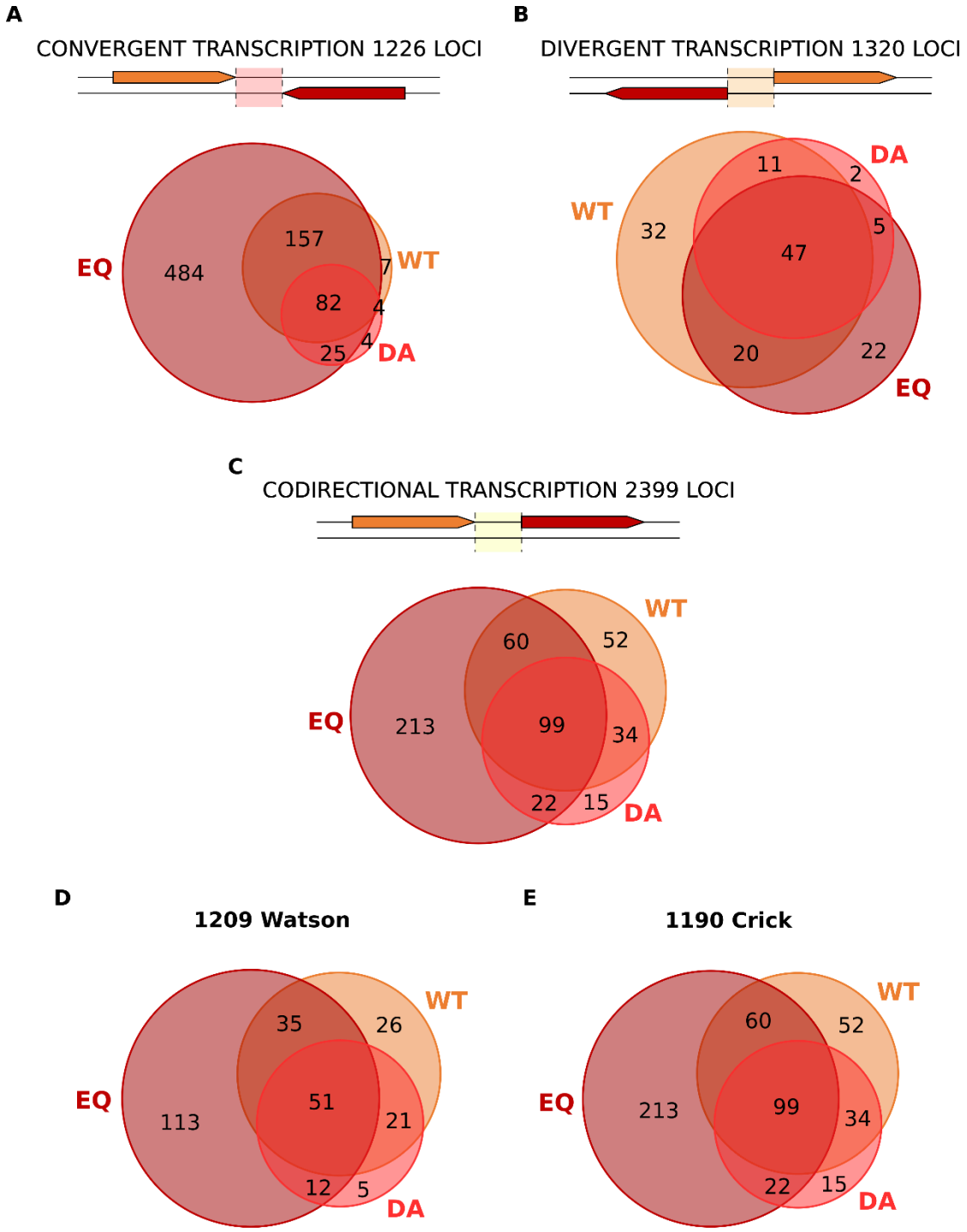

Figure 23. Convergent transcription sites are loci where the Smc5/6 complex loads onto chromatin. Venn diagrams obtained from the sequencing results of a chromatin immunoprecipitation (ChIP) of cells arrested in G2/M with nocodazole (Nz). Endogenous Smc5 was tagged with an auxin inducible degron (AID) to deplete it with the addition of auxin (IAA). These cells did also have a plasmid integrated into the TRP1 locus to express either a wild type or an ATPase mutant copy of Smc5 tagged with 6 copies of the FLAG epitope. Cultures were arrested in G1, then auxin was added and they were released into a synchronous S phase in the presence of auxin before being arrested again with Nz. Immunoprecipitation was performed using a mouse monoclonal antibody against FLAG epitope (clone M2). Each Venn diagram shows the number of peaks of each sample overlapping a type of intergenic transcription site: **(A)** convergent, **(B)** divergent, **(C)** all codirectional regions, **(D)** codirectional on Watson or **(E)** codirectional on Crick.

Strains in this figure: YMT5550, YMT5551, YMT5553 & YMT5554

This data was also analyzed using the read number along the genome. We normalized the number of reads and confirmed the overlapping analysis. The EQ mutant variant of Smc5 displays a higher number of reads on convergent transcription sites and, to a minor extent, also on codirectional transcription sites, both on Watson and Crick strands (Figure 24). When divergent transcription is analyzed, we could not observe any significative difference on the number of reads on any Smc5 variant compared to the UnTag sample.

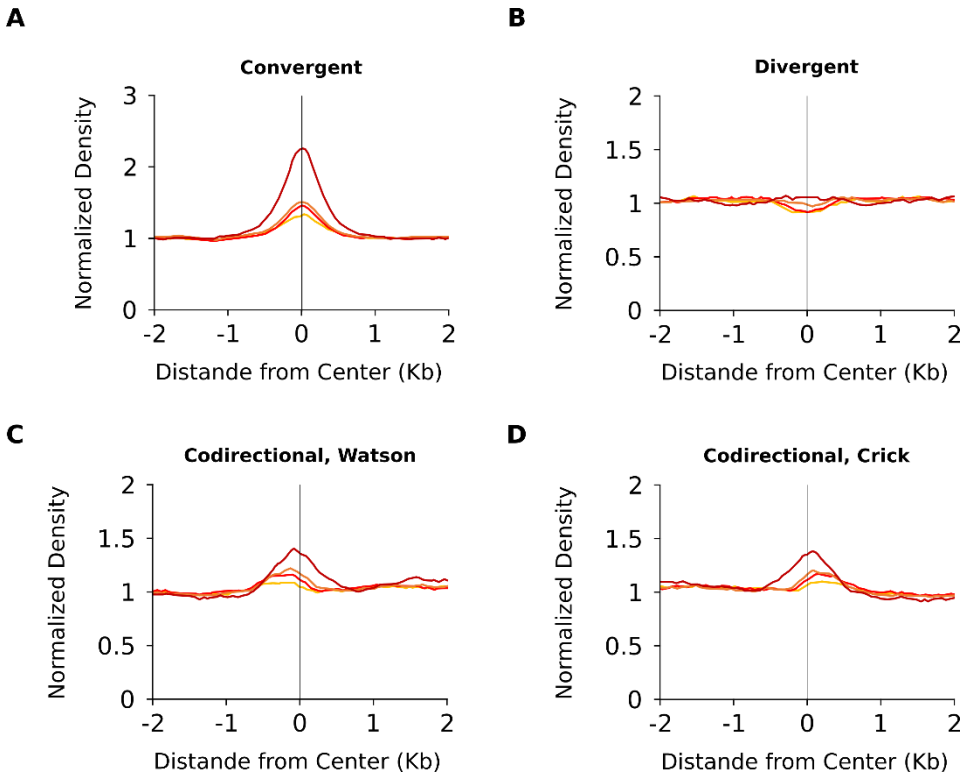

Figure 24. Convergent transcription sites are loci where the Smc5/6 complex loads onto chromatin, number of reads. Histogram plotted from the sequencing results of a chromatin immunoprecipitation (ChIP) of cells arrested in G2/M with nocodazole (Nz). Endogenous Smc5 was tagged with an auxin inducible degron (AID) to deplete it with the addition of auxin (IAA). These cells did also have a plasmid integrated into the TRP1 locus to express either a wild type or an ATPase mutant copy of Smc5 tagged with 6 copies of the FLAG epitope. Cultures were arrested in G1, then auxin was added and they were released into a synchronous S phase in the presence of auxin before being arrested again with Nz. Immunoprecipitation was performed using a mouse monoclonal antibody against FLAG epitope (clone M2). Each histogram shows the number of reads of each sample overlapping each position of a specific type of transcription intergenic regions: **(A)** convergent, **(B)** divergent, **(C)** codirectional on Watson or **(D)** codirectional on Crick.

Strains in this figure: YMT5550, YMT5551, YMT5553 & YMT5554

To validate these findings using a more quantitative approach, we individually tested specific genomic locations by ChIP-qPCR. We tested the coimmunoprecipitation of DNA bound to Smc5 by quantitative PCR. We selected two origins of replication, one of them bound by wild type Smc5 (ARS418) and another one that showed no Smc5-

binding in the ChIP-seq (ARS1617), and one convergent transcription site (382 Kb into chromosome III). The qPCR confirmed a higher enrichment of mutant Smc5-EQ relative to wild type Smc5 at both ARS sequences and the convergent transcription region (Figure 25). In contrast, when Smc5 was not able to bind ATP, we could not see a clear DNA coimmunoprecipitation on any of these sites (Figure 25). We conclude that the higher binding of Smc5-EQ to chromatin stems from increased association of the mutant protein to replication origins and convergent transcription sites.

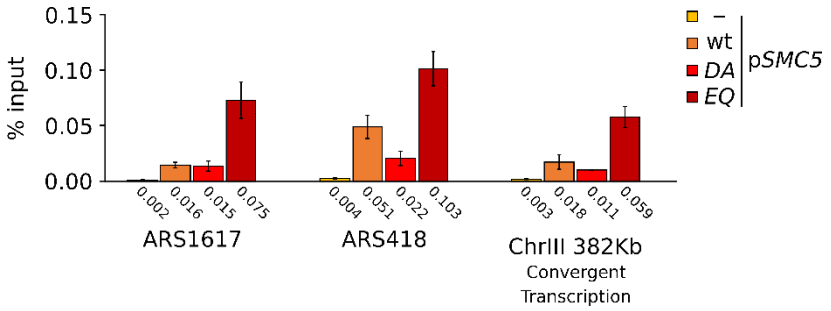

Figure 25. The EQ ATPase mutant allele of Smc5 binds preferably to replication origins and sites of convergent transcription. Barplot showing the results for a quantitative PCR (qPCR) analysis of a chromatin immunoprecipitation (ChIP) of cells arrested in G2/M with nocodazole (Nz). Endogenous Smc5 was tagged with an auxin inducible degron (AID) to deplete it with the addition of auxin (IAA). These cells did also have a plasmid integrated into the TRP1 locus to express either a wild type or an ATPase mutant copy of Smc5 tagged with 6 copies of the FLAG epitope. Cultures were arrested in G1, then auxin was added and they were released into a synchronous S phase in the presence of auxin before being arrested again with Nz. Immunoprecipitation was performed using a mouse monoclonal antibody against FLAG epitope (clone M2). The quantitative technique demonstrates the higher affinity of Smc5-EQ for replication origins (ARS1617 and ARS418) and convergent transcription sites compared to any other variant of Smc5, included the WT.

Strains in this figure: YMT5550, YMT5551, YMT5553 & YMT5554

4.2.4. Binding of the Smc5-EQ protein to the rDNA

The Smc5/6 complex binds to the rDNA array (Torres-Rosell, Machín, et al., 2005) with specific enrichment at NTS1 and NTS2 sequences (Moradi-Fard et al., 2021). As *smc5-EQ* binds to more origins of replication (Figure 21), we used ChIP-qPCR to test whether it affects binding to the ARS in the NTS2 of the rDNA array (rARS). Additionally, we tested if it also affects binding to the replication fork block (RFB) sequence present in NTS1.

We designed oligonucleotides to amplify 100 bp regions of the rARS, the RFB and the 35S rDNA. The latter was selected as a region where Smc5 is not suspected to bind. As expected, we did not see any enrichment of these regions in the UnTag sample. However, Smc5 showed an enrichment on both rARS and the RFB whereas it was less

enriched at the 35S rDNA (Figure 26). Surprisingly, blocking the binding of ATP to Smc5 abolished the binding of the protein to the rARS and RFB, but not to the 35S rDNA. Finally, the ChIP performed on Smc5-EQ showed a clear enrichment at the rARS and RFB, which became the loci with a higher enrichment of all those tested in the genome.

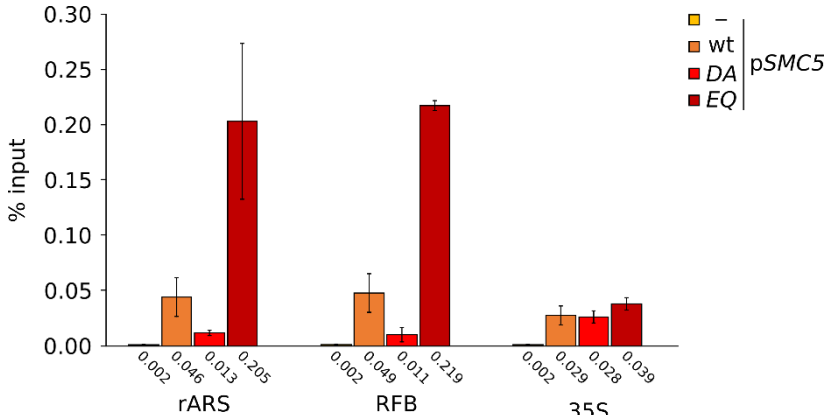

Figure 26. The EQ ATPase mutant allele of Smc5 is hightly enriched at the NTS1 and NTS2 sequences. Barplot showing the results for a quantitative PCR (qPCR) analysis of a chromatin immunoprecipitation (ChIP) of cells arrested in G2/M with nocodazole (Nz). Endogenous Smc5 was tagged with an auxin inducible degron (AID) to deplete it with the addition of auxin (IAA). These cells did also have a plasmid integreated into the TRP1 locus to express either a wild type or an ATPase mutant copy of Smc5 tagged with 6 copies of the FLAG epitope. Cultures were arrested in G1, then auxin was added and they were released into a synchronous S phase in the presence of auxin before being arrested again with Nz. Immunoprecipitation was performed using a mouse monoclonal antibody against FLAG epitope (clone M2). The quantitative technique demonstrates the higher affinity of Smc5-EQ for the rDNA, especially for NTS1 (rARS) and NTS2 (RFB).

Strains in this figure: YMT5550, YMT5551, YMT5553 & YMT5554

4.2.5. rDNA Disjunction is Dependent on the ATPase Activity of Smc5

Different activities co-inhabit in Smc5/6 complex, including a SUMO ligase, a ubiquitin ligase and an ATPase. We thus wondered to what extent the ATPase activity of the complex participates in rDNA segregation. To this end, we used a strain expressing a tetracycline repressor fused to YFP and carrying a battery of tetracycline operators (tetO) at 491 Kb in chromosome XII, at the telomeric side of the rDNA (Figure 27A) (Torres-Rosell, Machín, et al., 2005). Then, to control the degradation of wild type Smc5 in the cell, we integrated a Tir1-9myc expression vector and we tagged the endogenous copy of *SMC5* with an auxin inducible degron. Next, we added alpha factor to exponentially growing cells to arrest them in G1. Once arrested, we treated them with 1 mM auxin at 25 ºC for 30 minutes. Finally, we released cells into a synchronous cell cycle in the absence of Smc5 and collected samples at different time points after release

from the G1 arrest. At times 80-120, DNA masses were equally partitioned between mother and daughter cells. However, when we looked at the specific loci that contained the tetO battery, we observed that 50% of cells failed to segregate it (Figure 27B), in accordance with previous findings using thermosensitive alleles in the Smc5/6 complex (Torres-Rosell, de Piccoli, et al., 2007; Torres-Rosell, Machin, et al., 2005).

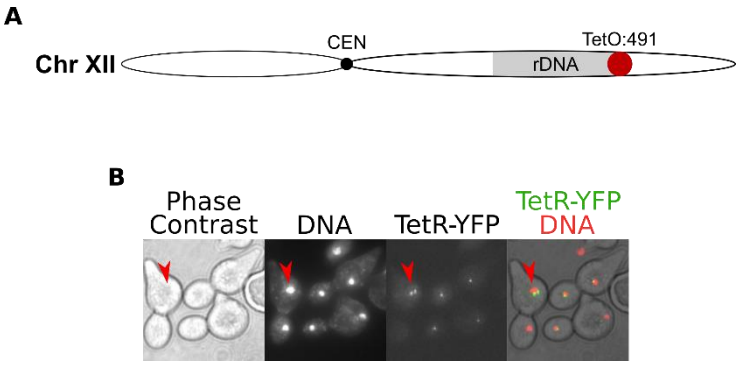

Figure 27. A system to study single locus segregation. (A) Scheme of Saccharomyces cerevisiae's chromosome XII, which contains the multicopy region of the ribosomal DNA (rDNA). A battery of tetracycline operators (tetO) has been integrated downstream of the rDNA. **(B)** Microscopy images of cells bearing the tetO, as described in panel (A). A tetracycline repressor fused to yellow fluorescent protein (tetR-YFP) is also expressed by these cells. DNA was stained with Hoechst. The images have been processed to add colors, tetR-YFP has been colored with green and DNA with red. Cells were arrested in G1 and then released into a synchronous S phase in the absence of Smc5. Apparently, all cells have segregated their genomic DNA properly. However, the tetO permits seeing that the locus downstream of the rDNA has been missegregated in some cells (red arrow).

Strain in this figure: YTR1437

Next, we complemented *smc5-AID* cells with plasmids expressing wild type or ATPase mutant alleles of *SMC5* and treated them as described in the previous paragraph. Samples from the synchronic culture were examined microscopically. First, we observed that budding was not affected in ATPase mutants, starting in all cases 20 minutes after G1 release (Figure 28B). At 120 minutes into the time course, some cells finished the cell cycle, decreasing the budding index. Entry into anaphase, scored as an elongated nucleus, also started synchronously 60 minutes after G1 release in all strains (Figure 28C). Nuclear segregation occurred a little bit later than anaphase, reaching a peak at 120 minutes, and with similar kinetics in all strains (Figure 28D). Finally, we scored cells that had segregated the tetO:491 dot. In the absence of Smc5, or when the protein cannot bind ATP, 20% of the cells displayed segregated tetO:491 foci at time 120 minutes (Figure 28E). Expression of wild type Smc5 increased the number of cells with segregated tetO:491 signals to 60%. Surprisingly, less than 5% of cells expressing the *smc5-EQ* allele were able to segregate this locus.

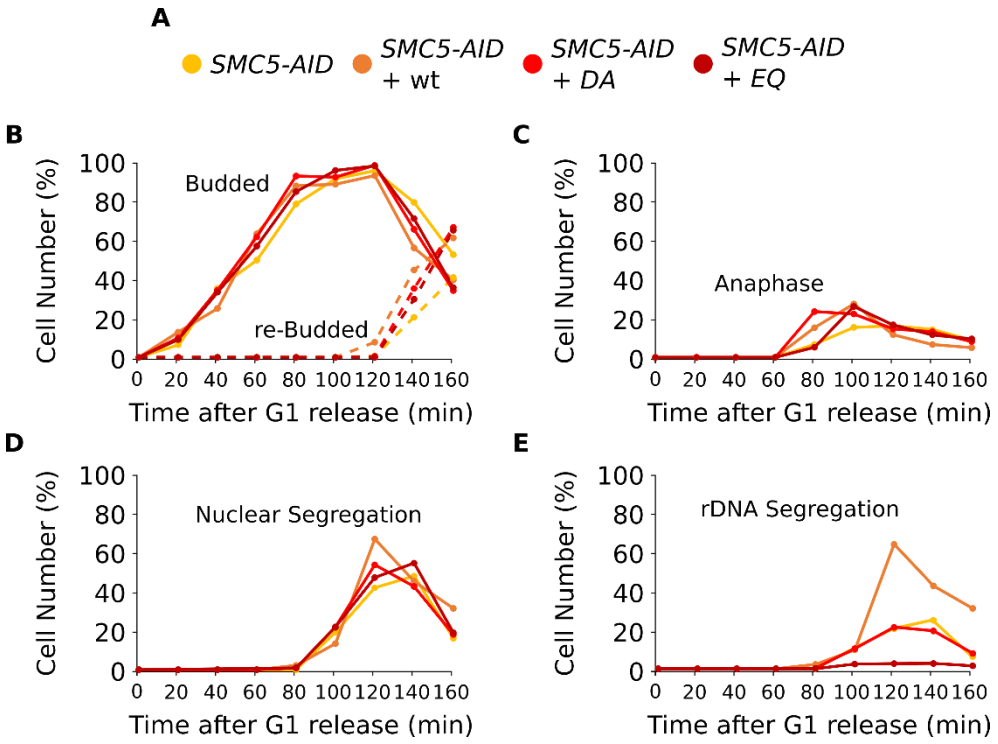

Figure 28. The ATPase activity of Smc5 is essential for a correct segregation of the rDNA locus. (A) Color legend used in the plots for the panels (B, C, D and E). Strains used for this experiment have got the endogenous Smc5 tagged with an auxin inducible degron (AID) to deplete it with the addition of auxin (IAA). Each of them has got either no plasmid, or a plasmid containing a wild type copy of Smc5 or one of the ATPase mutant alleles. For this experiment, cultures were arrested in G1, treated with auxin and released into a synchronous S phase in the presence of auxin. Samples were taken every 20 minutes after release. **(B)** Quantification of bud appearance along time after G1 release (solid lanes) and re-budding after first mitosis (discontinuous lanes). All strains in the experiment grew buds at same time, in a synchronous manner. Entrance into a second cell cycle with re-budding happens also at same time for all strains, starting at 120 minutes after G1 release. **(C)** Quantification of anaphases observed along time after G1 release. All strains display a similar number of anaphases and at same the same moment, reaching a maximum at 80 minutes after G1 release. **(D)** Quantification of cells displaying two separated nuclei, one into each of the buds. This indicates the end of the first mitosis and all the strains reach this point at same rhythm. **(E)** Quantification of the cells that have segregated the rDNA locus properly, with a bright dot into each of their two buds. Three different options can be observed: the strain with a wild type Smc5 in which most of the cells segregate the rDNA locus in a proper way; the strains either with no Smc5 or a Smc5 that cannot bind ATP, in which an intermediate quantity of cells can segregate the rDNA into the daughter cells; and the strain with the mutant allele unable to hydrolyze ATP, in which almost none of the cells can segregate the rDNA.

Strains in this figure: YTR1437, YMT4270, YMT4272 & YMT4656

As described in Figure 26B, we pooled all counted binucleate cells from time points 80 to 120 minutes and classified them as having or not segregated tetO:491 signals. In the absence of Smc5, 50% of the cells in the culture had segregated the telomeric side of the rDNA (Figure 29A). The strain expressing a wild type Smc5 recovered segregation to 95%. However, *smc5-DA* expressing cells showed a phenotype similar to Smc5-depleted cells, with 43% of cells segregating the tetO:491 battery. Interestingly, the *smc5-EQ* mutant allele of Smc5 led to an almost complete failure in tetO:491 segregation, with only 7% of the binucleate cells showing rDNA segregation. These results suggest that expression of the smc5-EQ allele severely interferes with segregation of the rDNA, actually worsening its segregation in cells that would otherwise manage to disjoin this locus.

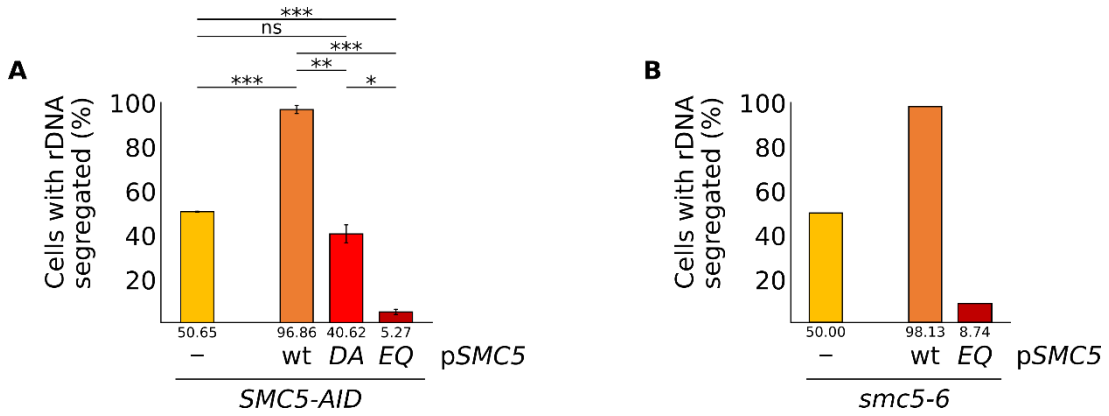

Figure 29. Mutating the Smc5 ATPase to block its hydrolytic activity results in abnormal levels of rDNA missegregation. (A) Absolut quantification of rDNA segregation in cultures that have undergone a synchronous S phase after a G1 arrest. Endogenous Smc5 was tagged with an auxin inducible degron (AID) to deplete it with the addition of auxin (IAA). Each of the strains used has got either no plasmid, or a plasmid containing a wild type copy of Smc5 or one of the ATPase mutant alleles. If there is no expression of Smc5, a half of the cells in the culture missegregate the rDNA. Expression of a wild type copy of Smc5 recovers rDNA segregation for all cells in the culture. Blocking ATP binding has no effect, half of the cells missegregate the rDNA as if there was no Smc5. Blockage of ATP hydrolysis results in only a 5% of cells segregating the rDNA properly. **(B)** Repetition of the experiment described in panel (A). Instead of using an AID tag, depletion of endogenous Smc5 is achieved by using a thermosensitive allele and performing the experiment at 37ºC. Results observed in this case are the same as in panel (A).

Significance levels are indicated with the following key: p>0,05 (ns), p≤0,05 (*), p≤0,01 (**), p≤0,001 (***), p≤0,0001 (****).

Strains in this figure: YTR969, YTR1437, YMT4270, YMT4272, YMT4656, YMT4890 & YMT4892

To confirm this result, we repeated the experiments using a thermosensitive allele of *SMC5* (*smc5-6*), which can be inactivated by shift to the restrictive temperature. We arrested exponentially growing cells in G1, we then shifted them to 36 ºC for 30 minutes and released them into a synchronous cell cycle at the restrictive temperature. As previously reported (Torres-Rosell, Machín, et al., 2005), only 50% of *smc5-6* cells segregated the rDNA (Figure 29B). The expression of wild type restored rDNA

segregation to 98% while expression of a mutant allele *smc5-EQ* prevented rDNA segregation in 91% of cells. Overall, these results indicate that the smc5-EQ allele negatively impacts on rDNA segregation, most probably through a gain of function activity that impedes separation of sister rDNA arrays.

4.2.6. rDNA Segregation Defects in *smc5*-EQ Mutants are Only Partially Dependent on the RFB or Recombination

Unexpectedly, we had seen that most *smc5-EQ* cells missegregated the telomeric side of the rDNA. This observation suggests that the Smc5-EQ protein promotes the appearance of a toxic structure that prevents rDNA disjunction. To gain further insight into the nature of the problems generated by preventing hydrolysis of ATP in Smc5, we deleted either *FOB1* or *RAD51* in *smc5-AID* cells. These deletions preclude the arrest of forks at the RFB or homologous recombination-dependent strand invasion, respectively (Menolfi et al., 2015). Importantly, both types of intermediates, arrested forks and recombination intermediates, accumulate in the rDNA of smc5/6 mutants and contribute to their rDNA segregation defects (Torres-Rosell, de Piccoli, et al., 2007).

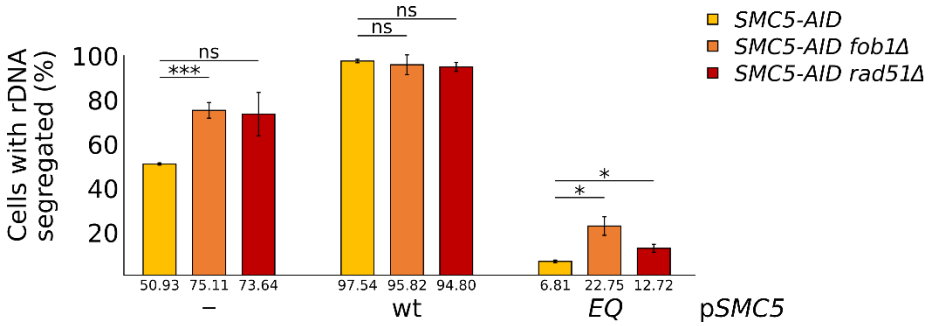

Figure 30. Missegregation of the rDNA locus promoted by the EQ mutant allele of Smc5 is not related to RFB or HR. Absolut quantification of rDNA segregation in cultures that have undergone a synchronous S phase after a G1 arrest. Endogenous Smc5 was tagged with an auxin inducible degron (AID) to deplete it with the addition of auxin (IAA). The strains were either wild type or mutant for fob1 or rad51. Each of the strains used has got either no plasmid, or a plasmid containing a wild type copy of Smc5 or the ATPase mutant allele smc5-EQ. Both rad51 and fob1 deletions permit a better segregation of the rDNA locus in both cells without Smc5 and with the EQ mutant allele of Smc5. However, there is no better recovery for strains with the EQ mutant allele than for those without Smc5.

Significance levels are indicated with the following key: p>0,05 (ns), p≤0,05 (*), p≤0,01 (**), p≤0,001 (***), p≤0,0001 (****).

Strains in this figure: YTR1437, YMT4270, YMT4656, YMT4896, YMT4898, YMT4900, YMS5026, YMS5029 & YMS5030

The *fob1Δ* or *rad51Δ* mutations did not have a perceptible effect on *smc5-AID* cells expressing wild type Smc5, with more than 95% of cells segregating the rDNA. In the absence of Smc5 expression, deletion of *FOB1* or *RAD51* allowed the segregation of tetO:491 in 75% of cells, which is a substantial improvement compared to the 50% segregation scored in the *smc5-AID* single mutant (Figure 30). Finally, deletion of either gene in a strain expressing the *smc5-EQ* mutant allele improved segregation, to different extents, of the rDNA from 5% in *smc5-AID smc5-EQ* cells to 23% in *smc5-AID smc5-EQ fob1Δ* and 13% in smc5-AID smc5-EQ *rad51Δ* cells. Thus, we conclude that the problems generated by expression of the smc5-EQ allele are partially dependent on forks arrested at the RFB and Rad51-dependent processes.

4.2.7. Cytokinesis Deficient Cells Segregate the rDNA Locus in the absence of Smc5

In an attempt to simplify the quantification of rDNA segregation, we decided to arrest cells in telophase through Cdc15 inhibition. We tagged Cdc15 with an auxin inducible degron and depleted it alongside Smc5. We first noted that the amount of auxin used in experiments for Smc5 inactivation (1 mM) was not sufficient to arrest cells in telophase by depletion of Cdc15-AID, with both mother and daughter cells growing a new bud despite inhibiting cytokinesis. This problem was corrected by increasing the auxin concentration to 6 mM, which effectively prevented both cytokinesis and mitotic exit.

We took samples every 45 minutes between 90 and 180 minutes after G1 release. The degradation of Cdc15 did not have any effect on cells expressing wild type Smc5, and >95% of cells in the culture segregated the tetO:491 at all time points (Figure 31). Surprisingly, cells deficient for Smc5 were able to segregate the rDNA when given sufficient time in the absence of cytokinesis. At 90 minutes into the time course, 50% of the *smc5-AID* cells had segregated the rDNA; however, this value increased to 85% at 180 minutes time point (Figure 31). We could also observe an equivalent improvement in *smc5-EQ* cells, going up from less than 5% of cells segregating the rDNA at 90 minutes to 20% at 180 minutes (Figure 31).

Overall, these observations indicate that, if given sufficient time, rDNA non-disjunction events in *smc5* mutant cells can be resolved through Smc5-independent pathways. Thus, the proteins involved in rDNA disjunction are not completely inactive in *smc5* mutant cells.

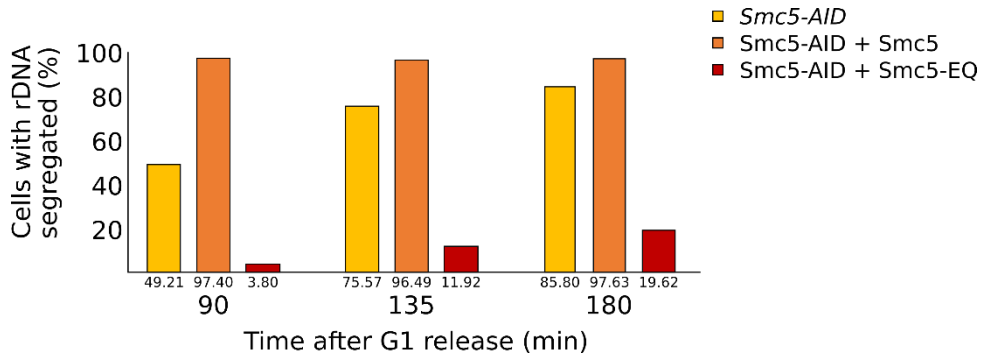

Figure 31. In the absence of cytokinesis, cells without Smc5 are able to segregate the telomeric side of the ribosomal DNA repetitive locus. Absolut quantification of rDNA segregation in cultures that have undergone a synchronous S phase after a G1 arrest. Endogenous Smc5 was tagged with an auxin inducible degron (AID) to deplete it with the addition of auxin (IAA). A second AID tag was fused to CDC15. Each of the strains used has got either no plasmid, or a plasmid containing a wild type copy of Smc5 or the ATPase mutant allele smc5-EQ. Degradation of Cdc15 avoids cytokinesis, which permits cells lacking Smc5 to better segregate the rDNA locus in both cells without Smc5 and with the EQ mutant allele of Smc5. However, there is no better recovery for strains with the EQ mutant allele than for those without Smc5.

Strains in this figure: YTR5375, YMT5817 & YMT581

4.2.8. DNA Damage Impairs Segregation in Smc5 ATPase Mutant Strains

The rDNA is highly sensitive to Smc5/6 function. This characteristic made us wonder whether the effect of the *smc5-EQ* allele on segregation is specific for the rDNA or if it also affects other chromosome locations. To analyze the effect of ATPase mutant expression in chromosome disjunction, we followed synchronous cultures of cells by flow cytometry.

We cultured *smc5-AID* cells expressing wild type or ATPase mutant alleles of *SMC5*. Exponentially growing cultures were treated with alpha factor to arrest them in G1. Once cells were arrested, we added 1mM auxin to degrade endogenous Smc5-AID and 0.01% MMS to generate DNA damage. After 30 minutes, we removed MMS and alpha factor by pelleting cells twice in fresh media and released them into a synchronous S-Phase in the presence of 1 mM IAA to maintain *smc5-AID* degradation. We took samples from synchronic cultures every 15 minutes for a total of 3 hours.

As shown in Figure 9, replication started 30 minutes after G1 release in all strains (Figure 32A). At time 75 minutes, some cells finished DNA replication, appearing a 2N peak. Cytokinesis occurred at time 135 minutes after G1 release, as evidenced by reappearance of a 1N peak in cells expressing wild type *SMC5*. In contrast, cells expressing no Smc5 had problems in nuclear segregation, with an evident sub-1N at later time points in the time course, indicating chromosome loss (black arrow on Figure

32A). Both DA and EQ ATPase mutant alleles missegregated their genomic DNA as observed in the strain with no Smc5 expression. However, and differently to the growth on plates (Figure 17) and rDNA segregation (Figure 29), we could not detect a dominant negative effect of *smc5-EQ* mutant expression on bulk nuclear segregation.

To verify chromosome segregation defects, we observed cells under the microscope. Hoechst staining revealed nuclear missegregation in cells with no Smc5 or expressing an ATPase mutant allele of the gene (Figure 32B). Remarkably, most cells with unequal nuclear segregation displayed a bigger nuclear mass in the daughter than in the mother cell. The mother cell was identified by the characteristic schmoo shape acquired during alpha factor treatment. This phenotype was confirmed when we plotted the DNA content of the cells against their size obtained from the FACS data. After cytokinesis, both small cells (daughter cells) with a DNA content over 2N and large cells (mother cells) with sub-1N DNA content could be observed in cultures of cells with no Smc5 or expressing the DA or EQ ATPase mutant versions (Figure 32C). We conclude that none of the ATPase mutants supports proper chromosome segregation in the presence of low levels of alkylation damage.

4.2.9. Recruiting *smc5-EQ* to a non-rDNA Locus Can Endanger its Segregation

As we did not see increased chromosome missegregation by expression of the smc5-EQ allele by monitoring bulk DNA segregation we decided to use a tetO battery placed upstream of the rDNA (tetO:455) in chromosome XII, a region that can be segregated in *smc5/6* mutants. In addition, we promoted the active recruitment of wild type or ATPase hydrolysis mutant Smc5/6 complexes to this site. To do so, we fused a single domain camelid nanobody (NB) against GFP/YFP to the C-terminal end of Smc6. In combination with expression of tetR-YFP, we expected to tether the Smc6-NB molecules, together with the other subunits of the complex, to the centromeric side of the rDNA.

Expression of Smc6-NB did not affect the segregation of the tetO:455 locus and over 95% of cells could segregate it. Expression of an additional copy of wild type Smc5 promoted a slight yet significant decrease of the cells capable to segregate the loci, just below 95%. Finally, expression of the Smc5-EQ protein limited the segregation of the locus upstream of the rDNA to 85% of cells. It is worth noting that this experiment was performed in competition with the endogenous *SMC5* wild type gene. Thus, the recruitment of Smc5-EQ ATPase mutant proteins to a specific locus results in increased missegregation at that genomic position (Figure 33). Moreover, although the effect of the mutant protein is more notorious downstream of the rDNA, it is not restricted to that region.

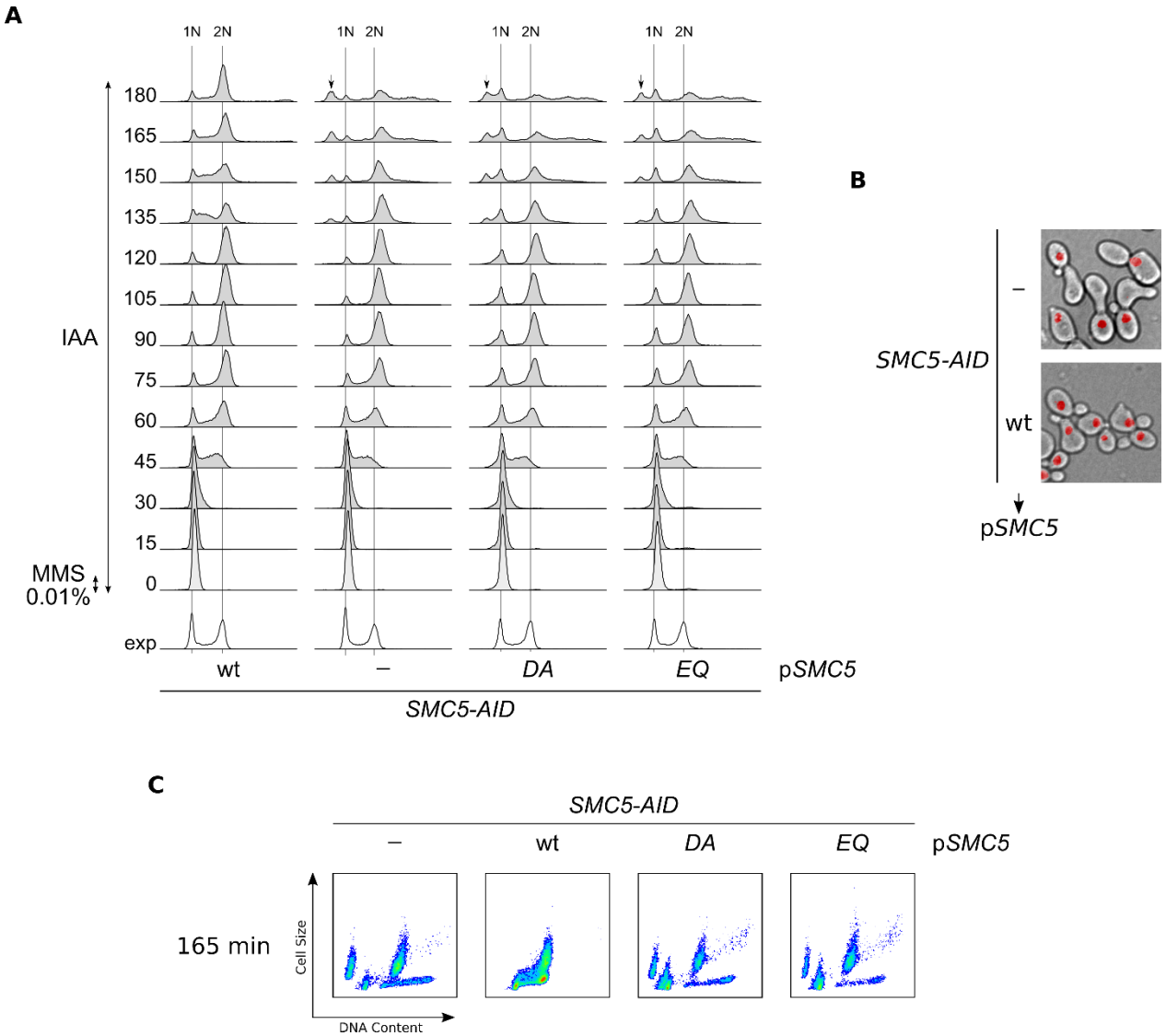

Figure 32. DNA segregation in the presence of induced damage is dependent on the ATPase activity of Smc5. (A) FACS profiles showing the DNA content of cells bearing with induced damage in the presence of the different ATPase mutant alleles of Smc5. Endogenous Smc5 was tagged with an auxin inducible degron (AID) to deplete it with the addition of auxin (IAA). The cultures were synchronized in G1 with alpha factor. Endogenous Smc5 was depleted before release and 0,01% MMS was added to induce DNA damage. Release into a synchronous S phase was performed in the presence of IAA and samples were taken every 15 minutes. Absence of Smc5 induces missegregation of genomic DNA which can be seen by the appearance of a peak bellow 1N DNA content. ATPase mutant alleles generate the same phenotype, while addition of a wild type copy of Smc5 recovers a normal segregation. **(B)** Representative microscopy images of a sample taken at 150 minutes into the time course. The images result from the merge of a bright field image and Hoechst-stained DNA. The images have been processed to add red color to DNA. DNA missegregation can be observed in cells with no Smc5 expression, as the whole nuclear content can be observed into the daughter cell. Cells expressing wild type *SMC5* segregate the DNA with a wild type phenotype. **(C)** Density plot of the 165-minute sample's FACS plotted in panel (A). When a wild type copy of Smc5 is present, three main populations can be observed: 1N small sized, replicating mid-sized and 2N big sized (and growing). In contrast, absence of Smc5 ATPase activity display four different populations: 1N small sized, 2N big sized (and growing), high DNA content with small size and low DNA content with big size. These different populations can be related to the DNA segregation pattern observed in panel (B).

Strains in this figure: YTR1437, YMT4270, YMT4272 & YMT4656.

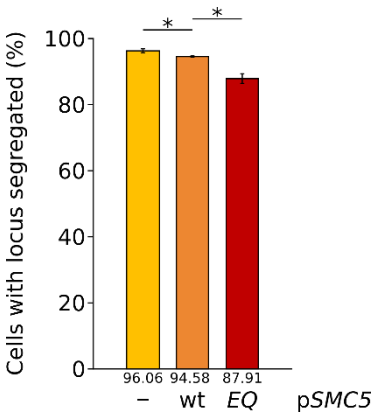

Figure 33. Recruitment of smc5-EQ to a genomic locus promotes its missegregation during anaphase. Absolut quantification of tetO:455 segregation in cultures that have undergone a synchronous S phase after a G1 arrest. The strains used for this experiment express a fusion of Smc6 with a nanobody against GFP (YFP). Addition of an extra copy of WT Smc5 slightly decreases the segregation of the studied locus. Expression of smc5-EQ further increases this effect.

Significance levels are indicated with the following key: p>0,05 (ns), p≤0,05 (*), p≤0,01 (**), p≤0,001 (***), p≤0,0001 (****).

Strains in this figure: YMT5784, YMT5797 & YMT5799

4.3. Analysis of the *smc6-EQ* ATPase Mutant

The ATPase at the head domains of cohesin and condensin is asymmetric, as binding and hydrolysis at each SMC subunit do not happen simultaneously (Arumugam et al., 2006; Elbatsh et al., 2016; Hassler et al., 2019; Thadani et al., 2018). To test whether the ATPase in Smc5/6 is also asymmetric, we introduced ATPase mutations on *SMC6* to test whether the *smc6-EQ* ATP hydrolysis mutant displays the same phenotype as the *smc5-EQ* allele.

4.3.1. Generation of Smc6 ATPase Mutants and Phenotypical Analysis

To study the ATPase activity of Smc6, we cloned a genomic copy of the gene into a centromeric plasmid. Then, we mutagenized it by site directed mutagenesis in order to generate the mutant alleles described in section 4.2.1. The alignments of SMC proteins in *Saccharomyces cerevisiae* (Figure 16) indicate that the residues and mutations for Smc6 are: D1047A (DA), S1020R (SR) and E1048Q (EQ).

4.3.1.1. The ATPase Activity of Smc6 is Essential for Cell Growth

The *smc6* mutagenized alleles were also lethal for cells, as we had observed for the *smc5* ATPase mutant alleles. We transformed the plasmids expressing the different *SMC6* alleles into a *GALp-SMC6* strain. Similar to Smc5, we observed a recessive

phenotype of the ATPase mutant alleles of *SMC6* when co-expressed with wild type *SMC6*.

We plated serial dilutions of *GALp-SMC6* strains containing the different variants of *SMC6* on plates containing either galactose or glucose. All the strains grew in the presence of galactose. However, in the presence of glucose we could observe that the strain with no expression of *SMC6* could not grow (Figure 34). The ectopic expression of *SMC6* recovered a wild type phenotype. In contrast, the expression of ATPase mutant alleles of *SMC6* did not rescue the phenotype of the *GALp-SMC6* cells in glucose.

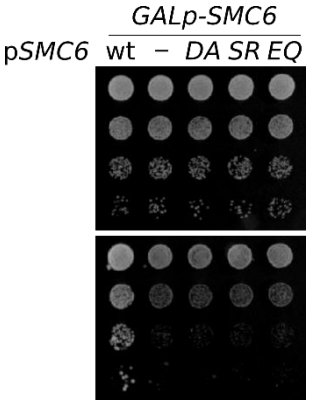

Figure 34. Smc6 ATPase mutations result in loss of viability. Plates displaying serial dilutions of a strain dependent on the different ATPase mutant alleles. The endogenous SMC6 was under control of a galactose promoter to control its expression depending on the carbon source. None of the ATPase mutant alleles can sustain cell viability, while a wild type copy of Smc6 recovers normal growth.

Strains in this figure: YTR3713, YTR3714, YTR3715, YTR3716 & YTR3717

4.3.1.2. DNA Damage Impairs Segregation in Smc6 ATPase Mutant Strains

Next, we analyzed if the ATPase activity of Smc6 is required for the role of Smc5/6 on disjunction of sister chromatids in the response to mild DNA damage. We cultured *GALp-SMC6* cells overnight in galactose before shifting the carbon source to glucose for 5 hours to deplete *SMC6* expression and arresting them in G1 using alpha-factor for two hours. Afterwards, we treated these cells with 0.01% MMS for 30 minutes to induce DNA damage and formation of sister chromatid junctions. Finally, we washed these cells to release them into a synchronous cell cycle and collected samples every 20 minutes for the first hour and every 15 minutes until reaching 165 minutes in the time course.

FACS analysis revealed that DNA replication started at 40 minutes after the release from G1 and finished at time 60-75 minutes in all samples (Figure 35A). Cytokinesis was completed at 120 minutes after release. We observed that *GALp-SMC6* cells displayed a sub-1N peak after mitosis (black arrow on Figure 35A), which coincided with microscopical analysis of these cells with Hoechst staining, with which we observed cells with big buds after anaphase and the whole nuclear content into the daughter cell.

Expression of the wild type Smc6 protein recovered a normal DNA segregation. As happened in *GALp-SMC6* cells, *smc6* ATPase mutant alleles displayed nuclear missegregation after cytokinesis, with a sub-1N peak. Again, this result correlated with microscopy images and, similar to *smc5* ATPase mutants, the missegregated nuclear material was preferentially localized in the daughter cells (Figure 35B).

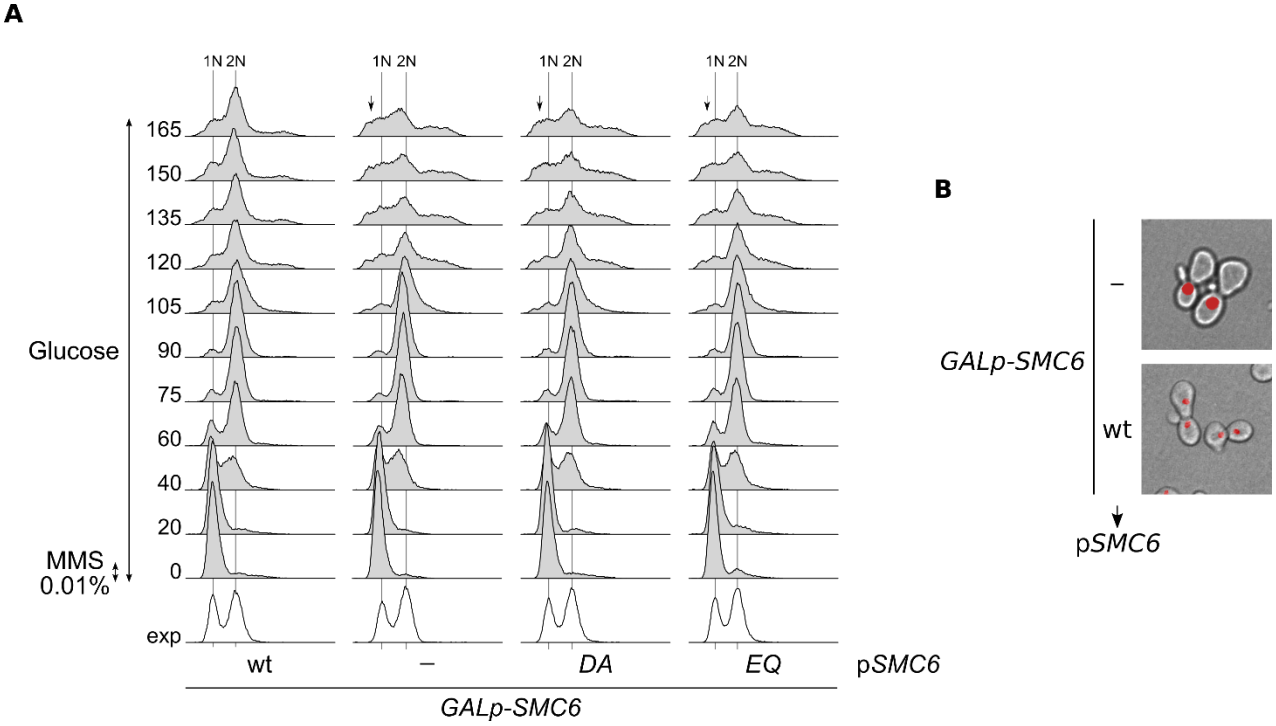

Figure 35. DNA segregation in the presence of induced damage is dependent on the ATPase activity of Smc6. (A) FACS profiles showing the DNA content of cells bearing with induced damage in the presence of the different ATPase mutant alleles of *SMC6*. Endogenous *SMC6* was under the control of a galactose promoter (GALp) in order to control its expression by shifting the carbon source in the media. The cultures were grown overnight in galactose, shifted to glucose for 5 hours and synchronized in G1 with alpha factor for 2 hours before treating them with 0,01% MMS for 30 minutes to induce DNA damage. Release into a synchronous S phase was performed in the presence of glucose and samples were taken every 20 minutes. Absence of Smc6 induces missegregation of genomic DNA which can be seen by the appearance of a peak bellow 1N DNA content. ATPase mutant alleles generate the same phenotype, while addition of a wild type copy of Smc6 recovers a normal segregation. **(B)** Representative microscopy images of a sample taken at 150 minutes into the time course. The images result from the merge of a bright field image and Hoechst-stained DNA. The images have been processed to add red color to DNA. DNA missegregation can be observed in cells with no *SMC6* expression, as daughter cells contain the whole genomic material. This phenotype cannot be observed in cells expressing wild type *SMC6* ectopically.

Strains in this figure: YTR3713, YTR3714, YTR3715 & YTR3717

4.3.2. A Fully Functional ATPase on Smc6 is Required for Binding to DNA

Next, we tested whether the ATPase activity of Smc6 was also required for the interaction of the complex with chromatin. We used chromosome spreads to test the

binding of wild type and ATPase mutant Smc6-6xHA proteins to chromatin in *smc6-AID* cells, which allow degradation of the endogenous Smc6 protein.

We could not observe any fluorescent signal in *smc6-AID* cells (Figure 36), as expected for no expression of any HA tag. Surprisingly, the quantity of Smc6-EQ protein bound to chromatin was significatively reduced in comparison to the wild type protein (Figure 36). Although Smc6-EQ might bind chromatin, as indicated by the significative difference with *smc6-AID*, this result indicated that hydrolysis of ATP is required for efficient binding of Smc6 to chromatin. Moreover, the different behavior of Smc5-EQ and Smc6-EQ in comparison with their respective wild type versions indicates that the ATPase in the Smc5/6 complex is asymmetric.

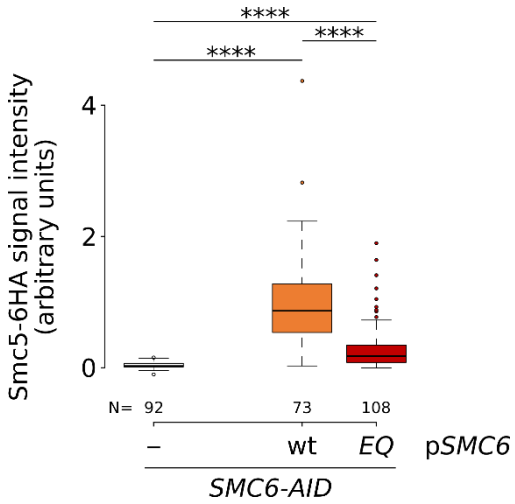

Figure 36. **Binding of Smc6 to chromatin is dependent on its ATPase activity. Quantification of the signal obtained in chromosome spreads images.** The N represents the number of nuclei quantified for each sample. All images were taken with the same settings in the microscope. All samples contained an internal standard to normalize all the quantifications. Hydrolysis of ATP is required for Smc6 to bind to DNA.

Significance levels are indicated with the following key: p>0,05 (ns), p≤0,05 (*), p≤0,01 (**), p≤0,001 (***), p≤0,0001 (****).

Strains in this figure: 5153, 5157 & 5160

4.3.3. Segregation of the rDNA Locus requires the ATPase Activity of Smc6 but is not Worsened by *smc6-EQ*

We have shown that the ATPase activity of Smc5 is essential for rDNA segregation. Moreover, the Smc5-EQ protein impaired rDNA segregation in almost all cells. The differential binding of Smc5-EQ and Smc6-EQ suggested that the rDNA segregation defects could be restricted to impaired ATP hydrolysis specifically in the Smc5 head.

To test this possibility, we transformed the centromeric plasmids containing the different versions of *SMC6* into a strain expressing the *smc6-9* thermosensitive allele. Using the tetO:491 system, we analyzed the segregation of the telomeric side of the rDNA in Smc6 ATPase mutants. We arrested cultures growing at 25 ºC in G1 and transferred them to 37 ºC for 30 minutes to inactivate the Smc6 thermosensitive protein. Then, we released the cultures into a synchronous cell cycle and collected samples to quantify the segregation of the rDNA. We observed that only 38% of *smc6-9* cells could segregate the tetR-YFP signal (Figure 37). Expression of wild type Smc6 protein recovered rDNA segregation to 85% of cells. Interestingly, 33% of Smc6-EQ cells segregated the telomeric side of the rDNA.

Overall, these results indicate that the ATPase activity of Smc6 is required for rDNA segregation. However, the impaired binding of Smc6-EQ to chromatin probably avoids a toxic function on DNA. Altogether, we conclude that the ATPase activity of Smc5/6, like that of cohesin and condensin, is asymmetric.

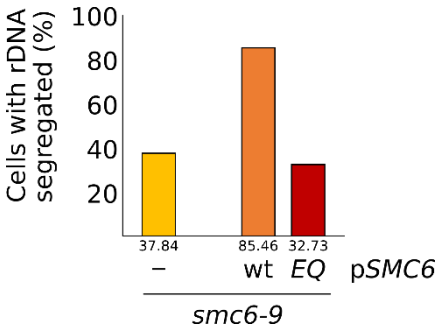

Figure 37. The ATPase activity of Smc6 is required for a correct segregation of the rDNA locus. Absolut quantification of rDNA segregation in cultures that have undergone a synchronous S phase after a G1 arrest. Endogenous Smc6 depletion is achieved by using a thermosensitive allele and performing the experiment at 37ºC. Each of the strains used has got either no plasmid, or a plasmid containing a wild type copy of Smc6 or the EQ mutant allele. If there is no expression of Smc6, a half of the cells in the culture missegregate the rDNA. Expression of a wild type copy of Smc6 recovers rDNA segregation for all cells in the culture. Blocking ATP hydrolysis has no effect, half of the cells missegregate the rDNA as if there was no Smc6.

Strains in this figure: YTR172, YMT4799 & YMT4800

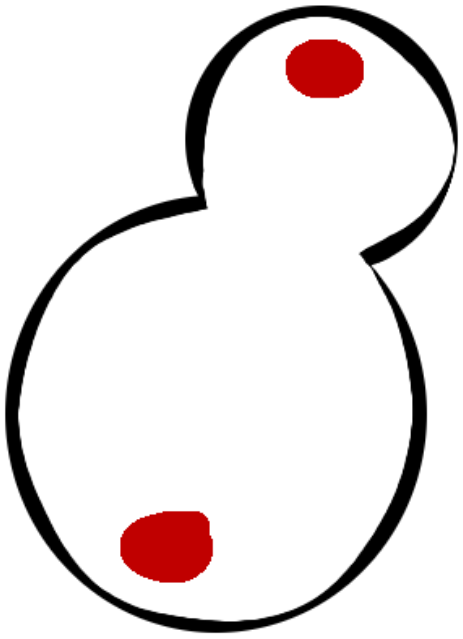

5 DISCUSSION

5. DISCUSSION

5.1. Requirements for the Binding of Smc5 to Chromatin

5.1.1. The Binding of the Smc5/6 Complex to DNA Requires the ATPase Activity of Smc5 and the Nse1/3/4 and Nse5/6 Subcomplexes

SMC complexes have to directly engage with chromatin to promote loop extrusion and organize chromosomes. Different functions, able to regulate the interaction with DNA, have been attributed to structural domains within SMC complexes. For the two most well-studied SMC complexes, cohesin and condensin, the ATPase activity is essential for their association with DNA (Arumugam et al., 2003; Thadani et al., 2018). Recent *in vitro* experimental data also points to a role of the ATPase in the Smc5/6 complex in binding to DNA (Gutierrez-Escribano et al., 2020; Kanno et al., 2015; Taschner et al., 2021). However, there is very little information about the role of the ATPase activity *in vivo*. In this thesis, we have observed that the binding of Smc5/6 to chromatin is regulated by both its ATPase activity (Figure 18) and the presence of different non-SMC subunits in the Nse1/3/4 and Nse5/6 subcomplexes (Figure 14, 15).

The expression of Smc5 ATPase mutant alleles *in vivo* confirmed, as observed *in vitro* (Gutierrez-Escribano et al., 2020; Taschner et al., 2021), that: (1) ATP binding to Smc5 is required for the complex to interact with DNA; and (2) blocking of ATP hydrolysis enhances the association of Smc5 with chromatin (Figure 18). When compared to other SMC complexes in budding yeast, this regulation is similar to cohesin (Hu et al., 2011) while it differs from condensin, in which Smc2 binding to ATP is apparently not even required for the recruitment of the complex to DNA (Thadani et al., 2018). It is difficult to ascertain whether this is due to a differential coordination of the ATPase cycle with chromatin binding or to the different penetrance of the ATPase mutations in different SMC complexes.

All SMC complexes have a common core, a trimer composed of two SMC proteins and one kleisin subunit. We have shown that Nse4, the kleisin subunit of the Smc5/6 complex, is required for Smc5 to interact with chromatin (Figure 14). In condensin, the kleisin subunit of the complex, is necessary for its interaction with chromatin (Kschonsak et al., 2017). The kleisin subunit Nse4 is not only interacting with the Smc5/6 dimer, but it also forms a subcomplex with two other subunits: Nse1 and Nse3. Earlier studies defined a winged-helix domain on the C-terminal of Nse3 that interacts with DNA (Zabrady et al., 2016). This interaction is necessary for the association of Smc5/6 with chromatin (Moradi-Fard et al., 2021; Zabrady et al., 2016) (Figure 15). Hence, since the lack of Nse4 brings a subsequent loss of interaction of Nse3 with the Smc5/6 complex, the loss of Nse4 might indirectly prevent the recruitment of the complex to DNA though the winged-helix domain of Nse3.

Nse1 and Nse3 are KITE subunits, which are unique in eukaryotic SMC complexes, as both cohesin and condensin non-SMC subunits are large proteins

belonging to the HAWK family of kleisin associated factors (J. J. Palecek & Gruber, 2015; Wells et al., 2017). The requirement of the KITE subunit Nse3 for the binding of Smc5/6 to chromatin mirrors the role of HAWK subunits in cohesin and condensin, which are also required for the binding of these complexes to DNA. In condensin, the DNA binding domains at the C-terminal end of Ycg1 functions together with Brn1 to promote the binding of condensin to chromatin (Kschonsak et al., 2017). In cohesin, two HAWK subunits, Pds5 and Scc2, have opposite roles: Pds5 inhibits ATP hydrolysis, while Scc2 enhances it (Petela et al., 2018). Interestingly, cohesin complexes that contain Scc2 can be loaded onto chromatin and translocate away from the loading site, while those that contain Pds5 would be the ones that can be released from chromosomes (Petela et al., 2018). A second comparison can be made between Nse3 and the KITE subunits found in bacterial SMC, for example MukE in the MukBEF complex, which seem to be evolutionary related (J. J. Palecek & Gruber, 2015). This bacterial KITE subunit is an inhibitor of the MukBEF ATPase activity (Zawadzka et al., 2018) and can interact with DNA to recruit MukF, a kleisin subunit that recruits the MukB dimer (Bürmann et al., 2021). The relation between Nse1/3 and the ATPase activity of the Smc5/6 complex remains unknown and, an inhibitory or activator effect of these subunits on the ATPase activity of the complex, could also explain why Smc5 displays a lower interaction with chromatin in the absence of Nse3.

Recent reports indicate that, in vitro, the Nse5/6 subcomplex has an inhibitory effect on the ATPase activity of the Smc5/6 complex (Hallett et al., 2021; Taschner et al., 2021). Our results indicate that, when Nse5 is depleted, the binding of the complex to DNA is reduced (Figure 15), agreeing with previous published data (Bustard et al., 2016). However, these results do not correlate with in vitro observations that an hexameric Smc5/6 complex without Nse5/6 binds to DNA (Taschner et al., 2021). Interestingly, it seems that Nse5/6 could play a role comparable to MukE, which inhibits the ATPase activity of MukBEF but is needed for the interaction of the complex with DNA (Bürmann et al., 2021; Zawadzka et al., 2018).

We can make a dual interpretation of our result. First, the most plausible option is that the Smc5/6 complex needs all its subunits to bind chromatin. Second, the lack of Nse5/6 should mean a faster ATPase activity that could be translated in either a higher turnover of the complex on chromatin or unproductive ATP hydrolysis. It would be interesting to test a double *nse5 smc5-EQ* mutant, which we would expect to differentiate between these two hypotheses. If the absence of Nse5 generates a higher turnover of the wild type Smc5/6 complex, the *smc5-EQ* mutation would block it, retaining its higher interaction with chromatin. On the other side, if Nse5 prevents unproductive ATP hydrolysis, its absence would have no effect on the Smc5-EQ mutant protein, which is already unable to hydrolyze ATP. However, it is difficult to anticipate whether Smc5-EQ would still be able to interact with chromatin in our first hypothesis. We do not know whether Smc5/6 requires all its subunits due to a specific role of each of them or to structural reasons. For example, a recently described connection between Nse5/6 and

Rtt107 supports the idea that each subunit plays a specific role on the loading of the Smc5/6 complex onto chromatin (Leung et al., 2011). The Nse6 N-terminal domain interacts with Rtt107, a protein that also interacts with γH2A, an ATR-phosphorylated histone, which accumulates in the vicinity of damaged DNA or forks (Li et al., 2012; Wan et al., 2019; Williams et al., 2010). The bridging role exerted by Rtt107 could explain the need for the Nse5/6 complex and ultimately Nse5 to recruit Smc5/6 to damaged chromatin.

Finally, both the ATPase activity of the Smc5/6 complex and its interaction with ssDNA activate the SUMO ligase activity of Nse2 (Bermúdez-López et al., 2010; Varejão et al., 2018). The hyper-sumoylation that we observed on Smc5-EQ proves that the catalytic activity of the ATPase in Smc5 is not necessary for the activation of the SUMO ligase activity of Nse2. ATP binding to Smc5 activates the Nse2 SUMO ligase. Moreover, we can now correlate both Nse2 SUMO-ligase regulatory events. The binding of ATP to Smc5/6 induces a conformational change of the coiled-coils and also regulates the interaction of the complex with DNA (Figure 18). Two possibilities could explain the hyper-sumoylation of Smc5-EQ: (1) the conformational change induced by ATP binding and DNA stimulation have an additive effect on the activation of the SUMO-ligase of Nse2 or (2) the accumulation of Nse2 and Smc5 molecules on chromatin account for a higher concentration of sumoylated Smc5 in protein extracts.

Overall, we have observed that the binding of the Smc5/6 complex to DNA is dependent on both the binding of ATP to Smc5 and the presence of the Nse1/3/4 and Nse5/6 subcomplexes. Although we have focused our work on the loading of the complex onto DNA, we can also confirm that the unloading mechanism requires at least the hydrolysis of ATP by Smc5.

5.1.2. Smc5 Binds to Replication Origins, Convergent Transcription Sites and Stalled Replication Forks

The binding of the Smc5/6 complex to DNA has been mainly using ChIP and *in vitro* experiments (de Piccoli et al., 2006; Jeppsson et al., 2014; Lindroos et al., 2006; Moradi-Fard et al., 2021; M.-A. Roy et al., 2011; M.-A. Roy & D'Amours, 2011; Zabrady et al., 2016). In this work, we have studied additional parameters to characterize the interaction of Smc5/6 with nucleic acids. Our results indicate that the Smc5/6 complex binds to DNA during replication (Figure 8, 9), suggesting that it has important roles at the time of DNA replication. In support of this hypothesis, it was previously shown, using temperature sensitive alleles in combination with inactivation of Smc5/6 at specific cell cycle phases, that the function of the complex was critical during S phase, but not after a metaphase arrest, to promote rDNA segregation (Torres-Rosell, de Piccoli, et al., 2007). In accordance with this observation, the human Smc5/6 is also specifically required during S phase, and not in mitosis, to promote chromosome disjunction (Venegas et al., 2020). In contrast, Menolfi et al., 2015 used S-phase and G2-phase

specific promoters-degron combinations to limit the expression of Smc5/6 proteins to specific phases of the cell cycle. Expression of the subunits only during S-phase had adverse effects in cell viability, while restricting expression in G2/M had a wild type phenotype. The differences might be due to the growth regimes and mutant alleles used in each work (i.e. thermosensitive and auxin-sensitive degron alleles in the first studies versus promoter change plus fusion to a cyclin degron box in the latter). Interestingly, the Smc5/6 seems to display maximum binding to chromatin in cells arrested in metaphase (Figure 7). However, we still do not know what mechanism could regulate the increased association of Smc5/6 with chromatin along the cell cycle. We hypothesize about two different possibilities, operating through unknown mechanisms, to explain the increased association of the complex with chromatin as the cell cycle advances: (1) a higher binding rate in combination with a stable unloading rate, compared to earlier stages of the cell cycle; or (2) a decrease in the turnover of the complex on DNA due to a more stable interaction in G2/M. It is possible that, if the complex is recruited to specific structures, such as replication forks or cohesin-binding sites (see below), Smc5/6 association to chromatin will increase if these structures become more abundant as the cell cycle progresses.

Chromatin immunoprecipitation of Smc6 and Nse1 in hydroxyurea-arrested cells revealed the binding of the Smc5/6 complex to early origins of replication (Lindroos et al., 2006). Based on this observation, it was proposed that the complex binds to either stalled replication forks or recently replicated DNA. The hydroxyurea treatment depletes the nucleotide pool in the cell and inhibits replication, causing replication forks to stall. This means that the binding of Smc6 to these origins was observed in cells with activated checkpoint responses. In this thesis, we have used an *smc5-EQ* allele as a reporter of the loading sites used by the Smc5/6 complex during the cell cycle. This mutant allele cannot hydrolyze ATP but is able to interact with DNA both *in vitro* (Taschner et al., 2021) and *in vivo* (Figure 19). The equivalent EQ mutation on Smc1 or Smc3 provokes the enrichment of cohesin on centromeric sequences, displaying a sharp peak on those regions that is much wider in wild type Smc1 and Smc3 experiments (Hu et al., 2011). This phenotype has been related to the inability of ATP-hydrolysis cohesin mutants to translocate along DNA. Since both translocation and loop extrusion require ATP hydrolysis, EQ mutants in SMC complexes remain anchored at their original loading sites. So, we propose that the ChIP-seq of the Smc5-EQ mutant represents a still photograph of all binding events occurring in a cell cycle from G1 to metaphase.

Our ChIP analysis of the Smc5-EQ protein revealed that it binds to replication origins (Figure 21, 22, 25). Interestingly, we have demonstrated that stalling of replication forks is not required for Smc5 to bind origins of replication. However, we do not know whether the binding of the complex to these sites is transient (restricted to newly activated origins) or is extended, translocating from loading sites at origins and escorting the replication fork. Similarly to Smc5/6, bacterial SMC complexes are loaded close to the origin, in each sister chromatid, physically separating sister DNA molecules through

a loop extrusion-mechanism (Karaboja et al., 2021). Thus, we hypothesize that the Smc5/6 complex could have an analogous function in eukaryotes, promoting the disjunction of sister chromatids from the very first moment they are synthesized. In fact, bacterial SMCs and the Smc5/6 complex seem to be close relatives, from the evolutionary and structural point of view (J. J. Palecek & Gruber, 2015). Interestingly, the detection of Smc5-EQ binding at origins of replication in G2/M-arrested cells suggests that the mutant complex could have a considerable half-life on DNA. Experiments with cell cycle-dependent expression of the *smc5-EQ* allele will be needed to clarify whether the interaction with origins of replication has to be established during replication or can occur at later cell cycle stages.

Other reports have shown that the Smc5/6 complex binds to convergent transcription sites around the centromeres (Jeppsson et al., 2014). Using the *smc5-EQ* allele as a reporter for loading sites, we have observed that the complex does not only bind to convergent transcription sites around the centromeres but also at most other sites in the genome (Figure 23,24, 25). For the wild type protein, the convergent transcription sites around the centromeres were places in which the Smc5/6 complex colocalized with cohesin (Jeppsson et al., 2014). In accordance, (1) cohesin translocates to convergent transcription sites, (2) the binding of Smc6 to chromatin is dependent on cohesin and (3) other studies indicate that both complexes co-localize in over 60% of the Smc6 peaks (Lengronne et al., 2004; Lindroos et al., 2006). The transcription machinery was proposed to be the responsible for the translocation of cohesin, pushing the complex to the 3' end of the transcribed gene. Since the Smc5-EQ mutant protein is most probably unable to translocate along chromatin, our hypothesis is that the convergent transcription sites are loading sites for the Smc5/6 complex.

Together, the loading of the Smc5/6 complex to ARS and convergent transcription sites account for 70% of the Smc5-EQ observed peaks. The main known role of the Smc5/6 complex is on resolution of sister chromatid junctions, which are believed to be mainly recombination and replication intermediates (Bermúdez-López et al., 2010). It is unclear if Smc5/6 binds directly to sister chromatid junctions, or if it promotes long distance effects to trigger their removal. In fact, the appearance of such structures is supposed to be mostly random and, if Smc5/6 bound to them, it would not generate defined peaks in the ChIP-seq. Thus, it is possible that Smc5/6 organizes chromatin to promote the remote elimination of sister chromatid junctions from its location at its most common binding site, convergent transcription regions. Alternatively, convergent transcription might be a chromosomal feature more prone to trigger DNA junctions, due to the increased topological burden, and a site more frequently bound by Smc5/6.

In this work, we have also studied the binding of Smc5 to chromatin after MMS treatment, when damaged replication forks accumulated in the genome. We have taken advantage that these forks are processed to inhibit different steps of their remodeling and repair, leading to the accumulation of different types of DNA structures (Figure 10). Since the absence of the Smc5/6 complex is related to defects on chromosome

disjunction, we expected to see an accumulation of Smc5 on chromatin when these structures could not be resolved. Surprisingly, after MMS treatment, mutants impaired in dissolution of replication and recombination intermediates did not accumulate Smc5 on chromatin to a higher extent than wild type cells (Figure 11). We also tested a set of mutant strains unable to trigger template switch on damaged replication forks. Interestingly, the quantity of Smc5 bound to chromatin was increased in this situation (Figure 12). Previous reports show the implication of the Smc5/6 complex on regulating different DNA repair pathways, mainly at early stages (Bonner et al., 2016; Xue et al., 2014; Zapatka et al., 2019). We propose that Smc5/6 could load onto replication origins and follow fork progression from a close distance. Thus, the complex would be already at the replication fork upon encountering DNA damage, which would explain the roles regulating early phases of DNA repair pathways. For instance, the ssDNA at the collapsed replication fork could directly activate the SUMO ligase of Nse2, that results in Smc5 sumoylation and activation of Mph1 to start fork regression (Varejão et al., 2018; Zapatka et al., 2019). However, this would not explain why there is more binding of Smc5 to chromatin in mms2Δ or rad5Δ cells. We think that, the affinity of the hinge domain for ssDNA (Alt et al., 2017), the higher affinity of Smc5 and Smc6 for ssDNA (M.-A. Roy et al., 2011; M.-A. Roy & D'Amours, 2011) and the activation of the SUMO ligase activity of Nse2 by ssDNA (Varejão et al., 2018) could indicate that Smc5/6 loads onto DNA at regions with accumulation of ssDNA. This is also in accordance with the presence of ssDNA at origins of replication, shortly after entrance into S-phase (Feng et al., 2006).

5.2. The Smc5/6 Complex Promotes the Formation of a DNA Intermediate During its Loading on Chromatin

5.2.1. Cell Survival Depends on the ATPase Activity of Smc5

The function of the ATPase heads in the Smc5/6 complex has not been analyzed in detail. In fact, few studies have used ATPase mutants in the Smc5/6 complex. Three of them do it *in vitro* with a purified Smc5/6 complex and were recently published (Hallett et al., 2021; Kanno et al., 2015; Taschner et al., 2021). Another article used the ATPase mutant alleles of the *S. pombe* complex in a two-hybrid assay to study the role of the KITE subunits on the interactions between the kleisin and the SMC subunits (Vondrova et al., 2020). In this thesis, we have studied ATPase mutants in the Smc5/6 complex *in vivo* through their ectopic expression in temperature or auxin sensitive mutants. ATPase mutant alleles are recessive and permit the wild type allele to sustain cell growth (Figure 17, 34). Surprisingly, the *smc5-EQ* allele, unable to hydrolyze ATP, was the most sensitive to downregulation of the wild type protein (Figure 17). We hypothesize that the Smc5-EQ protein remains bound to DNA for longer times than the wild type protein. In addition, it is probably affected in translocation on DNA, or in the presumptive loop extrusion activity of the Smc5/6 complex, which could be the key to understand its severe phenotype. In contrast, the Smc5-DA protein, which cannot bind ATP and is unable to

interact with DNA displays a growth phenotype identical to the absence of Smc5 (Figure 17). Thus, it is preferable not to have any Smc5 bound to chromatin than to have a mutant protein that binds DNA but does not complete the hydrolysis cycle.

5.2.2. Impaired ATP Hydrolysis by Smc5 Induces rDNA Missegregation

Work from several labs indicate that the rDNA locus is particularly sensitive to Smc5/6 activity, with important functions in replication and repair of this repetitive array (Menolfi et al., 2015; X. P. Peng et al., 2018; Torres-Rosell, de Piccoli, et al., 2007; Torres-Rosell, Machín, et al., 2005; Torres-Rosell, Sunjevaric, et al., 2007). For example, inactivation of the Smc5/6 complex prevents rDNA disjunction and proper segregation in anaphase. In general, this phenotype is exhibited by half of the cells in a population, reaching a maximum of around 60% in some thermosensitive mutants (Torres-Rosell, de Piccoli, et al., 2007). It is currently unknown why some cells missegregate the rDNA and others do not. It could be due to the random appearance of sister chromatid junctions in only some cells in the population, or to cell-to-cell variability, for example due to differences between mother and daughter cells, different metabolic rates or rRNA expression levels, etc. Strikingly, expression of the *smc5-EQ* allele prevented the disjunction of the rDNA in almost all cells (>95%) (Figure 29). There are (at least) two possible explanations for this observation. The first one is that thermosensitive or auxin-sensitive alleles may not be strong enough to completely inactivate Smc5/6. Alternatively, *smc5-EQ* might represent a gain-of-function allele with deleterious consequences for chromosome segregation. In relation to the first hypothesis, it is difficult to ascertain to what extent a thermosensitive allele inactivates protein function. In fact, Smc5/6 thermosensitive alleles display different penetrances; for example, *smc5-6* is less tight than *smc6-9* in terms of temperature sensitivity, DNA damage sensitivity or rDNA missegregation (Torres-Rosell, Machín, et al., 2005). Thus, it is possible that Smc5/6 function cannot be completely inactivated in the temperature sensitive alleles used in this study. Similarly, one of the possible problems of auxin-dependent degrons is the leakiness of the system, as fast and complete degradation of all AID-tagged molecules is probably very difficult. We can speculate that the little amount of Smc5-AID protein remaining after addition of auxin may be enough to form a functional complex and, in some cells, remove the sister chromatid junctions that prevent rDNA segregation. In contrast, the Smc5-EQ protein could form Smc5/6 complexes, capturing other subunits and preventing the formation of residual but active wild type Smc5/6 complexes. However, we do not favor this hypothesis, as *smc5-DA* expression does not further impair rDNA segregation in *smc5-AID* cells (Figure 29), although we cannot discard that the *smc5-DA* allele fails at interacting with some subunits of the complex. Thus, we propose that the Smc5-EQ protein has a gain-of-function that interferes with cell growth and chromosome segregation by promoting the accumulation of sister chromatid junctions.

One of the reasons for impaired rDNA segregation in *smc5/6* mutants is the accumulation of forks arrested at the replication fork block (RFB) (X. P. Peng et al., 2018). The deletion of *FOB1* reduces this accumulation, alleviating the segregation problems of the Smc5 deletion (J. Peng & Feng, 2016; Torres-Rosell, de Piccoli, et al., 2007). The deletion of *RAD51* also alleviates the segregation problems in *smc5*/6 mutants, it reduces the accumulation of recombination intermediates by blocking strand invasion (Menolfi et al., 2015). Indeed, both ***fob1Δ*** and ***rad51Δ*** improved the segregation of the rDNA in the absence of Smc5 (Figure 30). The combination of these mutations with *smc5-EQ* expression also alleviates the rDNA segregation defects, although a higher percentage of cells can segregate the rDNA in ***fob1Δ*** *smc5-EQ* than in ***rad51Δ*** *smc5-EQ*. This indicates that the problems observed at the rDNA in *smc5-EQ* stem more frequently from forks stalling at the RFB than to Rad51-dependent recombination intermediates. However, the suppression of *smc5-EQ* by ***fob1Δ*** or ***rad51Δ*** did not reach the levels of rDNA segregation in Smc5 depleted cells (*smc5-AID*). This observation suggests that most of the problems arising in *smc5-EQ* cells are not due to the accumulation of forks arrested at the RFB.

The relevant questions here are (1) how does the Smc5-EQ protein aggravate the rDNA segregation defects of Smc5/6 mutants, and (2) whether this effect is reporting on the mechanisms used by the wild type Smc5/6 complex to associate with DNA during a normal ATPase cycle. We hypothesize that Smc5/6 complex alters the topology of DNA during the loading reaction (before ATP hydrolysis), generating an intermediate that can potentially link the two sister chromatids and that is eventually removed once ATP is hydrolyzed. It is currently unclear how this intermediate would look like. Based on current models about SMC function, ATP binding and hydrolysis is used to extrude loops of DNA through a series of conformational changes in the SMC molecule that imply substantial rearrangements in protein-protein and protein-DNA contacts in the complex. In their ATP-bound state, before ATP hydrolysis, SMC complexes are invariably bound to at least one molecule of DNA, which is sandwiched between the ATPase heads and the kleisin-KITE/HAWK subunits. But SMC complexes must bind a second DNA molecule during their ATPase cycle, to either condense a chromosome or entrap the sister chromatid. We thus propose that in the ATP-bound state, Smc5/6 is binding to two different DNA molecules, most probably two strands belonging to the two sister chromatids. Other activities in the cell, such as helicases, topoisomerases, etc, could then transform this intermediate into a pathological structure that prevents segregation.

The conformation of the SMC complex in its ATP-bound form probably does not allow it to move away from its loading site. However, it is possible that the pathological structure connecting both sisters may migrate away. In fact, this structure must be removable through the action of a second Smc5/6 molecule, since wild type Smc5/6 can counteract the deleterious effect of the *smc5-EQ* allele. We conclude that the pathological structures must be mobile elements, migrating from the site where they are formed by the Smc5-EQ protein to new sites where they can be removed by wild type

Smc5/6. This hypothesis opens a new question: what is the intermediate structure generated by Smc5/6 during its loading onto DNA? We thought of two possible answers to this question. First, the link between the two sister chromatids could be protein-mediated, either direct, by topological entrapment into the lumen of the own Smc5/6 complex, or indirect, using other proteins to bridge the two sister chromatids. Second, the intermediate could be a DNA structure, either a HJ-like structure or catenated sisters. The fact that the pathological structure should translocate along the chromosome to be repaired by the wild type Smc5 protein suggests that, most likely, the intermediate is a DNA structure. The observation that linkages can be removed if the cell is given sufficient time before mitotic exit (Figure 31) is in agreement with the presence of mobile structures that can be dissipated towards the telomere.

A drawback of our hypothesis is that the Smc5-EQ protein is bound at different points along the genome but, in the absence of replicative stress, the missegregation problems only occur at the rDNA. We think that, the higher concentration of Smc5-EQ bound to the ARS and RFB sequences in the rDNA, compared to any other locus in the genome (Figure 26), could amplify a low frequency event and generate sister chromatid linking structures. In this thesis, we have designed a system to recruit the Smc5/6 complex to a specific locus in the DNA. In this case, we recruited Smc5-EQ to the 455 Kb sequence in chromosome XII. This region is upstream of the rDNA and does not display missegregation in *smc5/6* mutant cells (Figure 33). Recruitment of Smc5-EQ protein to this region significantly increased its missegregation (Figure 33), proving that artificial recruitment of Smc5-EQ to DNA affects chromosome disjunction and indicating that Smc5-EQ can generate toxic structures not only at the rDNA but also at other locations in the genome. Future experiments should include the study of other genomic loci, since we studied a locus in close proximity with the rDNA, what could sensitize it to suffer from missegregation. Moreover, the recruitment of Smc5/6 to the desired loci should be quantified to test to what extent the effect of the protein is dependent on its enrichment at a specific locus. Finally, the study of the segregation at telomeric sites in *smc5-EQ* cells would help to corroborate that Smc5-EQ deleterious effect is not restricted to the rDNA.

Additionally, we have observed that artificially extending mitosis improves segregation of the rDNA in *smc5-AID* cells (Figure 31). This result suggests that the accumulation of stalled replication forks and recombination intermediates can eventually be removed by an alternative pathway, independent of Smc5/6. Moreover, the artificial elongation of mitosis using *cdc15-AID* is also beneficial for *smc5-AID smc5-EQ* cells. However, the percentage of cells that segregate the rDNA in this strain is still low (20%) a few hours after completion of anaphase, which combined with the low segregation observed in both the *fob1Δ smc5-EQ* and *rad51Δ smc5-EQ* cells, indicates that most of the problems observed in *smc5-EQ* cells are not related to fork stalling or resolution/dissolution of recombination intermediates.

The difference on growth and rDNA segregation that we observed between the EQ and the DA alleles of Smc5 in the absence of DNA damage could not be appreciated when we looked at bulk genomic segregation after a treatment with MMS (Figure 32). Both the absence of Smc5 and the presence of any ATPase mutant prevented chromosome segregation. We think that this lack of differences is not related to the specific function performed by the EQ allele. A more plausible explication is that a huge amount of damage is generated by even a short pulse of alkylation damage and is enough to mask the differential phenotype produced by the ATP hydrolysis mutant allele. The damage generated by the MMS treatment is enough to prevent chromosome disjunction, as can be observed both under the microscope and by FACS analysis. The described missegregation of the genomic DNA is always in the same direction, carrying all the chromatin into the bud, away from the mother cell.

Overall, we have demonstrated that the ATPase activity of Smc5 is essential for cell viability. The impairment of the catalytic ability of the ATPase of Smc5 promotes a persistent loading of the protein onto DNA. The accumulation of this protein on a genomic locus enhances the probability of generating a pathological DNA structure that prevents segregation of sister chromatids. We believe that these DNA structures are accumulated on the rDNA in the absence of replicative stress due to the higher quantity of Smc5-EQ loaded onto this repetitive sequence of the genome. Moreover, these structures are only marginally related to concentration of arrested replication forks or recombination intermediates at the rDNA.

Accumulating the evidences along this work, we speculate that the toxic structure generated by ATP-hydrolysis mutant Smc5/6 complexes might be catenations. (1) We have observed that the loading sites of Smc5/6 include regions that exhibit supercoiling such as convergent transcription sites (Figure 23). (2) Moreover, this toxic structure can be translocated along the genomic sequence to be eliminated in the presence of the wild type Smc5 protein (Figure 17). (3) On top of that, the toxic structure created by Smc5-EQ is only marginally dependent on forks stalled at the RFB and recombination dependent intermediates (Figure 30). (4) Topoisomerases play a role during transcription at the rDNA (Brill et al., 1987; French et al., 2011) and Smc5 physically interacts and co-immunopurifies with Top2 and its association with chromatin increases in *top2* mutants, when sister chromatids become catenated (Kanno et al., 2015). (5) Finally, recent studies indicate that Smc5/6 would bind to and stabilize plectonemes and supercoiled structures in vitro (Serrano 2020; Gutierrez-Escribano 2020), an activity that is also compatible on binding two juxtaposed sister molecules, promoting their catenation.

5.3. The ATPase of the Smc5/6 Complex Displays an Asymmetric Behavior

The SMC proteins belong to the ABC type family of ATPases, many of which are transmembrane transporters (Holland & Blight, 1999). Studies on the P-glycoprotein multidrug transporter (Pgp) indicated that, two ATPase domains work in a coordinated

manner to hydrolyze ATP and provide the energy to pump different substrates across the membrane (Senior et al., 1995). However, the hydrolysis of ATP is never simultaneous in both ATPase domains in Pgp, it is alternate since the ATP bound on one catalytic site prevents hydrolysis at the second site. Later on, an asymmetric behavior was described for some heterodimeric ABC transporters (Procko et al., 2009). This asymmetry is due to the fact that only one of the subunits in the transporter can hydrolyze ATP. Finally, a more complex asymmetry was described for condensin (Hassler et al., 2019). In this case, both the binding and the hydrolysis of ATP at each subunit of the heterodimer controls both conformational changes and the binding to different subunits of the complex. The different steps in this asymmetric ATPase cycle would permit the loop extrusion by condensin.

Comparison of the phenotype exhibited by the *smc5-EQ* and *smc6-EQ* alleles, suggests that the Smc5/6 complex could also have an asymmetrical behavior. While the Smc5-EQ protein binds more strongly to chromatin and aggravates the growth and rDNA segregation defects of *smc5* mutants, defective association of the Smc6-EQ to chromatin (Figure 36) avoids additive effects on growth or segregation of the ribosomal DNA locus in *smc6* mutant cells (Figures 34 and 37). The mutations used in our study are equivalent to those used for description of an asymmetric ATPase cycle in condensin (Hassler et al., 2019; Thadani et al., 2018). On the other hand, it is worth keeping in mind that there are limitations in our study. The differential binding to chromatin observed for the Smc5-EQ and Smc6-EQ mutant proteins (Figure 36) could be explained by either the normal asymmetric behavior of the complex or by the artificial blockage of ATP hydrolysis in mutant alleles. Thus, we currently cannot exclude the possibility that the EQ mutants create an artificial condition that is never encountered by the wild type Smc5/6 complex.

The asymmetric behavior of the ATPase mutant alleles of the Smc5/6 complex is common in all SMC complexes in budding yeast (Elbatsh et al., 2016; Hassler et al., 2019; Thadani et al., 2018). An asymmetric behavior might be profitable to trigger sequential conformational changes, particularly if there is a strict order of ATP hydrolysis by the two heads, a mechanism that could promote progressive loop extrusion by reeling in DNA from the same direction.

From our observations, we cannot tell whether the active site of Smc5 or Smc6 is the first one to hydrolyze ATP. However, a recently published study presents a Cryo-EM structure of an hexameric Smc5/6 with EQ mutant Smc5 and Smc6 proteins (Yu et al., 2022). The structure described in the publication shows an interaction of this double mutant with the subcomplex Nse1-3-4 and also with DNA. Since the Smc5-EQ mutant protein also binds strongly to chromatin, the simplest hypothesis that the single Smc5-EQ mutant complex might interact with DNA in a similar way as the double Smc5-EQ/Smc6-EQ mutant complex. If this hypothesis is right, then the wild type Smc6 protein that pairs with the mutants Smc5-EQ proteins must be unable to hydrolyze ATP, waiting for Smc5 to do it first. This would imply that Smc5 hydrolyzes ATP before Smc6. In contrast, the single Smc6-EQ mutant complexes would allow the hydrolysis of ATP at

the catalytic site in Smc5, but not at Smc6. This would move the Smc5/6 complex one step forward in the sequence of conformational changes, leading to an intermediate that is more easily disengaged from chromatin. However, there are other possible and more complex scenarios that we currently cannot discard. For example, the way in which the single Smc5-EQ mutant is engaged with DNA might imply a completely different structure as the double Smc5-EQ/Smc6-EQ mutant.

Even though further studies should be performed to understand the asymmetry of the complex, we conclude that, at first sight, the Smc5/6 complex contains an ATPase with an asymmetric behavior. This piece of data opens the door to study more in depth this ATPase, for instance using combinations of the different ATPase mutants (unable to bind ATP, to dimerize the ATPase heads or to hydrolyze ATP) of Smc5 and Smc6, which could help to clarify the sequence of events during the ATPase cycle, the ensuing effects on the structure of the complex and its functions.

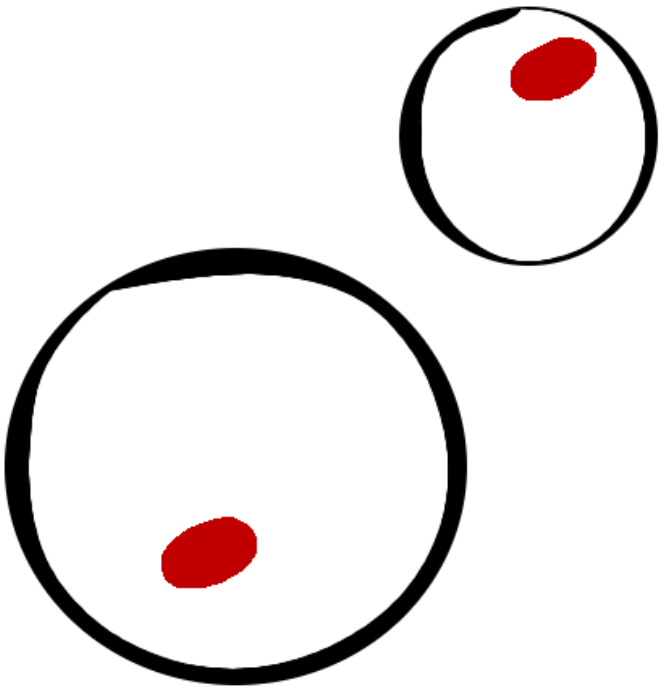

6 CONCLUSIONS

6. CONCLUSIONS

First. Association of Smc5 with chromatin progressively increases during DNA replication and is reduced upon entry into mitosis.

Second. Association of Smc5 with chromatin increases in mutants of template switch lesion bypass pathway but remains unaffected in the absence of recombination intermediate dissolution/resolution.

Third. The Nse1/3/4 and the Nse5/6 subcomplexes are required for the chromatin association of the Smc5/6 complex.

Fourth. The ATPase activity of Smc5 and Smc6 heads is essential for proliferation.

Fifth. The *smc5-E1015Q* allele, unable to hydrolyze ATP, has a gain of function that is toxic to the cell if not counteracted by sufficient levels of wild type *SMC5* expression.

Sixth. ATP binding to Smc5 is required for association of Smc5/6 with chromatin while ATP hydrolysis is required to prevent the accumulation of Smc5/6 molecules on chromatin.

Seventh. ChIP-seq analysis of the s*mc5-D1014A* ATP-binding mutant reveals a lower number of binding sites on chromatin while the hydrolysis mutant has increased binding sites when compared to the wild type protein.

Eighth. ChIP-seq analysis of the Smc5-E1015Q mutant protein reveals new binding sites for the Smc5/6 complex.

Ninth. Compared to wild type Smc5 protein, the ATPase mutant Smc5-E1015Q protein is enriched at the rDNA, tRNA genes, replication origins, codirectional and convergent transcription intergenic sites, but slightly depleted at centromeres.

Tenth. The *smc5-E1015Q* ATP hydrolysis mutant has a negative impact in segregation of the rDNA.

Eleventh. rDNA segregation defects in *smc5-E1015Q* cells are only partially dependent on forks arrested at the RFB and Rad51-dependent processes

Twelfth. Inhibition of cytokinesis provides extra time for segregation of the rDNA in cells with no Smc5 and alleviates rDNA segregation defects in *smc5-E1015Q* mutants.

Thirteenth. Artificial recruitment of the *smc5-E1015Q* mutant protein to a non-Smc5/6 binding site endangers its disjunction during chromosome segregation.

Fourteenth. Mild alkylating DNA damage similarly precludes nuclear segregation in cells with no Smc5/6 or expressing ATPase mutant alleles of Smc5 or Smc6.

Fifteenth. ATP hydrolysis at the Smc6 ATPase head domain is required for chromatin association of the Smc5/6 complex.

Sixteenth. rDNA disjunction is dependent on the ATPase activity of Smc6.

BIBLIOGRAPHY

BIBLIOGRAPHY

Alcasabas, A. A., Osborn, A. J., Bachant, J., Hu, F., Werler, P. J. H., Bousset, K., Furuya, K., Diffley, J. F. X., Carr, A. M., & Elledge, S. J. (2001). Mrc1 transduces signals of DNA replication stress to activate Rad53. *Nature Cell Biology*, *3*(11), 958–965. https://doi.org/10.1038/ncb1101-958

Alt, A., Dang, H. Q., Wells, O. S., Polo, L. M., Smith, M. A., McGregor, G. A., Welte, T., Lehmann, A. R., Pearl, L. H., Murray, J. M., & Oliver, A. W. (2017). Specialized interfaces of Smc5/6 control hinge stability and DNA association. *Nature Communications*, *8*(1), 14011. https://doi.org/10.1038/ncomms14011

Andrews, E. A., Palecek, J., Sergeant, J., Taylor, E., Lehmann, A. R., & Watts, F. Z. (2005). Nse2, a Component of the Smc5-6 Complex, Is a SUMO Ligase Required for the Response to DNA Damage. *Molecular and Cellular Biology*, *25*(1), 185–196. https://doi.org/10.1128/MCB.25.1.185-196.2005

Aragón, L. (2018). The Smc5/6 Complex: New and Old Functions of the Enigmatic Long-Distance Relative. *Annual Review of Genetics*, *52*(1), 89–107. https://doi.org/10.1146/annurev-genet-120417-031353

Arosio, D., Cui, S., Ortega, C., Chovanec, M., di Marco, S., Baldini, G., Falaschi, A., & Vindigni, A. (2002). Studies on the Mode of Ku Interaction with DNA. *Journal of Biological Chemistry*, *277*(12), 9741–9748. https://doi.org/10.1074/jbc.M111916200

Arumugam, P., Gruber, S., Tanaka, K., Haering, C. H., Mechtler, K., & Nasmyth, K. (2003). ATP hydrolysis is required for cohesin's association with chromosomes. *Current Biology : CB*, *13*(22), 1941–1953. https://doi.org/10.1016/j.cub.2003.10.036

Arumugam, P., Nishino, T., Haering, C. H., Gruber, S., & Nasmyth, K. (2006). Cohesin's ATPase activity is stimulated by the C-terminal Winged-Helix domain of its kleisin subunit. *Current Biology : CB*, *16*(20), 1998–2008. https://doi.org/10.1016/j.cub.2006.09.002

Banigan, E. J., van den Berg, A. A., Brandão, H. B., Marko, J. F., & Mirny, L. A. (2020). Chromosome organization by one-sided and two-sided loop extrusion. *ELife*, *9*. https://doi.org/10.7554/eLife.53558

Bauer, B. W., Davidson, I. F., Canena, D., Wutz, G., Tang, W., Litos, G., Horn, S., Hinterdorfer, P., & Peters, J.-M. (2021). Cohesin mediates DNA loop extrusion by a "swing and clamp" mechanism. *Cell*, *184*(21), 5448-5464.e22. https://doi.org/10.1016/j.cell.2021.09.016

Bell, S. P., & Stillman, B. (1992). ATP-dependent recognition of eukaryotic origins of DNA replication by a multiprotein complex. *Nature*, *357*(6374), 128–134. https://doi.org/10.1038/357128A0

Bermejo, R., Doksani, Y., Capra, T., Katou, Y.-M., Tanaka, H., Shirahige, K., & Foiani, M. (2007). Top1- and Top2-mediated topological transitions at replication forks ensure fork progression and stability and prevent DNA damage checkpoint activation. *Genes & Development*, *21*(15), 1921–1936. https://doi.org/10.1101/gad.432107

Bermejo, R., Katou, Y. M., Shirahige, K., & Foiani, M. (2009). ChIP-on-chip analysis of DNA topoisomerases. *Methods in Molecular Biology (Clifton, N.J.)*, *582*, 103–118. https://doi.org/10.1007/978-1-60761-340-4_9

Bermúdez-López, M., & Aragon, L. (2016). Smc5/6 complex regulates Sgs1 recombination functions. *Current Genetics*. https://doi.org/10.1007/s00294-016-0648-5

Bermúdez-López, M., Ceschia, A., de Piccoli, G., Colomina, N., Pasero, P., Aragón, L., & Torres-Rosell, J. (2010). The Smc5/6 complex is required for dissolution of DNA-mediated sister chromatid linkages. *Nucleic Acids Research*, *38*(19), 6502–6512. https://doi.org/10.1093/nar/gkq546

Bermúdez-López, M., Pociño-Merino, I., Sánchez, H., Bueno, A., Guasch, C., Almedawar, S., Bru-Virgili, S., Garí, E., Wyman, C., Reverter, D., Colomina, N., & Torres-Rosell, J. (2015). ATPase-Dependent Control of the Mms21 SUMO Ligase during DNA Repair. *PLOS Biology*, *13*(3), e1002089. https://doi.org/10.1371/journal.pbio.1002089

Beshnova, D. A., Cherstvy, A. G., Vainshtein, Y., & Teif, V. B. (2014). Regulation of the Nucleosome Repeat Length In Vivo by the DNA Sequence, Protein Concentrations and Long-Range Interactions. *PLoS Computational Biology*, *10*(7), e1003698. https://doi.org/10.1371/journal.pcbi.1003698

Bhavsar-Jog, Y. P., & Bi, E. (2017). Mechanics and regulation of cytokinesis in budding yeast. *Seminars in Cell & Developmental Biology*, *66*, 107–118. https://doi.org/10.1016/j.semcdb.2016.12.010

Bizard, A. H., & Hickson, I. D. (2014). The Dissolution of Double Holliday Junctions. *Cold Spring Harbor Perspectives in Biology*, *6*(7), a016477–a016477. https://doi.org/10.1101/cshperspect.a016477

Blanco, M. G., Matos, J., Rass, U., Ip, S. C. Y., & West, S. C. (2010). Functional overlap between the structure-specific nucleases Yen1 and Mus81-Mms4 for DNA-damage repair in S. cerevisiae. *DNA Repair*, *9*(4), 394–402. https://doi.org/10.1016/j.dnarep.2009.12.017

Bonner, J. N., Choi, K., Xue, X., Torres, N. P., Szakal, B., Wei, L., Wan, B., Arter, M., Matos, J., Sung, P., Brown, G. W., Branzei, D., & Zhao, X. (2016). Smc5/6 Mediated Sumoylation of the Sgs1-Top3-Rmi1 Complex Promotes Removal of Recombination Intermediates. *Cell Reports*,

16(2), 368–378. https://doi.org/10.1016/j.celrep.2016.06.015

Borrego-Soto, G., Ortiz-López, R., & Rojas-Martínez, A. (2015). Ionizing radiation-induced DNA injury and damage detection in patients with breast cancer. *Genetics and Molecular Biology*, *38*(4), 420. https://doi.org/10.1590/S1415-475738420150019

Bowen, N., Smith, C. E., Srivatsan, A., Willcox, S., Griffith, J. D., & Kolodner, R. D. (2013). Reconstitution of long and short patch mismatch repair reactions using Saccharomyces cerevisiae proteins. *Proceedings of the National Academy of Sciences*, *110*(46), 18472–18477. https://doi.org/10.1073/pnas.1318971110

Branzei, D., Seki, M., & Enomoto, T. (2004). Rad18/Rad5/Mms2-mediated polyubiquitination of PCNA is implicated in replication completion during replication stress. *Genes to Cells*, *9*(11), 1031–1042. https://doi.org/10.1111/j.1365-2443.2004.00787.x

Brewer, B. J., & Fangman, W. L. (1988). A replication fork barrier at the 3′ end of yeast ribosomal RNA genes. *Cell*, *55*(4), 637–643. https://doi.org/10.1016/0092-8674(88)90222-X

Brill, S. J., DiNardo, S., Voelkel-Meiman, K., & Sternglanz, R. (1987). Need for DNA topoisomerase activity as a swivel for DNA replication for transcription of ribosomal RNA. *Nature*, *326*(6111), 414–416. https://doi.org/10.1038/326414a0

Broomfield, S., Chow, B. L., & Xiao, W. (1998). MMS2 , encoding a ubiquitin-conjugating-enzyme-like protein, is a member of the yeast error-free postreplication repair pathway. *Proceedings of the National Academy of Sciences*, *95*(10), 5678–5683. https://doi.org/10.1073/pnas.95.10.5678

Buck, S. W., Maqani, N., Matecic, M., Hontz, R. D., Fine, R. D., Li, M., & Smith, J. S. (2016). RNA Polymerase I and Fob1 contributions to transcriptional silencing at the yeast rDNA locus. *Nucleic Acids Research*, *44*(13), 6173–6184. https://doi.org/10.1093/nar/gkw212

Bürmann, F., Funke, L. F. H., Chin, J. W., & Löwe, J. (2021). Cryo-EM structure of MukBEF reveals DNA loop entrapment at chromosomal unloading sites. *Molecular Cell*, *81*(23), 4891-4906.e8. https://doi.org/10.1016/j.molcel.2021.10.011

Bürmann, F., Lee, B.-G., Than, T., Sinn, L., O'Reilly, F. J., Yatskevich, S., Rappsilber, J., Hu, B., Nasmyth, K., & Löwe, J. (2019). A folded conformation of MukBEF and cohesin. *Nature Structural & Molecular Biology*, *26*(3), 227–236. https://doi.org/10.1038/s41594-019-0196-z

Bustard, D. E., Ball, L. G., & Cobb, J. A. (2016). Non-Smc element 5 (Nse5) of the Smc5/6 complex interacts with SUMO pathway components. *Biology Open*, *5*(6), 777–785. https://doi.org/10.1242/bio.018440

Bustard, D. E., Menolfi, D., Jeppsson, K., Ball, L. G., Dewey, S. C., Shirahige, K., Sjögren, C., Branzei, D., & Cobb, J. A. (2012). During Replication Stress, Non-Smc Element 5 (Nse5) Is Required for Smc5/6 Protein Complex Functionality at Stalled Forks. *Journal of Biological Chemistry*, *287*(14), 11374–11383. https://doi.org/10.1074/jbc.M111.336263

Byers, B., & Goetsch, L. (1975). Behavior of spindles and spindle plaques in the cell cycle and conjugation of Saccharomyces cerevisiae. *Journal of Bacteriology*, *124*(1), 511–523. https://doi.org/10.1128/jb.124.1.511-523.1975

Calil, F. A., Li, B. Z., Torres, K. A., Nguyen, K., Bowen, N., Putnam, C. D., & Kolodner, R. D. (2021). Rad27 and Exo1 function in different excision pathways for mismatch repair in Saccharomyces cerevisiae. *Nature Communications 2021 12:1*, *12*(1), 1–10. https://doi.org/10.1038/s41467-021-25866-z

Champoux, J. J. (2001). DNA Topoisomerases: Structure, Function, and Mechanism. *Annual Review of Biochemistry*, *70*(1), 369–413. https://doi.org/10.1146/annurev.biochem.70.1.369

Chatterjee, N., & Siede, W. (2013). Replicating Damaged DNA in Eukaryotes. *Cold Spring Harbor Perspectives in Biology*, *5*(12), a019836–a019836. https://doi.org/10.1101/cshperspect.a019836

Chen, Y.-H., Choi, K., Szakal, B., Arenz, J., Duan, X., Ye, H., Branzei, D., & Zhao, X. (2009). Interplay between the Smc5/6 complex and the Mph1 helicase in recombinational repair. *Proceedings of the National Academy of Sciences*, *106*(50), 21252–21257. https://doi.org/10.1073/pnas.0908258106

Cherry, J. M., Hong, E. L., Amundsen, C., Balakrishnan, R., Binkley, G., Chan, E. T., Christie, K. R., Costanzo, M. C., Dwight, S. S., Engel, S. R., Fisk, D. G., Hirschman, J. E., Hitz, B. C., Karra, K., Krieger, C. J., Miyasato, S. R., Nash, R. S., Park, J., Skrzypek, M. S., … Wong, E. D. (2012). Saccharomyces Genome Database: the genomics resource of budding yeast. *Nucleic Acids Research*, *40*(D1), D700–D705. https://doi.org/10.1093/nar/gkr1029

Choi, K., Szakal, B., Chen, Y.-H., Branzei, D., & Zhao, X. (2010). The Smc5/6 Complex and Esc2 Influence Multiple Replication-associated Recombination Processes in Saccharomyces cerevisiae. *Molecular Biology of the Cell*, *21*(13), 2306–2314. https://doi.org/10.1091/mbc.e10-01-0050

Ciosk, R., Zachariae, W., Michaelis, C., Shevchenko, A., Mann, M., & Nasmyth, K. (1998). An ESP1/PDS1 Complex Regulates Loss of Sister Chromatid Cohesion at the

Metaphase to Anaphase Transition in Yeast. *Cell*, *93*(6), 1067–1076. https://doi.org/10.1016/S0092-8674(00)81211-8

Coller, H. A. (2022). Stressed-out yeast do not pass GO. *Journal of Cell Biology*, *221*(1). https://doi.org/10.1083/jcb.202111032

Constantinou, A., Chen, X. B., McGowan, C. H., & West, S. C. (2002). Holliday junction resolution in human cells: Two junction endonucleases with distinct substrate specificities. *EMBO Journal*, *21*(20), 5577–5585. https://doi.org/10.1093/EMBOJ/CDF554

Cooke, M. S., Evans, M. D., Dizdaroglu, M., & Lunec, J. (2003). Oxidative DNA damage: mechanisms, mutation, and disease. *The FASEB Journal*, *17*(10), 1195–1214. https://doi.org/10.1096/fj.02-0752rev

Cortez, D. (2015). Preventing replication fork collapse to maintain genome integrity. *DNA Repair*, *32*, 149–157. https://doi.org/10.1016/j.dnarep.2015.04.026

Cottingham, F. R., & Hoyt, M. A. (1997). Mitotic Spindle Positioning in Saccharomyces cerevisiae Is Accomplished by Antagonistically Acting Microtubule Motor Proteins. *Journal of Cell Biology*, *138*(5), 1041–1053. https://doi.org/10.1083/jcb.138.5.1041

Crickard, J. B., Moevus, C. J., Kwon, Y., Sung, P., & Greene, E. C. (2020). Rad54 Drives ATP Hydrolysis-Dependent DNA Sequence Alignment during Homologous Recombination. *Cell*, *181*(6), 1380-1394.e18. https://doi.org/10.1016/j.cell.2020.04.056

D'Amours, D., & Amon, A. (2004). At the interface between signaling and executing anaphase—Cdc14 and the FEAR network. *Genes & Development*, *18*(21), 2581–2595. https://doi.org/10.1101/gad.1247304

D'Amours, D., Stegmeier, F., & Amon, A. (2004). Cdc14 and condensin control the dissolution of cohesin-independent chromosome linkages at repeated DNA. *Cell*, *117*(4), 455–469. https://doi.org/10.1016/S0092-8674(04)00413-1/ATTACHMENT/296C9597-C582-493F-9473-63ACAB90289B/MMC1.PDF

Datta, A., Adjiri, A., New, L., Crouse, G. F., & Jinks Robertson, S. (1996). Mitotic crossovers between diverged sequences are regulated by mismatch repair proteins in Saccaromyces cerevisiae. *Molecular and Cellular Biology*, *16*(3), 1085–1093. https://doi.org/10.1128/MCB.16.3.1085

Davidson, I. F., Bauer, B., Goetz, D., Tang, W., Wutz, G., & Peters, J.-M. (2019). DNA loop extrusion by human cohesin. *Science*, *366*(6471), 1338–1345. https://doi.org/10.1126/science.aaz3418

Davidson, I. F., & Peters, J.-M. (2021). Genome folding through loop extrusion by SMC complexes. *Nature Reviews Molecular Cell Biology*, *22*(7), 445–464. https://doi.org/10.1038/s41580-021-00349-7

de Bont, R. (2004). Endogenous DNA damage in humans: a review of quantitative data. *Mutagenesis*, *19*(3), 169–185. https://doi.org/10.1093/mutage/geh025

de Piccoli, G., Cortes-Ledesma, F., Ira, G., Torres-Rosell, J., Uhle, S., Farmer, S., Hwang, J.-Y., Machin, F., Ceschia, A., McAleenan, A., Cordon-Preciado, V., Clemente-Blanco, A., Vilella-Mitjana, F., Ullal, P., Jarmuz, A., Leitao, B., Bressan, D., Dotiwala, F., Papusha, A., … Aragón, L. (2006). Smc5–Smc6 mediate DNA double-strand-break repair by promoting sister-chromatid recombination. *Nature Cell Biology*, *8*(9), 1032–1034. https://doi.org/10.1038/ncb1466

de Wit, E., Vos, E. S. M., Holwerda, S. J. B., Valdes-Quezada, C., Verstegen, M. J. A. M., Teunissen, H., Splinter, E., Wijchers, P. J., Krijger, P. H. L., & de Laat, W. (2015). CTCF Binding Polarity Determines Chromatin Looping. *Molecular Cell*, *60*(4), 676–684. https://doi.org/10.1016/j.molcel.2015.09.023

Deans, A. J., & West, S. C. (2011). DNA interstrand crosslink repair and cancer. *Nature Reviews Cancer*, *11*(7), 467–480. https://doi.org/10.1038/nrc3088

DePamphilis, M. L. (1993). Eukaryotic DNA replication: anatomy of an origin. *Annual Review of Biochemistry*, *62*(1), 29–63. https://doi.org/10.1146/annurev.bi.62.070193.000333

Dexheimer, T. S. (2014). DNA repair pathways and mechanisms. *DNA Repair of Cancer Stem Cells*, 19–32. https://doi.org/10.1007/978-94-007-4590-2_2

Dizdaroglu, M. (1992). Oxidative damage to DNA in mammalian chromatin. *Mutation Research/DNAging*, *275*(3–6), 331–342. https://doi.org/10.1016/0921-8734(92)90036-O

Dogliotti, E., Fortini, P., Pascucci, B., & Parlanti, E. (2001). The mechanism of switching among multiple BER pathways. In *Progress in Nucleic Acid Research and Molecular Biology* (Vol. 68, pp. 3–27). Academic Press Inc. https://doi.org/10.1016/S0079-6603(01)68086-3

Donaldson, A. D., Fangman, W. L., & Brewer, B. J. (1998). Cdc7 is required throughout the yeast S phasetoactivatereplication origins. *Genes & Development*, *12*(4), 491–501. https://doi.org/10.1101/gad.12.4.491

Dorsett, D., & Merkenschlager, M. (2013). Cohesin at active genes: a unifying theme for cohesin and gene expression from model organisms to humans. *Current Opinion in Cell Biology*, *25*(3), 327–333. https://doi.org/10.1016/j.ceb.2013.02.003

Doyle, J. M., Gao, J., Wang, J., Yang, M., & Potts, P. R. (2010). MAGE-RING Protein Complexes Comprise a Family of

E3 Ubiquitin Ligases. *Molecular Cell*, *39*(6), 963–974. https://doi.org/10.1016/j.molcel.2010.08.029

Duan, X., Sarangi, P., Liu, X., Rangi, G. K., Zhao, X., & Ye, H. (2009). Structural and functional insights into the roles of the Mms21 subunit of the Smc5/6 complex. *Molecular Cell*, *35*(5), 657–668. https://doi.org/10.1016/j.molcel.2009.06.032

Duan, X., Yang, Y., Chen, Y.-H., Arenz, J., Rangi, G. K., Zhao, X., & Ye, H. (2009). Architecture of the Smc5/6 Complex of Saccharomyces cerevisiae Reveals a Unique Interaction between the Nse5-6 Subcomplex and the Hinge Regions of Smc5 and Smc6. *The Journal of Biological Chemistry*, *284*(13), 8507–8515. https://doi.org/10.1074/jbc.M809139200

Egidi, A., di Felice, F., & Camilloni, G. (2020). Saccharomyces cerevisiae rDNA as super-hub: the region where replication, transcription and recombination meet. *Cellular and Molecular Life Sciences*, *77*(23), 4787–4798. https://doi.org/10.1007/S00018-020-03562-3

Egly, J.-M., & Coin, F. (2011). A history of TFIIH: Two decades of molecular biology on a pivotal transcription/repair factor. *DNA Repair*, *10*(7), 714–721. https://doi.org/10.1016/j.dnarep.2011.04.021

Elbatsh, A. M. O., Haarhuis, J. H. I., Petela, N., Chapard, C., Fish, A., Celie, P. H., Stadnik, M., Ristic, D., Wyman, C., Medema, R. H., Nasmyth, K., & Rowland, B. D. (2016). Cohesin Releases DNA through Asymmetric ATPase-Driven Ring Opening. *Molecular Cell*, *61*(4), 575–588. https://doi.org/10.1016/j.molcel.2016.01.025

Emili, A. (1998). MEC1-Dependent Phosphorylation of Rad9p in Response to DNA Damage. *Molecular Cell*, *2*(2), 183–189. https://doi.org/10.1016/S1097-2765(00)80128-8

Enserink, J. M. (2011). Cell Cycle Regulation of DNA Replication in S. cerevisiae. In H. Seligmann (Ed.), *DNA Replication-Current Advances* (1st ed., pp. 391–408). InTech. https://doi.org/10.5772/19055

Escoté, X., Zapater, M., Clotet, J., & Posas, F. (2004). Hog1 mediates cell-cycle arrest in G1 phase by the dual targeting of Sic1. *Nature Cell Biology*, *6*(10), 997–1002. https://doi.org/10.1038/ncb1174

Fachinetti, D., Bermejo, R., Cocito, A., Minardi, S., Katou, Y., Kanoh, Y., Shirahige, K., Azvolinsky, A., Zakian, V. A., & Foiani, M. (2010). Replication Termination at Eukaryotic Chromosomes Is Mediated by Top2 and Occurs at Genomic Loci Containing Pausing Elements. *Molecular Cell*, *39*(4), 595–605. https://doi.org/10.1016/j.molcel.2010.07.024

Feng, W., Collingwood, D., Boeck, M. E., Fox, L. A., Alvino, G. M., Fangman, W. L., Raghuraman, M. K., & Brewer, B. J. (2006). Genomic mapping of single-stranded DNA in hydroxyurea-challenged yeasts identifies origins of replication. *Nature Cell Biology*, *8*(2), 148. https://doi.org/10.1038/NCB1358

Fousteri, M. I., & Lehmann, A. R. (2000). A novel SMC protein complex in Schizosaccharomyces pombe contains the Rad18 DNA repair protein. *The EMBO Journal*, *19*(7), 1691–1702. https://doi.org/10.1093/emboj/19.7.1691

Freeman, L., Aragon-Alcaide, L., & Strunnikov, A. (2000). The Condensin Complex Governs Chromosome Condensation and Mitotic Transmission of Rdna. *Journal of Cell Biology*, *149*(4), 811–824. https://doi.org/10.1083/jcb.149.4.811

French, S. L., Sikes, M. L., Hontz, R. D., Osheim, Y. N., Lambert, T. E., el Hage, A., Smith, M. M., Tollervey, D., Smith, J. S., & Beyer, A. L. (2011). Distinguishing the Roles of Topoisomerases I and II in Relief of Transcription-Induced Torsional Stress in Yeast rRNA Genes. *Molecular and Cellular Biology*, *31*(3), 482–494. https://doi.org/10.1128/MCB.00589-10

Frenz, L. M., Lee, S. E., Fesquet, D., & Johnston, L. H. (2000). The budding yeast Dbf2 protein kinase localises to the centrosome and moves to the bud neck in late mitosis. *Journal of Cell Science*, *113*(19), 3399–3408. https://doi.org/10.1242/jcs.113.19.3399

Fudenberg, G., Imakaev, M., Lu, C., Goloborodko, A., Abdennur, N., & Mirny, L. A. (2016). Formation of Chromosomal Domains by Loop Extrusion. *Cell Reports*, *15*(9), 2038–2049. https://doi.org/10.1016/j.celrep.2016.04.085

Funabiki, H., & Wynne, D. J. (2013). Making an effective switch at the kinetochore by phosphorylation and dephosphorylation. *Chromosoma*, *122*(3), 135–158. https://doi.org/10.1007/s00412-013-0401-5

Gaines, W. A., Godin, S. K., Kabbinavar, F. F., Rao, T., VanDemark, A. P., Sung, P., & Bernstein, K. A. (2015). Promotion of presynaptic filament assembly by the ensemble of S. cerevisiae Rad51 paralogues with Rad52. *Nature Communications*, *6*(1), 7834. https://doi.org/10.1038/ncomms8834

Galanti, L., & Pfander, B. (2018). Right time, right place—DNA damage and DNA replication checkpoints collectively safeguard S phase. *The EMBO Journal*, *37*(21). https://doi.org/10.15252/EMBJ.2018100681

Ganji, M., Shaltiel, I. A., Bisht, S., Kim, E., Kalichava, A., Haering, C. H., & Dekker, C. (2018). Real-time imaging of DNA loop extrusion by condensin. *Science*, *360*(6384), 102–105. https://doi.org/10.1126/science.aar7831

Gerald, J. N. F., Benjamin, J. M., & Kron, S. J. (2002). Robust G1 checkpoint arrest in budding yeast: dependence on DNA damage signaling and repair. *Journal of Cell*

Science, *115*(8), 1749–1757. https://doi.org/10.1242/jcs.115.8.1749

Giannattasio, M., Zwicky, K., Follonier, C., Foiani, M., Lopes, M., & Branzei, D. (2014). Visualization of recombination-mediated damage bypass by template switching. *Nature Structural & Molecular Biology*, *21*(10), 884–892. https://doi.org/10.1038/nsmb.2888

Gilbert, C. S., Green, C. M., & Lowndes, N. F. (2001). Budding Yeast Rad9 Is an ATP-Dependent Rad53 Activating Machine. *Molecular Cell*, *8*(1), 129–136. https://doi.org/10.1016/S1097-2765(01)00267-2

Gómez, R., Jordan, P. W., Viera, A., Alsheimer, M., Fukuda, T., Jessberger, R., Llano, E., Pendás, A. M., Handel, M. A., & Suja, J. A. (2013). Dynamic localization of SMC5/6 complex proteins during mammalian meiosis and mitosis implies functions in distinct chromosome processes. *Journal of Cell Science*, *126*(Pt 18), 4239–4252. https://doi.org/10.1242/jcs.130195

Greene, A. L., Snipe, J. R., Gordenin, D. A., & Resnick, M. A. (1999). Functional Analysis of Human FEN1 in Saccharomyces Cerevisiae and Its Role in Genome Stability. *Human Molecular Genetics*, *8*(12), 2263–2273. https://doi.org/10.1093/hmg/8.12.2263

Gruber, S., Arumugam, P., Katou, Y., Kuglitsch, D., Helmhart, W., Shirahige, K., & Nasmyth, K. (2006). Evidence that Loading of Cohesin Onto Chromosomes Involves Opening of Its SMC Hinge. *Cell*, *127*(3), 523–537. https://doi.org/10.1016/j.cell.2006.08.048

Gruber, S., Haering, C. H., & Nasmyth, K. (2003). Chromosomal Cohesin Forms a Ring. *Cell*, *112*(6), 765–777. https://doi.org/10.1016/S0092-8674(03)00162-4

Guacci, V., Koshland, D., & Strunnikov, A. (1997). A Direct Link between Sister Chromatid Cohesion and Chromosome Condensation Revealed through the Analysis of MCD1 in S. cerevisiae. *Cell*, *91*(1), 47–57. https://doi.org/10.1016/S0092-8674(01)80008-8

Gutierrez-Escribano, P., Hormeño, S., Madariaga-Marcos, J., Solé-Soler, R., O'Reilly, F. J., Morris, K., Aicart-Ramos, C., Aramayo, R., Montoya, A., Kramer, H., Rappsilber, J., Torres-Rosell, J., Moreno-Herrero, F., & Aragon, L. (2020). Purified Smc5/6 Complex Exhibits DNA Substrate Recognition and Compaction. *Molecular Cell*, *80*(6), 1039-1054.e6. https://doi.org/10.1016/j.molcel.2020.11.012

Guzder, S. N., Prakash, L., Prakash, S., & Sung, P. (1999). Synergistic Interaction between Yeast Nucleotide Excision Repair Factors NEF2 and NEF4 in the Binding of Ultraviolet-damaged DNA. *Journal of Biological Chemistry*, *274*(34), 24257–24262. https://doi.org/10.1074/jbc.274.34.24257

Guzder, S. N., Sommers, C. H., Prakash, L., & Prakash, S. (2006). Complex Formation with Damage Recognition Protein Rad14 Is Essential for Saccharomyces cerevisiae Rad1-Rad10 Nuclease To Perform Its Function in Nucleotide Excision Repair In Vivo. *Molecular and Cellular Biology*, *26*(3), 1135–1141. https://doi.org/10.1128/MCB.26.3.1135-1141.2006

Guzder, S. N., Sung, P., Prakash, L., & Prakash, S. (1998). The DNA-dependent ATPase Activity of Yeast Nucleotide Excision Repair Factor 4 and Its Role in DNA Damage Recognition. *Journal of Biological Chemistry*, *273*(11), 6292–6296. https://doi.org/10.1074/jbc.273.11.6292

Haering, C. H., Löwe, J., Hochwagen, A., & Nasmyth, K. (2002). Molecular architecture of SMC proteins and the yeast cohesin complex. *Molecular Cell*, *9*(4), 773–788. https://doi.org/10.1016/s1097-2765(02)00515-4

Hahn, A. T., Jones, J. T., & Meyer, T. (2009). Quantitative analysis of cell cycle phase durations and PC12 differentiation using fluorescent biosensors. *Cell Cycle*, *8*(7), 1044–1052. https://doi.org/10.4161/cc.8.7.8042

Hallett, S. T., Schellenberger, P., Zhou, L., Beuron, F., Morris, E., Murray, J. M., & Oliver, A. W. (2021). Nse5/6 is a negative regulator of the ATPase activity of the Smc5/6 complex. *Nucleic Acids Research*, *49*(8), 4534–4549. https://doi.org/10.1093/nar/gkab234

Hartwell, L. H., Culotti, J., Pringle, J. R., & Reid, B. J. (1974). Genetic Control of the Cell Division Cycle in Yeast. *Science*, *183*(4120), 46–51. https://doi.org/10.1126/science.183.4120.46

Hassler, M., Shaltiel, I. A., & Haering, C. H. (2018). Towards a Unified Model of SMC Complex Function. *Current Biology : CB*, *28*(21), R1266–R1281. https://doi.org/10.1016/j.cub.2018.08.034

Hassler, M., Shaltiel, I. A., Kschonsak, M., Simon, B., Merkel, F., Thärichen, L., Bailey, H. J., Macošek, J., Bravo, S., Metz, J., Hennig, J., & Haering, C. H. (2019). Structural Basis of an Asymmetric Condensin ATPase Cycle. *Molecular Cell*, *74*(6), 1175-1188.e9. https://doi.org/10.1016/j.molcel.2019.03.037

Hauf, S., Cole, R. W., LaTerra, S., Zimmer, C., Schnapp, G., Walter, R., Heckel, A., van Meel, J., Rieder, C. L., & Peters, J.-M. (2003). The small molecule Hesperadin reveals a role for Aurora B in correcting kinetochore–microtubule attachment and in maintaining the spindle assembly checkpoint. *Journal of Cell Biology*, *161*(2), 281–294. https://doi.org/10.1083/jcb.200208092

Heidenreich, E., Novotny, R., Kneidinger, B., Holzmann, V., & Wintersberger, U. (2003). Non-homologous end joining as an important mutagenic process in cell cycle-arrested cells. *The EMBO Journal*, *22*(9), 2274–2283. https://doi.org/10.1093/emboj/cdg203

Higashi, T. L., Eickhoff, P., Sousa, J. S., Locke, J., Nans, A., Flynn, H. R., Snijders, A. P., Papageorgiou, G., O'Reilly, N., Chen, Z. A., O'Reilly, F. J., Rappsilber, J., Costa, A., & Uhlmann, F. (2020). A Structure-Based Mechanism for DNA Entry into the Cohesin Ring. *Molecular Cell*, *79*(6), 917-933.e9. https://doi.org/10.1016/j.molcel.2020.07.013

Higashi, T. L., Pobegalov, G., Tang, M., Molodtsov, M. I., & Uhlmann, F. (2021). A Brownian ratchet model for DNA loop extrusion by the cohesin complex. *ELife*, *10*. https://doi.org/10.7554/eLife.67530

Higashi, T. L., & Uhlmann, F. (2022). SMC complexes: Lifting the lid on loop extrusion. *Current Opinion in Cell Biology*, *74*, 13–22. https://doi.org/10.1016/j.ceb.2021.12.003

Hiom, K. (2001). Recombination: Homologous recombination branches out. *Current Biology*, *11*(7), R278–R280. https://doi.org/10.1016/S0960-9822(01)00138-5

Hirano, M. (2001). Bimodal activation of SMC ATPase by intra- and inter-molecular interactions. *The EMBO Journal*, *20*(12), 3238–3250. https://doi.org/10.1093/emboj/20.12.3238

Hirano, T. (2002). The ABCs of SMC proteins: two-armed ATPases for chromosome condensation, cohesion, and repair. *Genes & Development*, *16*(4), 399–414. https://doi.org/10.1101/gad.955102

Hirano, T., & Mitchison, T. J. (1994). A heterodimeric coiled-coil protein required for mitotic chromosome condensation in vitro. *Cell*, *79*(3), 449–458. https://doi.org/10.1016/0092-8674(94)90254-2

Holland, I. B., & Blight, M. A. (1999). ABC-ATPases, adaptable energy generators fuelling transmembrane movement of a variety of molecules in organisms from bacteria to humans. *Journal of Molecular Biology*, *293*(2), 381–399. https://doi.org/10.1006/jmbi.1999.2993

Holliday, R. (1964). A mechanism for gene conversion in fungi. *Genetical Research*, *5*(2), 282–304. https://doi.org/10.1017/S0016672300001233

Holliday, R., & Ho, T. (1998). Gene silencing and endogenous DNA methylation in mammalian cells. *Mutation Research/Fundamental and Molecular Mechanisms of Mutagenesis*, *400*(1–2), 361–368. https://doi.org/10.1016/S0027-5107(98)00034-7

Holm, C., Goto, T., Wang, J. C., & Botstein, D. (1985). DNA topoisomerase II is required at the time of mitosis in yeast. *Cell*, *41*(2), 553–563. https://doi.org/10.1016/S0092-8674(85)80028-3

Hombauer, H., Srivatsan, A., Putnam, C. D., & Kolodner, R. D. (2011). Mismatch Repair, But Not Heteroduplex Rejection, Is Temporally Coupled to DNA Replication. *Science*, *334*(6063), 1713–1716. https://doi.org/10.1126/science.1210770

Hu, B., Itoh, T., Mishra, A., Katoh, Y., Chan, K.-L., Upcher, W., Godlee, C., Roig, M. B., Shirahige, K., & Nasmyth, K. (2011). ATP hydrolysis is required for relocating cohesin from sites occupied by its Scc2/4 loading complex. *Current Biology : CB*, *21*(1), 12–24. https://doi.org/10.1016/j.cub.2010.12.004

Hu, B., Liao, C., Millson, S. H., Mollapour, M., Prodromou, C., Pearl, L. H., Piper, P. W., & Panaretou, B. (2005). Qri2/Nse4, a component of the essential Smc5/6 DNA repair complex. *Molecular Microbiology*, *55*(6), 1735–1750. https://doi.org/10.1111/j.1365-2958.2005.04531.x

Hwang, L. H., Lau, L. F., Smith, D. L., Mistrot, C. A., Hardwick, K. G., Hwang, E. S., Amon, A., & Murray, A. W. (1998). Budding Yeast Cdc20: A Target of the Spindle Checkpoint. *Science*, *279*(5353), 1041–1044. https://doi.org/10.1126/science.279.5353.1041

Interthal, H., & Heyer, W.-D. (2000). MUS81 encodes a novel Helix-hairpin-Helix protein involved in the response to UV- and methylation-induced DNA damage in Saccharomyces cerevisiae. *Molecular and General Genetics MGG*, *263*(5), 812–827. https://doi.org/10.1007/s004380000241

Ip, S. C. Y., Rass, U., Blanco, M. G., Flynn, H. R., Skehel, J. M., & West, S. C. (2008). Identification of Holliday junction resolvases from humans and yeast. *Nature*, *456*(7220), 357–361. https://doi.org/10.1038/nature07470

Irmisch, A., Ampatzidou, E., Mizuno, K., O'Connell, M. J., & Murray, J. M. (2009). Smc5/6 maintains stalled replication forks in a recombination-competent conformation. *The EMBO Journal*, *28*(2), 144–155. https://doi.org/10.1038/emboj.2008.273

Ivanova, T., Maier, M., Missarova, A., Ziegler-Birling, C., Dam, M., Gomar-Alba, M., Carey, L. B., & Mendoza, M. (2020). Budding yeast complete DNA synthesis after chromosome segregation begins. *Nature Communications 2020 11:1*, *11*(1), 1–13. https://doi.org/10.1038/s41467-020-16100-3

Iyer, B. V. S., Kenward, M., & Arya, G. (2011). Hierarchies in eukaryotic genome organization: Insights from polymer theory and simulations. *BMC Biophysics*, *4*(1), 8. https://doi.org/10.1186/2046-1682-4-8

Iyer, D., & Rhind, N. (2017). The Intra-S Checkpoint Responses to DNA Damage. *Genes*, *8*(2), 74. https://doi.org/10.3390/genes8020074

Jansen, A., & Verstrepen, K. J. (2011). Nucleosome Positioning in Saccharomyces cerevisiae. *Microbiology and Molecular Biology Reviews*, *75*(2), 301–320. https://doi.org/10.1128/MMBR.00046-10

Jaspersen, S. L., Giddings, T. H., & Winey, M. (2002). Mps3p is a novel component of the yeast spindle pole body that interacts with the yeast centrin homologue Cdc31p. *Journal of Cell Biology*, *159*(6), 945–956. https://doi.org/10.1083/jcb.200208169

Jaspersen, S. L., & Winey, M. (2004). THE BUDDING YEAST SPINDLE POLE BODY: Structure, Duplication, and Function. *Annual Review of Cell and Developmental Biology*, *20*(1), 1–28. https://doi.org/10.1146/annurev.cellbio.20.022003.114106

Jeppsson, K., Carlborg, K. K., Nakato, R., Berta, D. G., Lilienthal, I., Kanno, T., Lindqvist, A., Brink, M. C., Dantuma, N. P., Katou, Y., Shirahige, K., & Sjögren, C. (2014). The Chromosomal Association of the Smc5/6 Complex Depends on Cohesion and Predicts the Level of Sister Chromatid Entanglement. *PLoS Genetics*, *10*(10), e1004680. https://doi.org/10.1371/journal.pgen.1004680

Jin, F., Richmond, D., & Wang, Y. (2009). The multilayer regulation of the metaphase-to-anaphase transition. *Cell Cycle*, *8*(5), 700–704. https://doi.org/10.4161/cc.8.5.7678

Johnston, G. C., Pringle, J. R., & Hartwell, L. H. (1977). Coordination of growth with cell division in the yeast Saccharomyces cerevisiae. *Experimental Cell Research*, *105*(1), 79–98. https://doi.org/10.1016/0014-4827(77)90154-9

Johzuka, K., & Horiuchi, T. (2002). Replication fork block protein, Fob1, acts as an rDNA region specific recombinator in S. cerevisiae. *Genes to Cells*, *7*(2), 99–113. https://doi.org/10.1046/j.1356-9597.2001.00508.x

Kadyrov, F. A., Dzantiev, L., Constantin, N., & Modrich, P. (2006). Endonucleolytic Function of MutLα in Human Mismatch Repair. *Cell*, *126*(2), 297–308. https://doi.org/10.1016/j.cell.2006.05.039

Kanno, T., Berta, D. G., & Sjögren, C. (2015). The Smc5/6 Complex Is an ATP-Dependent Intermolecular DNA Linker. *Cell Reports*, *12*(9), 1471–1482. https://doi.org/10.1016/j.celrep.2015.07.048

Karaboja, X., Ren, Z., Brandão, H. B., Paul, P., Rudner, D. Z., & Wang, X. (2021). XerD unloads bacterial SMC complexes at the replication terminus. *Molecular Cell*, *81*(4), 756-766.e8. https://doi.org/10.1016/j.molcel.2020.12.027

Kim, E., Kerssemakers, J., Shaltiel, I. A., Haering, C. H., & Dekker, C. (2020). DNA-loop extruding condensin complexes can traverse one another. *Nature*, *579*(7799), 438–442. https://doi.org/10.1038/s41586-020-2067-5

Kim, R. A., & Wang, J. C. (1989). Function of DNA topoisomerases as replication swivels in Saccharomyces cerevisiae. *Journal of Molecular Biology*, *208*(2), 257–267. https://doi.org/10.1016/0022-2836(89)90387-2

Kitada, K., Johnson, A. L., Johnston, L. H., & Sugino, A. (1993). A multicopy suppressor gene of the Saccharomyces cerevisiae G1 cell cycle mutant gene dbf4 encodes a protein kinase and is identified as CDC5. *Molecular and Cellular Biology*, *13*(7), 4445–4457. https://doi.org/10.1128/MCB.13.7.4445

Klemenz, R., & Geiduschek, E. P. (1980). The 5′ terminus of the precursor ribosomal RNA of Saccharomyces cerevisiae. *Nucleic Acids Research*, *8*(12), 2679–2690. https://doi.org/10.1093/nar/8.12.2679

Knop, M., Siegers, K., Pereira, G., Zachariae, W., Winsor, B., Nasmyth, K., & Schiebel, E. (1999). Epitope tagging of yeast genes using a PCR-based strategy: more tags and improved practical routines. *Yeast*, *15*(10B), 963–972. https://doi.org/10.1002/(SICI)1097-0061(199907)15:10B<963::AID-YEA399>3.0.CO;2-W

Kobayashi, I., & Ikeda, H. (1983). Double holliday structure: A possible in vivo intermediate form of general recombination in Escherichia coli. *Molecular and General Genetics MGG*, *191*(2), 213–220. https://doi.org/10.1007/BF00334816

Kobayashi, T., Heck, D. J., Nomura, M., & Horiuchi, T. (1998). Expansion and contraction of ribosomal DNA repeats in Saccharomyces cerevisiae : requirement of replication fork blocking (Fob1) protein and the role of RNA polymerase I. *Genes & Development*, *12*(24), 3821–3830. https://doi.org/10.1101/gad.12.24.3821

Kobayashi, T., Hidaka, M., Nishizawa, M., & Horiuchi, T. (1992). Identification of a site required for DNA replication fork blocking activity in the rRNA gene cluster in Saccharomyces cerevisiae. *Molecular and General Genetics MGG*, *233*(3), 355–362. https://doi.org/10.1007/BF00265431

Kobayashi, T., & Horiuchi, T. (1996). A yeast gene product, Fob1 protein, required for both replication fork blocking and recombinational hotspot activities. *Genes to Cells*, *1*(5), 465–474. https://doi.org/10.1046/j.1365-2443.1996.d01-256.x

Kolesar, P., Stejskal, K., Potesil, D., Murray, J. M., & Palecek, J. J. (2022). Role of Nse1 Subunit of SMC5/6 Complex as a Ubiquitin Ligase. *Cells*, *11*(1), 165. https://doi.org/10.3390/cells11010165

Kolodner, R. D., & Marsischky, G. T. (1999). Eukaryotic DNA mismatch repair. *Current Opinion in Genetics & Development*, *9*(1), 89–96. https://doi.org/10.1016/S0959-437X(99)80013-6

Krokan, H. E., & Bjoras, M. (2013). Base Excision Repair. *Cold Spring Harbor Perspectives in Biology*, *5*(4), a012583–a012583. https://doi.org/10.1101/cshperspect.a012583

Kschonsak, M., Merkel, F., Bisht, S., Metz, J., Rybin, V., Hassler, M., & Haering, C. H. (2017). Structural Basis for a Safety-Belt Mechanism That Anchors Condensin to Chromosomes. *Cell*, *171*(3), 588-600.e24. https://doi.org/10.1016/j.cell.2017.09.008

Kunkel, T. A. (2009). Evolving Views of DNA Replication (In)Fidelity. *Cold Spring Harbor Symposia on Quantitative Biology*, *74*, 91–101. https://doi.org/10.1101/sqb.2009.74.027

Kunkel, T. A., & Erie, D. A. (2005). DNA mismatch repair. *Annual Review of Biochemistry*, *74*(1), 681–710. https://doi.org/10.1146/annurev.biochem.74.082803.133243

Kushnirov, V. v. (2000). Rapid and reliable protein extraction from yeast. *Yeast*, *16*(9), 857–860. https://doi.org/10.1002/1097-0061(20000630)16:9<857::AID-YEA561>3.0.CO;2-B

Lavoie, B. D., Hogan, E., & Koshland, D. (2002). In vivo dissection of the chromosome condensation machinery. *Journal of Cell Biology*, *156*(5), 805–815. https://doi.org/10.1083/jcb.200109056

Lei, M., Kawasaki, Y., Young, M. R., Kihara, M., Sugino, A., & Tye, B. K. (1997). Mcm2 is a target of regulation by Cdc7–Dbf4 during the initiation of DNA synthesis. *Genes & Development*, *11*(24), 3365–3374. https://doi.org/10.1101/gad.11.24.3365

Leitao, R. M., & Kellogg, D. R. (2017). The duration of mitosis and daughter cell size are modulated by nutrients in budding yeast. *The Journal of Cell Biology*, *216*(11), 3463–3470. https://doi.org/10.1083/jcb.201609114

Lengronne, A., Katou, Y., Mori, S., Yokobayashi, S., Kelly, G. P., Itoh, T., Watanabe, Y., Shirahige, K., & Uhlmann, F. (2004). Cohesin relocation from sites of chromosomal loading to places of convergent transcription. *Nature*, *430*(6999), 573–578. https://doi.org/10.1038/nature02742

Leung, G. P., Lee, L., Schmidt, T. I., Shirahige, K., & Kobor, M. S. (2011). Rtt107 Is Required for Recruitment of the SMC5/6 Complex to DNA Double Strand Breaks. *Journal of Biological Chemistry*, *286*(29), 26250–26257. https://doi.org/10.1074/jbc.M111.235200

Li, X., Liu, K., Li, F., Wang, J., Huang, H., Wu, J., & Shi, Y. (2012). Structure of C-terminal Tandem BRCT Repeats of Rtt107 Protein Reveals Critical Role in Interaction with Phosphorylated Histone H2A during DNA Damage Repair. *Journal of Biological Chemistry*, *287*(12), 9137–9146. https://doi.org/10.1074/jbc.M111.311860

Li, X., & Nicklas, R. B. (1995). Mitotic forces control a cell-cycle checkpoint. *Nature*, *373*(6515), 630–632. https://doi.org/10.1038/373630a0

Liang, F., Richmond, D., & Wang, Y. (2013). Coordination of Chromatid Separation and Spindle Elongation by Antagonistic Activities of Mitotic and S-Phase CDKs. *PLoS Genetics*, *9*(2), e1003319. https://doi.org/10.1371/journal.pgen.1003319

Lindahl, T. (1974). An N -Glycosidase from Escherichia coli That Releases Free Uracil from DNA Containing Deaminated Cytosine Residues. *Proceedings of the National Academy of Sciences*, *71*(9), 3649–3653. https://doi.org/10.1073/pnas.71.9.3649

Lindroos, H. B., Ström, L., Itoh, T., Katou, Y., Shirahige, K., & Sjögren, C. (2006). Chromosomal association of the Smc5/6 complex reveals that it functions in differently regulated pathways. *Molecular Cell*, *22*(6), 755–767. https://doi.org/10.1016/j.molcel.2006.05.014

Litwin, I., Pilarczyk, E., & Wysocki, R. (2018). The Emerging Role of Cohesin in the DNA Damage Response. *Genes*, *9*(12), 581. https://doi.org/10.3390/genes9120581

Livingston, C. M., Ramakrishnan, D., Strubin, M., Fletcher, S. P., & Beran, R. K. (2017). Identifying and Characterizing Interplay between Hepatitis B Virus X Protein and Smc5/6. *Viruses*, *9*(4). https://doi.org/10.3390/v9040069

Lopez-Serra, L., Lengronne, A., Borges, V., Kelly, G., & Uhlmann, F. (2013). Budding Yeast Wapl Controls Sister Chromatid Cohesion Maintenance and Chromosome Condensation. *Current Biology*, *23*(1), 64–69. https://doi.org/10.1016/j.cub.2012.11.030

Löwe, J., Cordell, S. C., & van den Ent, F. (2001). Crystal structure of the SMC head domain: an ABC ATPase with 900 residues antiparallel coiled-coil inserted11Edited by R. Huber. *Journal of Molecular Biology*, *306*(1), 25–35. https://doi.org/10.1006/jmbi.2000.4379

Maclean, M. J., Aamodt, R., Harris, N., Alseth, I., Seeberg, E., Bjoras, M., & Piper, P. W. (2003). Base excision repair activities required for yeast to attain a full chronological life span. *Aging Cell*, *2*(2), 93–104. https://doi.org/10.1046/j.1474-9728.2003.00041.x

Marcos-Alcalde, Í., Mendieta-Moreno, J. I., Puisac, B., Gil-Rodríguez, M. C., Hernández-Marcos, M., Soler-Polo, D., Ramos, F. J., Ortega, J., Pié, J., Mendieta, J., & Gómez-Puertas, P. (2017). Two-step ATP-driven opening of cohesin head. *Scientific Reports*, *7*(1), 3266. https://doi.org/10.1038/s41598-017-03118-9

Marians, K. J. (2018). Lesion Bypass and the Reactivation of Stalled Replication Forks. *Annual Review of Biochemistry*, *87*(1), 217–238. https://doi.org/10.1146/annurev-biochem-062917-011921

Marini, F., Pellicioli, A., Paciotti, V., Lucchini, G., Plevani, P., Stern, D. F., & Foiani, M. (1997). A role for DNA primase in coupling DNA replication to DNA damage response.

The EMBO Journal, *16*(3), 639–650. https://doi.org/10.1093/emboj/16.3.639

Mayan, M., & Aragón, L. (2010). Cis-interactions between non-coding ribosomal spacers dependent on RNAP-II separate RNAP-I and RNAP-III transcription domains. *Cell Cycle*, *9*(21), 4328–4337. https://doi.org/10.4161/cc.9.21.13591

McCulloch, S. D., & Kunkel, T. A. (2008). The fidelity of DNA synthesis by eukaryotic replicative and translesion synthesis polymerases. *Cell Research*, *18*(1), 148–161. https://doi.org/10.1038/cr.2008.4

McInerney, P., & O'Donnell, M. (2004). Functional Uncoupling of Twin Polymerases. *Journal of Biological Chemistry*, *279*(20), 21543–21551. https://doi.org/10.1074/jbc.M401649200

Mehta, A., & Haber, J. E. (2014). Sources of DNA Double-Strand Breaks and Models of Recombinational DNA Repair. *Cold Spring Harbor Perspectives in Biology*, *6*(9), a016428–a016428. https://doi.org/10.1101/cshperspect.a016428

Melby, T. E., Ciampaglio, C. N., Briscoe, G., & Erickson, H. P. (1998). The Symmetrical Structure of Structural Maintenance of Chromosomes (SMC) and MukB Proteins: Long, Antiparallel Coiled Coils, Folded at a Flexible Hinge. *Journal of Cell Biology*, *142*(6), 1595–1604. https://doi.org/10.1083/jcb.142.6.1595

Melvin, T., Botchway, S. W., Parker, A. W., & O'Neill, P. (1996). Induction of Strand Breaks in Single-Stranded Polyribonucleotides and DNA by Photoionization: One Electron Oxidized Nucleobase Radicals as Precursors. *Journal of the American Chemical Society*, *118*(42), 10031–10036. https://doi.org/10.1021/ja961722m

Menolfi, D., Delamarre, A., Lengronne, A., Pasero, P., & Branzei, D. (2015). Essential Roles of the Smc5/6 Complex in Replication through Natural Pausing Sites and Endogenous DNA Damage Tolerance. *Molecular Cell*, *60*, 835–846. https://doi.org/10.1016/j.molcel.2015.10.023

Michaelis, C., Ciosk, R., & Nasmyth, K. (1997). Cohesins: Chromosomal Proteins that Prevent Premature Separation of Sister Chromatids. *Cell*, *91*(1), 35–45. https://doi.org/10.1016/S0092-8674(01)80007-6

Mieczkowski, P. A., Lemoine, F. J., & Petes, T. D. (2006). Recombination between retrotransposons as a source of chromosome rearrangements in the yeast Saccharomyces cerevisiae. *DNA Repair*, *5*(9–10), 1010–1020. https://doi.org/10.1016/j.dnarep.2006.05.027

Mitchell, D. L., & Karentz, D. (1993). The Induction and Repair of DNA Photodamage in the Environment. *Environmental UV Photobiology*, 345–377. https://doi.org/10.1007/978-1-4899-2406-3_12

Moradi-Fard, S., Mojumdar, A., Chan, M., Harkness, T. A. A., & Cobb, J. A. (2021). Smc5/6 in the rDNA modulates lifespan independently of Fob1. *Aging Cell*, *20*(6), e13373. https://doi.org/10.1111/acel.13373

Moradi-Fard, S., Sarthi, J., Tittel-Elmer, M., Lalonde, M., Cusanelli, E., Chartrand, P., & Cobb, J. A. (2016). Smc5/6 Is a Telomere-Associated Complex that Regulates Sir4 Binding and TPE. *PLOS Genetics*, *12*(8), e1006268. https://doi.org/10.1371/journal.pgen.1006268

Moyer, S. E., Lewis, P. W., & Botchan, M. R. (2006). Isolation of the Cdc45/Mcm2–7/GINS (CMG) complex, a candidate for the eukaryotic DNA replication fork helicase. *Proceedings of the National Academy of Sciences*, *103*(27), 10236–10241. https://doi.org/10.1073/pnas.0602400103

Mullen, J. R., Kaliraman, V., Ibrahim, S. S., & Brill, S. J. (2001). Requirement for three novel protein complexes in the absence of the Sgs1 DNA helicase in Saccharomyces cerevisiae. *Genetics*, *157*(1), 103. https://doi.org/10.1093/genetics/157.1.103

Muramatsu, S., Hirai, K., Tak, Y.-S., Kamimura, Y., & Araki, H. (2010). CDK-dependent complex formation between replication proteins Dpb11, Sld2, Pol ε, and GINS in budding yeast. *Genes & Development*, *24*(6), 602–612. https://doi.org/10.1101/gad.1883410

Nasmyth, K., & Haering, C. H. (2005). The structure and function of SMC and kleisin complexes. *Annual Review of Biochemistry*, *74*(1), 595–648. https://doi.org/10.1146/annurev.biochem.74.082803.133219

Nerusheva, O. O., Galander, S., Fernius, J., Kelly, D., & Marston, A. L. (2014). Tension-dependent removal of pericentromeric shugoshin is an indicator of sister chromosome biorientation. *Genes & Development*, *28*(12), 1291–1309. https://doi.org/10.1101/gad.240291.114

Newlon, C. S., & Theis, J. F. (1993). The structure and function of yeast ARS elements. *Current Opinion in Genetics & Development*, *3*(5), 752–758. https://doi.org/10.1016/S0959-437X(05)80094-2

Nicklas, R. B., & Koch, C. A. (1969). CHROMOSOME MICROMANIPULATION. *Journal of Cell Biology*, *43*(1), 40–50. https://doi.org/10.1083/jcb.43.1.40

Ouspenski, I. I., Cabello, O. A., & Brinkley, B. R. (2000). Chromosome Condensation Factor Brn1p Is Required for Chromatid Separation in Mitosis. *Molecular Biology of the Cell*, *11*(4), 1305–1313. https://doi.org/10.1091/mbc.11.4.1305

Page, B. D., & Snyder, M. (1993). CHROMOSOME SEGREGATION IN YEAST. *Annual Review of*

Microbiology, *47*(1), 231–261. https://doi.org/10.1146/annurev.mi.47.100193.001311

Palecek, J. J., & Gruber, S. (2015). Kite Proteins: a Superfamily of SMC/Kleisin Partners Conserved Across Bacteria, Archaea, and Eukaryotes. *Structure*, *23*(12), 2183–2190. https://doi.org/10.1016/j.str.2015.10.004

Palecek, J., Vidot, S., Feng, M., Doherty, A. J., & Lehmann, A. R. (2006). The Smc5-Smc6 DNA repair complex. Bridging of the Smc5-Smc6 heads by the KLEISIN, Nse4, and non-Kleisin subunits. *The Journal of Biological Chemistry*, *281*(48), 36952–36959. https://doi.org/10.1074/jbc.M608004200

Palmer, R. E., Sullivan, D. S., Huffaker, T., & Koshland, D. (1992). Role of astral microtubules and actin in spindle orientation and migration in the budding yeast, Saccharomyces cerevisiae. *Journal of Cell Biology*, *119*(3), 583–593. https://doi.org/10.1083/jcb.119.3.583

Pebernard, S., Schaffer, L., Campbell, D., Head, S. R., & Boddy, M. N. (2008). Localization of Smc5/6 to centromeres and telomeres requires heterochromatin and SUMO, respectively. *The EMBO Journal*, *27*(22), 3011–3023. https://doi.org/10.1038/emboj.2008.220

Pellicioli, A., Lucca, C., Liberi, G., Marini, F., Lopes, M., Plevani, P., Romano, A., di Fiore, P. P., & Foiani, M. (1999). Activation of Rad53 kinase in response to DNA damage and its effect in modulating phosphorylation of the lagging strand DNA polymerase. *The EMBO Journal*, *18*(22), 6561–6572. https://doi.org/10.1093/emboj/18.22.6561

Peng, J., & Feng, W. (2016). Incision of damaged DNA in the presence of an impaired Smc5/6 complex imperils genome stability. *Nucleic Acids Research*, *44*(21), 10216–10229. https://doi.org/10.1093/nar/gkw720

Peng, X. P., Lim, S., Li, S., Marjavaara, L., Chabes, A., & Zhao, X. (2018). Acute Smc5/6 depletion reveals its primary role in rDNA replication by restraining recombination at fork pausing sites. *PLoS Genetics*, *14*(1), e1007129. https://doi.org/10.1371/journal.pgen.1007129

Petela, N. J., Gligoris, T. G., Metson, J., Lee, B.-G., Voulgaris, M., Hu, B., Kikuchi, S., Chapard, C., Chen, W., Rajendra, E., Srinivisan, M., Yu, H., Löwe, J., & Nasmyth, K. A. (2018). Scc2 Is a Potent Activator of Cohesin's ATPase that Promotes Loading by Binding Scc1 without Pds5. *Molecular Cell*, *70*(6), 1134-1148.e7. https://doi.org/10.1016/j.molcel.2018.05.022

Peter, B. J., Ullsperger, C., Hiasa, H., Marians, K. J., & Cozzarelli, N. R. (1998). The Structure of Supercoiled Intermediates in DNA Replication. *Cell*, *94*(6), 819–827. https://doi.org/10.1016/S0092-8674(00)81740-7

Pfander, B., & Matos, J. (2017). Control of Mus81 nuclease during the cell cycle. *FEBS Letters*, *591*(14), 2048–2056. https://doi.org/10.1002/1873-3468.12727

Piper, P. W. (1993). Molecular events associated with acquisition of heat tolerance by the yeast Saccharomyces cerevisiae. *FEMS Microbiology Reviews*, *11*(4), 339–355. https://doi.org/10.1111/j.1574-6976.1993.tb00005.x

Plank, J. L., Wu, J., & Hsieh, T. (2006). Topoisomerase IIIα and Bloom's helicase can resolve a mobile double Holliday junction substrate through convergent branch migration. *Proceedings of the National Academy of Sciences*, *103*(30), 11118–11123. https://doi.org/10.1073/pnas.0604873103

Prakash, S., & Prakash, L. (2000). Nucleotide excision repair in yeast. *Mutation Research/Fundamental and Molecular Mechanisms of Mutagenesis*, *451*(1–2), 13–24. https://doi.org/10.1016/S0027-5107(00)00037-3

Prinz, S., Hwang, E. S., Visintin, R., & Amon, A. (1998). The regulation of Cdc20 proteolysis reveals a role for the APC components Cdc23 and Cdc27 during S phase and early mitosis. *Current Biology*, *8*(13), 750–760. https://doi.org/10.1016/S0960-9822(98)70298-2

Procko, E., O'Mara, M. L., Bennett, W. F. D., Tieleman, D. P., & Gaudet, R. (2009). The mechanism of ABC transporters: general lessons from structural and functional studies of an antigenic peptide transporter. *FASEB Journal : Official Publication of the Federation of American Societies for Experimental Biology*, *23*(5), 1287–1302. https://doi.org/10.1096/fj.08-121855

Qiu, S., & Huang, J. (2021). MRN complex is an essential effector of DNA damage repair. *Journal of Zhejiang University-SCIENCE B*, *22*(1), 31–37. https://doi.org/10.1631/jzus.B2000289

Raghuraman, M. K., Winzeler, E. A., Collingwood, D., Hunt, S., Wodicka, L., Conway, A., Lockhart, D. J., Davis, R. W., Brewer, B. J., & Fangman, W. L. (2001). Replication Dynamics of the Yeast Genome. *Science*, *294*(5540), 115–121. https://doi.org/10.1126/science.294.5540.115

Ray, P. D., Huang, B.-W., & Tsuji, Y. (2012). Reactive oxygen species (ROS) homeostasis and redox regulation in cellular signaling. *Cellular Signalling*, *24*(5), 981–990. https://doi.org/10.1016/j.cellsig.2012.01.008

Raynard, S., Bussen, W., & Sung, P. (2006). A Double Holliday Junction Dissolvasome Comprising BLM, Topoisomerase IIIα, and BLAP75. *Journal of Biological Chemistry*, *281*(20), 13861–13864. https://doi.org/10.1074/jbc.C600051200

Reid, D. A., Keegan, S., Leo-Macias, A., Watanabe, G., Strande, N. T., Chang, H. H., Oksuz, B. A., Fenyo, D., Lieber, M. R., Ramsden, D. A., & Rothenberg, E. (2015).

Organization and dynamics of the nonhomologous end-joining machinery during DNA double-strand break repair. *Proceedings of the National Academy of Sciences*, *112*(20), E2575–E2584. https://doi.org/10.1073/pnas.1420115112

Robertson, A. B., Klungland, A., Rognes, T., & Leiros, I. (2009). DNA Repair in Mammalian Cells. *Cellular and Molecular Life Sciences*, *66*(6), 981–993. https://doi.org/10.1007/s00018-009-8736-z

Robinow, C. F., & Marak, J. (1966). A FIBER APPARATUS IN THE NUCLEUS OF THE YEAST CELL. *Journal of Cell Biology*, *29*(1), 129–151. https://doi.org/10.1083/JCB.29.1.129

Roy, M.-A., & D'Amours, D. (2011). DNA-binding properties of Smc6, a core component of the Smc5-6 DNA repair complex. *Biochemical and Biophysical Research Communications*, *416*(1–2), 80–85. https://doi.org/10.1016/j.bbrc.2011.10.149

Roy, M.-A., Siddiqui, N., & D'Amours, D. (2011). Dynamic and selective DNA-binding activity of Smc5, a core component of the Smc5-Smc6 complex. *Cell Cycle (Georgetown, Tex.)*, *10*(4), 690–700. https://doi.org/10.4161/cc.10.4.14860

Roy, U., & Greene, E. C. (2021). The Role of the Rad55–Rad57 Complex in DNA Repair. *Genes*, *12*(9), 1390. https://doi.org/10.3390/genes12091390

San Filippo, J., Sung, P., & Klein, H. (2008). Mechanism of Eukaryotic Homologous Recombination. *Annual Review of Biochemistry*, *77*(1), 229–257. https://doi.org/10.1146/annurev.biochem.77.061306.125255

Santivasi, W. L., & Xia, F. (2014). Ionizing Radiation-Induced DNA Damage, Response, and Repair. *Antioxidants & Redox Signaling*, *21*(2), 251–259. https://doi.org/10.1089/ars.2013.5668

Sato, N. (1997). Human and Xenopus cDNAs encoding budding yeast Cdc7-related kinases: invitro phosphorylation of MCM subunits by a putative human homologue of Cdc7. *The EMBO Journal*, *16*(14), 4340–4351. https://doi.org/10.1093/emboj/16.14.4340

Scheller, J., Schürer, A., Rudolph, C., Hettwer, S., & Kramer, W. (2000). MPH1 , A Yeast Gene Encoding a DEAH Protein, Plays a Role in Protection of the Genome From Spontaneous and Chemically Induced Damage. *Genetics*, *155*(3), 1069–1081. https://doi.org/10.1093/genetics/155.3.1069

Schneider, C. A., Rasband, W. S., & Eliceiri, K. W. (2012). NIH Image to ImageJ: 25 years of image analysis. *Nature Methods 2012 9:7*, *9*(7), 671–675. https://doi.org/10.1038/nmeth.2089

Schurer, K. A. (2004). Yeast MPH1 Gene Functions in an Error-Free DNA Damage Bypass Pathway That Requires Genes From Homologous Recombination, but Not From Postreplicative Repair. *Genetics*, *166*(4), 1673–1686. https://doi.org/10.1534/genetics.166.4.1673

Schwab, M., Lutum, A. S., & Seufert, W. (1997). Yeast Hct1 Is a Regulator of Clb2 Cyclin Proteolysis. *Cell*, *90*(4), 683–693. https://doi.org/10.1016/S0092-8674(00)80529-2

Senior, A. E., Al-Shawi, M. K., & Urbatsch, I. L. (1995). The catalytic cycle of P-glycoprotein. *FEBS Letters*, *377*(3), 285–289. https://doi.org/10.1016/0014-5793(95)01345-8

Sergeant, J., Taylor, E., Palecek, J., Fousteri, M., Andrews, E. A., Sweeney, S., Shinagawa, H., Watts, F. Z., & Lehmann, A. R. (2005). Composition and architecture of the Schizosaccharomyces pombe Rad18 (Smc5-6) complex. *Molecular and Cellular Biology*, *25*(1), 172–184. https://doi.org/10.1128/MCB.25.1.172-184.2005

Serrano, D., Cordero, G., Kawamura, R., Sverzhinsky, A., Sarker, M., Roy, S., Malo, C., Pascal, J. M., Marko, J. F., & D'Amours, D. (2020). The Smc5/6 Core Complex Is a Structure-Specific DNA Binding and Compacting Machine. *Molecular Cell*, *80*(6), 1025-1038.e5. https://doi.org/10.1016/j.molcel.2020.11.011

Sherr, C. J., & Roberts, J. M. (2004). Living with or without cyclins and cyclin-dependent kinases. *Genes & Development*, *18*(22), 2699–2711. https://doi.org/10.1101/gad.1256504

Shin, S., Hyun, K., Kim, J., & Hohng, S. (2018). ATP Binding to Rad5 Initiates Replication Fork Reversal by Inducing the Unwinding of the Leading Arm and the Formation of the Holliday Junction. *Cell Reports*, *23*(6), 1831–1839. https://doi.org/10.1016/j.celrep.2018.04.029

Shirayama, M., Tóth, A., Gálová, M., & Nasmyth, K. (1999). APCCdc20 promotes exit from mitosis by destroying the anaphase inhibitor Pds1 and cyclin Clb5. *Nature*, *402*(6758), 203–207. https://doi.org/10.1038/46080

Shou, W., Seol, J. H., Shevchenko, A., Baskerville, C., Moazed, D., Chen, Z. W. S., Jang, J., Shevchenko, A., Charbonneau, H., & Deshaies, R. J. (1999). Exit from Mitosis Is Triggered by Tem1-Dependent Release of the Protein Phosphatase Cdc14 from Nucleolar RENT Complex. *Cell*, *97*(2), 233–244. https://doi.org/10.1016/S0092-8674(00)80733-3

Sidorova, J. M., & Breeden, L. L. (1997). Rad53-dependent phosphorylation of Swi6 and down-regulation of CLN1 and CLN2 transcription occur in response to DNA damage in Saccharomyces cerevisiae. *Genes & Development*, *11*(22), 3032–3045. https://doi.org/10.1101/gad.11.22.3032

Siede, W., Friedberg, A. S., Dianova, I., & Friedberg, E. C. (1994). Characterization of G(1) Checkpoint Control in

the Yeast Saccharomyces Cerevisiae following Exposure to DNA-Damaging Agents. *Genetics*, *138*(2), 271. https://doi.org/10.1093/genetics/138.2.271

Siede, W., Friedberg, A. S., & Friedberg, E. C. (1993). RAD9-dependent G1 arrest defines a second checkpoint for damaged DNA in the cell cycle of Saccharomyces cerevisiae. *Proceedings of the National Academy of Sciences*, *90*(17), 7985–7989. https://doi.org/10.1073/pnas.90.17.7985

Simon, M.-N., Churikov, D., & Géli, V. (2016). Replication stress as a source of telomere recombination during replicative senescence in Saccharomyces cerevisiae. *FEMS Yeast Research*, *16*(7), fow085. https://doi.org/10.1093/femsyr/fow085

Siow, C. C., Nieduszynska, S. R., Muller, C. A., & Nieduszynski, C. A. (2012). OriDB, the DNA replication origin database updated and extended. *Nucleic Acids Research*, *40*(D1), D682–D686. https://doi.org/10.1093/nar/gkr1091

Skryabin, K. G., Eldarov, M. A., Larionov, V. L., Bayev, A. A., Klootwijk, J., de Regt, V. C., Veldman, G. M., Planta, R. J., Georgiev, O. I., & Hadjiolov, A. A. (1984). Structure and function of the nontranscribed spacer regions of yeast rDNA. *Nucleic Acids Research*, *12*(6), 2955–2968. https://doi.org/10.1093/nar/12.6.2955

Sogo, J. M., Lopes, M., & Foiani, M. (2002). Fork Reversal and ssDNA Accumulation at Stalled Replication Forks Owing to Checkpoint Defects. *Science*, *297*(5581), 599–602. https://doi.org/10.1126/science.1074023

Soh, Y.-M., Bürmann, F., Shin, H.-C., Oda, T., Jin, K. S., Toseland, C. P., Kim, C., Lee, H., Kim, S. J., Kong, M.-S., Durand-Diebold, M.-L., Kim, Y.-G., Kim, H. M., Lee, N. K., Sato, M., Oh, B.-H., & Gruber, S. (2015). Molecular basis for SMC rod formation and its dissolution upon DNA binding. *Molecular Cell*, *57*(2), 290–303. https://doi.org/10.1016/j.molcel.2014.11.023

Stegmeier, F., Huang, J., Rahal, R., Zmolik, J., Moazed, D., & Amon, A. (2004). The Replication Fork Block Protein Fob1 Functions as a Negative Regulator of the FEAR Network. *Current Biology*, *14*(6), 467–480. https://doi.org/10.1016/j.cub.2004.03.009

Stelter, P., & Ulrich, H. D. (2003). Control of spontaneous and damage-induced mutagenesis by SUMO and ubiquitin conjugation. *Nature*, *425*(6954), 188–191. https://doi.org/10.1038/nature01965

Sterling, C. H., & Sweasy, J. B. (2006). DNA Polymerase 4 of Saccharomyces cerevisiae Is Important for Accurate Repair of Methyl-Methanesulfonate-Induced DNA Damage. *Genetics*, *172*(1), 89–98. https://doi.org/10.1534/genetics.105.049254

Stern, B. M., & Murray, A. W. (2001). Lack of tension at kinetochores activates the spindle checkpoint in budding yeast. *Current Biology*, *11*(18), 1462–1467. https://doi.org/10.1016/S0960-9822(01)00451-1

Stinchcomb, D. T., Struhl, K., & Davis, R. W. (1979). Isolation and characterisation of a yeast chromosomal replicator. *Nature*, *282*(5734), 39–43. https://doi.org/10.1038/282039A0

Stone, J. E., Kumar, D., Binz, S. K., Inase, A., Iwai, S., Chabes, A., Burgers, P. M., & Kunkel, T. A. (2011). Lesion bypass by S. cerevisiae Pol ζ alone. *DNA Repair*, *10*(8), 826–834. https://doi.org/10.1016/j.dnarep.2011.04.032

Strunnikov, A. v., Hogan, E., & Koshland, D. (1995). SMC2, a Saccharomyces cerevisiae gene essential for chromosome segregation and condensation, defines a subgroup within the SMC family. *Genes & Development*, *9*(5), 587–599. https://doi.org/10.1101/gad.9.5.587

Sullivan, M., Higuchi, T., Katis, V. L., & Uhlmann, F. (2004). Cdc14 Phosphatase Induces rDNA Condensation and Resolves Cohesin-Independent Cohesion during Budding Yeast Anaphase. *Cell*, *117*(4), 471–482. https://doi.org/10.1016/S0092-8674(04)00415-5

Sun, J., Lee, K.-J., Davis, A. J., & Chen, D. J. (2012). Human Ku70/80 Protein Blocks Exonuclease 1-mediated DNA Resection in the Presence of Human Mre11 or Mre11/Rad50 Protein Complex. *Journal of Biological Chemistry*, *287*(7), 4936–4945. https://doi.org/10.1074/jbc.M111.306167

Sung, P. (1997). Function of Yeast Rad52 Protein as a Mediator between Replication Protein A and the Rad51 Recombinase. *Journal of Biological Chemistry*, *272*(45), 28194–28197. https://doi.org/10.1074/jbc.272.45.28194

Sung, P., Reynolds, P., Prakash, L., & Prakash, S. (1993). Purification and characterization of the Saccharomyces cerevisiae RAD1/RAD10 endonuclease. *The Journal of Biological Chemistry*, *268*(35), 26391–26399. http://www.ncbi.nlm.nih.gov/pubmed/8253764

Sung, P., & Robberson, D. L. (1995). DNA strand exchange mediated by a RAD51-ssDNA nucleoprotein filament with polarity opposite to that of RecA. *Cell*, *82*(3), 453–461. https://doi.org/10.1016/0092-8674(95)90434-4

Takata, M., Sasaki, M. S., Sonoda, E., Morrison, C., Hashimoto, M., Utsumi, H., Yamaguchi-Iwai, Y., Shinohara, A., & Takeda, S. (1998). Homologous recombination and non-homologous end-joining pathways of DNA double-strand break repair have overlapping roles in the maintenance of chromosomal integrity in vertebrate cells. *The EMBO Journal*, *17*(18), 5497–5508. https://doi.org/10.1093/emboj/17.18.5497

Tamborrini, D., Juanes, M. A., Ibanes, S., Rancati, G., & Piatti, S. (2018). Recruitment of the mitotic exit network to yeast centrosomes couples septin displacement to actomyosin

constriction. *Nature Communications 2018 9:1*, *9*(1), 1–15. https://doi.org/10.1038/s41467-018-06767-0

Taschner, M., Basquin, J., Steigenberger, B., Schäfer, I. B., Soh, Y., Basquin, C., Lorentzen, E., Räschle, M., Scheltema, R. A., & Gruber, S. (2021). Nse5/6 inhibits the Smc5/6 ATPase and modulates DNA substrate binding. *The EMBO Journal*, *40*(15). https://doi.org/10.15252/embj.2021107807

Tatum, D., & Li, S. (2011). Nucleotide Excision Repair in S. cerevisiae. In *DNA Repair - On the Pathways to Fixing DNA Damage and Errors*. InTech. https://doi.org/10.5772/22129

Thadani, R., Kamenz, J., Heeger, S., Muñoz, S., & Uhlmann, F. (2018). Cell-Cycle Regulation of Dynamic Chromosome Association of the Condensin Complex. *Cell Reports*, *23*(8), 2308–2317. https://doi.org/10.1016/j.celrep.2018.04.082

Toh, G. W.-L., & Lowndes, N. F. (2003). Role of the Saccharomyces cerevisiae Rad9 protein in sensing and responding to DNA damage. *Biochemical Society Transactions*, *31*(1), 242–246. https://doi.org/10.1042/bst0310242

Tomkinson, A. E., Bardwell, A. J., Tappe, N., Ramos, W., & Friedberg, E. C. (1994). Purification of Rad1 Protein from Saccharomyces cerevisiae and Further Characterization of the Rad1/Rad10 Endonuclease Complex. *Biochemistry*, *33*(17), 5305–5311. https://doi.org/10.1021/bi00183a038

Torres-Rosell, J., de Piccoli, G., Cordon-Preciado, V., Farmer, S., Jarmuz, A., Machin, F., Pasero, P., Lisby, M., Haber, J. E., & Aragón, L. (2007). Anaphase Onset Before Complete DNA Replication with Intact Checkpoint Responses. *Science*, *315*(5817), 1411–1415. https://doi.org/10.1126/science.1134025

Torres-Rosell, J., Machin, F., & Aragón, L. (2005). Smc5-Smc6 complex preserves nucleolar integrity in S. cerevisiae. *Cell Cycle (Georgetown, Tex.)*, *4*(7), 868–872. https://doi.org/10.4161/cc.4.7.1825

Torres-Rosell, J., Machín, F., Farmer, S., Jarmuz, A., Eydmann, T., Dalgaard, J. Z., & Aragón, L. (2005). SMC5 and SMC6 genes are required for the segregation of repetitive chromosome regions. *Nature Cell Biology*, *7*(4), 412–419. https://doi.org/10.1038/ncb1239

Torres-Rosell, J., Machín, F., Jarmuz, A., & Aragón, L. (2004). Nucleolar segregation lags behind the rest of the genome and requires Cdc14 phosphatase activation by the FEAR network. *Cell Cycle*, *3*(4), 496–502. https://doi.org/10.4161/CC.3.4.802

Torres-Rosell, J., Sunjevaric, I., de Piccoli, G., Sacher, M., Eckert-Boulet, N., Reid, R., Jentsch, S., Rothstein, R., Aragón, L., & Lisby, M. (2007). The Smc5–Smc6 complex and SUMO modification of Rad52 regulates recombinational repair at the ribosomal gene locus. *Nature Cell Biology*, *9*(8), 923–931. https://doi.org/10.1038/ncb1619

Toth, A., Ciosk, R., Uhlmann, F., Galova, M., Schleiffer, A., & Nasmyth, K. (1999). Yeast Cohesin complex requires a conserved protein, Eco1p(Ctf7), to establish cohesion between sister chromatids during DNA replication. *Genes & Development*, *13*(3), 320–333. https://doi.org/10.1101/gad.13.3.320

Tran, N. T., Laub, M. T., & Le, T. B. K. (2017). SMC Progressively Aligns Chromosomal Arms in Caulobacter crescentus but Is Antagonized by Convergent Transcription. *Cell Reports*, *20*(9), 2057–2071. https://doi.org/10.1016/j.celrep.2017.08.026

Tran, P. T., Simon, J. A., & Liskay, R. M. (2001). Interactions of Exo1p with components of MutLα in Saccharomyces cerevisiae. *Proceedings of the National Academy of Sciences*, *98*(17), 9760–9765. https://doi.org/10.1073/pnas.161175998

Uhlmann, F., Lottspelch, F., & Nasmyth, K. (1999). Sister-chromatid separation at anaphase onset is promoted by cleavage of the cohesin subunit Scc1. *Nature 1999 400:6739*, *400*(6739), 37–42. https://doi.org/10.1038/21831

van der Kemp, P. A., de Padula, M., Burguiere-Slezak, G., Ulrich, H. D., & Boiteux, S. (2009). PCNA monoubiquitylation and DNA polymerase ubiquitin-binding domain are required to prevent 8-oxoguanine-induced mutagenesis in Saccharomyces cerevisiae. *Nucleic Acids Research*, *37*(8), 2549–2559. https://doi.org/10.1093/nar/gkp105

Varejão, N., Ibars, E., Lascorz, J., Colomina, N., Torres-Rosell, J., & Reverter, D. (2018). DNA activates the Nse2/Mms21 SUMO E3 ligase in the Smc5/6 complex. *The EMBO Journal*, *37*(12). https://doi.org/10.15252/embj.201798306

Vas, A. C. J., Andrews, C. A., Kirkland Matesky, K., & Clarke, D. J. (2007). In Vivo Analysis of Chromosome Condensation in Saccharomyces cerevisiae. *Molecular Biology of the Cell*, *18*(2), 557–568. https://doi.org/10.1091/mbc.e06-05-0454

Venegas, A. B., Natsume, T., Kanemaki, M., & Hickson, I. D. (2020). Inducible Degradation of the Human SMC5/6 Complex Reveals an Essential Role Only during Interphase. *Cell Reports*, *31*(3), 107533. https://doi.org/10.1016/j.celrep.2020.107533

Visintin, R., Craig, K., Hwang, E. S., Prinz, S., Tyers, M., & Amon, A. (1998). The Phosphatase Cdc14 Triggers Mitotic Exit by Reversal of Cdk-Dependent Phosphorylation. *Molecular Cell*, *2*(6), 709–718. https://doi.org/10.1016/S1097-2765(00)80286-5

Visintin, R., Hwang, E. S., & Amon, A. (1999). Cfi 1 prevents premature exit from mitosis by anchoring Cdc14 phosphatase in the nucleolus. *Nature*, *398*(6730), 818–823. https://doi.org/10.1038/19775

Visser, P., Snelder, E., Kop, A., Boelen, P., Buma, A., & van Duyl, F. (1999). Effects of UV radiation on DNA photodamage and production in bacterioplankton in the coastal Caribbean Sea. *Aquatic Microbial Ecology*, *20*(1), 49–58. https://doi.org/10.3354/ame020049

Vondrova, L., Kolesar, P., Adamus, M., Nociar, M., Oliver, A. W., & Palecek, J. J. (2020). A role of the Nse4 kleisin and Nse1/Nse3 KITE subunits in the ATPase cycle of SMC5/6. *Scientific Reports 2020 10:1*, *10*(1), 1–13. https://doi.org/10.1038/s41598-020-66647-w

Waga, S., & Stillman, B. (1994). Anatomy of a DNA replication fork revealed by reconstitution of SV40 DNA replication in vitro. *Nature*, *369*(6477), 207–212. https://doi.org/10.1038/369207a0

Wan, B., Wu, J., Meng, X., Lei, M., & Zhao, X. (2019). Molecular Basis for Control of Diverse Genome Stability Factors by the Multi-BRCT Scaffold Rtt107. *Molecular Cell*, *75*(2), 238-251.e5. https://doi.org/10.1016/j.molcel.2019.05.035

Waterman, D. P., Haber, J. E., & Smolka, M. B. (2020). Checkpoint Responses to DNA Double-Strand Breaks. *Annual Review of Biochemistry*, *89*(1), 103–133. https://doi.org/10.1146/annurev-biochem-011520-104722

Wells, J. N., Gligoris, T. G., Nasmyth, K. A., & Marsh, J. A. (2017). Evolution of condensin and cohesin complexes driven by replacement of Kite by Hawk proteins. *Current Biology*, *27*(1), R17–R18. https://doi.org/10.1016/j.cub.2016.11.050

West, S. C., Blanco, M. G., Chan, Y. W., Matos, J., Sarbajna, S., & Wyatt, H. D. M. (2015). Resolution of Recombination Intermediates: Mechanisms and Regulation. *Cold Spring Harbor Symposia on Quantitative Biology*, *80*, 103–109. https://doi.org/10.1101/sqb.2015.80.027649

Whalen, J. M., Dhingra, N., Wei, L., Zhao, X., & Freudenreich, C. H. (2020). Relocation of Collapsed Forks to the Nuclear Pore Complex Depends on Sumoylation of DNA Repair Proteins and Permits Rad51 Association. *Cell Reports*, *31*(6), 107635. https://doi.org/10.1016/j.celrep.2020.107635

Williams, J. S., Williams, R. S., Dovey, C. L., Guenther, G., Tainer, J. A., & Russell, P. (2010). γH2A binds Brc1 to maintain genome integrity during S-phase. *The EMBO Journal*, *29*(6), 1136–1148. https://doi.org/10.1038/emboj.2009.413

Winey, M., Mamay, C. L., O'Toole, E. T., Mastronarde, D. N., Giddings, T. H., McDonald, K. L., & McIntosh, J. R. (1995). Three-dimensional ultrastructural analysis of the Saccharomyces cerevisiae mitotic spindle. *Journal of Cell Biology*, *129*(6), 1601–1615. https://doi.org/10.1083/jcb.129.6.1601

Wu, L., & Hickson, I. D. (2003). The Bloom's syndrome helicase suppresses crossing over during homologous recombination. *Nature*, *426*(6968), 870–874. https://doi.org/10.1038/nature02253

Wu, L., Liu, Y., & Kong, D. (2014). Mechanism of chromosomal DNA replication initiation and replication fork stabilization in eukaryotes. *Science China Life Sciences*, *57*(5), 482–487. https://doi.org/10.1007/s11427-014-4631-4

Wu, N., & Yu, H. (2012). The Smc complexes in DNA damage response. *Cell & Bioscience*, *2*(1), 5. https://doi.org/10.1186/2045-3701-2-5

Wu, X., Braithwaite, E., & Wang, Z. (1999). DNA Ligation during Excision Repair in Yeast Cell-Free Extracts Is Specifically Catalyzed by the CDC9 Gene Product. *Biochemistry*, *38*(9), 2628–2635. https://doi.org/10.1021/bi982592s

Wutz, G., Várnai, C., Nagasaka, K., Cisneros, D. A., Stocsits, R. R., Tang, W., Schoenfelder, S., Jessberger, G., Muhar, M., Hossain, M. J., Walther, N., Koch, B., Kueblbeck, M., Ellenberg, J., Zuber, J., Fraser, P., & Peters, J. (2017). Topologically associating domains and chromatin loops depend on cohesin and are regulated by CTCF, WAPL, and PDS5 proteins. *The EMBO Journal*, *36*(24), 3573–3599. https://doi.org/10.15252/embj.201798004

Wyatt, H. D. M., & West, S. C. (2014). Holliday Junction Resolvases. *Cold Spring Harbor Perspectives in Biology*, *6*(9), a023192–a023192. https://doi.org/10.1101/CSHPERSPECT.A023192

Xue, X., Choi, K., Bonner, J. N., Chiba, T., Kwon, Y., Xu, Y., Sanchez, H., Wyman, C., Niu, H., Zhao, X., & Sung, P. (2014). Restriction of replication fork regression activities by a conserved SMC complex. *Molecular Cell*, *56*(3), 436–445. https://doi.org/10.1016/j.molcel.2014.09.013

Yatskevich, S., Rhodes, J., & Nasmyth, K. (2019). Organization of Chromosomal DNA by SMC Complexes. *Annual Review of Genetics*, *53*(1), 445–482. https://doi.org/10.1146/annurev-genet-112618-043633

Yu, Y., Li, S., Ser, Z., Kuang, H., Than, T., Guan, D., Zhao, X., & Patel, D. J. (2022). Cryo-EM structure of DNA-bound Smc5/6 reveals DNA clamping enabled by multi-subunit conformational changes. *Proceedings of the National Academy of Sciences*, *119*(23). https://doi.org/10.1073/pnas.2202799119

Yu, Y., Li, S., Ser, Z., Sanyal, T., Choi, K., Wan, B., Kuang, H., Sali, A., Kentsis, A., Patel, D. J., & Zhao, X. (2021).

Integrative analysis reveals unique structural and functional features of the Smc5/6 complex. *Proceedings of the National Academy of Sciences*, *118*(19), e2026844118. https://doi.org/10.1073/pnas.2026844118

Zabrady, K., Adamus, M., Vondrova, L., Liao, C., Skoupilova, H., Novakova, M., Jurcisinova, L., Alt, A., Oliver, A. W., Lehmann, A. R., & Palecek, J. J. (2016). Chromatin association of the SMC5/6 complex is dependent on binding of its NSE3 subunit to DNA. *Nucleic Acids Research*, *44*(3), 1064–1079. https://doi.org/10.1093/nar/gkv1021

Zapatka, M., Pociño-Merino, I., Heluani-Gahete, H., Bermúdez-López, M., Tarrés, M., Ibars, E., Solé-Soler, R., Gutiérrez-Escribano, P., Apostolova, S., Casas, C., Aragon, L., Wellinger, R., Colomina, N., & Torres-Rosell, J. (2019). Sumoylation of Smc5 Promotes Error-free Bypass at Damaged Replication Forks. *Cell Reports*, *29*(10), 3160-3172.e4. https://doi.org/10.1016/j.celrep.2019.10.123

Zawadzka, K., Zawadzki, P., Baker, R., Rajasekar, K. v., Wagner, F., Sherratt, D. J., & Arciszewska, L. K. (2018). MukB ATPases are regulated independently by the N- and C-terminal domains of MukF kleisin. *ELife*, *7*. https://doi.org/10.7554/eLife.31522

Zegerman, P., & Diffley, J. F. X. (2007). Phosphorylation of Sld2 and Sld3 by cyclin-dependent kinases promotes DNA replication in budding yeast. *Nature*, *445*(7125), 281–285. https://doi.org/10.1038/nature05432

Zhang, X., & Paull, T. T. (2005). The Mre11/Rad50/Xrs2 complex and non-homologous end-joining of incompatible ends in S. cerevisiae. *DNA Repair*, *4*(11), 1281–1294. https://doi.org/10.1016/j.dnarep.2005.06.011

Zhao, X., & Blobel, G. (2005). A SUMO ligase is part of a nuclear multiprotein complex that affects DNA repair and chromosomal organization. *Proceedings of the National Academy of Sciences*, *102*(13), 4777–4782. https://doi.org/10.1073/pnas.0500537102

Zhu, Z., Chung, W.-H., Shim, E. Y., Lee, S. E., & Ira, G. (2008). Sgs1 Helicase and Two Nucleases Dna2 and Exo1 Resect DNA Double-Strand Break Ends. *Cell*, *134*(6), 981–994. https://doi.org/10.1016/j.cell.2008.08.037

Zou, L., Mitchell, J., & Stillman, B. (1997). CDC45, a novel yeast gene that functions with the origin recognition complex and Mcm proteins in initiation of DNA replication. *Molecular and Cellular Biology*, *17*(2), 553–563. https://doi.org/10.1128/MCB.17.2.553